22

HAMBURGER WASSERBAU-SCHRIFTEN

Herausgegeben von Prof. Dr.-Ing. Peter Fröhle

2020

Sandra Hellmers

Integrating local scale drainage measures in meso scale hydrological modelling of backwater affected catchments

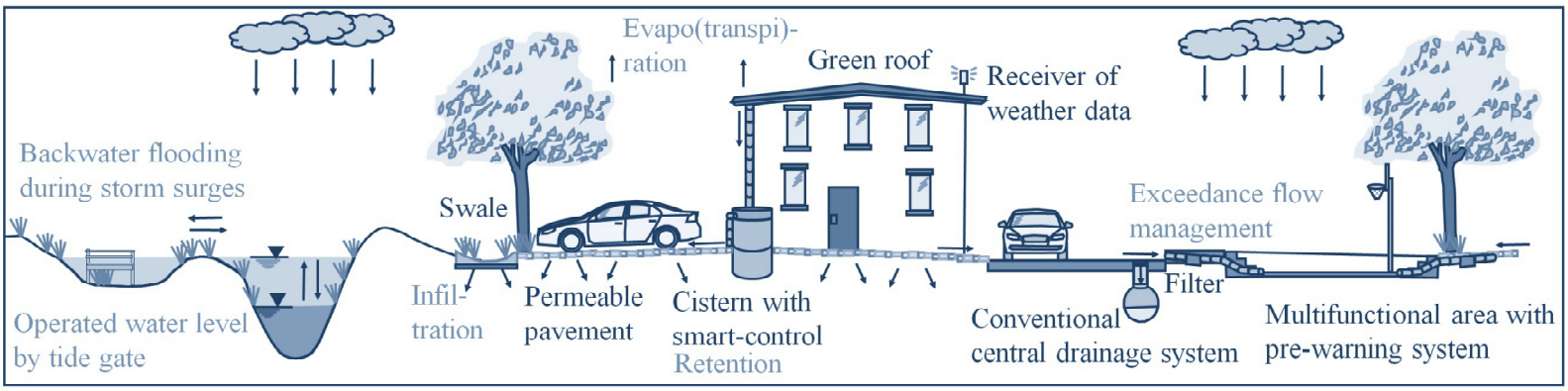

WASSERBAU
River and Coastal Engineering

Integrating local scale drainage measures in meso scale hydrological modelling of backwater affected catchments

von Sandra Hellmers

Institut für Wasserbau, Technische Universität Hamburg

Hamburger Wasserbauschriften, Band 22
Herausgegeben von Prof. Dr.-Ing. Peter Fröhle

Bibliografische Information der Deutschen Nationalbibliothek
Die Deutsche Nationalbibliothek verzeichnet diese Publikation in der Deutschen Nationalbibliothek; detaillierte Daten sind im Internet über http://www.dnb.de abrufbar.

Impressum

Institut für Wasserbau
Denickestrasse 22
21073 Hamburg
Tel.: +49 40 42878-3761
Fax: +49 40 4273-10199
E-Mail: wasserbau.office@tuhh.de

1. Auflage Februar 2020

DOI: https://doi.org/10.15480/882.2627
Sandra Hellmers: https://orcid.org/0000-0002-1216-3259

Integrating local scale drainage measures in meso scale hydrological modelling of backwater affected catchments

Vom Promotionsausschuss der
Technischen Universität Hamburg

zur Erlangung des akademischen Grades
Doktor-Ingenieurin (Dr.-Ing.)

genehmigte Dissertation

von
Sandra Hellmers

aus
Brake (Unterweser)

2020

Gutachter:

1. Prof. Dr.-Ing. Peter Fröhle
2. Prof. Dr.-Ing. Zoran Vojinović

Tag der mündlichen Prüfung: 06.12.2019

Vorwort

Mecklenburg-Vorpommern (2011), Münster (2014), Simbach (Bayern, 2016), Berlin (2017) aber auch Australien (2012 und 2019), Japan (2018) oder Tel Aviv (2020) sind einige wenige Beispiele für Starkregenereignisse der letzten Jahre. Solche Ereignisse sind besondere Herausforderungen für Verwaltungen und den Katastrophenschutz, aber auch für Planungsbüros oder wissenschaftliche Einrichtungen in der Hydrologie, der Wasserwirtschaft und im Wasserbau. Ereignisse und deren Abläufe sind zu verstehen, zu quantifizieren und als Grundlage für die Bemessung statistisch zu bewerten und möglicherweise zu extrapolieren. Maßnahmen und Bauwerke zur Minderung der Auswirkungen von Starkniederschlägen und zum Schutz vor dem Wasser sind zu entwickeln, zu planen und dann auch umzusetzen.

In diesem Zusammenhang stellt das dezentrale aber auch das zentrale Management von Regenwasser in urbanen und ländlichen Räumen derzeit weltweit eine der großen Aufgaben für konkrete Planungsprozesse dar. Vor dem Hintergrund steigender Niederschlagsmengen einzelner Ereignisse und insbesondere auch vor dem Hintergrund steigender Niederschlagsintensitäten im speziellen für konvektive Niederschlagsereignisse, die in den letzten Jahrzehnten und Jahren vermehrt beobachtet wurden und die signifikante Schäden an lokalen Infrastrukturen, Häusern und anderen Werten zur Folge hatten und haben, ist das Erfordernis der realitätsnahen Quantifizierung der Auswirkungen von Starkniederschlägen und natürlich auch der Quantifizierung der Wirkungen von zentralen und dezentralen Regenwasser-Rückhaltestrukturen aus Sicht der Planer evident. Für diese Quantifizierung wurden und werden vielfach hydrologisch-numerische Modelle eingesetzt. Im Institut für Wasserbau der Technischen Universität Hamburg wird in enger Kooperation mit dem Ingenieurbüro Björnsen seit rund 20 Jahren das hydrologisch-numerische Einzugsgebietsmodell KalypsoHydrology entwickelt und gepflegt.

Klassische hydrologische Einzugsgebietsmodelle lösen bisher je nach Detaillierungsgrad der Teil-Einzugsgebiete die Wirkungen und Auswirkungen insbesondere lokalskaliger dezentraler Speicher- und Entwässerungsmaßnahmen nicht oder lediglich integriert auf Teil-Einzugsgebietsebene auf. Zeitlich variate hydrologische Prozesse in den eigentlichen hydrologisch wirksamen Elementen, die die Speicherleistung und den Rückhalt von Wasser stark beeinflussen, werden in Modellen nicht oder nur rudimentär berücksichtigt. Zudem bleibt ein möglicher Rückstau im Einzugsgebiet, im Teil-Einzugsgebiet oder innerhalb eines Bauwerks, beispielsweise als Folge der Entwässerung gegen wechselnde Wasserstände z.B. im Tidegebiet oder als Folge limitierter Entwässerungskapazitäten der Regenwasserkanalisation im Einzugsgebiet oder direkt im Vorfluter in klassischen hydrologischen Modellen ebenfalls praktisch immer unberücksichtigt.

Hier setzt die in diesem 22. Band der Hamburger Wasserbauschriften veröffentlichte Dissertationsschrift von Frau Dr. Sandra Hellmers an. Sie hat in Ihrer Dissertation nachstehend

aufgeführte überzeugende Ansätze und Methoden für hydrologische Einzugsgebietsmodelle entwickelt:

- Realisierung einer flexiblen räumlich-zeitlichen Auflösung,
- Realisierung einer flexiblen und bedarfsorientierten Generierung hydrologischer Netzwerke in Abhängigkeit von der jeweils aktuellen Entwässerungssituation,
- Realisierung von Kontrollfunktionen für die Steuerung hydraulischer Bauwerke,
- Modellierung von hydrologischen Prozessen auf der Bauwerks- und der lokalen Ebene innerhalb von Einzugsgebieten,
- Modellierung des Überschreitungsabflusses und -nachlaufs einschließlich der Hochwasserführung innerhalb von Kontrollstrukturen,
- Modellierung von Rückstaueffekten unter Verwendung eines generischen und skalenunabhängigen Ansatzes in unterschiedlichen Ebenen der hydrologischen Einzugsgebietsmodellierung:
  - in lokalen Entwässerungsstrukturen,
  - in (Teil-) Einzugsgebieten und
  - in Vorflutern.

Diese Ansätze und Methoden wurden dann auch in das hydrologische Modellsystem KalypsoHydrology implementiert, für praktische Fragestellung aufbereitet und basierend auf Feld- und Labordaten verifiziert sowie bewertet.

Den Schwerpunkt legt Frau Dr. Hellmers hierbei auf dezentrale und lokal wirkende Entwässerungsmaßnahmen (LSDM – Local Scale Drainage Measures). Da die entsprechenden Ansätze und Methoden von ihr zumeist generisch und skalenunabhängig entwickelt wurden, sind diese somit entsprechend auf allen relevanten Zeit- und Raumskalen hydrologischer Modelle anwendbar. Ein wie ich finde großer Schritt in der Entwicklung hydrologischer Modelle und Modellsysteme.

Die vorliegende Arbeit baut auf den vielfältigen Projekterfahrungen von Frau Dr. Hellmers auf. Sie hat am Institut insbesondere in den Vorhaben KLIMZUG-Nord, KLEE und nicht zuletzt im Vorhaben StucK gearbeitet und hieraus die vorgenannte Fülle von Fragestellungen abgeleitet und dann entsprechend aufbereitet und umgesetzt.

Es freut mich persönlich sehr, dass Frau Dr. Hellmers ihr Dissertationsvorhaben zu einem ausgezeichneten Ende gebracht hat. Nach meiner Ansicht stellt diese Arbeit eine inspirierende Quelle für Hydrologen und für die Entwickler hydrologischer Modelle dar und ich bin überzeugt, dass die von ihr entwickelten Ansätze und Methoden auch in andere hydrologische Modelle einfließen werden.

Peter Fröhle
Leiter des Instituts für Wasserbau der TUHH

Danksagung

An dieser Stelle möchte ich mich bei all denjenigen bedanken, die mich während der Anfertigung der vorliegenden Dissertation fachlich, sowie persönlich unterstützt, gefördert und motiviert haben.

Mein Dank gilt zunächst meinem Doktorvater Herrn Prof. Dr.-Ing. Peter Fröhle für die Unterstützung, Betreuung und Begutachtung meiner Dissertation. Sein fachlicher Rat, die konstruktiven Diskussionen und der wissenschaftliche Austausch förderten und motivierten mich maßgeblich in der Fertigstellung dieser Arbeit. Für die fortwährend gute, vertrauensvolle und zuverlässige Zusammenarbeit während meiner Promotion, den Tätigkeiten in Projekten und der Lehre am Institut für Wasserbau der Technischen Universität Hamburg bedanke ich mich herzlich.

Herrn Prof. Dr.-Ing. Zoran Vojinović vom IHE Delft (Institute for Water Education) danke ich sehr für die Übernahme des zweiten Gutachtens und den fachlichen internationalen Austausch. Für die Übernahme des Vorsitzes der Prüfungskommission danke ich Herrn Prof. Dr.-Ing. Otto von Estorff.

Danken möchte ich im Besonderen auch unserem ehemaligen Institutsleiter Herrn Prof. Dr.-Ing. Erik Pasche für die Nahebringung der Thematik Hydrologie, sowie seiner vermittelten Begeisterung für die Weiterentwicklung von numerischen hydrologischen Modellen. Die für mich äußerst interessanten Arbeiten unter seiner Leitung während des Studiums und anschließend als wissenschaftliche Mitarbeiterin waren wesentliche Impulse zur Anfertigung der hier vorliegenden Dissertation. Sein früher Tod im Jahr 2010 war für mich und das ganze Institut aus persönlicher und fachlicher Sicht ein schwerwiegender Verlust.

Herrn Dr. Karl-Friedrich Daemrich danke ich sehr für die fachliche und persönliche Unterstützung während seiner Zeit als kommissarischer Leiter unseres Instituts und den dadurch gewachsenen sowie fortlaufenden Austausch, welcher mir viel bedeuted. Bedanken möchte ich mich bei ihm für sein Interesse, die Anregungen und das Korrekturlesen meiner hier vorliegenden Dissertation. Gerne erinnere ich mich auch an den Institutsausflug auf dem Fluß Seeve inklusive einer ungewollten Kenterung unseres Doppelkanus ins kalte Wasser mit anschließender Weiterfahrt, die mit viel Lachen zu einem unvergesslichen Erlebnis wurde.

Mein Dank geht auch an alle aktuellen und ehemaligen Kollegen des Instituts für Wasserbau für die außerordentlich gute Zusammenarbeit, die zum Gelingen der vorliegenden Arbeit beigetragen hat. Insbesondere bedanke ich mich bei meinen Kollegen Herrn Justus Patzke und Herrn Giovanni Palmaricciotti für die Entwicklung und die Umsetzung des Regensimulators, sowie Aufbau und Inbetriebnahme der Gründachversuche. Die umfangreichen Versuchsdurchführungen, Datenaufbereitungen und numerischen Modelluntersuchungen wurden durch zahlreiche betreute studentische Arbeiten umgesetzt. Auch dafür möchte ich meinen aufrichtigen Dank aussprechen. Namentlich möchte ich hier Lina Sverdlova, Lena Stöbert,

Anton Schneider, Emmanuel Rodriguez, Fenja Schuyenburg, Paulina Mederos und Petra Pasdzior für ihre Arbeiten danken. Meinen Kollegen im Bereich Hydrologie, Christoph Sauer und Saskia Nagrelli, danke ich sehr für Ihr Interesse und Ihre Zeit des Korrekturlesens mehrerer Abschnitte der vorliegenden Dissertation. Für den Austausch in zahlreichen gemeinsamen Publikation danke ich meiner Kollegin Dr.-Ing. Nataša Manojlović. Für die Unterstützung zur Weiterentwicklung der Software Kalypso aus dem Bereich der Informationstechnik danke ich besonders meinen Kollegen Ilya Gershovich, Dejan Antanasković, Dr. Stefan Kurzbach, Nico Schrage und Gernot Belger (von Björnsen Beratende Ingenieure). Unserem Oberingenieur des Instituts für Wasserbau, Herrn Dr.-Ing. Edgar Nehlsen, danke ich sehr für die organisatorische und persönliche Unterstützung zur Fertigstellung der vorliegenden Dissertation.

Den Kollegen vom Landesbetrieb Straßen, Brücken und Gewässer möchte ich für die jahrelange gute Zusammenarbeit in mehreren Forschungs- und Entwicklungsprojekten (u.a. KLIMZUG Nord und StucK) danken. Den Firmen Optigrün International AG und HanseGrand danke ich für die Bereitstellung von Materialien für Forschungszwecke.

Meinen persönlichen und ganz besonders herzlichen Dank während dieser herausfordernden, aber auch ungemein lohnenden Zeit der Dissertation möchte ich meiner Familie, insbesondere meinen Eltern, für ihre fortwährende liebevolle Unterstützung aussprechen.

Der größte Dank gilt jedoch meinem Lebenspartner Vincent Gabalda für den wichtigen Ausgleich in unserem gemeinsamen Leben und die liebevolle Motivation zum Endspurt, die durch die zeitnahe Geburt unserer Tochter nochmals bekräftigt wurde.

Ebenso sei allen denen ein Dankeschön ausgesprochen, die nicht namentlich Erwähnung fanden, aber zum Gelingen dieser Arbeit beigetragen haben.

Sandra Hellmers
Hamburg, Februar 2020

Abstract

This work presents the development, implementation and evaluation of methods to overcome limitations in modelling local scale drainage measures (LSDMs) in backwater affected meso scale catchments with hydrological numerical models.

LSDMs manage stormwater close to its source by imitating natural processes of infiltration (e.g. by swales), evapotranspiration (e.g. by green roofs) and detention (e.g. by cisterns). Advantages of LSDMs lie in a larger flexibility for adaptation, multi-functionality as well as sustainability to retrofit existing central drainage systems. Especially in low lying catchments, the pressure on current storm water drainage systems increases due to combined impacts of urbanisation, mean sea level rise and heavy storm events in terms of increased intensity, frequency and duration. In these catchments, the linkage of local scale drainage measures in a cascading system is a promising concept to mitigate the magnitude of surface runoff volumes and rates.

The demand to compute LSDMs in meso scale catchments with hydrological numerical models arises, among others, by the need to analyse the performance of adaptation measures for the mitigation of the frequency and magnitude of flooding on a regional scale. To meet this demand, the following limitations in current numerical models to compute local scale hydrological processes and backwater effects in (tidal influenced) low lying lands are resolved in this work. The required flexible spatio-temporal resolution in applied methods was not sufficient. A parametrisation to model hydrological processes in LSDMs on the basis of measurements in laboratory or nature was not available. Hydrological methods to model backwater effects and approaches to generate hydrological networks on the local and meso scale were missing.

One strength of the developed methods is to zoom into the processes (physically, spatially and temporally) where reasonable values of parameters are available on the local scale (<1 m^2) and to zoom out of the processes on the meso scale (10 to 100 km^2) where conceptualized approaches are applied. Further on, it is accomplished to model backwater effects in streams, flood prone areas and LSDMs with a hydrological approach.

An evaluation of the extended numerical model is performed by verification and validation of simulated results in application studies on local and regional scale. The results of the applied evaluation criteria demonstrate very good congruency between simulated model outputs and observed data from laboratory as well as from gauging stations in nature. It is proved, with a sufficient exactness from a practical point of view, that the developed model is an appropriate instrument to analyse the hydrological performance of LSDMs on the regional scale in backwater affected catchments.

Zusammenfassung

Diese Arbeit erläutert die Entwicklung, Implementierung und Evaluierung von Methoden zur Behebung von Mängeln in der Modellierung von lokalwirkenden Entwässerungsmaßnahmen in rückstaubeeinflussten mesoskaligen Einzugsgebieten mit hydrologischen numerischen Modellen.

Lokalwirkende Entwässerungsmaßnahmen LSDMs (aus dem Englischen: Local Scale Drainage Measures) bewirtschaften das Niederschlagswasser durch natürliche Prozesse, wie Infiltration (z.B. mit Mulden), Verdunstung (z.B. mit begrünten Dächern) und Rückhalt (z.B. mit Zisternen). Die Vorteile von LSDMs zur Ergänzung bestehender zentraler Entwässerungssysteme liegen in der flexiblen Anpassungsfähigkeit und den multifunktionalen sowie nachhaltigen Eigenschaften. Insbesondere in tiefliegenden Gebieten erhöht sich der Druck auf aktuelle Entwässerungssysteme durch die kombinierte Belastung aus Urbanisierung, Meeresspiegelanstieg und intensivere, sowie länger andauernde Starkniederschläge. In diesen Gebieten ist die Vernetzung von lokalwirkenden Maßnahmen in kaskadierenden Entwässerungssystemen ein erfolgsversprechendes Konzept zur Minderung von Oberflächenabflüssen.

Die Nachfrage zur numerischen Modellierung von LSDMs auf Einzugsgebietsebene erwächst unter anderem aus dem Bedarf zur Analyse der Wirksamkeit von Anpassungsmaßnahmen zur Minderung der Häufigkeit und des Ausmaßes von Überflutungen auf der regionalen Skala. Aus diesem Grund wurden die folgenden Unzulänglichkeiten in numerischen Modellen behoben, um lokalwirkende Maßnahmen und Rückstaueffekte zu modellieren. Die erforderliche flexible raum-zeitliche Auflösung in den angewendeten Methoden fehlte. Eine Parametrisierung von lokalwirkenden Maßnahmen auf Basis von Messdaten aus dem Labor oder aus der Natur war nicht verfügbar. Hydrologische Methoden zur Modellierung von Rückstaueffekten und Ansätze zur Generierung hydrologischer Netzpläne auf der lokalen, sowie auf der mesoskaligen Ebene waren nicht vorhanden.

Eine Stärke der entwickelten Methoden ist das Hineinzoomen in die Prozesse (physikalisch, räumlich und zeitlich), für die ausreichende Werte der Parameter auf lokaler Ebene ($<1\,m^2$) verfügbar sind und ein Herauszoomen aus den Prozessen, für die konzeptionelle Ansätze auf der mesoskaligen Ebene (10 bis $100\,km^2$) angewendet werden. Im Weiteren ist erreicht worden, Rückstaueffekte in Flussabschnitten, Überflutungsflächen und LSDMs mit einem hydrologischen Ansatz zu berechnen.

Zur Prüfung des erweiterten Models erfolgte die Verifizierung und Validierung von simulierten Ergebnissen in Anwendungsstudien auf lokaler und regionaler Skala. Die Ergebnisse der Prüfungskriterien zeigen eine sehr gute Übereinstimmung der simulierten Werte im Vergleich zu gemessenen Daten im Labor und von Stationsdaten in der Natur. Es ist mit aus praktischer Sicht hinreichender Genauigkeit nachgewiesen worden, dass das Modell ein geeignetes Instrument ist, um die Wirkung von lokalen Entwässerungsmaßnahmen auf der regionalen Skala in rückstaubeeinflussten Einzugsgebieten zu analysieren.

Contents

Glossary

afflux

An afflux describes the impounding of water combined with a rise in water level immediately upstream of a natural or artificial obstruction which causes the narrowing or closing of a cross section. A consequence of an afflux is a **backwater effect** in upstream direction.

algorithm

An algorithm is a structured workflow which defines the order of functions, instructions or calculation routines to execute a computation. Algorithms are depicted in this work in flow charts to illustrate the computational structures with marked symbols, boxes and notations.

allocatable array

In programming, the dimension of allocatable arrays is specified during the execution of the computation. In this way, memory storage for arrays of parameters is assigned only temporary for the specific needs of the models. This **on-the-fly** procedure supports to safe memory storage and computation resources during the execution of a model.

backwater effect

A backwater effect is caused when the water level at a downstream section exceeds the water level at an upstream section. The effect of impounded water causing a rise of downstream water level is also known as **afflux**. Flooding of areas caused by backwater effects in streams is defined as **backwater flooding**.

calculation code

A calculation code is an executable file which is created by compilation of a **source code** into a computer readable language.

calculation routine

A calculation routine is a part of a computational algorithm and comprises functions and instructions. A calculation routine which is repeated several times within an algorithm is defined as **computational loop**. Each unit in such a loop is a **computation run**.

catchment

A catchment is defined as a spatial unit where water drains to one outlet. The scale of a catchment ranges from a plot of some m^2 (for instance the roof area of a building) up to 1000 km^2 for large river basins. In this work catchments are modelled on the regional scale of river basins with sizes larger than 100 km^2 including subcatchments on the meso scale with a size of 1 to 10 km^2.

data structure

In this work, data structures are defined as elements within a **hydrological network** which are specified by a set of **parameters** (namely a parametrisation). In this work, the elements such as subcatchments, stream segments, junction nodes and LSDMs are described as data structures.

driver time series

Driver time series are computed or measured time series of an element (= a "driver") in the hydrological network. These time series are checked for reaching threshold values (criteria) during the execution of a control function to activate or deactivate a function.

feature

A feature describes effective attributes and functionalities of a structure or model.

flood routing

The procedure to determine the magnitude and time of outflow of a stream on the basis of an inflow into the upstream part is defined as flood routing. It describes the propagation of discharge through streams from up- to downstream, whereby translation and retention effects along the stream change the shape of the hydrograph.

flux

A flux is the quantity of water passing through a unit area ($1\,m^2$) within the actual computing time step size Δt given in $mm/\Delta t = l/m^2/\Delta t$ in a specified direction. When modelling the processes in a storage volume, a differentiation is done between influx and outflux direction.

free flow conditions

Free flow conditions are present if the flow propagation through a stream is not affected by downstream obstructions. This means that effects derived from obstacles downstream of a considered stream segment (such as **affluxes**) have no impact on the upstream flow regime.

hydrological (numerical) modelling

In this work, the term "hydrological modelling" as well as the term "hydrodynamical modelling" describe the numerical simulation of processes with a computational model. Physical models with respect to simulate processes with a model in laboratory or in nature are not the main focus of this work.

hydrological network

A hydrological network describes the distribution, drainage properties and links among elements (here: **data structures**) within a hydrological model. Elements of a hydrological network are defined as areas (**subcatchments** or **LSDMs**), **stream segments** (reaches of a river) or **junction nodes**.

ideal year

A parametrisation based on an ideal year describes the input values with a time series from 1st January until 31st December. An ideal year has a length of 365 days or for leap years 366 days. In this work, input parameters which are given in the form of ideal years are for example, rainwater harvesting and vegetated cover values.

international system of units

Values of parameters are given in units which correspond to the international system of units ("SI" = Système International (d'unités)). The unit symbols such as "m" (metre), "kg" (kilogram), "km" (kilometre) and "s" (seconds) are applied. Further unit symbols are "h" (hour), "l" (litre) and "mm" (millimeter).

junction nodes

Junction nodes define the linkage between stream segments and the inflow points of subcatchments into streams within a **hydrological network**. Additionally, control functions to distribute water are defined at junction nodes.

KC-approach

The Kozeny-Carman (KC-) approach was proposed by Kozeny [1927] and verified by Carman [1937] to compute the hydraulic conductivity on the basis of the soil material characteristics. This approach describes the "hydraulic radius theory" with the assumption that porous soil is treated like a bundle of capillary tubes of equal length as described in Bear [1988] (p. 166).

LSDM

The term "local scale drainage measure" (LSDM) describes a drainage structure which operates close to the location where surface runoff is generated. By means of a cascade of local measures, storm water is managed in a natural and sustainable way by using the processes of infiltration, evapo(transpi)ration and rainwater harvesting. Alternative terms with nuanced definitions are for example "Low Impact Development" (LID), "Sustainable (urban) Drainage System" (SUDS), "Water Sensitive Urban Design" (WSUD), "Best Management Practice" (BMP), "Alternative Technique" (AT) and "Green Infrastructure" (GI).

m a.s.l.

The reference height is defined in "meter above (mean) sea level = m a.s.l." also known as altitude. This corresponds to NHN = "Meter über Normalhöhennull (m ü. NHN)" in Germany.

model calibration

Input parameters into a numerical model are either derived by measurements or based on conceptual approaches. Especially for meso or regional scale modelling, observed data is limited. Therefore, conceptual approaches are applied which demand for an adjustment of values. This adjustment is performed in a "model calibration" procedure of input parameter values. The procedure of model calibration aims to reproduce the response of reality within a range of accuracy specified for the model application.

model validation

Model validation aims to analyse if the model results are within a sufficient range of accuracy for the proposed but as well limited field of application. In this work, model validation is performed by comparing the simulated results with observed data from laboratory and gauging stations in nature.

model verification

Model verification aims to test the functional and mathematical correctness of the numerical model with a limited set of evaluation criteria. It is restricted to a specified field of application which is described in this work.

on-the-fly processing

A data processing which is **allocated**, changed and updated continuously during the execution of a computation is defined as "on-the-fly (data) processing". It reduces computation resources and manual interventions.

overlay data structure

An overlay data structure comprises specified parameters which are lying, in order of priority, over basic parameters and replace them if values are defined.

parameter

A parameter is an effective value that describes a component of a system. Selecting a set of parameters to describe for example, a **data structure** is named **parametrisation**. A differentiation is done between formal parameters and actual input parameters (also known as **arguments**). Formal parameters are processed as input and output in calculation routines. Actual input parameters are the arguments given by the modeller to define specific characteristics of the data structures to be modelled.

parsimonious model

A parsimonious model aims to be defined as simple as possible, but complex enough to perform the simulation of processes in an appropriate way. This concept leads to a reduction of the number and a definition of a required resolution of actual input parameters in a numerical model.

run

A **run** defines the execution of a simulation or monitoring study with defined conditions. A **simulation run** is the execution of a computation over a specific time duration (such as a shortterm, longterm or cycle run). A simulation run with a time step size of a few minutes is defined as **shortterm run** of specific events. Simulation runs of several decades utilize a time step size in days are defined as **longterm runs**. A **cycle run** comprises the simulation of processes within one specified event or per year within a longterm run. Further on, an **experimental run** describes the execution of an experimental study in the laboratory with defined conditions and over a specified period of time.

run-on process

The run-on process describes the flow routing from a source area (for example a LSDM) in the direction to a target (namely a sink) area. In comparison, a run-on process is the reverse of a runoff process.

scaling

Scaling is the process to transfer data from one spatial or temporal level to another one. For example, a differentiation of spatial scales is defined among micro (<1 m^2), local (<10 m^2), district (<1000 m^2), meso (<100 km^2) and regional scales (>100 km^2) in this work.

shape

A shape is a spatial data structure in form of a file which describes parameters with geographical reference and attributes in a **GIS**-based coordinate system.

source code

A source code is the written form of a computational algorithm which gives the structure of the calculation routines using a programming language (for example Fortran or C++). For the execution of the computational algorithm with a computer, the source code is compiled to a **calculation code**.

stream segment

A stream segment is a defined part of a stream. The segmentation aims to define per segment a characteristic profile. Each stream segment starts and ends with a **junction node** within a **hydrological network**.

WVQ-relation

A relation between water level (W), volume (V) and discharge (Q) is derived for steady-state flow conditions per stream segment in the flood routing approach for a reasonable small stream segment.

Acronyms

ASCII American Standard Code for Information Interchange

CFL-criterion Courant-Friedrichs-Lewy criterion

DEM Digital Elevation Model

eq. equation

GIS Geographic Information System

HRU Hydrological Response Unit

RMSD Root Mean Square Difference

RS-TUHH Rainfall-Simulator of the Hamburg University of Technology

1. Introduction

The demand for quantifying the performance of local scale hydrological structures to mitigate the occurrence of flooding in backwater affected catchments on meso scale with hydrological (numerical) models is growing. Hydrological modelling deals with the computation of water fluxes driven by the exchange of energy and mass through divers compartments made up of heterogeneous media like soil, air and water. The spatial sizes of the hydrological structures range from local scales of less than 100 m^2 to regional scales of several 100 km^2. Thereby, the availability of data on spatio-temporal detailed scales and thus the kind of parametrisation differs significantly. On the one hand, for regional scale modelling, observable data is available in most cases only on rough spatio-temporal scales to reconstruct the complex architecture of a hydrological system. Technical resources of observation methods below as well as above the surface and temporal changes of the structures pose a challenge to obtain a detailed description of the hydrological processes. On the other hand, for study areas on local scale, the media and structures are described with data on more detailed spatio-temporal resolutions with available observation technics and human resources.

To integrate the gained knowledge from local scale studies in current meso scale hydrological numerical models two key features are missing: on the one hand, adequate "flexible" spatio-temporal scales in the methods to model local scale hydrological systems and on the other hand, approaches to model backwater effects in low lying lands. These weaknesses of numerical models are specified and resolved in this work by means of integrating local scale drainage measures (LSDMs) in meso scale hydrological modelling of backwater affected catchments.

Background. The need for adaptation of drainage systems arises by the impacts of urbanisation and climate change which pose major challenges to many cities worldwide to both, the mitigation of flooding and water scarcity. More than 55 % of the world's population, which means 4.2 billion, already lives in urban areas as referred by UN DESA [2018][1]. This urbanisation rate increased from 30 % in 1950 and is predicted to reach 68 % in 2050. In Europe, the population living in urban areas was reported to be 74 % in the year 2018 (UN DESA [2018]) and is expected to reach 80 % in 2050 (UN DESA [2014]).

[1] UN DESA = United Nations Department of Economic and Social Affairs.

The effects of urbanisation on the water balance are manifold with regard to physical, chemical and biological modifications as reported in Butler and Davies [2011] and Gessner et al. [2014]. By changing a vegetated into an impervious surface (such as parking places, houses or streets) a smaller quantity of water infiltrates, evapotranspirates or is retained in these areas. At the same time, the magnitude and intensity of surface runoff reaching the catchment outlet are increased. This leads to larger runoff volumes, higher peak flow rates as a consequence of shorter retention time and an increase of the probability of flooding in low lying areas. These and further impacts of urbanisation are reported for instance by Butler and Davies [2011]; Fletcher et al. [2013]; Haase [2009]; McGrane [2016]; O'Driscoll et al. [2010]; Vojinović and Abbott [2012] and Zevenbergen et al. [2011].

Low lying lands in coastal regions are situated close to or below the reference height of the "mean sea level" also known as altitude. In the progress of land cultivation and urbanisation, low lying lands are reclaimed by installing dykes, tide gates and pumping stations. Lowered water levels in these areas are controlled by pumping out exceeding water or by drainage during low tidal water levels. In low lying urban lands the pressure on the storm water drainage systems to prevent flooding arises by combined impacts of climate change on mean sea level rise (IPCC [2013c]), more intensive as well as longer heavy storm events (IPCC [2013a, 2013b]) and urbanisation (UN DESA [2018]). The range of predicted impacts by climate change on the intensity of heavy precipitation[2] in Central and Eastern Europe varies between 15 % to 35 % until 2100 (Jacob et al. [2014]).

Studies about the combined risk of high tides and storm events are given by Lian et al. [2013] for a case study at the southeast coast of China and by Nehlsen [2017] for tributary areas of the Elbe river, North Germany. The situation in flood prone areas of the Netherlands is reported by Klijn et al. [2012] and Zeeberg [2009] as examples of the upcoming challenges in Europe. Huong and Pathirana [2013] analysed the impacts on urban flooding in the low lying lands of the Mekong River Delta in the city Can Tho, Vietnam and Sweet et al. [2017] gives a review about the predicted changes in flooding in low lying lands along the coast of the United States. These are selected examples showing a conformity about a tendency that low lying lands will face higher pressures to mitigate flooding in the future, while the range in the predicted magnitude of impacts is large.

The demand for local, flexible, adaptable and sustainable drainage measures. To address the margin of uncertainty in the impacts of urbanisation and climate change, flexible as well as sustainable solutions are required as described for example in "The EU strategy on adaptation to climate change" (EC [2013]).

In the past century, centralised (conventional) drainage systems were implemented in urban areas such as underground constructed pipe networks or straight open channels aiming for a fast non-retained conveyance of stormwater runoff from the source (properties) to protect structures, prevent flooding and for public health maintenance. The size adjustment of a conventional central drainage system after the construction demands in most cases for a large

[2]Heavy precipitation is defined as the intensity of the 95th percentile of daily precipitation (Jacob et al. [2014]).

amount of financial and human resources. There is a limited flexibility of these systems to be adjusted for changes derived by urbanisation, climate change or both impacts (see Gersonius et al. [2013]; Radhakrishnan [2017]; Sieker et al. [2008]; Zevenbergen et al. [2011]). Further on, conventional drainage systems contribute less to mitigate impacts of urbanisation regarding water quality, health, ecology and increased surface water runoff, because the stormwater is conveyed to receiving water bodies directly with little or no adequate treatment or retention (see M. J. Burns et al. [2012]). To improve the urban drainage management a combination of conventional centralised with local scale drainage measures (LSDMs) is required to develop a sustainable adaptation in cities as described for example in Vojinović [2015].

The definition of local scale drainage measures (LSDMs). LSDMs manage storm- and rainwater[3] close to its source by imitating the natural processes of infiltration, evapotranspiration and retention. The concept of LSDMs accentuate the integration of a combination of "soft" (natural) and "hard" (engineered) systems to collect, drain, treat, attenuate and reduce stormwater runoff by activating these hydrological processes in urban areas (see Butler and Davies [2011]; Wong. et al. [2013]; Woods Ballard et al. [2015] and Askarizadeh et al. [2015]). Additionally, rainwater harvesting considers rainwater as a resource and less as a load. At the same time, the implementation of LSDMs provides a larger flexibility to be adapted for impacts derived by urbanisation or climate change in comparison to conventional central stormwater drainage systems. LSDMs consist of source control structures such as swales, green roofs or cisterns with a limited capacity and a specific design threshold volume. In case of storm events that exceed the capacity of these local measures, the control of exceedance flow is of particular concern. If the design value of a LSDM (for instance green roof) is exceeded, the exceedance flow (namely overflow) can be conveyed by roads or streets to multifunctional areas (for example a park or open green space) or a retention pond. By linking LSDMs into such cascades, a flexible adaptable system is created.

In Li et al. [2017], a review of 31 studies about modelling and monitoring LSDMs provides an insight into the performance of implemented structures. That paper concludes that the implementation of LSDMs reduces surface runoff and peak discharge while increasing retention times and base flow. These attributes of LSDMs mitigate the extend and occurrence of flooding, but because of the different complexities in each hydrological system, a general valid statement about the potential performance of LSDMs can not be derived. Thus, LSDMs as parts of different individual catchments need to be modelled with their primary attributes.

LSDMs are studied, monitored, modelled and implemented worldwide using varying terms. In recent years, the terminology to define these practices and principles in urban stormwater management increased in complexity as explained in Fletcher et al. [2014]. Different terms are described according to the international origin and nuanced definition like "Low Impact Development" (LID; North America, New Zealand), "Sustainable (urban) Drainage System" (SUDS; United Kingdom), "Water Sensitive Urban Design" (WSUD; Middle East and

[3]Rainwater is the portion of rain falling directly on the area. Stormwater comprise the drained rainwater runoff from different areas, while containing more contaminants in dependence on the land use.

Australia), "Best Management Practice" (BMP; United States and Canada), "Alternative Technique" (AT; France) and "Green Infrastructure" (GI, United States). In recent years the term "Blue-Green" infrastructure is used to describe the management of stormwater runoff, rainwater harvesting and the multiple benefits regarding water quality, quantity and environmental issues (see Bozovic et al. [2017]; Brears [2018] and Maksimović et al. [2015]).

In Germany the term: "Dezentrale Regenwasserbewirtschaftung", meaning "decentralised stormwater management", was introduced during the 1990s to set a focus on the change from central to decentral (namely localised) measures (see FHH [2000]). From a modellers perspective, the differences between conventional and decentral drainage systems are the functional scales. Therefore, the term "local scale drainage measure" (LSDM) is defined in this work to point out the focus on modelling the local scale performance of drainage measures on a size of a few square metres (1 to 100 m^2) within meso scale catchments having a size of several square kilometres (>10 km^2).

The status of policy, frameworks and regulations to implement LSDMs. To facilitate the implementation of LSDMs in urban areas a change in policy, frameworks, regulations, urban planning and last but not least individual acceptance of stakeholders is required. These demands are described for example in Hoang and Fenner [2015]; Kuller et al. [2017]; Petrucci et al. [2013]; Vojinović [2015]; Wong. et al. [2013] and Zevenbergen et al. [2011]. Nowadays, several organisations, research institutes and associations promote and support the implementation of LSDMs in urban areas. In Singapore, the PUB (Singapore's national water agency) initiated in 2006 the "Active, Beautiful and Clean"(ABC) Waters programme, which aims to transform the storm water drainage network into a sustainable system by promoting the implementation of LSDMs (Yau et al. [2017]). In the United Kingdom the organisation CIRIA (Construction Industry Research and Information Association) provides information for practitioners to implement sustainable drainage measures since 2007 (CIRIA [2018]). In Australia eWater (evolving Water management) supports the integration of water sensitive urban designs and governance (eWater [2012]). In the United States the organisation EPA (U.S. Environmental Protection Agency) supports efforts to implement green infrastructures under the "Clean Water Act" and "Safe Drinking Water Act" (EPA [2018b]). Examples of implemented "blue-green" infrastructures are given by Maksimović et al. [2015] for the cities Seoul, Melbourne, Philadephia, Wallington and Brisbane. Additionally, the report by Brears [2018] describes the implementation stages of "blue-green" infrastructures in the cities of Copenhagen, New York, Rotterdam, Singapore and Hamburg, among others.

A review about regulations and policies supporting the implementation of LSDMs in Germany is given by T. Schütze [2013]. In Hamburg, the Ministry for Urban Development and Environment provides examples of implemented LSDMs in a report (see BSU [2013]). Further on, the "Gründachstrategie", meaning "green roof strategy", running from 2014 till 2019 in Hamburg exemplifies how the demand of regulations ("fordern"), the financial support ("fördern") and the support by information ("informieren") facilitates the implementation of LSDMs in a complementing and supportive way (BUE [2015]).

The demand to resolve limitations and weaknesses in hydrological numerical models. To analyse the performance of LSDMs, for example by the means of flood mitigation in meso scale catchments, numerical modelling is required. Hydrological models, as a category of numerical models, aim to simulate the dominant processes based on available (although limited) descriptions of the totality of large scale hydrological systems (see Law and Kelton [1991]). Using hydrological models for the analysis of the performance of LSDMs can assist planners and decision makers at various stages for evaluating, planning and implementing LSDMs.

The demand in quantifying the performance of LSDMs on catchment scale (for example >100 km^2) with hydrological models is increasing, although still rarely realised (see Li et al. [2017]). The reason lies in the limitations and weaknesses in modelling LSDMs and backwater effects with currently available hydrological catchment models. Prevailing limitations of such models are tackled in this work: First, the missing, but required high spatial and temporal resolution. Second, the unavailable, but needed parametrisation of LSDMs for the numerical computation on the basis of measurements. Third, the missing, but required approaches to model backwater effects on the local and meso scale in hydrological models to simulate the performance of LSDMs in low lying lands.

Objectives of this work. This work aims to resolve limitations and weaknesses in modelling LSDMs in backwater affected meso scale catchments by extending recent and developing new methods for the implementation in hydrological numerical models. One objective is the definition of a physical-based parametrisation with a high spatio-temporal resolution to compute a detailed simulation of hydrological processes in LSDMs. A second objective is to integrate LSDMs in the meso scale catchment model structure. For this purpose, a hydrological network needs to be generated including drainage structures on the meso, local and micro scale. New elements as well as linkages are required to be defined for hydrological modelling. A third objective is to develop a methodology to compute backwater effects and control systems within streams as well as areas. Additionally, methods are required to model subsequent hydrological processes on submerged local areas which are affected by backwater flooding. These processes comprise for example, open water evaporation and subsequent controlled drainage. The scope of work to realise these objectives for the integration[4] of methods in a meso scale hydrological numerical model is described in chapter 3.

Outline. In the following chapters the literature review, scope of work, methodology and results to integrate LSDMs in meso scale hydrological (numerical) modelling of backwater affected catchments are explained. The outline of this work is illustrated in figure 1.1. The weaknesses in current hydrological modelling to be resolved in this work are distinguished after a literature review in chapter (2). The specific objectives and theoretical approaches to resolve the detected weaknesses are described in chapter (3). The methodology is divided

[4]The term "integration" evokes the perception of completeness, but is obtained in hydrological (numerical) modelling within the limited boundaries of specified aspects which are presented in this work.

in three consecutive parts and comprises several methods. In chapter (4) the methods to revise and extent the catchment model algorithms are described. A method is developed for flexible spatio-temporal scaling to model LSDMs with geographical location and with an explicit hydrological network generation. The presented methods accomplish short computing times and a parsimonious parametrisation. In chapter (5) methods are described to model the hydrological processes in LSDMs on a local and micro scale using recent knowledge gained in practice and laboratory studies for a physical-based parametrisation. Modelling the techniques of LSDMs like real-time control devices and rainwater harvesting in multifunctional systems is realised by the development of new control functions using the criteria of precipitation intensities, water levels and discharges. In chapter (6) the developed methods to model flood routing among interlinked LSDMs, control structures in stream segments as well as methods to model backwater effects in LSDMs and low lying lands are explained.

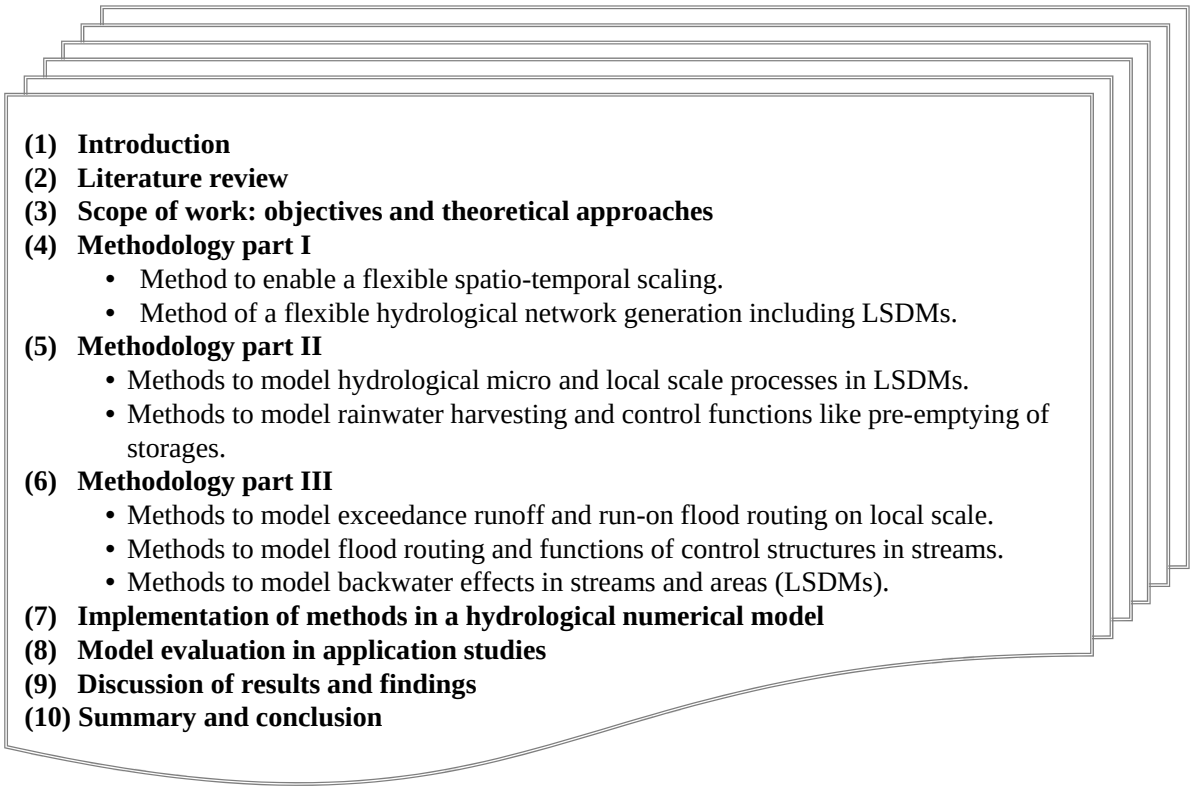

Figure 1.1: Outline and chapter's content of this work.

The implementation of the developed methods in a numerical model is realised in the semi-distributed hydrological catchment model KalypsoNA and the module KalypsoHydrology. The implementation and the parametrisation are described in chapter 7. The results of application studies using evaluation parameters and criteria are analysed and presented in chapter (8) to confirm the model validity and applicability for the defined purposes. The discussion of results in chapter (9) provides a comparison of methods and findings to related studies from literature and an outlook for further research in this topic. A summary of the key findings and a conclusion finalises this work in chapter (10).

2. Literature review

The demand for implementing local scale drainage measures (LSDMs) to retrofit and complement centralised stormwater drainage systems in urban areas increased over the past decades as described in Fletcher et al. [2014]. In Europe, the interest in these measures raised along with the publication of the EU (European Union) Water Framework Directive in 2000 (EC [2000], §13) which postulates a sustainable river basin management while preferring the implementation of local measures close to the source of runoff formation. Thereafter, the EU Floods Directive was published in 2007 which requires the EU member states to take adequate and coordinated action to reduce the flood risk (EC [2007], §7.3).

In this chapter the literature review in section 2.1 summarises main hydrological and technological features of LSDMs as well as the need to model backwater effects when these measures are implemented in low lying lands or tidal influenced catchments close to the coast. Based on a review of hydrological numerical models in section 2.2, a classification scheme of model categories is worked out to discuss the pros and cons of current model features. This serves as basis in order to select required model categories for the objectives of this work. The review concludes in section 2.3 with a summary of the limitations and weaknesses in the determined categories of hydrological numerical models to integrate LSDM features and backwater effects. The chapter's outline is illustrated in figure 2.1

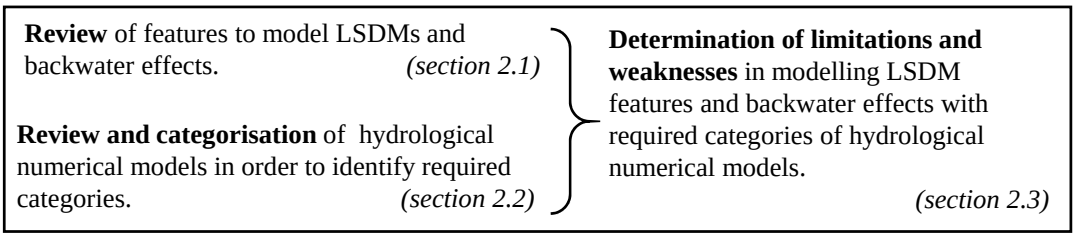

Figure 2.1: Outline of the literature review to determine the limitations and weaknesses in modelling LSDM features and backwater effects in meso scale catchments using hydrological numerical models.

2.1 Review of local scale drainage measures and backwater effects

A prerequisite to develop a methodology for a numerical model is to understand the system components and processes that have to be modelled. For that purpose, the hydrological and technical features of LSDMs are reviewed in this section on the basis of literature, laboratory and monitored study results. This work places emphasis on modelling water quantity issues like drainage and retention processes as well as backwater effects in low lying (tidal influenced) catchments. The scheme in figure 2.2 illustrates some examples of LSDMs and backwater flooding which are described in the following paragraphs.

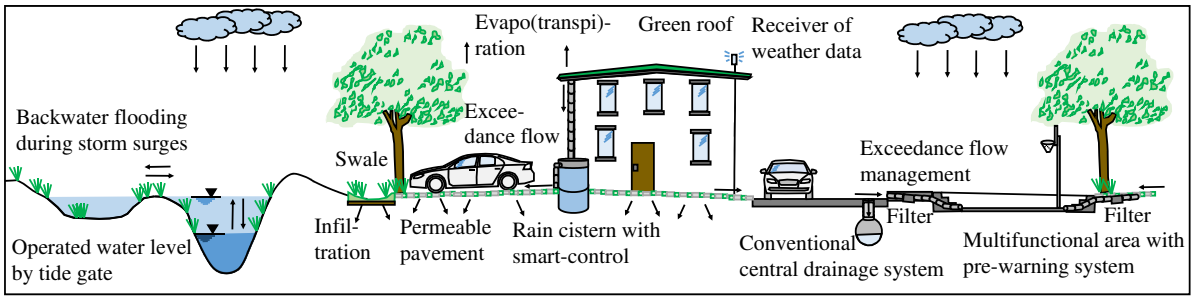

Figure 2.2: Examples of LSDMs in low lying backwater affected lands.

2.1.1 Required spatio-temporal resolution and parametrisation to model LSDMs

The sizes of LSDMs range from cistern or rain barrel scale (1 to 10 m^2), to roof scale (100 to 1000 m^2) and up to parking lots utilised as multifunctional areas (500 to 2000 m^2)[1]. To assess their retention performance and corresponding hydrological system components in urban areas, the spatio-temporal scale in hydrological models has to be reasonably small to represent the heterogeneous and fast responding characteristics of LSDMs. One important aspect in spatial scaling of LSDMs within catchments is the geographical location. This issue has been mentioned previously by Versini et al. [2016] where it is exemplified with the location of green roofs. However, the study by Versini et al. [2016] lacks an approach to model the flood routing among LSDMs.

With regard to the temporal scaling, laboratory and local field monitoring studies show that the permeable material in LSDMs provokes short reaction times in infiltration and fast runoff processes when the storage capacity is reached. For example, extensive green roofs are LSDMs with thin layers of porous media and the results of laboratory and monitoring studies demonstrate a responds time to rainfall which ranges from seconds to minutes. Water infiltrates and is partially retained in the porous media before runoff is generated with a high rising limb (see Patzke et al. [2017]; Vesuviano and Stovin [2013] and Stovin et al. [2015]). The infiltration processes and the point in time where the runoff is generated need to be modelled in a time step size smaller than 1 minute. Therefore, a high temporal resolution in seconds is required to simulate hydrological processes and their interactions in LSDMs in an appropriate

[1] In this work, unit symbols are given in accordance with the international system of units as described in the glossary.

way.

Additionally, it is an open task to define which parameters are required to model LSDMs using a hydrological catchment model. The knowledge gained by laboratory analysis (for instance by De-Ville [2017]; Szota et al. [2017] and Stovin et al. [2015]) regarding green roof field monitoring studies and Abbaspour et al. [2018] considering underdrain systems are not yet integrated in the parametrisation of hydrological catchment models. Water losses through evapotranspiration is often assumed to be a monthly constant or the potential evapotranspiration with the vegetation type is ignored as described in Li et al. [2017]. Therefore, a current limitation in parametrisation exists for modelling evaporation processes. Likewise, a parametrisation of LSDMs to describe the characteristics of the porous materials and drainage structures is only rarely available.

Further on, the complexity of the parametrisation using meso scale hydrological models needs to be limited. For the purpose of integrating the parametrisation of LSDM features into the modelling of meso scale subcatchments (1 - 10 km^2) which are part of regional catchments (>100 km^2) the model complexity needs to be kept as "simple" as possible, but detailed enough to represent the hydrological processes on the respective scales. The complexity depends, amongst others, on the data availability and resolution for the actual parameters to create the numerical model. Unsuitable or insufficient data sources for the parameter estimation may lead to uncertainties and unreliable model results. This issue is also known as "over-parametrisation" as described by Beven [2012]; Perrin et al. [2001]; Petrucci and Bonhomme [2014] and Salvadore et al. [2015]. Reaching a balance between model data structure complexity and data availability, while explaining the dynamics of the data still complex enough, aims to provide a parsimonious model (see Fenicia et al. [2008]).

2.1.2 Hydrological processes in LSDMs

The hydrological processes in LSDMs comprise infiltration, percolation and water retention, which differ in magnitude and dynamic from water balance processes in natural soils. Knowledge about the performance of LSDMs by field monitoring and laboratory studies is collected and reported for example in Ahiablame et al. [2012] and Li et al. [2017]. Available study results provide information about the aspects of runoff reduction of permeable pavements in Winston et al. [2016], of bioswales in Askarizadeh et al. [2015] and of green roofs in De-Ville et al. [2017]; Patzke et al. [2017]; Szota et al. [2017] and Stovin et al. [2015]. In this way, first knowledge about LSDMs is gathered with respect to the retention performance of different materials and drainage technologies. At the same time, in research and practice the demand for hydrological numerical models to compute these features is growing. For that purpose, a parametrisation of LSDMs to model the hydrological processes is required. The application of laboratory results for a parametrisation of empirical numerical green roof models with one or two layers is presented by Versini et al. [2015]; Zimmer and Geiger [1997] and Stovin et al. [2015]. They apply an adapted form of the linear-reservoir theory with the retention coefficients k and n. These numerical approaches have significant limitations in the transfer of derived parameters to other studies because of lacking physical-based meaning. For that pur-

pose, further research is required for the finding of physical-based parameters and methods to describe the hydrological processes in drainage and vegetated substrate layers.

2.1.3 Flexible multiple and interlinked layered structures

LSDMs are made up of different materials in multi-layered structures. Permeable materials are used for retention and drainage layers in green roofs or swale-drainage-systems. Thereby, these structures are designed with interlinked layers. For example an overflow outlet draining the exceeding water of the upper storage directly to the bottom storage is already implemented in practice (such as in a bioretention facility in Washington presented in Anacostia Waterfront Trust [2017]). Other retention layers are constructed with a cascade of storages or as a meandering system to prolong the flow path. This is realised for example in the patented 30 mm or 60 mm meander drainage segments by Optigrün international AG [2018a]. The example of Myers et al. [2011] using permeable pavement installation for rainwater harvesting illustrates how flexible the different technologies of LSDMs are applied in research and practice. Among these multiple layers the flow direction is reversed when infiltrated water reaches a saturated lower layer with impounded water. In consequence, water is backed-up in the upper layers. These retention and drainage processes within multiple and interlinked layered structures need to be simulated in a representative way, but are rarely resolved in current hydrological numerical catchment models.

2.1.4 Rainwater harvesting, multifunctional use and control features

LSDMs are often hybrid systems to improve a more natural accentuated drainage management and rainwater harvesting with rain tanks. According to the region and climate conditions, LSDMs serve different demands. Thereby, rainwater harvesting has higher priority in dry climate conditions while stormwater retention to reduce runoff volume and rate has higher priority in wet climate conditions. The non-potable water reuse comprises for instance toilet flushing but as well bathing, laundry, gardening or car washing in dependence of hygienic standards of the countries. The benefits of rainwater harvesting are studied worldwide. For example, in Australia by Xu et al. [2018] and in comparison to Kenia by Amos et al. [2016]. In the UK a study is published by Melville-Shreeve et al. [2016] and with regard to social involvement by Ward and Butler [2016]. In the Netherlands, rainwater harvesting is applied for the Airport Schiphol as reported in Kuller et al. [2016]. In the United States the potential of rainwater harvesting is studied recently by Alamdari et al. [2018] for climate change scenarios illustrating the large variety in rainwater harvesting implementations in different climate zones ranging from Marine Westcoast in Seattle, tropical wet/dry seasons in Miami to the semiarid steppe in Denver. A similar study is presented for four climate zones in China by Jing et al. [2018].

For Germany, the cost efficiency of rainwater harvesting with regard to replace the demand of potable water is low as published in Umweltbundesamt [2005]. But these studies do not take into account possible benefits in retaining stormwater for flood mitigation. In

T. Schütze [2013] larger benefits are reviewed by taking into account both aspects of rainwater harvesting and stormwater retention. Guidance in planning, installation, operation and maintenance of rainwater harvesting structures for Germany is given in DIN [2002].

Recent progress in the development of technologies is detected in dual storage facilities by combining the benefits of rainwater harvesting and flood mitigation in one facility. A storage volume like a cistern, barrel or tank is divided into two compartments with a bottom storage for retention (namely rainwater harvesting) and an upper storage volume for stormwater detention purpose. The upper one is linked with the lower one to make the inflow for rainwater harvesting possible. Such a system is presented for instance in Rohrer and Armitage [2017] which is implemented in South Africa.

Further progress is made by installing control devices in multifunctional areas. The benefits of multifunctional areas is studied for example in the project RISA for different case studies in Hamburg (Waldhoff et al. [2012]) and the State Ministry for Urban Development and Environment of Hamburg (HSE & BUE [2015]). The legislations and definitions of multifunctional areas ('Mitbenutzung von Flächen') for Hamburg are described in the report by the KompetenzNetzwerk [2010]. Control systems serve two purposes. On the one hand, multifunctional areas which are used by the public (for example as sport fields) have to be evacuated in time before a storm event occurs over a specific threshold using a rainfall forecast system. On the other hand, the retained stormwater has to be drained after the flood event in a controlled manner.

An operational system for evacuating multifunctional areas and emptying cisterns in time before a larger storm event occurs, provides safety and a higher available retention capacity. Whereas storing the water before longer dry periods has beneficial effects for the water reuse by irrigation, toilet flushing and for washing machines. According to Novotry [2009] water management including rainwater harvesting in future cities could close the urban hydrological cycle. In this way, cities practising water conservation and harvesting, consider stormwater as resource with an economic value rather than a load.

Both concepts for multifunctional areas and cisterns require real-time control of storage volumes linked to weather forecast systems. A control system manages, directs and regulates the performance or behaviour of a system in the dependency of control criteria. Such criteria depend on the actual stored water volume, the actual water stage at the drainage outlet and detailed rainfall forecasts based on radar data for several days like presented in a case study of a cistern control system in Keser and Mietzel [2014].

The technology of real-time control by adding sensors to the systems of stormwater retention and rainwater harvesting provides an improved management of these facilities. With regard to dual stage systems of rainwater harvesting and stormwater retention, the criteria of these sensors (namely the control device) is coupled with weather forecast (namely radar rainfall systems) and with water level sensors as illustrated in figure 2.3 (a).

Similar technologies to increase the retention volume on roofs are represented by storage layers which retain water with a control valve. Examples of these systems are retention layers with control valves which function as water storage for the vegetation and are emptied

according to criteria of forecasted storm event intensities. For example the performance of so called "Hydroactive Smart Roof Systems - Hydroventiv" is studied in the project "Climate Innovation Window Studies"[2]. This system is innovated by the company Le Prieuré [2018] and studied in the scope of a European Union's Horizon2020 research project running from 2016 to 2020 (see CIW [2018]). This system is illustrated in figure 2.3 (b). Other systems are available for instance in Germany like the Smart Flow Control 4.0 system invented by Optigrün international AG [2018b]. These products are selected to exemplify the actual interest in combining real-time control systems with technologies in LSDMs.

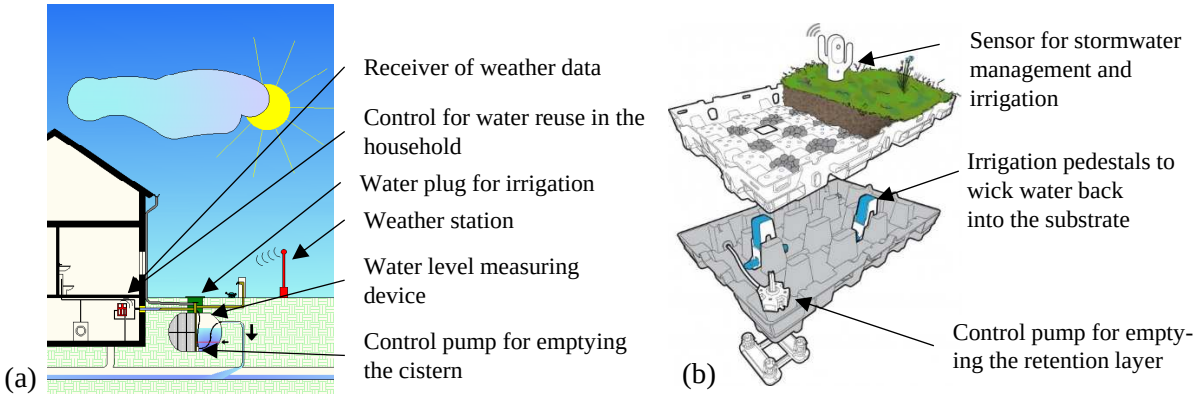

Figure 2.3: Examples of real-time control systems in LSDMs: (a) Cistern with retention and emptying control system (modified from Keser and Mietzel [2014]) and (b) Hydroactive Smart Roof System - Hydroventiv (modified from vegetal i.D. [2018]).

Until nowadays, the approach of real-time control is mainly used in detention basins and drainage systems for the mitigation of combined sewer overflows, for drainage networks with real-time control sensors of water levels or flow velocities as described in Gaborit et al. [2013]; García et al. [2015]; Henonin et al. [2013]; M. Schütze et al. [2016]; Vojinović and Abbott [2012]. But local scale installations of cisterns which are controlled by rainfall forecasts data are still rare. Two allotment studies presented by Keser and Mietzel [2012] and by Xu et al. [2018] illustrate promising results to improve the water retention performance. Additionally, good functionality is demonstrated by an already installed rainwater harvesting tank in Denver which is equipped with a control valve to monitor the irrigation demand and uses weather forecast data (UDFCD [2014]).

To realise the implementation of calculation routines to model control systems on the local scale with hydrological models, the computing time is an important feature. Real-time computing is constraint by short computing times. Operational systems in real-time require a response within a specified time frame which is actually smaller than real time. Vaze et al. [2012] assessed the computing time of hydrological models on typically available computer platforms in 2012 for different model categories to compute 100 years of daily data[3]. For empirical models a computing time of a few seconds, for a conceptual model up to 60 seconds and for fully-distributed models computing times up to several hours are determined

[2] see www.climateinnovationwindow.eu/
[3] The size of the analysed area is not provided in the report by Vaze et al. [2012].

in that study. This assessment depends on many other factors, but serves here to present the difference in computing times among these model categories.

The findings of this review and the results of application studies show the potential of the approach to couple the technology of rainwater harvesting, stormwater retention, real-time control and forecast strategies with LSDMs. These technologies receive more and more attention in research studies like presented in Goncalves et al. [2018]; Rohrer and Armitage [2017]; Xu et al. [2018] and is stated to be an open task for further research as well as for the implementation of these upcoming features in hydrological modelling.

2.1.5 Exceedance and run-on flow routing among interlinked LSDMs

Local scale drainage measures are designed with a limited capacity to retain and detain water. As consequence, exceedance flow is generated when the capacity of a LSDM or any stormwater system is reached. The design capacity is defined for instance in Woods Ballard et al. [2015] for the United Kingdom and in Germany the sizes for LSDMs are recommended in DWA [2016]. Knowledge about exceedance flow control and guidelines are described in a report by Balmforth et al. [2006]. To reduce the impacts of flooding by exceedance flow, an effective design of central underground ("major") systems in combination with decentral ("minor") overland flood conveyance by setting up a cascade of LSDMs (namely "SUDSs"[4]) is suggested in that report.

The routing of flow from an area (namely the source) to the area of interest (namely the sink or target) is defined as "run-on process". This is the reverse process of runoff from a system. The feature of a LSDM to receive water from other LSDMs has to be described in detail to model an interlinked drainage system. Although in analogue studies with respect to water quality issues a treatment train or management train is described (for example in Woods Ballard et al. [2015] (p. 303) to buffer high pollution, such an approach is not analysed for exceedance flow quantities up to now. The exceedance flow control is considered as an important feature to be modelled with hydrological models. But so far, appropriate calculation routines are missing in current meso scale hydrological models to compute the flood routing among LSDMs. This issue is reviewed in more detail in section 2.2.6.

2.1.6 Backwater effects in structures on the local and micro scale

A backwater effect is caused when the water stage at a downstream section is higher than at an upstream section. The retention of water which rises a downstream water level is also known as afflux. In low lying areas backwater effects lead to flooding in drainage streams and adjacent areas, when an afflux is generated in the downstream sections (for instance by a closed tide gate). In this work, it is studied if a controlled flooding of areas (such as LSDMs) is beneficial to mitigate the occurrence of backwater flooding in flood prone areas. It is an open task to model the run-on, retention and controlled drainage processes in LSDMs which are affected

[4] "SUDS" are Sustainable (urban) Drainage Systems.

by backwater flooding. The occurrence of backwater effects and reverse flow in stormwater drainage systems is already recognised, but rarely simulated with hydrological models. So far mostly hydrodynamic-numerical models are applied like it is presented for instance in Yau et al. [2017] for modelling perforated pipes, outlets of rain gardens and gravel swales. Another aspect is the occurrence of backed-up water within vertical layers. Water percolates into lower soil layers as long as the saturation state is not reached. When the lower soil layer is saturated, water is backed-up in the upper layers. The issue of backwater flooding by streams into LSDMs and backed-up water within LSDM layers are rarely monitored, studied or modelled until now.

2.1.7 Summary of required features for modelling LSDMs in backwater affected catchments

The required features in hydrological (numerical) models to compute LSDMs and backwater effects are summarised in table 2.1 from (1) to (10) in the order of three main modelling aspects. In the first aspect of resolution, a high spatial (<1 m^2) and high temporal resolution (<1 minute) are important features to model the performance of LSDMs in meso scale catchments.

Table 2.1: Summary of required features to model LSDMs in backwater affected catchments.

Modelling aspects	Required features in hydrological (numerical) models to compute LSDMs		
Resolution and applicability	(1) Spatial local scale resolution (<1m²) and geographical organisation.		(2) Temporal small scale resolution (< 1 minute).
	(3) Applicability for spatio-temporal meso scale modelling.		(4) Short computing times.
Hydrological processes and LSDM technologies	(5) Modelling LSDM features with an applicable parametrisation.		
	(6) Modelling multiple and interlinked layered structures.	(7) Modelling rainwater harvesting functions.	(8) Modelling control features in areas (a) and streams (b).
Flood routing	(9) Modelling the flood routing among LSDMs.		(10) Modelling backwater effects in streams, areas and LSDMs.

The applicability to model LSDM features on the meso scale requires a parsimonious parametrisation and short computing times. A parsimonious parametrisation is needed to find a balance between the complexity to model hydrological processes on meso scale and the data availability. Short computing times are required to model control functions in operational systems of local scale measures like cisterns or multifunctional areas. For modelling the hydrological processes in LSDMs a parametrisation and methods based on knowledge from laboratory and field monitoring studies are important. The rainwater harvesting and real-time control features of storage volumes in LSDMs are considered as upcoming effective features. Flexible multiple and interlinked layered structures are required to be modelled to represent new

technologies. Exceedance and run-on flow routing among interlinked LSDMs are significant features for the simulation of exceedance flow control in urban areas. Additionally, backwater effects are mostly neglected in LSDM studies up to now, although it is an important feature to be modelled concerning the computation of flood routing in low lying catchments.

2.2 Review and categorisation of hydrological numerical models

A review of hydrological (numerical) catchment models is worked out with a focus on the requirements to integrate features of LSDMs and backwater effects. The findings are discussed in this section with regard to pros, cons and weaknesses in current hydrological models.

These models are used to simulate the processes in the compartments of the land-based water cycle. The processes represent for instance the proportion of precipitation contributing to infiltration, evaporation, soil water storage, overland runoff, river flow and groundwater recharge. These land-based processes of the hydrological water cycle are distinguished into four compartments as illustrated in figure 2.4.

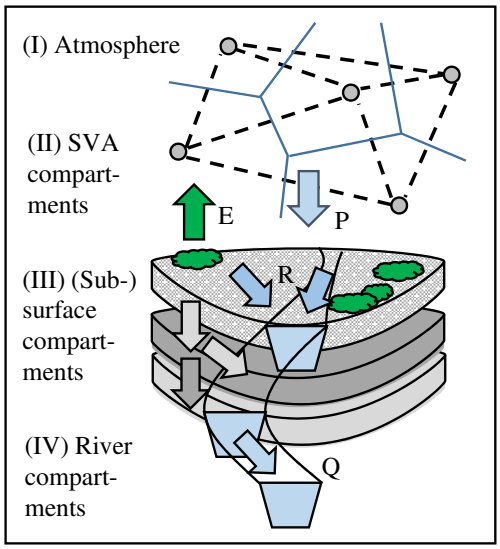

Explanation of compartments:

I. Regionalisation of meteorological data (for example precipitation = **P**) using for instance the Thiessen method.

II. Modelling the fluxes (for example evapotranspiration = **E**) and retention at the interface of the soil-vegetation-atmosphere (**SVA**) compartments.

III. Modelling the (sub-) surface runoff, interflow and baseflow which contribute to form stream flow at the basin outlet = **R**.

IV. Modelling the flood routing (**Q**) along the river compartments including reservoirs.

Figure 2.4: Scheme of hydrological processes in four main compartments as parts of a hydrological (numerical) catchment model.

Hydrological catchment models are applied for a variety of objectives, depending on the question that needs to be answered. These models are used on the one hand to represent the actual state of the catchment, but they are used as well to investigate the impacts caused by predicted changes in urbanisation or climate and the efficiency of adaptation measures. Another application purpose is flood forecasting with forecast rainfall data which is described for instance in Hingray et al. [2014]; Pechlivanidis et al. [2011] and Maniak [2016].

History of hydrological (numerical) model development. Empirical knowledge about the hydrological systems was gathered already in the ancient times, Middle Ages and Renaissance. Early mathematical and physical basics are defined at the soil-vegetation-atmosphere interface, for example, by Green & Ampt [1911] and Horton [1933]. In the field of rainfall data

processing, methods are published such as by "Thiessen" [1911]. Hydrological approaches to compute the flood routing are defined for example in the Muskingum routing approach described by McCarthy in [1938] and in the approach by Kalinin & Milyukov published in [1957]. The development of the first lumped models in the 1960s grew fast to more complex catchment models which support the simulation of manifold processes of water fluxes and flow physics as described in Donigian and Imhoff [2006]. Numerical model development is depending on the gained knowledge about hydrological processes, legislation and computer technology. Beven [2012] recognized a "survival of the fittest", meaning that new inventions in numerical modelling are driven by new knowledge or new technologies and the best fitting numerical models serving the demand are developed further. A description of the model development history based on the growing knowledge in hydrological processes, the subsequent definition of shortcomings in hydrological modelling and the optimisation of these weaknesses is given by Todini [2007].

Categorisation of hydrological numerical models. To develop, select and apply a hydrological model for a defined objective, it is important to understand the model features and to place the available features of the numerical model into a context. This is achieved by the definition of categorisation criteria and the creation of a classification scheme which facilitates a discussion and comparison of similarities or discrepancies. Comparing hydrological catchment models by using a structured classification scheme is presented for instance by Clarke [1973]; Devia et al. [2015]; Jajarmizad et al. [2012]; Kampf and Burges [2007]; Mulligan [2004]; Pechlivanidis et al. [2011]; Salvadore et al. [2015]; Vaze et al. [2012] and Zoppou [2001].

The reviewed model classification schemes illustrate prevalent types of categories which are more often applied than others. One early and distinctive review of model classification schemes is presented by Clarke [1973]. He suggests to classify models with the following main categories: empirical versus conceptual, lumped versus distributed and deterministic versus stochastic. Additional categories are defined according to the purpose of this work to discuss the suitability and limitations of hydrological catchment models for the integration of LSDM features and modelling backwater effects. The temporal representation comprises the differentiation in event- or continuous simulation models and different time scale based resolutions. The subsurface discretization classifies models into single- or multi-layered models. The different flood routing methods distinguish models into empirical, conceptual-physical or coupled hydrodynamic-numerical models.

Criteria to select an applicable model category for a specified objective comprise the issue of model uncertainty and data availability. A review about criteria and assessing the uncertainty in numerical modelling is given in attachment A.1 of this work. One important issue of model uncertainty is the lack in quality and quantity of input data in the required spatial and temporal resolution. The complexity of the model, with regard to the number of input parameters, is only suitable as far as respective detailed data is available (Perrin et al. [2001]). Otherwise, over-parametrisation caused by unsuitable data sources for parameter estimation and calibration leads to uncertainties and unreliable model results as described by Petrucci and Bonhomme

[2014]. The objective is a balance between model complexity and data availability to keep the model as simple as possible, but complex enough to explain the dynamics of the data and processes. A model structure serving these requirements is known as parsimonious model. The study results by Perrin et al. [2001] and Fenicia et al. [2008] pointed out that parsimonious models can yield more promising results, whereas complex models show more weaknesses in applications. These aspects in model selection criteria are considered as well in the following sections to discuss the pro and cons of hydrological catchment models.

Review about hydrological catchment models applied for LSDM modelling. Different hydrological and hydrodynamic-numerical models are applied and reviewed for LSDM modelling mainly on the local scale (<100 m^2), while only a few studies are available up to now on a meso scale (>10 km^2). The importance to analyse the performance of LSDMs on the meso scale and not only on the local scale is described for instance in Shuster and Rhea [2013] as well as in Li et al. [2017]. The primary developed hydrodynamic-numerical model "SWMM"[5] is used in many reviewed publications with more or less considerations of its limitations in the application (see attached list of reviews in table A.1). The numerical model "MUSIC" (namely the Model for Urban Stormwater Improvement and Conceptualizations) is a tool especially developed for LSDM modelling by eWater [2018]. It is characterised as a conceptual model for the planning phase (DPLG [2010]), but limited with regard to apply physical-based approaches. Complex fully-distributed hydrological models like MIKE SHE[6] are applicable for local scale modelling (see for example Rujner et al. [2018]), but not for LSDM studies on the meso or larger catchment scales, because of missing data resources to setup these models (see Devia et al. [2015]). An overview of these models and published reviews to model LSDMs is given in attachment A.3.

In recent application studies, various weaknesses and limitations to compute features of LSDMs with current hydrological catchment models are revealed. On the one hand, these models lack in representing local ("on-site") devices for catchment scale modelling including geographic locations and sufficient detailed spatio-temporal scales (see Ahiablame et al. [2012]; Elliott and Trowsdale [2007] and Li et al. [2017]). On the other hand, the need to account for subsurface conditions is required, but rarely resolved (see Ahiablame et al. [2012]). Further on, there is a need for applicable (namely "easy-to-use") tools in practice (see Ahiablame et al. [2012]; Elliott and Trowsdale [2007] and Li et al. [2017]). Additionally it is described, that the flood routing from source LSDMs over pathways to the catchment outlet as well as the flood routing via pathways between LSDMs are still not modelled and require further research (see Li et al. [2017]). Hence, a review of model categories is done in this work to discuss the pros, cons and weaknesses of current hydrological (numerical) catchment models. The selected model classes are summarised at the end in section 2.2.8.

[5] The model SWMM is a Stormwater Management Model, which is primary developed by the United States Environmental Protection Agency (EPA) as hydrodynamic-numerical model and accounts for hydrological processes in urban/suburban areas (see EPA [2018]) with the module “Bio-retention Cell" for LSDM modelling.

[6] MIKE SHE is a distributed detailed hydrological numerical model developed by the Danish Hydraulic Institute (DHI).

2.2.1 Review of model categories to describe hydrological processes

A widely applied categorisation differentiates between the approaches to describe the hydrological processes in an (i) empirical, (ii) physically-based or (iii) conceptual manner.

(i) Empirical approaches. Empirical approaches apply observed relations between input and output values of processes. These are labelled as well as "black-box" approaches (Pechlivanidis et al. [2011]) and are based on calibrating the relations between influx and outflux of a catchment using regressions (Vaze et al. [2012]). The Unit Hydrograph theory for event-based catchment scale simulations developed by Sherman (in 1932) is for example an empirical approach. Such an approach may reproduce the observed parameters which are used for the calibration of the numerical model in a suitable way, but limits the applicability for modelling changed conditions with regard to urbanisation or climate change impacts as described for example in Devia et al. [2015].

(ii) Physical-based approaches. Numerical models which use physical-based approaches include primary laws of physics, as far as the laws and current knowledge is applicable for numerical modelling. Most input parameters need to be derived by measurements to apply physical-based approaches. A numerical model in this category represents dimensions and characteristic in a physical-based way to describe its behaviour in details (see Hingray et al. [2014]). These models are classified as "White Box" or "mechanistic"-models (see Devia et al. [2015]; Jajarmizad et al. [2012] and Pechlivanidis et al. [2011]). A drawback of the physical-based approach is the strong reliability and dependency on the availability of spatially and temporary detailed data as argued for example by Savenije, H. H. G. [2009]. The requirement of larger computer resources, a more complex model setup and higher risk of over-parametrisation are further drawbacks of this approach when the purpose is to model meso to regional scale catchments (>100 km^2). The issue of over-parametrisation is discussed and reviewed in more detail in attachment A.2.

(iii) Conceptual approaches. Numerical models based on conceptual approaches represent the catchment conceptually by using for example, a series of cascading reservoirs (such as the Nash model). For a conceptual model the parameters are derived partly by measurements and partly by numerical adjustment (namely a calibration procedure). Models based on conceptual approaches are defined as "grey-box" or "parametric" models and are a compromise between empirical and physical-based models as stated by Devia et al. [2015]; Jajarmizad et al. [2012] and Hingray et al. [2014]. When a conceptual model uses more observed relations, it tends towards the features of an empirical model. When it comprises a larger amount of parameters to describe the physical characteristics in details, it tends towards a physical-based model.

Discussion of pros and cons of aforementioned model categories concerning the objectives of this work. The defined LSDM features (see table 2.1) affect hydrological processes of

catchments on a local scale including for instance evapotranspiration, interception, infiltration, depression losses, surface and subsurface runoff. The results of local scale studies show that the description of hydrological processes on the local scale require conceptual or physical-based approaches (see Mobilia et al. [2014]; Palla et al. [2012]; She and Pang [2010]; Sherrard and Jacobs [2012] and Vesuviano et al. [2014]). Catchment models based on empirical approaches do not fulfil the requirements to transfer the results and parametrisation to other scales. Two studies, Palla et al. [2012] and Devia et al. [2015], compared the applicability of conceptual and physical-based approaches for LSDM modelling. In Palla et al. [2012], conceptual and physical-based approaches are applied to model green roof installations on local scale and demonstrate comparable results. In the meso scale catchment study by Devia et al. [2015] the conceptual semi-distributed models (here: TOPMODEL, HBV and SWAT) showed better applicability than the physical-based fully-distributed model (here: MIKE SHE). It is concluded that conceptual (partly) physical-based approaches are more promising for meso to regional scale catchment modelling (>100 km^2), but require a revision to be applied on the respective small temporal and spatial scales.

2.2.2 Review of deterministic and stochastic model categories

Models are categorised as deterministic when the results are explicitly determined through effective input data and parameter values. In deterministic approaches, a given set of inputs will produce the same output as long as the input parameter values of the models are not changed (see Hingray et al. [2014]; Pechlivanidis et al. [2011]).

In contrast, stochastic models represent the variability of processes using probability distributions and attempt to handle some of the inherent uncertainties in numerical modelling as well as the input data. As consequence, the output is produced according to a statistical distribution and different results are given per simulation run. The differentiation of these model categories is further described and discussed by Clarke [1973]; Devia et al. [2015]; Hingray et al. [2014]; Mulligan [2004]; Pechlivanidis et al. [2011] and Zoppou [2001].

Discussion of pros and cons of these model categories. For LSDM modelling the deterministic approaches are regarded as more applicable, because of the requirement to use an effective (physical-based) parametrisation to compute the processes in LSDMs on local as well as on meso scale. One objective is to transfer the findings in parametrisation on a physical basis from one to other catchment studies. For this purpose, a stochastic approach is not applicable.

2.2.3 Review of model categories using different spatial discretizations

Depending on the manner in which the physical medium is spatially represented and in dependence on how equations are used to describe the processes, the models can be categorised as (i) lumped, (ii) distributed or (iii) semi-distributed (see figure 2.5).

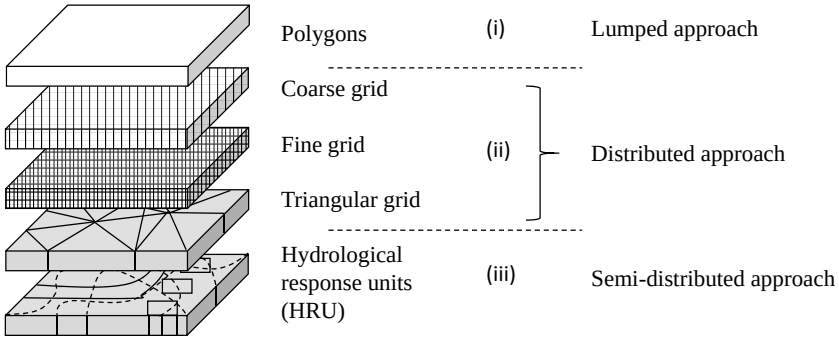

Figure 2.5: Categorisation of the spatial discretization approaches in numerical models.

(i) Lumped spatial discretization. Models which aggregate the data at the catchment scale do not take into account the spatial distribution of the input data, nor of the spatial organisation of parameters within a catchment. These models are based on lumped approaches (see Clarke [1973]; Hingray et al. [2014] and Mulligan [2004]).

(ii) Distributed spatial discretization. Models apply a distributed approach when the spatial heterogeneity of hydrological characteristics within a catchment is defined on (i) rectangular grids, (ii) TIN facets following contours or (iii) shapes on the basis of dominant hydrological features. Each grid cell is defined with hydrological characteristics. In this way, so called distributed models are created, which are capable of taking into account spatial heterogeneity in input data and boundary conditions to some extend according the resolution of the grid cells. Distributed models are a special kind of lumped models per grid cell, whereas the sub-grid processes are scaled up for each cell (Schumann [1993]). The flow paths among these cells are modelled for instance by applying the data of Digital Elevation Models (DEMs).

The disadvantage of using discretizations in the form of rectangular or TIN grid-cells is the fitting of irregular areas into a regular grid-based raster. In this manner, the information of the specific form of local scale hydrological systems is represented too roughly or a very high resolution of the cells is required. The application of such a model in urban areas depends on a small size of grid cells to represent the complex heterogeneity. For regional scale catchments (>100 km^2) with urban and larger agricultural or natural landuse areas, the required dimension of the raster varies enormously. As smaller the raster, as more data sets, computer resources and computing time is required (see Grayson and Blöschl [2001b]). The impact of fully-distributed models on using different spatial resolutions (100 m to 5 m) is analysed recently by Ichiba et al. [2018] for a 2.45 km^2 peri-urban area close to Paris using the distributed model Multi-Hydro which is developed by Ecole des Ponts ParisTech. The results illustrate the high dependency on an appropriate small spatial resolution for the application of a distributed model. It is stated that the selection of an appropriate resolution of a distributed model is comparable to a parameter calibration procedure of a grid-based approach (Ichiba et al. [2018]). A fully-distributed (physical-based) model like MIKE SHE applied by Rujner et al. [2018] on local scale of a swale with a size of about 30 m^2 or the model MultiHydro applied on neighbourhood scale of 2.45 km^2 by Ichiba et al. [2018] are not

preferred for the modelling of larger catchments (>100 km^2) because of the following four arguments: (i) the increased demand of input data coming along with a larger uncertainty in over-parametrisation as described in attachment A.1 & A.2, (ii) the complexity of the models which limits the applicability for specific research as well as engineering purposes, (iii) the difficulties in spatial scaling as described for example by Ichiba et al. [2018] and (iv) the required longer computing times which are not sufficient for (real-time) forecast application of a hydrological model.

(iii) Semi-distributed spatial discretization. The semi-distributed spatial discretization is based on shapes of dominant hydrological features (such as pedological, geologic and landuse data) in a conceptual way. It is applied early by Amerman [1965] to define "Unit-Source Areas" with a unique land use (namely defining the type of vegetation and urbanization), a single soil type (namely pedological and geological characteristics of the soils and subsoils) and as parts of the same watershed (or (sub-)catchment) with defined hydrographic characteristics.

The approach is applied later by Schumann [1993] utilizing Geographic Information Systems (GIS) to define the spatial heterogeneity of hydrological characteristics for each catchment. He defined the term "hydrologically similar unit" (HSU) to describe for each generated field element a reasonably homogeneous hydrological characteristic. In the following three decades varying further terms were created, for instance, HRU (hydrological response unit) which is applied by Bos et al. [2006]; Mulligan [2004] and Conradt [2013], REA (representative element area) used by Grayson and Blöschl [2001b], GRU (grouped response unit) applied by Kouwen et al. [1993], RHHU (Relatively Homogeneous Hydrological Unit) used by Hingray et al. [2014] or in urban areas the terms UHE (Urban Hydrological Element) by Rodriguez et al. [2008]; Salvadore et al. [2015] and UHRU (Urban Hydrological Response Unit) by Eric et al. [2013] are defined.

The common idea in models which use a semi-distributed approach, is the identification of spatial units which have a sufficient small size to represent the spatial heterogeneity of hydrological processes. These elements, for example UHEs or HRUs, represent urban blocks, buildings and surrounding areas such as cadastral parcels, single neighbourhoods or spatial objects (see Salvadore et al. [2015]).

When a model defines the flow paths among each "neighbouring" element with the information of an DEM, the model tends to be a spatial distributed model. This is the case for the models which utilise UHEs and UHREs which are applied for small scale urban study areas (<10 km^2) (see Eric et al. [2013]; Rodriguez et al. [2008]; Salvadore et al. [2015]). The disadvantages of distributed models, namely uncertainty in over-parametrisation and larger required computational resources, apply likewise. But in comparison to TIN or rectangular grid-based rasters, the spatial discretized input parameters are variable concerning the spatial resolution and shapes in the hydrological model. The semi-distributed approach is more flexible in using for instance, a rough spatial resolution for larger homogeneous natural areas than for urban areas where a higher heterogeneity is present. To reduce the required computing time and the parametrisation within watersheds, the HRUs with identical values

of their state variables are spatially aggregated per watershed. In that way, the number of the overall HRUs and hence the required computational costs of a simulation run are reduced. But on the same time, this posses a disadvantage because the generated smallest fields (here: HRUs) are laterally disconnected from each other. The geographical referencing of HRUs and the modelling of flood routing among HRUs is not supported in such a spatial semi-distributed discretization approach.

Discussion of pros and cons of these model categories. It is concluded, that the semi-distributed model approach points out more advantages concerning the objective to integrate the modelling of LSDMs in regional scale catchments (>100 km^2). In contrast to fully-distributed models, the benefits of semi-distributed approaches are a smaller demand of data processing, smaller computational costs and a more applicable parametrisation for large scale modelling purposes. The semi-distributed approach to model LSDMs is presented previously by Aryal et al. [2016]; Eric et al. [2013]; Krebs [2016]; Palla and Gnecco [2015]; Scherer et al. [2018]; Versini, Jouve, et al. [2014]; Versini et al. [2015] using the model SWMM and by Gagrani et al. [2014]; Hamel and Fletcher [2013] using the model MUSIC. But there are still significant weaknesses in semi-distributed models which need to be resolved. For instance, modelling the lateral dependency between LSDMs and a spatial organisation within the (sub-)catchments is required, but not supported yet in current semi-distributed model approaches for large scale modelling.

2.2.4 Review of model categories using different temporal resolutions

Models are differentiated according to applied time step sizes in the simulation runs, such as sub-hourly, sub-daily, daily, monthly and yearly time step sizes. The choice of this temporal resolution of a model depends on its intended use and the available input data. Salvadore et al. [2015] studied 43 hydrological and partly hydrodynamic-numerical models with respect to the used time step sizes. They concluded that most models use a time step size of 1 hour (25 % of the models) or 1 day (20 % of the models). He determined a dependency between catchment model studies smaller than 10 km^2 having a temporal resolution smaller or equal to 6 minutes, while for catchment studies larger than 10 km^2 the temporal resolution varies between 1 hour to 1 day. These time step sizes are not sufficient for modelling the fast processes of water fluxes in LSDMs with respond times less than 1 minute. The demand for small scale time step processing in LSDM modelling is stated by Elliott and Trowsdale [2007] and McAlister et al. [2006] while the demand for dynamical time step processing is stated by Kraft [2012] (p. 63) and recently by Leistert et al. [2018]. The response time of runoff and hydrological processes in LSDMs is likely in a range of minutes or even less (McAlister et al. [2006]).

A differentiation between event and continuous process driven models is described by Zoppou [2001], and reviewed in more detail later by Elliott and Trowsdale [2007]; Hingray et al. [2014]; Pechlivanidis et al. [2011] and Salvadore et al. [2015]. Event-based models are applied for shortterm simulations comprising one individual or a short series of storm events of some days. Continuous models simulate a catchment's overall water balance over long

periods of time (namely several years). In continuous longterm models the computation of antecedent moisture conditions before a storm event is implicated, but for event or design storm simulations this information is not included. In that case, the antecedent moisture conditions is computed by statistics or for instance with the principle of the "Antecedent Precipitation Index" as described in Hingray et al. [2014].

Discussion of pros and cons of the model categories. For LSDM modelling a small temporal resolution of time step sizes (<1 minute) is required, but not available yet in meso to regional scale modelling (>100 km^2). This limitation in a required high temporal resolution is tackled in this work by enabling a flexible time step size in hydrological catchment models. Further on, it is concluded that the simulation of antecedent moisture conditions is required and best done with a continuous longterm simulation of water balances. Nevertheless, event based model approaches show benefits to reduce computing times and modelling processes with small temporal time step sizes. Therefore, a coupled approach using event based simulation runs which are embraced by a continuous longterm simulation run is suggested in this work.

2.2.5 Review of approaches to discretise the sub-surface

The vertical sub-surface discretization is differentiated between a lumped or distributed approach for modelling multi-layered structures. The required discretization in the sub-surface depends on the processes which need to be modelled with the hydrological catchment model. A lumped single-layer approach is not sufficient for modelling different lateral sub-surface processes such as drainage through perforated pipes, interflow, baseflow and groundwater flow.

The sub-surface discretization is an important issue for modelling hydrological processes in LSDMs and catchments. In dependence on the pedology and geology, the subsurface flow processes (namely interflow and baseflow) contribute to the low flow conditions in streams. Wet antecedent low flow in the streams contributes to generate higher peak and volume flow rates during storm events as shown for instance by Tromp-van Meerveld and McDonnell [2006]. When the interflow is drained through soils with high hydraulic conductivity, it may contribute directly on the flood hydrograph and leads to a fast rise in peak flow (Tromp-van Meerveld and McDonnell [2006]). The impact of LSDMs on the baseflow and the flow in multi-layered structures in urban catchments requires further research as stated in Hamel and Fletcher [2013].

Summary of current limitations to model multi-layered LSDMs. Limitations exist in current hydrological catchment models to simulate LSDMs with multiple and interlinked layered structures taking into account exceedance and backed up water flow among layers. These limitations are tackled in this work to be resolved.

2.2.6 Review of approaches to model the flood routing in streams and areas

Flood routing describes the processes of translation and retention of a flood wave moving along a stream in downstream direction. Different flood routing approaches are available and classified here into: (i) pure black box (namely empirical, lumped), (ii) hydrological conceptual and physical-based or (iii) hydrodynamic-numerical approaches as described in Hingray et al. [2014] and Maniak [2016]. The applicable flood routing method needs to be chosen with respect to the modelling purpose and the available data. Detailed flood routing simulations for streams are solved by computations using hydrodynamic-numerical models. The numerical integration of the partial differential equations describing the flood routing processes in complex profiles as well as flood prone areas demands for 2D or 3D hydrodynamic-numerical simulations. A requirement for hydrodynamic-numerical modelling is a high resolution of data describing the topography of the main channel and the natural flood plain in the case of bank overflow. Hence, the availability of suitable detailed profile data from measurements is significant for hydrodynamic-numerical modelling. The comparatively long computing time for hydrodynamic-numerical model simulation runs is no limitation for answering special research questions, but it poses a limitation in real-time operational application of the model and for meso to regional scale catchment modelling.

For hydrological numerical modelling of regional catchments (>100 km^2) alternative approaches are required. Hydrologists developed and proposed conceptual approaches, such as the so called "storage routing" by Puls (1928), "Muskingum routing" described by McCarthy in (1938), "Kalinin and Miljukov routing" (1958) or "linear reservoir and channel cascade routing" presented by Maddaus in (1969) (see Todini [1991]). In hydrological catchment modelling it is still not considered as feasible to integrate a detailed description of sewers or drainage networks for meso to regional scale modelling (Salvadore et al. [2015] (p. 72). This differs from the urban hydrodynamic-numerical modelling concepts. For hydrological approaches conceptual or empirical parameters are calibrated based on observed events like in the widely used Muskingum method. A compromise are hydrological methods using profile data of stream reaches to apply basic hydrodynamical approaches, for example in the "Muskingum-Cunge" (see Cunge [1969]) as well as the Kalinin and Milyukov [1957] approach. These concepts use profile data in a conceptual way and require shorter computing times for meso scale modelling. The purpose of hydrological flood routing approaches is to compute the discharge hydrographs in the considered stream segments. The computation of flow depths, velocities and backwater effects in the streams as well as on the forelands are not modelled with hydrological approaches yet.

Discussion of pros, cons and weaknesses of current flood routing approaches. Empirical hydrological flood routing approaches do not enable a transfer of determined parameters in a physical-based way to other catchments and is therefore not applicable in this work. Applying a hydrodynamic-numerical model coupled with a hydrological model shows disadvantages in the application on meso to regional catchment scales (>100 km^2) and for operational model applications. Most promising to accomplish the objectives of this work is the extension of

a hydrological conceptual (partly physical-based) approach, which is directly implemented in a hydrological numerical model. As described above, the state-of-the-art hydrological approaches (for instance Muskingum-Cunge or Kalinin-Milyukov) do not compute water levels or backwater effects. For flood routing computation in low lying lands new hydrological approaches are required to resolve this limitation.

2.2.7 Review of the required parametrisation and computation resources

The complexity of the parametrisation and the required computational resources of a numerical model are important features for application purposes. The complexity of a parametrisation shows the strengths and weaknesses of a model concerning the applicability and reliability to resolve specific questions. The required computation resources comprise several aspects with respect to computing time, the number of calculation routines or functions to solve a calculation and the required memory space for the execution of the computation. The demand for applicable models with short computing times for the performance evaluation of LSDMs in flood forecasting systems increases (see Locatelli et al. [2014] and Webber et al. [2018]). An overview of existing real-time flood forecasting systems in urban areas of France, Bangkok, Denmark and Spain demonstrate the demand of such models as described in Henonin et al. [2013].

A differentiation of the parametrisation between simple, parsimonious and complex data models is described in Vaze et al. [2012] using the following modified criteria. An empirical model using one to five parameters and having a low risk of over-parametrisation is defined as a simple model. A conceptual (partly physical-based) model with a number of input parameters below 100 and having a moderate risk of over-parametrisation is defined as a parsimonious model. A fully-distributed physically-based model with up to 1000 parameters is defined as a complex model with a higher risk of over-parametrisation.

The objective is to balance the level of complexity used for the different representations or components of a model and the level of details of available data. A way to reduce the number of parameters, is the differentiation between local and meso scale parameters to describe a (sub-)catchment. The designation of a parameter to be defined on the local scale (for instance per HRU) or on the meso scale (per catchment) is an important decision for the model structure. According to Fenicia et al. [2016] this discussion requires a balancing between parsimony in parameters and a sufficient level of details to represent the spatial heterogeneity.

Concluding aspects. To reach the objectives of this work, it is required to find a balance between a parsimonious parametrisation, small computational costs and reliable methods for the simulation of processes on the small spatio-temporal resolutions of LSDMs within meso scale catchments.

2.2.8 Summary of required model categories

In this section, the previously explained pros and cons of hydrological numerical model categories are summarised to point out selected ones according to classification criteria. There exists a tendency that models which use a specific category of the description of processes are combined with a distinct category of the spatial discretization. For example, empirical models often use spatially lumped approaches, conceptual models tend to apply semi-distributed approaches and physical-based models tend to utilize fully-distributed approaches (see Mulligan [2004]). A widely-used combination of model categories is a conceptual, semi-distributed and deterministic model. In Germany the models NASIM (Hydrotec [2018]) and KalypsoHydrology (BCE [2018]), in the USA the models SWMM (EPA [2018]) and SWAT (Soil & Water Assessment Tool; USDA [2018]) and in Sweden the model HBV developed by the Swedish Meteorological and Hydrological Institute (Bergström [1992]) correspond with this category.

The classification criteria of model categories, which have been discussed in the previous sections, are itemised from (a) to (g) in table 2.2. Applicable model categories to accomplish the objectives of this work are selected from the above-mentioned discussions and marked in grey colour. Among these categories the differentiation can be contradictory (indicated with "↔") or combinable (indicated with "↔/&").

Table 2.2: Overview and selection of model categories to be applied in this work.

Classification criteria	List of reviewed model categories		
(a) Description of hydrological processes	Empirical	↔ / &	Physical
		Conceptual	
(b) Relation between the variables	Stochastic	↔	Deterministic
(c) Spatial discretization	Lumped	↔	Distributed
		semi-distributed	
(d) Temporal representation	Event based	↔ / &	Continious based
	small scale (Δt < 1h)	↔ / &	Large scale (Δt > 1d)
(e) Sub-surface discretization	Single layered	↔	Multiple layered
(f) Flood routing approach	Empirical approach	↔	Coupled hydro-dynamic-numerical models
		Hydrological conceptual or physical-based approach	
(g) Model complexity	Simple	↔	Complex
		Parsimonious	

Note: selected model categories are marked in ▭ . Model categories have contrary (" ↔ ") or combinable (" ↔ / &") attributes. Δt is the time step size for simulations.

According to these selected model categories, the required model is characterised as a combined conceptual physical-based deterministic model (a/b) with a semi-distributed spatial discretization (c), a flexible temporal resolution and coupled continuous simulation approach (d). The model requires to compute multi-layered structures (e), a hydrological conceptual or

physical-based flood routing approach (f) and a parsimonious parametrisation in the model structure (g). The limitations and weaknesses in these categories to model LSDMs and backwater effects are summarised in the following section.

2.3 Summary of current limitations and weaknesses to model LSDMs and backwater effects

The reviewed model categories and required modelling features are listed in a matrix to define the main limitations and weaknesses in modelling LSDMs as well as backwater effects with current hydrological catchment models. The matrix in table 2.3 intersects the list of required features to model LSDMs (from table 2.1) with the list of the defined model categories (from table 2.2). The required features to be modelled, from (1) to (10), are listed in the left column. These features for modelling LSDMs in backwater affected catchments are ordered in three groups. First, the aspects of resolution as well as applicability, secondly the aspects of hydrological processes as well as LSDM technologies and thirdly, the aspects of flood routing issues are pointed out. The model categories, from (a) to (g), are itemised in the top row. The black points indicate limitations and weaknesses in the defined model categories which require revisions. In the following paragraphs these points are explained in the order of required features from (1) to (10). White spaces indicate that the feature does not overlap with the model category and no revision is necessary.

Required features (1) to (4) in table 2.3 to resolve limitations in the spatio-temporal resolution and applicability. To model the exceedance flow control among different interlinked LSDMs, it is required to represent the geographical location, flow path length and topography. These local scale parameters are not available in meso scale (semi-distributed) hydrological catchment models up to now and new methods to compute the flood routing on the meso scale are required. The location of LSDMs within a (sub-)catchment has an impact on the overall runoff concentration at the outlet in the receiving stream. This issue is mentioned also by Versini et al. [2016], but not studied in detail yet. The direct (unretained) surface runoff from locations which are further away from the target (sink) element, superimpose with retained surface runoff closer to the outlet and may lead to a higher peak flow of the hydrograph at the outlet. The spatial resolution and the possibility to set the geographical location in semi-distributed models require a revision of calculation routines and are marked as weak points in table 2.3. This includes, in addition, the need to revise the flood routing computation among LSDMs and to accomplish at the same time an applicable parametrisation.

Further on, the integration of LSDM features into hydrological catchment modelling requires a revision of the temporal resolution to be more flexible. The demand for more flexible temporal resolutions in hydrological catchment modelling is discussed as well in Obled et al. [2009]; Ostrowski et al. [2010] and Salvadore et al. [2015]. For modelling hydrological processes in LSDMs a temporal scale of seconds is required, while a temporal scale of five minutes is considered to be sufficient to model the processes on the meso scale catchment. A flexible

Table 2.3: Matrix of weak points to model LSDM features (1 to 9) and backwater effects (10) in the determined hydrological model categories (a) to (g).

	Required features to be modelled		(a) Defined model categories	(b) Conceptual - physical based methods	(c) Deterministic methods	(d) Semi-distributed discretization	(e) Flexible temporal resolution	(f) Flexible multiple layered discretization	(g) Hydrological flood routing method / Parsimonious parametrisation
Resolution and application	Spatial local scale resolution (<1m²) and geographical organisation.	(1)			●			●	●
	Temporal small scale resolution (< 1 minute).	(2)				●			●
	Applicability for spatio-temporal meso scale modelling.	(3)	●	●	●	●			●
	Short computing times.	(4)			●	●			●
Hydrological processes and LSDM technologies	Modelling LSDM features with an applicable parametrisation.	(5)	●	●	●	●	●	●	●
	Modelling multiple and interlinked layered structures.	(6)					●		●
	Modelling rainwater harvesting functions.	(7)	●	●			●		●
	Modelling control features in areas (a) and streams (b).	(8)	●	●			●		●
Flood routing	Modelling the flood routing among LSDMs.	(9)	●	●	●			●	●
	Modelling backwater effects in streams, areas and LSDMs.	(10)	●	●	●	●	●	●	●

● = points indicate limitations and weaknesses in the determined model categories to compute processes in LSDMs and backwater effects.

differentiation (namely a dynamic time step size) within the numerical model structure is not available yet in hydrological catchment models. Additionally, antecedent moisture conditions need to be provided for detailed simulations. Therefore, an approach to embrace shortterm event based simulations with a longterm continuous water balance computation is required. These limitations are tackled in this work.

Reaching a balance between model structure details (namely complexity) and data availability is an important issue to keep the model as parsimonious as possible, but complex enough to explain the heterogeneity in the areas and the dynamics in the hydrological processes. The objective is a parsimonious parametrisation as described in section 2.2.7. For that purpose, it is required to revise the methods in calculation routines, spatial discretizations and parametrisations of meso scale catchment models.

Especially in urban areas with response times below one hour, a short lead time in forecast models is required (see WMO [2011] and Jasper-Tönnies et al. [2018]). The computing time is an important issue in real-time forecasting and for modelling control features. Computing times of a few minutes shall not be exceeded per simulation run which cover several days for regional catchments (>100 km^2). This work aims to resolve these weak points with respect to accomplish a high spatio-temporal resolution, while enabling a parsimonious parametrisation and keeping the computing time short for operational application.

Missing features in (5) to resolve limitations in parametrisation to model hydrological processes in LSDMs. The gathered knowledge by field monitoring and laboratory studies regarding infiltration, evaporation, drainage and retention processes in LSDMs are rarely integrated in the parametrisation of current hydrological catchment models yet.

The approach to define an outlet in a (virtual) storage tank to simulate the infiltration into the underground without taking into account the parametrisation of the subsurface, is insufficient from a modellers point of view. But this is the practice for example in the models SWMM and MIKE Urban[7] (see Elliott and Trowsdale [2007]). The infiltration in the mostly very permeable material requires a revision of modelling approaches. The drainage layer structures with prolonged flow paths or retention techniques are not considered with physical-based parameters yet. For the application of a calibrated model to changed conditions (for example to model changes in urbanisation, climate or LSDM structures) it is required to define a physical-based parametrisation. Another limitation exists in hydrological catchment models when neglecting the computation of open water evaporation from streams or submerged flood prone areas. These weak points in parametrisation of hydrological processes and methods are tackled in this work and are marked in table 2.3 row (5). The points affect all categories of the meso scale hydrological model.

Needed features in (6) to resolve weaknesses in modelling multiple and interlinked layered structures. A discretization of numerical models in multiple layers is required for simulating the drainage and retention processes in LSDMs as shown in the local scale studies by Locatelli et al. [2014] and Stovin et al. [2015]. The significance of longterm low flow (namely inter- and baseflow) modelling in multiple layers is stated by Hamel and Fletcher [2013]. The superposition of these low flows with the surface flow processes is especially important when the meso scale catchment is characterised by a larger diversity of natural, rural and urban areas. It has been examined in the project KLEE (see KLEE Verbund [2016]) that the implementation of green roofs and swales in small urban areas with mostly rural surroundings and larger interflow proportions may even increase the peak flow in river reaches. The storm water from roofs and parking places drains directly to the receiving river reaches after the event. By implementing LSDMs the infiltrated water increases the fraction of interflow and the retained flow of green roofs is superimposed with the larger flow fraction from rural natural areas.

Another aspect is the missing computation of the flow among interlinked layers in the

[7] MIKE URBAN is a one-dimensional hydrodynamic-numerical model by the Danish Hydraulic Institute (DHI).

reviewed hydrological catchment models (see section 2.1.3). These limitations in modelling the processes among multiple interlinked layered structures are solved in this work, while a parsimonious parametrisation is pursued.

Demanded features in (7) to resolve limitations in modelling rainwater harvesting functions. The demand to revise the modelling of rainwater harvesting functions is described recently in Li et al. [2017]. The water demand for rainwater harvesting techniques is estimated currently as an average based on the storage capacity of LSDMs (see for example in M. Burns et al. [2010]). In this manner, the variability in user behaviour per season and weekday is ignored. For a detailed simulation of rainwater harvesting functions, a parametrisation with a weekday differentiation is required. This is missing in the reviewed hydrological catchment models up to now. The computational methods, temporal resolutions and parametrisations in hydrological catchment models need to be revised to model rainwater harvesting functions in a detailed way.

Required features in (8) to resolve weaknesses in modelling control features. Control features (namely real-time control functions) are implemented in hydrodynamic-numerical models for urban drainage purposes (see García et al. [2015] and M. Schütze et al. [2016]), but only few hydrological (numerical) catchment models compute any control features. Simplified functions in hydrological models are applied to compute the performance of larger retention, detention basins or for hydro dams. Using the features of real-time control for modelling LSDMs (namely cisterns, multifunctional areas or retention roofs) with a link to weather forecast and rainwater harvesting functions is an open task as stated for example in Jayasooriya and Ng [2014]. This weak point in the features of hydrological models is tackled in this work and requires extensions in the current computational approaches as well as the parametrisation.

Needed features in (9) to resolve weaknesses in modelling exceedance and run-on flood routing among interlinked LSDMs. Exceedance and run-on flood routing are important features when modelling the performance of LSDMs in meso to regional scale catchments. The run-on flood routing is the reverse process to runoff from a system. It is the feature of LSDMs to receive water from linked LSDMs or other sources. In the CIRIA[8] Manuals (see Digman et al. [2012] and Woods Ballard et al. [2015] (p. 538)) the importance of linking LSDMs (namely "SUDSs") is expressed to be significant for exceedance flow control, so that flows can reach a destination by a connection or a cascade of measures to prevent uncontrolled flooding. Although this issue is known, details about the coupling or combination of measures are missing up to now. In Palmaricciotti et al. [2012], the theoretical approach of the connection of different LSDMs for exceedance flow control are illustrated. The decision frameworks by Alves et al. [2016] and Chow et al. [2014] support to choose whether LSDMs may show benefits in flood mitigation purposes, but the computation of the performance of linked cascades of LSDMs

[8]CIRIA = Construction Industry Research and Information Association in the United Kingdom.

are not discussed or modelled yet in detail with hydrological approaches on meso scales. As reviewed in Hellmers and Fröhle [2017], modelling the flood control among interlinked measures is still missing in current semi-distributed hydrological catchment models. When LSDMs are defined as fraction of subcatchments (like in SWMM as described in Rossman [2015]; p. 244 ff.), the flood routing among LSDMs is computed with the same parameters as defined for the (sub-)catchment on the meso scale. The geographical location and spatial order of LSDMs are not parametrised within the catchment. It is an open task to develop a hydrological approach to model the flood routing among LSDMs in a more detailed way for regional scale catchment modelling (>100 km^2).

Missing features in (10) to resolve limitations in modelling backwater effects in streams and LSDMs. Current hydrological flood routing approaches neglect the computation of backwater effects in lower reaches or low lying lands of the catchments as discussed in section 2.2.6. In hydrodynamic-numerical models like the aforementioned MIKE Urban and SWMM approaches, such as the dynamic-wave routing, are activated for modelling backwater effects in streams. But these hydrodynamical flood routing approaches are less suitable for regional scale catchment modelling (>100 km^2) because of the required parametrisation and large computational resources.

Only for district scale study areas (<1 km^2) these models are applied until now as presented for example by Yau et al. [2017]. In that presented study area, the hydrodynamical approaches of the model SWMM are applied for a case study in Singapore with a size smaller than 0.1 km^2 to model backwater effects and reverse flow in the examples of perforated pipes, orifice outlets of rain gardens and gravel swales. Coupled models like the aforementioned MIKE SHE coupled with MIKE Urban are available, but hold shortcomings in the applicability on meso to regional scales (>100 km^2) because of required large computing times and the complexity in parametrisation to setup such a large scale model.

For the hydrological catchment model NASIM (Hydrotec [2018]) a second executable NASIM HDR ("NASIM-Hydrodynamisch") has been recently reported to compute backwater effects (Dorp et al. [2017]). It is based on a one-dimensional hydrodynamical approach using the diffuse wave approximation. These hydrodynamic-numerical approaches compute backwater effects in linear stream elements (rivers, ditches or pipes), but the flood routing from a stream element into LSDMs or flood prone areas is not supported by these approaches. Subsequent evaporation of backed-up water from flood prone areas and LSDMs is neglected up to now in these hydrodynamical flood routing models.

Two related studies are reviewed for Northern Germany using approaches based on the linear storage cascade theory to model backwater effects. In the first study by Messal [2000], the hypodermic backwater flow among river streams and the subsurface flow in the river banks is computed. The second approach by Riedel [2004] models backwater effects among river streams by defining preset downstream boundary conditions. The methods are based on conceptual approaches neglecting backwater effects from stream elements into LSDMs or flood prone areas.

The model "ArcEGMO" takes into account backwater effects by hindering the downstream routing when the water level at the downstream section is larger than the upstream one (Pfützner [2018]). This method calculates a retained flow, but neither computes the flood routing in reversed flow direction nor the backwater flooding of adjacent areas.

It is concluded that previously published methods rarely enable the modelling of backwater effects in streams and areas with an applicable hydrological approach on meso to regional scale catchments. Methods for the computation of backwater affected processes in LSDMs or subsequent hydrological processes on flood prone areas are missing. These weak points in modelling backwater effects in streams and LSDMs with hydrological numerical catchment models are tackled in this work.

3. Objectives and theoretical approaches to model LSDMs and backwater effects

The literature review in the previous chapter revealed specific limitations and weaknesses in state-of-the-art hydrological numerical catchment models to simulate the processes in LSDMs and backwater effects. These shortcomings comprise insufficient small spatio-temporal resolutions, missing parametrisations for computing hydrological processes in LSDMs, lacking approaches to simulate control features, unavailable methods to model multiple and interlinked layered structures, needed approaches to calculate the exceedance as well as run-on flood routing among LSDMs and missing hydrological methods to model backwater effects in streams as well as areas. Additional demands on the hydrological model are a parsimonious parametrisation to model LSDMs on the meso scale and with short computing times for the application of the model in operational forecast systems.

To resolve these limitations and weaknesses of hydrological numerical models, a scope of work including theoretical approaches is described in this chapter. The scope of work is defined according to the SMART-principle[1] to determine specific objectives which are measurable, applicable, relevant and in-time achievable.

The objectives and theoretical approaches are described in this chapter with a focus on four main aspects. First, the approaches to improve the spatio-temporal resolution and network generation are explained in section 3.1. Thereafter, approaches to model the hydrological processes in LSDMs are determined in section 3.2. Further on, theoretical approaches to model LSDM technologies are given in section 3.3. In the last section 3.4, theoretical approaches to develop a flood routing method comprising the computation of backwater effects in streams and areas are described.

Each section begins with an explanation of the Specific objectives and the resolved part in the scope of this work according to the SMART-principle in the form of tables. Five Measurable evaluation parameters are determined to verify and validate the developed methods to be

[1] An early publication of the SMART-principle is given by Doran [1981], who defined the acronym for project objectives which are specific, measurable, assignable, realistic and time-related. An adapted version of that principle is applied in this work with a focus on the applicability and relevance of required features for numerical model development.

reliable, parsimonious and sensitive with respect to the application purposes of this work.

(i) The numerical model results are validated by comparing them with observed measurements from laboratory and gauge stations in meso scale catchments in nature.

(ii) The numerical model results are verified by checking the mass-conservation between input and output parameters in water balance processes and fluxes.

(iii) The functional correctness in the execution of the methods is verified by testing among others, the correctness in data processing.

(iv) Sensitivity studies are performed by varying the values for the input parameters of the structures and boundary conditions in the models of application studies.

(v) The computing times are tested to be reasonable short and the number of input parameters are checked to be in an applicable parsimonious range. The execution of the implemented local scale methods shall not increase significantly the computing times of (current) meso scale hydrological catchment models.

The sequence of sections are in accordance with the defined order from (1) to (10) of the required features to accomplish the Application of a hydrological numerical model to simulate LSDMs and backwater effects (see table 2.1; page 14). Furthermore, these features are Relevant to resolve open tasks in the development of meso scale hydrological catchment models. Such tasks are described in the literature review by using an alphabetical enumeration from (a) to (g) (see tables 2.2 and 2.3, page 26 ff.). An in-Time achievement of the objectives depends first on the successful development as well as implementation of methods in a hydrological numerical catchment model. Secondly, it depends on the availability of sufficient detailed data as well as measurements to setup application studies for the evaluation of the developed model.

3.1 Approaches to revise the spatio-temporal resolutions in hydrological numerical modelling

The algorithms[2] in hydrological numerical models are based on specified spatio-temporal scales. These currently supported scales need to be extended to integrate calculation routines for modelling processes in LSDMs and backwater effects. This part of the scope of work according to the SMART-principle is outlined in table 3.1. The specific objectives are defined and listed in the first column. The development of methods comprises a GIS-based local data mapping, a dynamic time step calculation routine, an explicit network generation and enabling short computing times as well as a parsimonious data structure for the application of the numerical model. A measurable evaluation of the model is done by testing the mass-conservation, functional correctness and computing time in application studies. An execution time shorter than 5 minutes for a 10 day simulation run of a regional scale catchment (>100 km^2) shall not be exceeded. The specific objectives resolve the demands for the

[2] An algorithm is a structured workflow of calculation routines or functions to resolve a problem (see Levi and Rembold [2003]).

application of the model to compute LSDM features which are listed in the third column in table 3.1. To realise these objectives, a revision of the meso scale hydrological model is relevant and required with regard to the spatial discretization, flexible temporal resolution and the data structure to provide a parsimonious model (see column four in table 3.1). To realise the objectives in-time, a revision of the calculation routines in the source code of an appropriate numerical model and the availability of parameter values for application studies are required.

Table 3.1: Scope of work to resolve limitations in modelling the spatio-temporal resolution, applicability and structure of algorithms in hydrological catchment models. (The enumeration is explained in footnote[3].)

Specific objectives	Measurable evaluation parameters	Applicability for LSDM modelling	Relevant revisions of current hydrological models	In-Time effort for the implementation and model tests
GIS-based local data mapping in meso scale catchments.	Verification of spatial consistency in areas (ii).	(1) High spatial resolution and geographical location.	Revision of the spatial discretization (c,f,g).	Revision of the source code of an applicable numerical model and availability of parameter values for local as well as meso scale studies.
Flexible nested time step intervals.	Verification of functional correctness (iii).	(2) High temporal resolution.	Enabling a flexible temporal resolution (d,g).	
Explicit network generation and data mapping.		(3) Flexible data processing in meso scale networks.	Revision of the spatial order and network structure of elements (a - d, g).	
Short computing times and parsimonious parametrisation.	Testing the computing time and the number of parameters (v).	(4) Short computing times.	Revision of the structure of calculation routines (c,d,g).	

The methodology to realise these objectives is described in chapter 4.

The objectives and theoretical approaches to revise the GIS-based data mapping, the spatio-temporal scaling, enabling an explicit network generation and to revise the structure of algorithms in hydrological catchment models are described in the following sections 3.1.1 to 3.1.3. The methodology to realise these objectives is described in chapter 4.

3.1.1 Approach to define a flexible spatio-temporal scaling

Hydrological processes occur over a wide range of spatial scales from unsaturated flow in a $1\,m^2$ wide soil profile to floods in river systems of a million square kilometres. This range

[3]The SMART-principle and measurable evaluation parameters (i) to (v) are described on page 33 ff. The weaknesses in the applicability of the current numerical models to compute the features of LSDMs and backwater effects are numbered from (1) to (10) and explained in table 2.1 (see page 14). The relevant and required revisions of model categories are labelled with (a) to (g) and are described in table 2.3 (see page 28).

distinguishes the heterogeneity in space. The temporal scales range from surface runoff processes which occur within a duration of a few minutes to flow processes in regional scale aquifers which are effective over hundreds of years. This range differentiates the variability in time. The spatial and temporal scales need to be appropriate to simulate the hydrological processes on local as well as on meso scales. Scaling and mapping are techniques to transfer data from one sized (namely scaled) data source to another scale using functions like down- or upscaling of data (see Paniconi and Putti [2015]). The term 'scale' refers to a specific or characteristic time or spatial proportion (see Blöschl and Sivapalan [1995]; Grayson and Blöschl [2001a] and Gleeson and Paszkowski [2013]). For the purpose to integrate LSDM features in meso scale catchment modelling, it is required to define the critical scales in spatial heterogeneity and temporal variability. A critical scale is defined as the spatial unit or time at which sufficient information is available and an effective parametrisation is realised to represent the processes (see Gentine et al. [2012]).

In the research field of hydrology, different perceptions of the scale terms exist. A definition of the terminology to describe the different scales is analysed by Gleeson and Paszkowski [2013]. For example, it is concluded that the terms "small", "site" and "local" scale are compatible, but the term "local" scale is recognised as more specific in practice of hydrology than "small" or "site" scale. The definitions of spatial and temporal scales used in this work are depicted in figure 3.1.

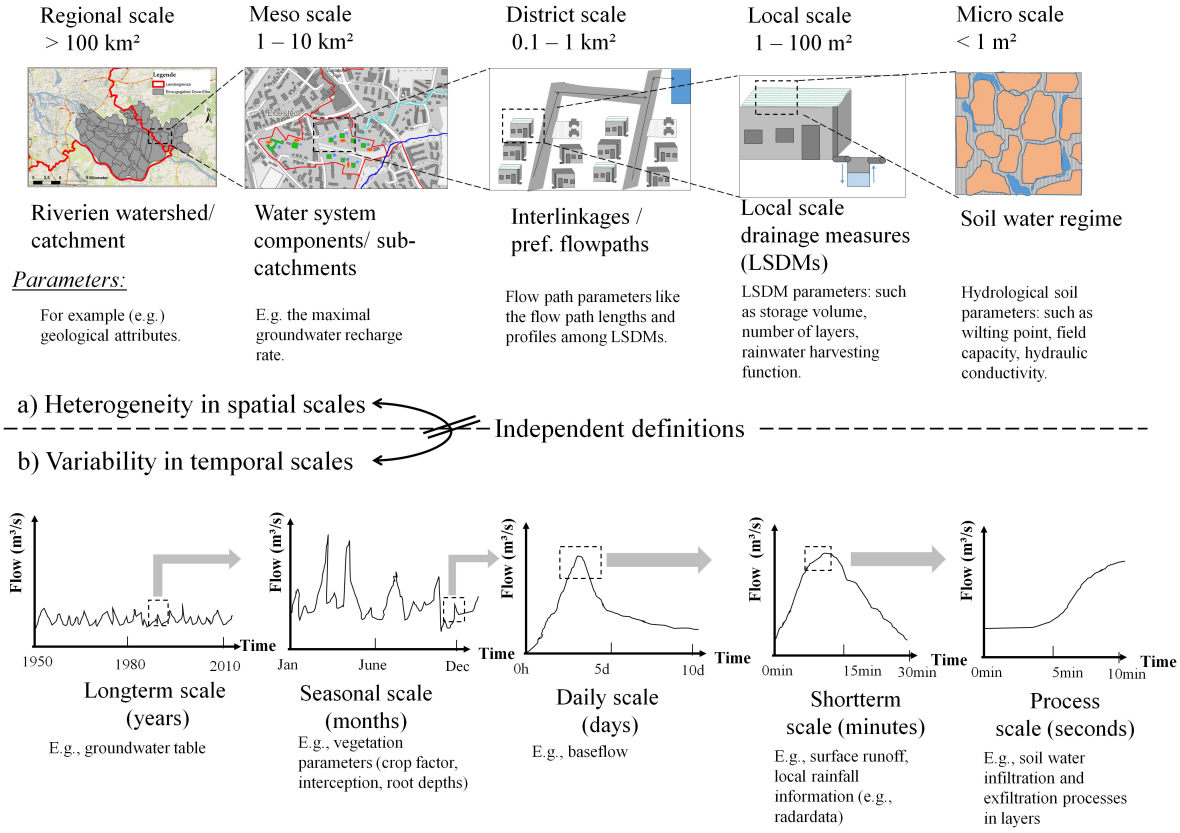

Figure 3.1: Differentiation between (a) the heterogeneity in spatial and (b) the variability in temporal scales (modified from Hellmers and Fröhle [2017]).

The catchment boundary of a riverine watershed is defined on the regional scale and can have a size larger than 100 km^2. The watershed components within the catchment (for instance the drainage systems) are defined on a meso scale (1 km^2 to 10 km^2) in "subcatchments". On the district scale, ranging for instance from 0.1 km^2 to 1 km^2, the flow paths among LSDMs are defined. On the local scale the flow and retention processes of drainage measures (such as in LSDMs) are modelled. These drainage measures have a size between 1 m^2 to about 100 m^2. A spatial micro scale is defined to model processes on a small size within multiple layers (<1 m^2) like the soil water regime and processes in vegetation. Spatial and temporal scales are independently defined. Temporal scales range from the analysis of rapid events like after local heavy rainfall events in less than an hour to seasonal impacts within 1 year to long term effects over 50 to 100 years. Hydrological processes, like the infiltration and exfiltration processes in porous material, are determined in even smaller temporal scales of seconds.

The smaller the spatial and temporal scales are defined, the more detailed input data is required in most application studies. Therefore, a model with a detailed spatio-temporal resolution in the required scales is often defined with a more complex data structure and the number of parameters is large (for example >100) to describe the hydrological system for regional catchments (>100 km^2). Parametrisation aims to define an adequate set of parameters to specify the system being modelled on the basis of measurable and non-measurable parameters. Thereby, non-measurable parameters induce a calibration procedure to obtain a model which simulates observed hydrological behaviour. With an increased number of non-measurable parameters, the model is calibrated on the basis of relatively few measurable information. Consequently, processes may remain undefined and the developed model may show insufficient predictive capabilities to model hydrological processes. One way to deal with this phenomenon is the definition of a moderate and flexible spatial distribution of parameters, which requires a data processing on multi-scales as presented for instance in Samaniego et al. [2010] and Zhang et al. [2013]. The objective is to model catchments with an adjustable spatial and temporal resolution of parameters within one model algorithm.

This work aims to develop a methodology to compute processes in LSDMs which are parametrised with knowledge from recent field monitoring, while meso scale approaches remain valid for the modelling of processes on the catchment scale. The objective is to develop a methodology which facilitates to zoom into the processes (physically, spatially and temporally) where detailed physical-based computation is required and to zoom out of the processes where a conceptualized parametrisation is applied. This approach to zoom in the local scale is exemplified in the scheme in figure 3.2 for a green roof structure.

3.1.2 Network generation based on drainage criteria among connected LSDMs

A network structure of the hydrological model elements has to be explicitly defined to compute the flood routing, run-on and backwater effects among LSDMs on the local, district as well as on meso scale. Explicitly means, that the hydrological network needs to be defined with a specific order of the elements. Circular or infinite connections of elements within networks must be prevented. To compute a multi-linked flood routing in the hydrological network,

it requires the definition of auxiliary (namely "virtual") elements according to the drainage criteria on the local scale. Explicit networks of elements in hydrological catchment models are created to describe the flood routing from upstream to downstream direction in a river system and consists of subcatchments, linear drainage streams and junction nodes. An objective of this work is to integrate data structures of LSDMs with an additional parametrisation to describe the source to sink (target) relations with drainage criteria.

The developed theoretical approach supports the computation of drainage and exceedance flow in a cascade of connected LSDMs and meso scale drainage elements. In that manner, the model accounts for the possibility that a single LSDM or designated area may both receive (with a run-on function) and distribute water (with a runoff function). This requires the model network to support additional linkages with drainage criteria to redistribute water from junction nodes (sources) to areas (sinks). A scheme of an exemplified model network with LSDMs is illustrated in figure 3.2. When the design capacity (V_d) of the elements on properties (namely green roofs, swales or cisterns) is exceeded by an inflow (V_{in}) the exceedance flow is distributed to retention areas in the larger system (such as multifunctional areas) or to the receiving drainage streams. Additionally, backwater effects in low lying lands may cause a reverse flow which is indicated with red arrows in the scheme between the receiving water body and the multifunctional areas. The approach to compute backwater effects among layers on the local scale is explained in the following section.

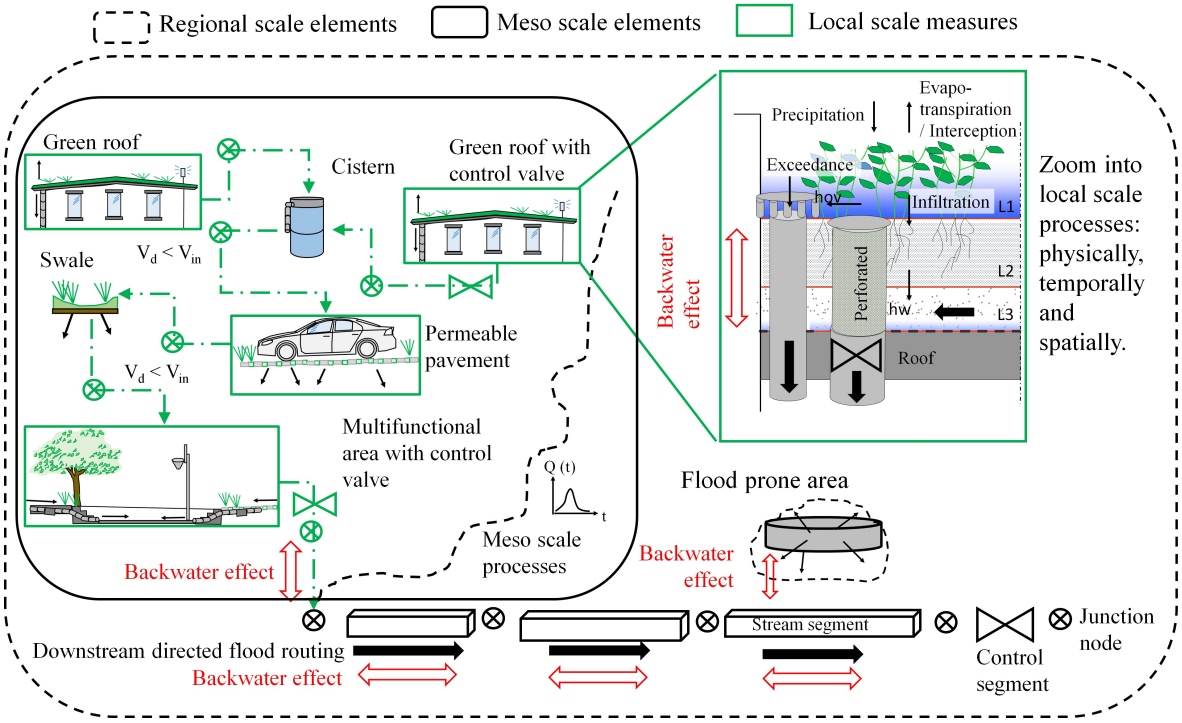

Figure 3.2: Theoretical approach to zoom in the processes on the local scale and the network generation based on drainage criteria on local scale. (The legend of flow chart symbols is given in attachment B.1).

3.1.3 Approaches to revise the structure of algorithms

A revision of algorithm in meso scale hydrological models is required with respect to two issues. First, a flexible spatial and temporal scaling needs to be realised. Second, a method to generate an explicit hydrological network on the basis of drainage criteria on the local scale is necessary. Hydrological catchment models consist of explicit computational algorithms. On the one hand, time loops are executed within a spatial tree structure (namely a time-before-space order). On the other hand, spatial loops are computed within a time tree structure (namely a space-before-time order). Explicit means here that the computation per element or time step is performed in a directed sequence from a starting ordinal to an ending one. Both approaches have advantages and disadvantages. A time-before-space computational structure is required when hydrological process simulations depend on the actual, previous and next state in time of the regarded or any previous element in the computation configuration. Whereas a space-before-time computational structure is required when downstream and upstream directed dependencies need to be computed within the network of elements per time step. The disadvantage of a space-before-time structure is a discrepancy of one time step because the computation is based on the conditions between the elements of the previous time step. To realise the objectives of this work a time-before-space structure is applied for the computation of hydrological processes. This ensures that the complete simulation results for the water balance computations of linked elements from upstream to downstream direction are taken into account. Additionally, a subsequent space-before-time computational structure is suggested to compute the backwater effects in streams and areas because the actual states of any element in the system needs to be computed simultaneously.

3.2 Approaches to model local and micro scale hydrological processes

The specific objectives to resolve limitations and weaknesses in simulating the hydrological processes in LSDMs with meso scale catchment models are summarised in table 3.2. The first objective is the definition of a physical-based parametrisation on the local scale. Secondly, a detailed simulation of processes on the micro scale needs to be accomplished. Thirdly, the computation of hydrological processes in LSDMs of backwater affected catchments is required. The measurable evaluation parameters to verify and validate the developed methods are listed in the second column in table 3.2. The specific objectives aim for the application of the numerical model to simulate hydrological processes on local and micro scale of LSDMs. A revision of the calculation routines in hydrological catchment models is relevant and required with regard to the hydrological approaches, the parametrisation, the sub-surface discretization and the computation of initial (antecedent) hydrological conditions. Antecedent moisture conditions are to be computed for event based simulation runs with small time step sizes. In this work, these shortterm simulations are embraced by longterm simulation runs over several years to compute the slow running processes of the water balances.

The parametrisation needs to be defined on physical-based derivable parameters to describe the characteristics of materials and structures. With respect to model LSDMs, the knowledge of field monitoring and laboratory studies need to be taken into account. Theoretical approaches for modelling hydrological processes in the vegetated cover, surface and subsurface are described in the following sections 3.2.1 to 3.2.3. The developed methodology to realise these objectives and theoretical approaches is explained in chapter 5.

Table 3.2: Scope of work to resolve weaknesses in modelling the hydrological processes in LSDMs with meso scale catchment models. (The enumeration is explained in footnote[3] on page 35.)

Specific objectives	Measurable evaluation parameters	Applicability for LSDM modelling	Relevant revisions of current hydrological models	In-Time effort for the implementation and model tests
Definition of a physical-based parametrisation for modelling LSDM features.	Validation with observed physical model data, verification of mass-conservation in computed processes and testing the sensitivity of input parameters (i,ii,iv).	(5) Modelling hydrological processes on local and micro scale.	Revision of hydrological approaches, subsurface discretization and parametrisation (a to g).	Revision of the source code of an applicable numerical model and availability of parameter values for local as well as meso scale studies.
Modelling hydrological processes on the spatio-temporal micro scale.				
Computing hydrological processes of LSDMs in backwater affected areas.				

The methodology to realise these objectives is described in chapter 5.

3.2.1 Approaches to model interception and evapotranspiration processes

The hydrological processes between the compartments of soil, vegetation and atmosphere comprise the processes of interception, evaporation and transpiration. The evaporation from interception storage (namely interception losses) takes place on the surface of vegetation. Evaporation from open water and bare soil occur on surfaces and varies in magnitude according to different landuse types. The evapotranspiration process is the sum of evaporation and transpiration from vegetation.

Different theoretical approaches are published in literature to compute the magnitude of intercepted, evaporated and evapotranspirated water. Empirical approaches to compute the evaporation are for example the HAUDE, Thorntwaite or TURC approach which are defined for specific regions. Physical-based approaches apply the Penman-Monteith model where knowledge about the root zone, the crop factor per season and meteorological input parameters (temperature, wind, sunshine duration, relative humidity and precipitation) are required (see R. G. Allen et al. [1998] and DVWK [1996] (p. 53ff.)).

Hydrological approaches differentiate between potential and actual evaporation. The potential evaporation represents the maximal reachable magnitude of evaporated water which is computed on the basis of meteorological data using energy-balance equations (see Hingray et al. [2014]; Maniak [2016] and DVWK [1996]). The magnitude of potentially evaporated

water does not depend on the available amount of water. To compute the evaporation in dependency of different vegetation types, the approach of the United Nations Food and Agriculture Organization (FAO) is applied (see R. Allen et al. [1994]). The FAO approach computes a so called "grass-reference evaporation" and is a derivative of the Penman-Monteith relation. To transfer the computed evaporation of the grass-reference to the actual vegetation types, a transfer function with an empirical coefficient (a crop factor) is determined. The actual evaporation magnitude is the sum of processes on vegetated, open water and bare soil surfaces. Thereby, the magnitude of actually evaporated water is limited in quantity by the available amount of water per time step.

The interdependent processes of interception, evaporation and transpiration are computed with different approaches. For a vegetated surface it is assumed that the total evaporation demand is first served by the losses from interception and the residual fraction represents the demand served by evapotranspiration (see Hingray et al. [2014]).

The process of interception detains water on the surface of vegetated covers. This process is modelled with conceptual approaches using one or several reservoirs. Especially for small and medium vegetation types the leaf storage is computed with one single reservoir. Only in case of large vegetations (such as trees) another reservoir is parametrised to present the attributes of branches and trunks as described in Hingray et al. [2014]. The initial interception storage volume is an important value to start a simulation run, while a preset constant value derived from statistics is not sufficient in real event simulations. The interception storage content is modelled over time by using a continuity equation which calculates the water content stored in the vegetated cover, combined with empirical equations used to estimate losses by evaporation, canopy dripping and stemflow. The magnitude of the interception loss varies according to the potential evaporation, intensity as well as duration of precipitation and the characteristic of the vegetated cover. A conceptual approach based on the linear reservoir theory to model interception processes and the magnitude of water fluxes on the surface of vegetated cover is published by Rutter et al. [1971]. That approach uses detailed information about the characteristics of the vegetation types, which are limited to be derived on the meso scale and consequently the parameters need to be estimated. The approach computes the drawdown and recovery of the interception storage during a precipitation event. It is an objective of this work to model the dynamic of interception losses during an event in a related manner, but limiting the required parametrisation to one single reservoir approach for meso scale modelling. The single reservoir of the interception storage depends on the vegetated cover characteristics which changes per season. A parametrisation of the vegetated cover on a monthly basis is required to model this variation. Important input parameters (arguments) are the leaf area index and the crop factor. After subtraction of interception losses from the total precipitation, the residual fraction is defined as effective precipitation reaching the soil surface.

The process of transpiration depends on the depth of the root zone and the available soil water above the wilting point in the subsurface per time step. The depth of the root zone changes per vegetative season. Therefore, the parametrisation is not constant, but

changes on a monthly basis. The defined theoretical approach in this work is based on separating the subsurface in several segments (multiple layers) which are parametrised with soil characteristics. In dependence on the actual root zone depth and the magnitude of available soil water above the wilting point of each layer, the transpiration process is computed. This approach requires a continuous simulation to model antecedent moisture conditions and a subsurface discretization of multiple layers in the (meso scale) hydrological model.

The computation of the evaporation from water surfaces of areas which are backwater affected is neglected up to now in hydrological catchment models. In the scope of this work, a method is introduced to model the evaporation of water from backwater affected flood prone areas, water surfaces of streams and submerged LSDM areas (see chapter 5).

3.2.2 Approaches to model depression losses on impervious surfaces

Water losses on impervious surfaces occur by filling up reliefs or micro-reliefs in depressed (sunken) parts of surfaces. In these depressions a certain amount of water is retained and subsequently evaporated. In current practice of hydrological modelling, empirical values of depression losses for landuse categories are applied (see Hingray et al. [2014] (p.134 ff.)). These empirical approaches neglect initial stages and temporal dynamic losses in depressions over longer periods of time. It is one objective of this work to introduce into the meso scale hydrological modelling a methodology to compute depression losses in dependence on the slope of the area, the surface properties (such as the roughness) and a time dependent filling and emptying of the depression storage capacities. Thus, the depression losses are computed in a conceptual time dependent way including the characteristics of the catchments. This approach is applicable for modelling depression losses in LSDMs as well as in meso scale catchments with a hydrological numerical model.

3.2.3 Approaches to model subsurface hydrological processes

Infiltration into permeable unsaturated soil takes place when effective precipitation or run-on fluxes reach the surface. Infiltration is a complex physical process depending on the antecedent soil moisture and hydrological characteristics, texture and structure of the media (soil). Thereby, the porosity is an effective parameter which is based upon the fraction and distribution of macro pores in the soil (see Beven and Germann [2013]). The infiltration process is driven by forces of gravity and pressure. The formation of lateral subsurface flow in the unsaturated zone is defined as interflow and in the saturated zone as baseflow. In catchments with dominantly high permeable soils, the subsurface flow may reach velocities in the same order as the surface flow (see Beven and Germann [1982]). A critical and detailed review about approaches which are used for modelling infiltration and lateral subsurface flow processes is given by Beven and Germann [2013]. The horizontal groundwater flow below the bed level of rivers, meaning which does not account for the runoff processes into receiving rivers, is not analysed in detail in this work.

Different approaches are applied on local and on meso scale to model subsurface flow

processes. The application of the widely used one-dimensional physical-based Richard's equation in the unsaturated zone and the three-dimensional version in the saturated zone in meso scale catchment modelling is subject of uncertainties because of the scale dependent parametrisation as described by Beven and Germann [2013]. The Richard's one-dimensional partial differential equation results from the combination of the Darcy model and the continuity equation (see Hingray et al. [2014]). According to the discussions presented in Beven and Germann [2013] and Hingray et al. [2014], the Richard's equation is not applicable on the meso scale as a suitable modelling approach.

Other approaches to model infiltration are based on empirical equations such as by Horton or the SCS-CN[4] method (see Hingray et al. [2014] and Maniak [2016]). Empirical equations are widely-applied because of their straightforward application, but contain parameters that are difficult to be predicted because they have no physical meaning. Other approaches use a parametrisation of the capillary suction at a wetting front in the soil, for instance in the Green and Ampt approach described in Mein and Larson [1973]. But, these functions in its basic form can not be applied to model the dynamic in bottom-up saturation and the recovery of the infiltration capacity of the soil over time (see Hingray et al. [2014]).

To tackle this limitation, an extended approach is based on the linear reservoir theory for modelling the infiltration and percolation processes in multi-layered structures. With this approach, each layer is computed as a reservoir with a continuity equation which combines the calculation of different hydrological processes. An example is the so called "infiltration excess model" (IEM) presented in Hingray et al. [2014], which facilitates the computation of the infiltrated and exceedance water fractions per time step of each subsurface reservoir. Surface runoff is generated when the precipitation intensity exceeds the infiltration capacity of the first layer. This approach is implemented for example in the hydrological catchment models "BlueM" (M. Bach [2011]; Ostrowski et al. [2010]) and KalypsoNA (TUHH-WB [2014]). This approach includes the simulation of the recovery of the soil infiltration capacity when the inflow in the soil layer is less than the infiltration capacity and the calculated outflow reduces the water content over time. It is applicable on the meso scale as parsimonious modelling approach with regard to the number of required input parameters and it is applicable for modelling LSDM techniques of multi-linked layers using detailed spatio-temporal scaled data.

To describe the hydrological characteristics of soil (namely any type of porous subsurface media), the pedological parametrisation comprises the maximal pore volume (maxPV), wilting point (WP), field capacity (FC) and the hydraulic conductivity (k). The volumetric soil water content below the "wilting point" (V_{WP}) corresponds to the water content that is held by capillary and hydroscopic forces and is not available for plants or drainage of the layer. The volumetric soil water content reaching the "field capacity" (V_{FC}) is the water content remaining in the soil layer by capillary forces after gravitational drainage is ceased and the water is available for plants. For regional scale catchment modelling (>100 km^2) it is reason-

[4] SCS is the Soil Conservation Service of the U.S. Department of Agriculture. CN is the Curve Number to describe the infiltration characteristics of a soil group.

able to use pedological field base maps in combination with a soil classification scheme to define this pedological parametrisation. For local scale modelling it is an objective to apply a more detailed approach using the "hydraulic radius theory" presented by Kozeny [1927] which is later verified by Carman [1937] to compute the hydraulic conductivity on the basis of the particle sizes of the material (see Bear [1988]). That approach is labelled in this work as Kozeny-Carman approach (KC-approach).

The hydraulic radius theory is based on the assumption that the porous soil can be treated as a bundle of capillary tubes of equal length as described in Bear [1988]. The cross-sections of the capillary tubes vary and Kozeny proposed to apply a numerical coefficient c_0 (namely the Kozeny's coefficient) to take into account a varying geometrical form of the capillary tubes. Kozeny (1927) derived the following base form of the equation with respect to a unit volume of porous soil (Bear [1988]; p. 166):

$$k = c_0 \cdot \frac{n^3}{(1-n)^2} \cdot \frac{1}{(M_s)^2} \tag{3.2.1}$$

where k is the hydraulic conductivity (mm/s), c_0 is the Kozeny's coefficient which describes the shape and tortuosity[5] of flow paths in the porous material (-) (see Chapuis and Aubertin [2003]), n is the porosity (-) and M_s is the specific surface of the material (mm). About ten years later Carman [1937] defined values for c_0 to be between $\frac{1}{2}$ and $\frac{1}{6}$. The specific surface M_s of a porous soil is related to the mean particle size $d_m = 6/M_s$ (see Bear [1988]). The equation is transformed in the following manner:

$$k = c_0 \cdot \frac{n^3}{(1-n)^2} \cdot (\frac{d_m}{6})^2 \tag{3.2.2}$$

Long time it was stated that the empirical form of the KC-approach is only valid for sandy soils. But the analysis by Chapuis and Aubertin [2003] and Urumović and Urumović Sr. [2016] proved on the basis of laboratory experiments that the equation is valid for further soils which can be described by Darcy's law. It has been shown by Urumović and Urumović Sr. [2016] that the KC-approach predicts fairly well the saturated hydraulic conductivity of most soils ranging with grain size (d_m) between 1.5 μm to 6 mm and hydraulic conductivities between 10^{-12} to 10^{-2} m/s. The equation has taken several forms (see Chapuis and Aubertin [2003]; Urumović and Urumović Sr. [2016]), including the following one:

$$k = c_0 \cdot \frac{g \cdot \rho}{\mu_w} \cdot \frac{n^3}{(1-n)^2} \cdot (\frac{d_m}{6})^2 \tag{3.2.3}$$

where k is the hydraulic conductivity (mm/s), μ_w is the dynamic viscosity of water (g/(mm*s)), ρ is the density of water (g/mm^3), g is the acceleration of gravity (9.81 m/s^2 = 9810 mm/s^2), n is the porosity (-) and d_m is the mean particle size (mm).

In this work the infiltration excess model which is based on the linear reservoir theory in combination with the KC-approach are applicable to reach the objectives of the defined scope of work.

[5]The tortuosity describes how many curves and turns exist along the flow paths within porous material.

3.3 Approaches to model LSDM technologies

The specific objectives of modelling LSDM technologies comprise the simulation of processes in retention layers, rainwater harvesting and (real-time) control functions. The scope of work to resolve these objectives is given in table 3.3. The evaluation of methods is done by comparing the numerical model output parameters with laboratory physical model results, a verification by computing the mass-conservation in processes and testing the functional correctness in data processing with the numerical model. In the hydrological catchment model, it is required to define a multi-layered structure to accomplish the modelling of drainage flow between the layers. Current hydrological numerical approaches need to be revised and a parsimonious parametrisation is required.

Table 3.3: Scope of work to resolve weaknesses and limitations in integrating LSDM technologies into current hydrological numerical models. (The enumeration is explained in footnote [3] on page 35).

Specific objectives	Measurable evaluation parameters	Applicability for LSDM modelling	Relevant revisions of current hydrological models	In-Time effort for the implementation and model tests
Modelling multiple layered structures.	Validation with physical model data from laboratory and verification by testing the mass-conservation in processes (i,ii).	(6) Facilitating the modelling of multiple layered structures.	Revision of the subsurface discretization (e & g).	Revision of the source code of an applicable numerical model and availability of parameter values for local as well as meso scale studies.
Modellling rainwater harvesting functions.	Verification of mass-conservation within in- and outflow processes (ii).	(7) Modelling rainwater harvesting functions.	Revision of current hydrological approaches and the parametrisation (a,b,e,g).	
Modelling control functions in LSDMs based on criteria.	Verification of the functional correctness in data processing (iii).	(8a) Modelling control features in the areas of LSDMs.		

The methodology to realise these objectives is described in chapter 5.

3.3.1 Definition of drainage processes in multi-layered and interlinked hydrological systems

To develop computational approaches to model hydrological processes in LSDMs, the system components and dependencies need to be clarified. For that purpose, schemes of multi-layered structures and the hydrological processes among layers are illustrated in figure 3.3. From left to right in these examples, a green roof structure is subdivided into three layers. The upper layer represents a storage and vegetation level. The second layer is a substrate layer with permeable soil and the lowest layer is a drainage level (see figure 3.3, a). In the substrate layer,

vegetation is planted according to an extensive or intensive use. The parametrisation of the root zone depth depends on the vegetated cover and the season. The root zone depth reaches over one or more layers. On the roof, a drainage layer is provided above a root protection and sealing to drain the water to a downpipe.

A swale-filter-drain system illustrates the features of interlinked layers. Exceedance flow of the first layer flows directly in the underground drainage layer after exceeding an overflow crest height (see figure 3.3, b). The example of a swale is illustrated likewise with an exceedance flow outlet and a defined overflow crest height. A cistern is represented with an inlet into a storage layer, an exceedance flow outlet and rainwater harvesting technical devices (pumps). Additionally, the storage layers can be equipped with control valves and linked with weather forecast sensors to manage the quantity of retained water.

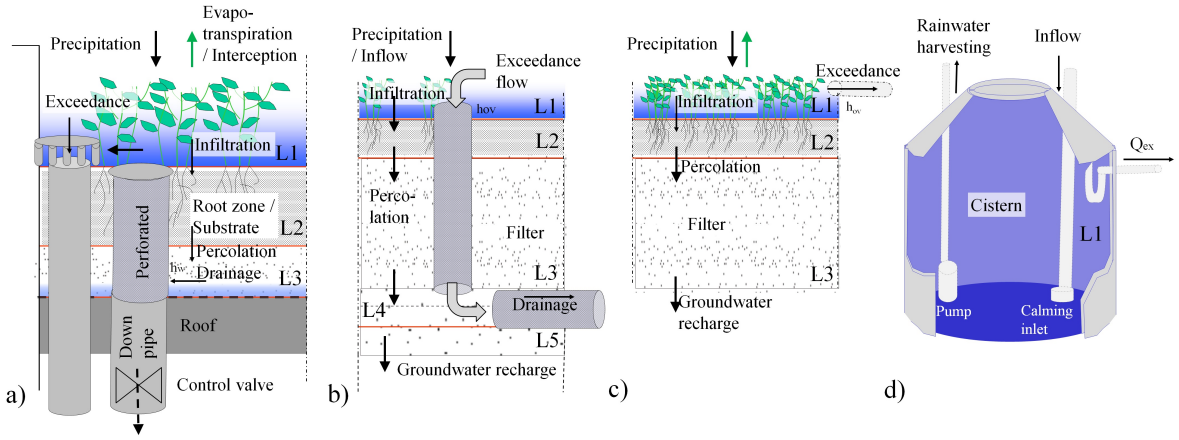

Figure 3.3: Design examples of LSDMs made up of multiple layers: (a) green roof with exceedance flow and down pipe outlet; (b) swale-filter-drain system with interlinked layers; (c) swale with exceedance flow control; (d) cistern with rainwater harvesting device (adopted from Hellmers and Fröhle [2017]).

3.3.2 Approaches to model rainwater harvesting and control features

The water quantity utilized for rainwater harvesting depends on seasons and weekdays for gardening as well as for domestic or industrial water demands. Therefore, rainwater harvesting quantities need to be defined on a daily or sub-daily temporal scale for modelling LSDMs. To model dual systems with rainwater harvesting and additional storage function for flood mitigation purposes, further criteria are required to determine extended control features. The objective of this work is to activate a control function per time step on the basis of control criteria for different driver parameters including precipitation intensities, water levels and discharges of elements in the hydrological network. According to these criteria, a comparison of the driver variable with a defined critical setpoint (threshold) is performed. If the setpoint is reached a control function is activated. The driver time series for the control functions are preset or computed on-the-fly. The preset time series are imported such as observed precipitation or flow gauge data series. On-the-fly computed control functions depend on process parameters which are calculated within the hydrological system during a simulation run. An

overview of driver time series and a scheme of a control system are illustrated in figure 3.4.

Integrating LSDM technologies within an operational system requires a continuous import and processing of data for instance rainfall forecast data. It is needed to couple different models and to achieve a fast data transfer. Further on, ensemble data of rainfall forecast systems give promising results to be used in future for the control of hydrological systems (see Jasper-Tönnies et al. [2018]). The computing time of the rainfall forecast as well as the hydrological model has to be reasonable short (<5 minutes) to facilitate a fast data transfer. These approaches to model control functions are developed for local scale hydrological systems, but are also applicable to model meso scale structures.

The developed methodology to extend current hydrological numerical approaches to model LSDM technologies is described in chapter 5.

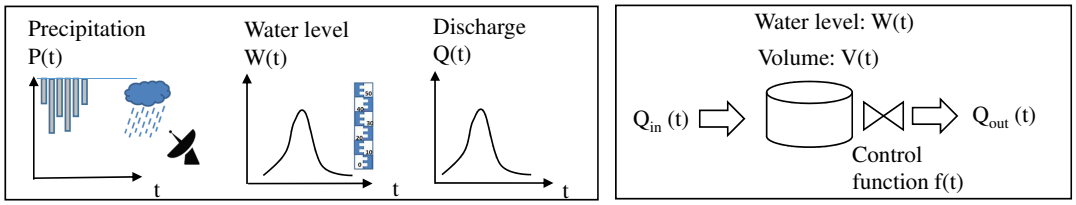

(a) Overview of driver time series (b) Scheme of a control system

Figure 3.4: (a) Overview of preset and on-the-fly computed driver time series. (b) Scheme of a control system to model local and meso scale systems.

3.4 Approaches to model flood routing and backwater effects in streams and areas

Flood routing describes the retention and translation processes of water flowing along a linear stream (such as an open channel, drainage pipe or ditch). These processes depend on the characteristics of the drainage network comprising the geometry of profiles, gradients and roughness of the streams. The review of hydrological numerical model categories in section 2.2 (page 16 ff.) revealed significant weaknesses in current hydrological approaches to compute backwater effects in streams and flood prone areas. It is an objective of this work to extend a hydrological approach to be applicable for the computation of flood routings and backwater effects in streams and among LSDMs on meso as well as local scale.

The scope of work and the specific objectives to extend current flood routing methods are summarised in table 3.4. This comprises the integration of control functions, flood routing computation among LSDMs and modelling backwater effects in streams as well as areas of low lying lands including LSDMs. The measurable evaluation parameters are defined with the objective to verify the functional correctness in data processing, to verify the mass-conservation in the computation of processes, to study the sensitivity of parameters in different LSDMs and to compare simulated results with observed flow gauge data to validate the flood routing and backwater effect calculations in larger as well as smaller streams. The approaches are applicable for LSDM modelling to define different control functions on the

basis of observed, forecasted or simulated time series (for example, precipitation intensities, water levels and discharges). The flood routing method and computation of backwater effects need to be applicable on the local and meso scale. Additionally, it is an objective to compute the evaporation of water from submerged areas and streams. For the hydrological numerical model development, it is relevant to revise the methods to compute surface runoff, flood routing in streams and open water evaporation from spatial as well as linear structures. To achieve the objectives in-time, the calculation routines in an applicable numerical model need to be revised and new methods are required to be integrated. Additionally, the parametrisation with respect to the geographical informations of LSDMs in meso scale hydrological models is needed.

Table 3.4: Scope of work to resolve weaknesses in modelling the flood routing among LSDMs and backwater effects with hydrological numerical models. (The enumeration is explained in footnote [3] on page 35).

Specific objectives	Measurable evaluation parameters	Applicability for LSDM modelling	Relevant revisions of current hydrological models	In-Time effort for the implementation and model tests
Modelling control features in streams.	Verification of the functional correctness in data processing (iii).	(8b) Modelling control features in streams of LSDMs.	Extension of a hydrological flood routing approach to accomplish the required features (a to g).	Revision of the source code of an applicable numerical model and availability of parameter values for local as well as meso scale studies.
Computing local scale and run-on flood routing in hydrological networks.	Verification of the mass-conservation in computed processes and testing parameters in sensitivity studies (ii,iv).	(9) Computing the runoff and run-on flood routing in interlinked LSDMs.		
Modelling backwater effects in local and meso scale streams and subsequent hydrological processes.	Validation with measured flow gauge data and verification of mass-conservation balances (i,ii).	(10) Modelling backwater effects in streams and LSDMs.		

The methodology to realise these objectives is described in chapter 6.

3.4.1 Hydrological approaches to model flood routing in streams and among LSDMs

To resolve current weaknesses in modelling the flood routing among LSDMs and backwater effects with hydrological numerical models, an appropriate approach needs to be determined and extended. To support the application of the approach on different scales and for computing different stream categories within one catchment, it is required to utilize a physical-based parametrisation.

Current hydrological methods to compute the flood routing are based, for example, on linear or non-linear Muskingum approaches (see section 2.2.6, page 2.2.6 ff). These approaches

require input parameters which are based on observed data in upstream and downstream sections of rivers. Because of missing physical-based parametrisation, these hydrological approaches are not suitable to be used for simulating changed conditions in the streams and where no observed data is available.

Two approaches are applicably which are based on physical characteristics such as river geometry, stream length, roughness coefficient and river bed slope. On the one hand, the Muskingum–Cunge (often used in the United States) and on the other hand, the Kalinin-Milyukov flood routing approach are applicable. For this work, the second one is chosen because of a wide field of application in Germany and Eastern Europe.

The theoretical approach of Kalinin and Milyukov [1957] (KM) divides a stream into a number of characteristic lengths as illustrated in figure 3.5 (a). Each length is considered to be small enough for assuming a quasi-stationary relationship on the basis of a hysteresis curve (see figure 3.5 (b)). Different derivations of the KM-approach are given in literature and are discussed for example by Koussis [2009].

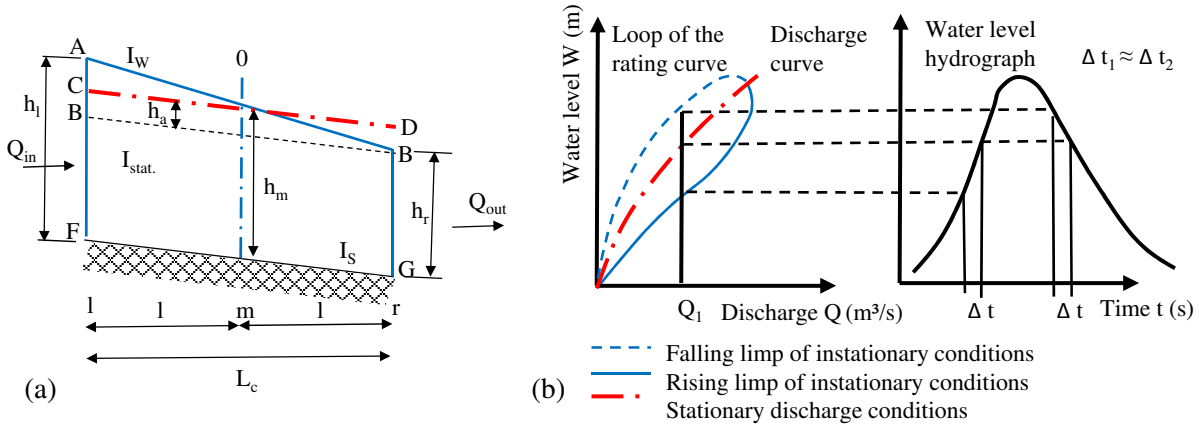

Figure 3.5: (a) Parametrisation of a characteristic length L_c of a stream segment.
(b) Illustration of a hysteresis curve, which describes the relation between discharge and water level for instationary and stationary conditions. Similar illustrations are given in Maniak [2016] (p. 398 ff.) and Koussis [2009].

The KM-approach is based on the assumption that in the quasi-stationary state, the discharge Q (m^3/s) is directly related to the water volume V (m^3) per characteristic stream segment. The slope of the function $V = f(Q)$ results in the retention coefficient K (s). Therewith, the relation $\Delta V = K \cdot \Delta Q$ is derived for each characteristic length L_c of a stream segment. The conditions under the instationary water level gradient I_w are compared with the stationary water level gradient I_{stat}. For each point in the discharge hydrograph (for example, Q_1), three corresponding water level stages are given in the hysteresis curve (figure 3.5 (b)). The water levels at the rising and falling limp of a stationary discharge curve appear a time step size Δt later than in the instationary flow process. The water-level-discharge-relation (WQ-relation) is derived by assigning the discharge $Q(t-1)$ to the water level $W(t)$. For a characteristic length L_c the water levels in a stationary and instationary conditions are labelled in figure 3.5 (a). The average water level at point (m) is transferred to point (r) on the basis of the WQ-relation. The volume in the stream segment in the instationary state (indicated with the points: A,B,G,F)

corresponds to the stationary state (indicated with: C,D,G,F). This results in a distinct water-level-volume-discharge-relation (namely "WVQ-relation"), which is valid for a characteristic length L_c with a constant water level slope I_W and an even cross-section as well as roughness along the stream length. This approach results in the computation of the instationary flow of a complete reach by a cascade of characteristic stationary linear reservoirs. Using the Nash-model principle with the gamma-function according to Dooge [1973] it becomes more flexible in using a real number of characteristic lengths. The parametrisation to apply this approach depends on profile geometry, slope and roughness coefficients. An analysis by Dooge [1973] shows that the KM-approach can closely reproduce the results of the linearized Saint-Venant solution.

3.4.2 Approaches to model control systems and backwater effects in streams and LSDMs

Control structures are required to be modelled to simulate operational and real-time control technologies in local, district and meso scale streams as well as LSDMs. Criteria to activate different control functions are based on water levels, discharges and precipitation intensities as illustrated likewise in figure 3.4 for LSDM control systems.

The review in chapter 2 revealed limitations in hydrological numerical models to simulate backwater effects in streams and areas with hydrological approaches. One objective of this work is to develop a method to model backwater effects in streams and areas on the local scale (such as LSDMs). To model backwater effects in low lying lands, the approach needs to be applicable to model tide-gate operations and the functionality of pumping stations on the local as well as on the meso scale.

To achieve these objectives, the developed approach in this work is based on extending the flood routing computation described in the previous section 3.4.1. The extension uses the results of the derived WVQ-relations for each characteristic stream segment to compute a backwater effect in case of afflux conditions in the downstream sections. Because of the direction of backwater effects from downstream to upstream, the order of calculation routines need to be adjusted likewise from downstream to upstream direction. These calculation routines need to take into account time-dependent (instationary) conditions. The developed approach is applicable for modelling backwater effects in streams as well as areas. The parametrisation is based on the hydrological approach to model flood routing processes and requires the definition of one characteristic stream profile geometry, stream length, roughness coefficient and river bed slope per stream segment. For regional scale catchment modelling (>100 km^2) the length of such a stream segment with one characteristic profile parametrisation may have a length of several kilometres, whereas a characteristic stream on the local scale may have a length of a few meters. In comparison to a hydrodynamic-numerical model approach, this parametrisation is considered as more parsimonious to be applied on different spatial scales within one data model structure. This approach is not intended to model details in the distribution of flow velocities within stream segments like a hydrodynamic-numerical model, but fulfils the requirements of a detailed physical-based hydrological approach directly

integrated in a numerical catchment model. The parsimonious parametrisation of streams and expected short computing times are considered as benefits of this hydrological approach to model backwater effects. Further on, the hydrological processes like evaporation of water or subsequent controlled drainage of water from submerged areas after backwater flooding is modelled directly with the presented hydrological calculation routines.

The methodology to resolve the presented weaknesses and limitations in hydrological models with the determined theoretical approaches to model control systems and backwater effects in streams and areas is described in chapter 6.

4. Methods of a flexible spatio-temporal scaling and network generation

The methodology is subdivided into three parts and comprises several methods. The first part is explained in this chapter to resolve shortcomings in hydrological numerical modelling for the integration of LSDMs. The required model features are numbered from (1) to (4) in the objectives of the scope of work (see table 3.1 on page 35). A prerequisite to integrate these features is a revision of the algorithms in the hydrological numerical model. Thereby, a flexible spatio-temporal resolution and an applicable parametrisation of data structures is necessary. In the field of numerical modelling, data structures describe the parametrisation of elements within a hydrological network. In this work, the main elements include subcatchments, stream segments, junction nodes, HRUs and LSDMs, which are defined as data structures.

This chapter is divided into three sections. First, a method is described to facilitate a flexible geographical data mapping on local and meso spatial scales (see section 4.1). To accomplish a flexible temporal scaling, a method is developed to compute the processes in LSDMs as well as meso scale data structures (see section 4.2). Further on, an on-the-fly network generation based on drainage criteria is developed which is explained in section 4.3. This method facilitates the simulation of interlinkages between network elements on different spatial scales. For regional scale catchment models (>100 km^2) including LSDMs with sizes between 1 m^2 to 100 m^2 the number of elements easily exceeds 1000s. In that case, the network generation can not be performed manually by the modeller, when selecting each linkage between the elements separately. This limitation in current hydrological numerical models is resolved with the developed method in this work which is also published in parts in the reviewed journal papers Hellmers et al. [2015], Hellmers, Manojlović, et al. [2016], Hellmers and Fröhle [2017].

4.1 Spatial order and scaling of georeferenced local data structures

The review of hydrological model categories in chapter 2 revealed the semi-distributed model approach as appropriate to realise the objectives of this work. The spatial discretization approach uses subcatchments as larger units within watershed delineations (catchments).

Each subcatchment is defined with a specific drainage outlet in the hydrological network. The spatial heterogeneity within subcatchments is represented by Hydrological Response Units (HRUs). An HRU describes the area according to homogeneous properties of pedology, geology and vegetated cover which contribute to represent a specific hydrological behaviour. A single HRU can be smaller than 1 m^2 on the local scale or larger than several 100 m^2 on the meso scale. This depends on the characteristic input data which is used for the intersection to create HRUs. The spatial scaling of parameters in semi-distributed models is flexible by using a nested approach. Data structures of HRUs are aggregated per subcatchment according to similar hydrological characteristics while loosing their geographical location. This aggregation concept on the subcatchment scale reduces the number of different HRU data structures and consequently the required computing resources (times). The runoff routing is computed on the meso scale with conceptual approaches. Although this approach is advantageous on the meso scale, it holds weaknesses when modelling the flood routing among local scale structures. A limitation by current semi-distributed approaches is the assumption of independency between the local data structures because the spatial organisation is ignored.

For modelling the performance of LSDMs on the meso scale, this limitation is tackled in this work by developing a method to define a parametrisation which includes the geographical location and specific drainage attributes of LSDMs. A specific LSDM attribute is for example a predefined drainage direction from a source to a target element by a drainage stream. The data structures without specific drainage attributes are aggregated as HRUs within a subcatchment. To map large numbers of heterogeneous local scale data structures per meso scale subcatchment Geographic Information System (GIS) data import and data processing functions are applied. For example, the distribution of green roofs depends on the availability of building contours, whereas the distribution of retention spaces and infiltration measures depends on the availability of free spaces. This demands for a modelling approach which can handle a large number of spatially distributed measures and a sufficiently detailed land use map matching the spatial detail of LSDMs within meso scale subcatchments. For this purpose, a spatial mapping with so called "overlay data structures" is created.

Spatial mapping by using overlay data structures. Because of the fact, that LSDM data structures are situated within the delineations of meso scale subcatchments, relevant preset parameters of meso scale attributes are adopted for modelling local scale data structures. These meso scale parameters are defined in shapes to describe the prevailing pedology, geology, landuse and watershed parametrisation. A shape is a file to describe the spatial data in a layer which provides input parameters with geographical reference in a GIS-based coordinate system. These shapes are intersected to create HRU data structures made up of different layers as illustrated in figure 4.1 (a). The selection and spatial mapping of LSDMs is performed on-the-fly with the criteria to select elements with specific drainage attributes and create overlay data structures as depicted in figure 4.1 (b). The LSDM parameters overlay the HRU parameters and replace them if values are defined. To split the LSDM data structures from the meso scale ones, another spatial intersection is performed as depicted in figure 4.1 (c). This step is

an intersection of local data structures on the basis of overlying LSDM and underlying HRU parameters. The parameters of LSDMs replace the ones of HRUs precisely for the delineated LSDM shapes. Specific drainage attributes of LSDMs are for instance the number and depths of layers, material descriptions, land use attributes on the surface and maximal groundwater recharge rates. These parameters are optional, meaning that the defined meso scale parameters are transferred on the local scale data structure if no "overlying" value is defined. In this manner, the meso scale data structures (HRUs) of the subcatchment are spatially reduced and overlay data structures (in this case, LSDMs) are created. Each LSDM data structure consists of at least one HRU. For detailed flood routing computation among structures on the local scale, the geographical location per LSDM is calculated to provide information about distance and flow path gradient between source and target LSDM structures.

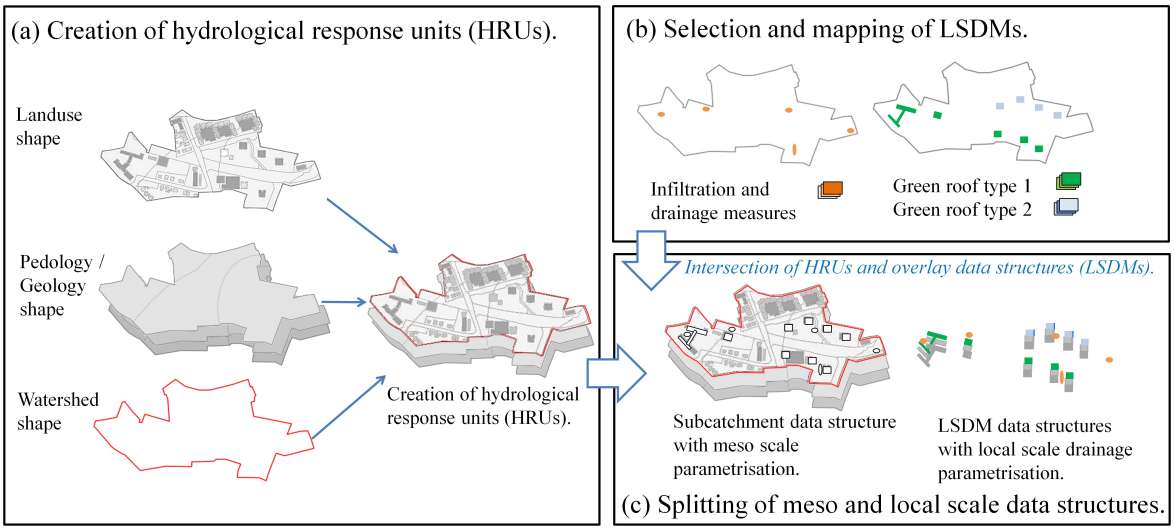

Figure 4.1: Procedure of the method to create LSDM data structures within meso scale subcatchment data structures (adopted from Hellmers et al. [2015]).

The developed method is based on GIS functions and supports a direct import of land use shape files. Digitised basic data pools from cartography of real land utilisation of provincial and municipal governments delineate building types, roof types and free spaces. These data sources are used to set the location of potential LSDMs like green roof installations and retention measures. Further on, the information of building types is applied to define rainwater harvesting time series.

Mapping LSDM data structures with geographical location and modelling an exceedance flow control. To model the exceedance flow on the local scale, a computation of the interlinked drainage and run-on flood routing is needed. For this purpose, LSDM data structures are defined with source and target (sink)[1] information in overlay shape files. These files include the geographical data of a defined coordinate system. If the geographical location of the overlay shapes is not available, an aggregation of corresponding parameters per subcatchment

[1] A source is defined as any element in the hydrological network which delivers water. In turn, a sink or target element receives the drained water.

is performed to reduce the data processing on the meso scale.

Three different levels of details to compute the flood routing among LSDMs within a subcatchment are depicted in figure 4.2. These examples of LSDMs include green roofs (GRs), swales (SWs), cisterns (Cs) and multifunctional areas (MFAs). In case (a), overlay data structures without geographical location are aggregated per meso scale subcatchment and the flood routing is computed with a meso scale approach. In case (b), geographical locations of LSDMs are imported. The parametrisation of the flood routing includes the length of the flow path, the gradient and geometrical profile data. In this way, the flood routing to the outlet is computed in a more detailed manner. The flow path is the longest distance a drop of water flows from a source to a target. In case (c), the parametrisation per source element provides additionally a drainage fraction to different target elements using junction nodes. The receiving junction nodes can be inside as well as outside of the subcatchment boundaries. Enabling the different cases (a) to (c) in one methodology provides a flexible model to serve different application demands according to the available data and objectives of modelling. Nonetheless, only the last case (c) facilitates a detailed computation of an exceedance flow control among interlinked LSDMs.

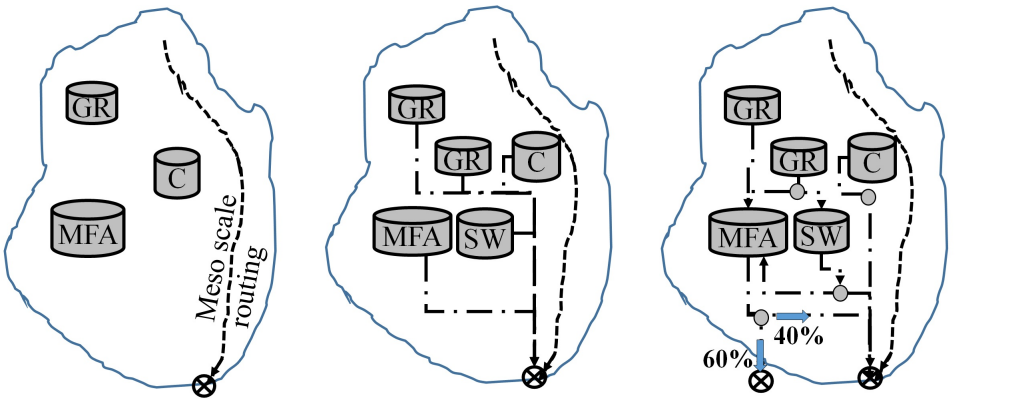

(a) Flood routing defined on the meso scale.

(b) Flood routing with defined geographical location of LSDMs.

(c) Flood routing among interlinked LSDMs on local scale.

Figure 4.2: Options to compute the flood routing within a subcatchment using different parametrisations of geographical data and drainage criteria among LSDMs.

The actual parameters to compute the flood routing among LSDMs are given per source data structure. The hydrological network of local scale interlinked streams is generated on-the-fly during the execution of the simulation run. For this purpose, junction nodes are created with a parametrisation to represent the water distribution between elements. An example in figure 4.2 (c) illustrates a drainage distribution of 40 % to the catchment outlet and 60 % to a different target node. The flow path length and gradient from the source to the target elements are computed based on the geographical locations and additional parametrisations of the source data structure. The computed flow path length is initially the shortest distance among the source and target. This initial flow path length is adjusted with an optional factor to model prolongations of the flow path over the surface to the target. Different data

structures can be selected as target such as other LSDMs, subcatchments or junction nodes. The computed gradient among the source and target (sink) is defined on the basis of DEM data and requires an adjustment if it decreases below a minimum gradient. Especially in urban areas, the stormwater drainage system in the subsurface is not necessarily in accordance with the topographical gradient on the surface. The developed method facilitates to model interlinked flood routing on local scale among LSDMs and on meso scale among river streams. Because of the large number of linkages among LSDMs, when modelling regional scale catchments (>100 km^2), the definition of each linkages by the modeller in a one-by-one selection procedure is not feasible. To resolve this limitation, a method to facilitate the generation of a hydrological network on-the-fly is developed and described in section 4.3.

4.2 Method to introduce a dynamic time step size computation

For the simulation of hydrological processes on the local and meso scale, the required time step sizes differ. To compute the hydrological processes on the local scale in permeable and thin layers, for instance infiltration, exfiltration and drainage processes, a time step size of a few seconds is necessary. On the other hand, a time step size of several minutes is appropriate for modelling processes on the meso scale. Additionally, a differentiation between longterm (using daily time step sizes) and event based simulation runs (using time step sizes in minutes) is defined. To model antecedent moisture conditions, longterm water balance simulations over several years are needed. To reduce the computing time, one longterm run embraces several detailed shortterm event based runs.

To integrate in one algorithm meso via local and longterm via shortterm demands, a dynamic time step size computation is required. A differentiation is introduced between the preset simulation time step size and the (internal) process-related time step size. The disaggregation to process-related time step sizes prevents the computation of undesired oscillatory behaviour. Such an oscillatory behaviour occurs when the influx of water into the regarded layer in one time step is larger than the available storage volume per unit area. This results in an "on-off" phenomenon, where in one time step a surplus of water can not be processed completely in the layer and in the following time step the surplus water content drops to zero. The dynamic time step size adjustment allows a more flexible and process-related soil water computation and improves the simulation accuracy of vertical water fluxes in layered structures compared to a constant time step size. The computation of the process-related time step size is based on a spatial and temporal water balance computation. The algorithm is presented in figure 4.3. The input criteria are the volume of water feeding the different subsurface layers within the actual simulation time step, the hydraulic conductivity of the material, the maximal pore volume, the actual water content in that layer and the layer thickness. A differentiation is done between a shortterm and a longterm simulation in the calculation routine "*Corr 1*" (figure 4.3). In case of longterm simulations with a daily time step size (Δt = 24 hours) the minimum process-related time step size for soil water calculations is $\Delta t'$ = 8 hours (=28 800s). The computation is performed in the following form and labelled as "Min. Δt longterm" in

figure 4.3.

$$\Delta t' = \frac{1}{3} \cdot \Delta t$$
$$\dot{V}_{in}(t') = \dot{V}_{in}(t) \cdot \frac{\Delta t'}{\Delta t} \tag{4.2.1}$$

where Δt is the preset simulation time step size (s), $\Delta t'$ is the process-related time step size (s), $\dot{V}_{in}(t)$ is the actual influx in the preset time step size (mm/s) and $\dot{V}_{in,i}(t')$ is the adjusted influx within the process-related time step size (mm/s). The actual free soil water storage (V_{free}) per time step is required to be at least 10 times larger than the inflow ($\dot{V}_{in,i}(t')$) per time step size $\Delta t'$ in the shortterm and longterm simulation to prevent oscillatory behaviour. As long as the following query "Test V_{free}" (see figure 4.3) is true, the time step size $\Delta t'$ is reduced:

$$\dot{V}_{in,i}(t') > 10 \cdot V_{free}(t)$$
$$\frac{\Delta t}{\Delta t'} < 100 \tag{4.2.2}$$

A decisive point is reached when the process-related time step size is much smaller than the predefined simulation time step size. To prevent infinity small time step sizes, the query checks that the process-related time step size is not 100 times smaller than the predefined time step size of the simulation run. The calculation routine ("*Corr 1*") is active as long as both queries (see e.q. 4.2.2) are true. For shortterm and longterm simulation runs a reduction in time step size and a corresponding adjustment of the inflow is computed as follows:

$$\Delta t' = \frac{1}{2} \cdot \Delta t$$
$$\dot{V}_{in,i}(t') = \dot{V}_{in,i}(t') \cdot \frac{\Delta t'}{\Delta t} \tag{4.2.3}$$

This calculation is labelled as "*Reduce* $\Delta t', \dot{V}_{in}(t')$" in figure 4.3. If an open storage is defined as top layer, the parameters of the next subsurface soil layer are taken as basis to compute the process-related time step size in "*Corr 1*". For longterm and shortterm simulations of HRU data structures, the dynamic time step size computation is finalised when the actual free soil water storage (V_{free}) per time step is at least 10 times larger than the inflow ($\dot{V}_{in,i}(t')$) per time step size $\Delta t'$. This query is labelled as "*Test* V_{free}" (see e.q. 4.2.2). For the computation of processes in thin substrate layers which have a high hydraulic conductivity and a large quantity of water enters within a short time, this dynamic time step size computation requires an additional correction. A critical state is reached when the infiltrated water into the regarded soil layer flows through more than one soil layer thickness within the computed time step size. These situations occur in drainage and permeable substrate layers of LSDMs.

Therefore, a second correction method is developed (see figure 4.3, "*Corr 2*") which is based on the Courant-Friedrichs-Lewy criterion (CFL-criterion) (Courant et al. [1928]). According to the CFL-criterion, the time step size is a function of the spatial dimension (here: layer thickness) and the velocity with which the water flows into the spatial element. The

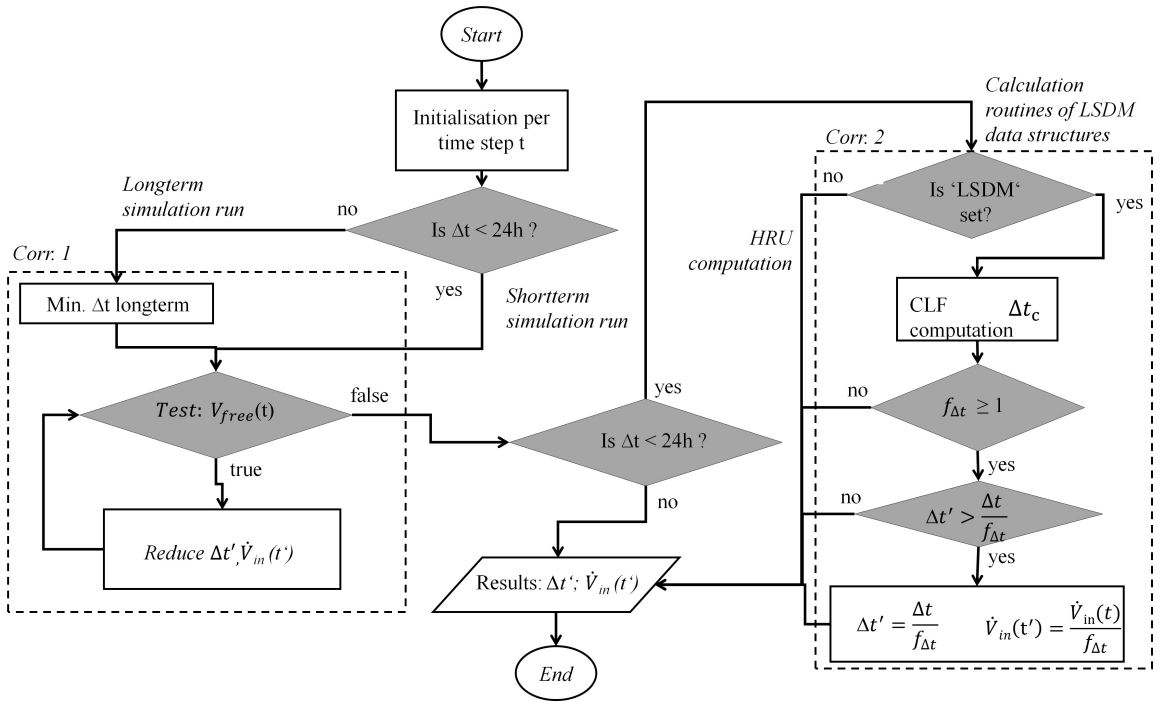

Figure 4.3: Developed algorithm of the dynamic time step size computation (adopted from Hellmers and Fröhle [2017]).

velocity is defined in this case by the hydraulic conductivity k of the soil or material in (mm/s). The CFL-criterion for the one dimensional case is defined as follows (Pinder [2002]):

$$C_r = \frac{u * \Delta t}{\Delta x} \leq C_{max} \tag{4.2.4}$$

where C_r is the CFL-criterion (-), Δt is the time step size (s), u is the magnitude of velocity (m/s), Δx is the spatial distance between in- and outflux border (m), and C_{max} is equal to 1 (for explicit calculations) (see Pinder [2002]). To assure that the CFL-criterion is fulfilled, a dynamic time step size computation is required taking into account the respective layer thickness (z) and the hydraulic conductivities (k) per layer. The equation (4.2.4) is transformed and applied in the following form:

$$\Delta t_c = MIN_{i=1}^{n} \frac{\Delta z_i}{k_i} \tag{4.2.5}$$

where Δt_c is the required small time step size to fulfil the CFL-criterion (s), i is the layer index (from 1 to n), n is the index of the deepest soil layer, Δz_i is the thickness of the actual soil layer i (mm) and k_i is the saturated hydraulic conductivity of the layer i (mm/s). The dynamic time step size computation runs over all layers to define the critical smallest time step size. An adaptation factor $f_{\Delta t}$ is calculated to test the validity of the CFL-criterion with:

$$f_{\Delta t} = \left\lceil \frac{\Delta t}{\Delta t_c} \right\rceil \tag{4.2.6}$$

If the time step size computed with the adaptation factor is smaller than the time step size

computed with "*Corr. 1*", the process-related time step size is computed with the adaptation factor and the actual input flux is corrected respectively:

$$\begin{aligned}
&\text{if these conditions are true: } f_{\Delta t} \geq 1 \text{ and } \Delta t'_{Corr1} > \frac{\Delta t}{f_{\Delta t}} \\
&\text{then } \Delta t' \text{ is computated with Corr 2: } \Delta t' = \frac{\Delta t}{f_{\Delta t}} \text{ and } \dot{V}_{in}(t') = \frac{\dot{V}_{in}(t)}{f_{\Delta t}} \\
&\text{else } \Delta t' = \Delta t'_{Corr1} \text{ and } \dot{V}_{in}(t') = \dot{V}_{in,Corr1}(t')
\end{aligned} \tag{4.2.7}$$

where $f_{\Delta t}$ is the adaptation factor according to the CFL-criterion, Δt is the preset simulation time step size (s), Δt_c is the required time step size to fulfil the CFL-criterion (s), $\Delta t'_{Corr1}$ is the corrected process-related time step size (s) of *Corr 1* (see e.q. 4.2.3), $\Delta t'$ is the final corrected process-related time step size (s) and $\lceil () \rceil$ is the mathematical notation of the ceiling function of integers. $\dot{V}_{in}(t)$ is the actual influx in the preset time step size (mm/s) and $\dot{V}_{in,i}(t')$ is the adjusted influx within the process-related time step size (mm/s).

4.3 Hydrological network generation including data structures on different scales

Additional methods are developed to generate the hydrological network for computing the flood routing among LSDMs and to model the interlinkages between meso, local and micro scale data structures. In state-of-the-art hydrological numerical models the network represents the interlinked order among three main types of elements: (1) directed stream segments (namely river segments, reservoirs, pipes, ditches or open rills), (2) junction nodes and (3) spatial structures such as subcatchments. The processes in stream segments are computed with flood routing methods. Each stream segment is connected with an inflow and outflow junction node. The junction nodes function as joint connections to set rules of flow redistribution in the network interconnections. Nodes can be directly connected with stream segments or other junction nodes to distribute the flow according to criteria. Subcatchment data structures configure the spatial and temporal parameters of drained areal compartments within the network. Any spatial data structure in the network has to be defined with an explicit position by the order of stream segments and the respective outlet junction node.

The applied method in this work is based on the theory of the Shreve's stream order (Shreve [1967]). The computational order is based on a directed data tree structure with an explicit start and an explicit end according to the stream segments along the main stream on the meso scale. It defines a directed graph with incoming tributaries. Different types of stream segments demand for a differentiation between "virtual" stream segments (auxiliary connections), "real" stream segments (connectors with flood routing features) and reservoir stream segments (connectors with detention and control features).

This primary method is extended in this work by integrating auxiliary stream segments and junctions nodes on the local scale. A directed graph is created to order the overlay data

structures (namely LSDMs) from the upstream source to the downstream target (sink) elements. The developed algorithm prevents the generation of closed loops in circular order among any network element. For each spatial data structure two auxiliary junction nodes and one auxiliary stream segment are generated on-the-fly to form a "base-unit". In figure 4.4 such base-units are depicted with auxiliary elements. A junction node with redistribution function is generated to provide the parametrisation to distribute runoff fractions to different target data structures. The downstream auxiliary node is by default linked to the subcatchment outlet junction node. LSDM data structures are connected with the meso scale subcatchment, but are computed separately. The primary network connections are depicted in the example in figure 4.4 as continuous lines. By these connections an explicit network is defined according to drainage attributes of LSDMs. In hydrological models spatial data structures (like subcatchments) are computed solely with a drainage function to route water to receiving rivers. This approach is enhanced by additional run-on (water uptake) and runoff (redistribution) functions, which are depicted with dotted lines in figure 4.4 for subcatchment (2) and (3). For this subcatchment the overland flow (here defined from sealed areas) is distributed as percentage to LSDM data structures (here: 10 % to swale type 1 and 20 % to swale type 2). The rest is drained to the receiving downstream junction node. To improve the informative value of illustrated flow charts, the auxiliary elements of the base-unit are not depicted in following diagrams. An example of a generated network of LSDMs within a subcatchment of the application study "Moorfleet" is given in attachment D23.

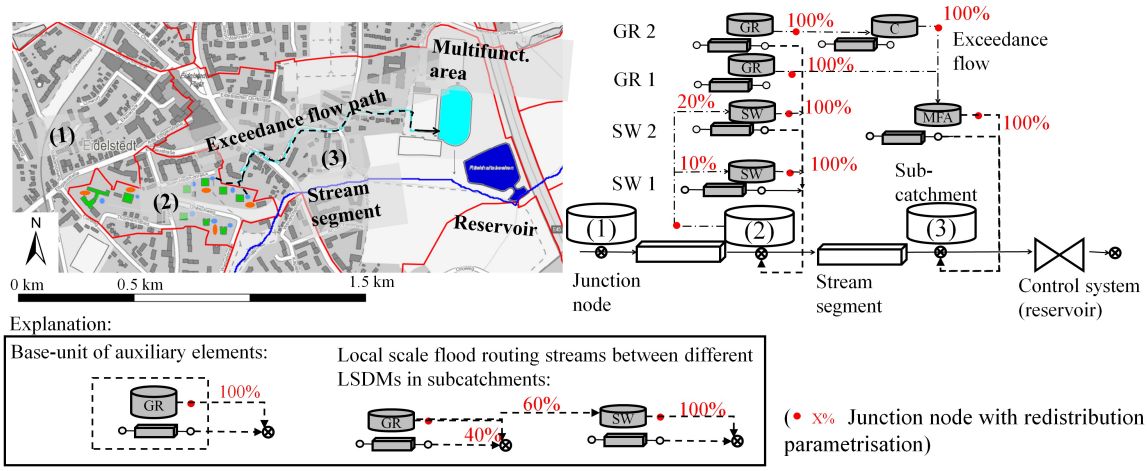

Figure 4.4: Example of a hydrological network which integrates multi-linked data structures including LSDMs (adopted from Hellmers and Fröhle [2017]). (A legend of symbols and acronyms applied in flow charts in this work is given in attachment B.1.)

Modelling the interlinkages between data structures on different scales. To model interlinkages among data structures on different scales, additional methods need to be developed. The subcatchments and stream segments are defined as meso scale data structures, whereas LSDM data structures are linked on the district and local scale. The interconnections between data structures on different scales are illustrated in figure 4.5. New methods are developed

especially for three types of interconnections: (i) the interlinkage between different meso and local scale elements; (ii) the interlinkage among local scale elements on the district scale; and (iii) the interlinkage between subsurface layers on the micro scale. In contrast to an unidirectional flood routing, the interlinkages take into account feedback and backwater effects (indicated with "↔").

For the computation of the flood routing on the meso scale (as depicted in figure 4.5, i and ii), the results of the micro and local scale structures are aggregated according to their location of contribution in the network. The developed method in this work includes the computation of the conveyance of drainage and exceedance flow in a cascade of LSDMs and meso scale retention structures. The exceedance flow is distributed to retention areas in the larger system (for example, multifunctional areas, such as sports fields) or to the drainage network, when the design capacity of the measures on the local scale is exceeded. For this purpose, the developed methodology computes a spatial data structure to receive and distribute water (see "run-on/runoff" routing in figure 4.5, ii, "↔").

The interconnection among subsurface layers is depicted in figure 4.5 (iii) and described in the following chapter 5. This method comprises the computation of multiple linkages between layers of LSDM structures.

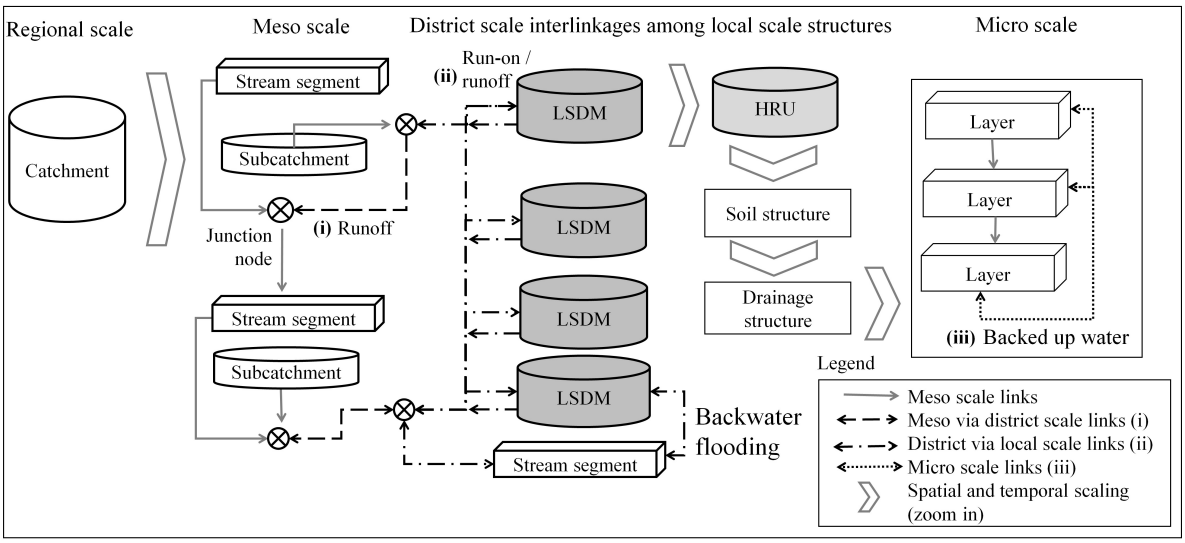

Figure 4.5: Scheme of the hydrological network structure of integrated linkages among elements on different scales. New represented interconnections are (i) among meso via local scale elements, (ii) among local scale elements and (iii) among subsurface layers (adopted from Hellmers and Fröhle [2017]).

5. Methods to model local scale hydrological processes

The second part of the methodology is explained in this chapter to overcome limitations in numerical model features (5) to (8a), which are explained in the tables 3.2 and 3.3 (page 40 ff.). The specific objectives and theoretical approaches are summarised in that aforementioned tables for the computation of hydrological processes on local as well as micro scale and to simulate drainage control functions in LSDMs. To achieve these objectives, the knowledge about hydrological processes in LSDMs from field monitoring studies in nature and physical models in laboratory testing need to be integrated in a physical-based parametrisation. Recently applied empirical or conceptual approaches restrict a transfer of parameter values from calibration conditions to changed ones. This limitation is solved in this work by the definition of a physical-based parametrisation to model multi-layered drainage structures. The strength of this developed part of the methodology is to zoom into the processes (physically, spatially and temporally) to compute the water balances on local scale and to zoom out where conceptual methods are applied to model the processes on the meso scale.

5.1 Algorithm to model hydrological processes in multi-layered structures

Spatial data structures (such as LSDMs) are subdivided into a sequence of layers for modelling the drainage and retention processes. The developed methods to calculate the hydrological processes and the drainage functions per layer are nested in the process-related time step calculation routine (explained in section 4.2). Flux interactions (such as backed up water) between the layers, the drainage features and rainwater harvesting functions are computed. The processes are calculated in three computational loops over the multi-layered structures as illustrated in figure 5.1. The vertically directed processes are computed as fluxes ($\dot{V}$) which is the volume of water (l) drained per unit area of 1 m^2 within the actual process-related time step size $\Delta t'$ ($l/m^2/s$). The horizontally directed processes form a discharge (Q) which is the water volume drained per time unit and given in (m^3/s). The storage volume (V) is the

present quantity of water within the actual process-related time step t' given in (m^3).

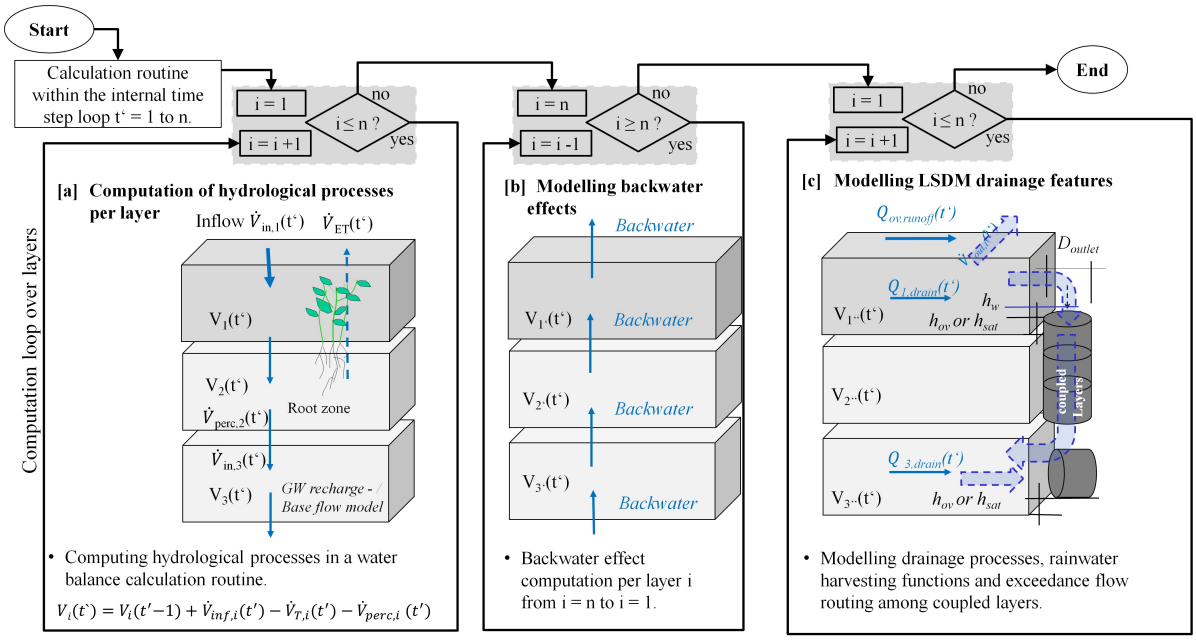

Figure 5.1: Flow chart of the algorithm to model hydrological processes in multi-layers on the spatio-temporal micro scale (adopted from Hellmers and Fröhle [2017]).

.

In the first computational loop of the layers (see figure 5.1, [a]) the processes of interception, evaporation, evapotranspiration, infiltration, percolation (namely exfiltration) and retention per layer are computed. The methods are based on the theoretical approaches described in section 3.2. For every soil layer on the spatio-temporal micro scale the soil water balance equation is solved. The deepest layer is the last soil layer above the groundwater regime or the last layer above a sealing.

In the second computational loop (see figure 5.1, [b]), the flux of backed-up water in the layers is calculated. Such a backwater effect occurs when the flux into the actual soil layer is larger than the respective free storage volume and when the percolated flux is larger than the maximal infiltration rate into the beneath lying soil or groundwater regime. In this case, the surplus water of each layer is rebalanced from the lowest layer to the layers above by a step wise calculation of the saturated water stages. When a complete saturation stage of the layers is reached, surface runoff is generated.

In the third computational loop (see figure 5.1, [c]) the horizontal drainage fluxes are computed. The methods are described in section 5.3 and comprise the computation of the runoff generation in multi-layered structures as well as the modelling of control features.

Differentiation in vertical and horizontal processes A differentiation between vertical and horizontal hydrological processes is done in this work to describe this part of the methodology. An overview of the processes is given in figure 5.2 per micro, local as well as meso scale. On the micro scale, the computations of hydrological processes per layer are executed. Effective vertical hydrological processes are evaporation from open water surfaces ($\dot{V}_{EW}$), in-

terception of water on vegetated surfaces ($\Delta\dot{V}_{I,S}$), transpiration ($\dot{V}_{T,i}$) from rooted soil layers in dependence on the type of vegetation, infiltration ($\dot{V}_{inf,i}$), percolation ($\dot{V}_{perc,i}$) and change in soil water storage (ΔV_i) per layer with the index (i). For the computation of the processes in the multi-layered structures a temporal scaling from the simulation time step size Δt to the process-related micro scale time step size ($\Delta t'$) is performed. The developed methods for the computation of vertical processes as fluxes ($\dot{V}$) on the micro and local scale are described in section 5.2. Horizontal processes like surface runoff, drainage flow, depression losses and flood routing are explained in section 5.3.

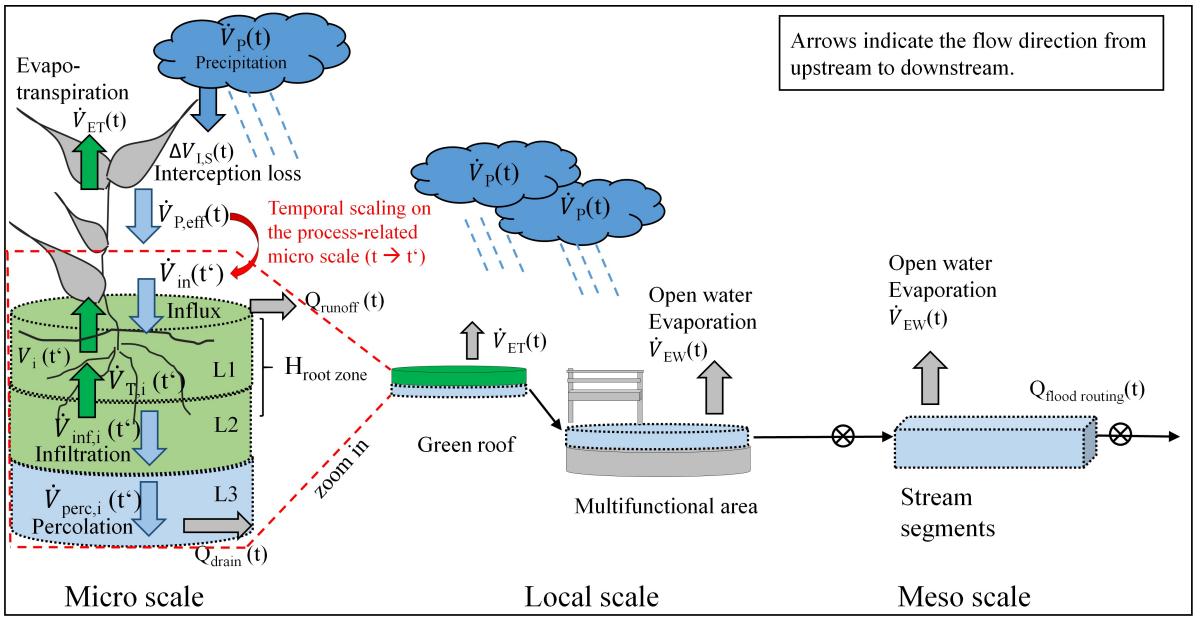

Figure 5.2: Scheme of modelled hydrological processes from vegetated and open water surfaces on micro, local and meso scale.

5.2 Methods to model the vertical hydrological processes on the spatio-temporal micro scale

The developed methods to compute the vertical processes on the spatio-temporal micro scale are described in the order of occurrence from the top to the lowest layers of the structures. First, the actual evapotranspiration is computed by calculating the specific potential evapotranspiration, interception and transpiration losses.

Computing the specific potential evapotranspiration $\dot{V}_{ET,pot}(t)$. The potential evapotranspiration from plants $\dot{V}_{ET,pot}(t)$ is calculated with the "FAO-Standard" approach which is based on the Penman-Monteith theory (see R. G. Allen et al. [1998] and DVWK [1996], p. 54). The input parameters for this approach are the crop factor R (-) to relate the actual vegetation to a grass reference vegetation, the root depth ($H_{root\ zone}$) for each land use class per season and the actual water content ($V_i(t)$) in the root zone per layer (i). The required meteorological input parameters in the model are the daily average values of the air temperature (°C), sunshine duration

in hours (h), average relative humidity (%), average wind speed (m/s) and the precipitation sum per time step size in (mm) on a daily ($\Delta t = 1$ day) or smaller ($\Delta t \leq 5$ minutes) temporal resolution. The specific potential evapotranspiration from vegetated cover is calculated with:

$$\dot{V}_{ET,pot}(t) = \dot{V}_0(t) \cdot R \tag{5.2.1}$$

where $\dot{V}_{ET,pot}(t)$ is the specific potential evapotranspiration from vegetated surfaces (mm), $\dot{V}_0(t)$ is the potential evapotranspiration for a standard grass-reference (see DVWK [1996]; p. 54) and R is the monthly defined crop coefficient for specific vegetation types (-) (see DVWK [1996]; p. 49 ff).

Calculation of the interception storage losses $\Delta\mathbf{V_{I,S}(t)}$. The potential evapotranspiration demand $\dot{V}_{ET,pot}(t)$ is first served by the retained water in the interception storage, while the rest is supplied by the transpiration process. The interception loss is computed on the basis of a single reservoir for the leaf storage as described in the theoretical approach in section 3.2.1 (p. 40) which is comparable to Rutter et al. [1971].

In the approach by Rutter et al. [1971] a differentiation of the canopy dripping rate, stemflow and a change in the surface storage capacity of leafs and stems is defined. The vegetated cover in LSDMs mainly consists of small vegetation and therefore the maximal storage capacity is only parametrised with the leafs, neglecting the smaller stem flow storage capacities in this work. The available interception storage capacity per time step $\Delta V_{I,S,pot}(t)$ (mm) is computed with:

$$\Delta V_{I,S,pot}(t) = V_{I,S,max} - V_{I,S}(t-1) \tag{5.2.2}$$

where $V_{I,S,max}$ is the maximal storage capacity (mm) and $V_{I,S}(t-1)$ is the interception storage content in the previous time step $(t-1)$. The maximal storage capacity $V_{I,S,max}$ is calculated with the following equation using vegetation characteristics:

$$V_{I,S,max} = c \cdot f \cdot \mathrm{LAI} \tag{5.2.3}$$

where LAI is the Leaf Area Index (-), f is the storage capacity per unit of leaf area (mm) (according to Hingray et al. [2014] between $f = 0.05$ and $f = 0.2$) and c is a vegetated cover index (-). In the presented method, the parametrisation of the vegetated cover for the canopy interception and evapotranspiration model are defined according to land use classes for an ideal year per month. Two cases are differentiated to compute the filling and depletion of the interception storage.

Case 1: Filling of the interception storage if $\dot{\mathbf{V}}_\mathbf{P}\mathbf{(t)} \geq \Delta\mathbf{V_{I,S,pot}(t)}$: If the gross precipitation $\dot{V}_P(t)$, reaching the vegetated surface (mm), is larger than the available interception storage capacity $\Delta V_{I,S,pot}(t)$, the interception storage is filled up completely (= $V_{I,S,max}$). In this case, the effective precipitation (throughfall) reaching the soil surface $\dot{V}_{P,eff}(t)$ (mm) is computed in the following manner:

$$\dot{V}_{P,eff}(t) = \dot{V}_P(t) - \Delta V_{I,S,pot}(t) \tag{5.2.4}$$

The interception storage content $V_{I,S}(t)$ is computed with a balance equation. If the specific potential evapotranspiration $\dot{V}_{ET,pot}(t)$ (see eq. 5.2.1) is smaller than the maximal available water in the interception storage (meaning: $\dot{V}_{ET,pot}(t) < V_{I,S,max}$), the actual interception storage content $V_{I,S}(t)$ (mm) is computed with:

$$V_{I,S}(t) = V_{I,S,max} - \dot{V}_{ET,pot}(t)$$

Otherwise, if the specific potential evapotranspiration demand is larger than the available water content in the interception storage (meaning: $\dot{V}_{ET,pot}(t) \geq V_{I,S,max}$), the retained water in the interception storage is completely evaporated ($V_{I,S}(t) = 0$). The rest of the potential evapotranspiration demand is processed in the computation of the transpiration.

$$\dot{V}_{ET,pot,rest}(t) = \dot{V}_{ET,pot}(t) - V_{I,S,max} \tag{5.2.5}$$

where $\dot{V}_{ET,pot,rest}(t)$ is the potential evapotranspiration demand which is potentially served by the transpiration process (see eq. 5.2.9).

Case 2: Depletion of the interception storage if $\dot{\mathbf{V}}_{\mathbf{P}}(\mathbf{t}) < \Delta\mathbf{V}_{\mathbf{I,S,pot}}(\mathbf{t})$: If the gross precipitation $\dot{V}_P(t)$ is smaller than the available interception storage capacity $\Delta V_{I,S,pot}(t)$, less water is added to the interception storage to meet the evaporative demand. In this case, there is no effective precipitation ($\dot{V}_{P,eff}(t) = 0$) reaching the soil. The gross precipitation is completely retained in the interception storage $V_{I,S}(t)$ which serves as source to meet the evapotranspiration demand. If the specific potential evapotranspiration $\dot{V}_{ET,pot}(t)$ is smaller than the available water in the interception storage (meaning: $\dot{V}_{ET,pot}(t) < V_{I,S}(t-1) + \dot{V}_P(t)$), the actual interception storage content $V_{I,S}(t)$ (mm) is computed with:

$$V_{I,S}(t) = V_{I,S}(t-1) + \dot{V}_P(t) - \dot{V}_{ET}(t) \tag{5.2.6}$$

Otherwise, if the specific potential evapotranspiration demand is larger than the available water content in the interception storage (meaning: $\dot{V}_{ET,pot}(t) \geq V_{I,S}(t-1) + \dot{V}_P(t)$), the retained water in the interception storage is completely evaporated ($V_{I,S}(t) = 0$). The residual potential evapotranspiration is computed with:

$$\dot{V}_{ET,pot,rest}(t) = \dot{V}_{ET,pot}(t) - V_{I,S}(t-1) - \dot{V}_P(t) \tag{5.2.7}$$

where $\dot{V}_{ET,pot,rest}(t)$ is likewise the potential evapotranspiration demand which is potentially served by the transpiration process as explained in the following paragraph. In this way, a depletion of the interception storage content ($V_{I,S}(t) \rightarrow 0$) is computed over time. The interception loss rate $\Delta V_{I,S}(t)$ (mm) is the change of the storage content over time.

$$\Delta V_{I,S}(t) = V_{I,S}(t) - V_{I,S}(t-1) \tag{5.2.8}$$

Computing the transpiration $\dot{V}_T(t)$ per layer. The actual magnitude of transpiration is computed on the micro scale for the fractions per rooted soil layer using the available soil water above the wilting point ($V_{WP,i}$) per layer and the rest of the potential evapotranspiration magnitude. The depth of rooted soil is computed over several layers until the absolute root depth is reached. A query checks if the topmost layers are defined as substrate in the rooted zone or free storage layers. The magnitude of potential transpiration $\dot{V}_{T,pot,rooted,i}(t)$ (mm) per rooted layer (i) depends on the available moisture contents in the rooted zone as follows:

$$\begin{aligned} \dot{V}_{T,pot,rooted,i}(t) &= \frac{H_{root,i}(t)}{\Sigma H_{rooted}(t)} \cdot \frac{V_{available,i}(t)}{\bar{V}_{available}(t)} \\ \text{with:} \quad V_{available,i}(t) &= \frac{V_i(t)}{(V_{maxPV,i} - V_{WP,i})} \\ \text{with:} \quad \bar{V}_{available}(t) &= \frac{1}{n} \cdot \sum_{i=1}^{n} \frac{V_i(t)}{(V_{maxPV,i} - V_{WP,i})} \end{aligned} \tag{5.2.9}$$

where $H_{root,i}(t)$ is the rooted depth of layer (i) (mm), $\Sigma H_{rooted}(t)$ is the total rooted depth in the soil horizon (mm), $V_{available,i}(t)$ is the available soil water content in that layer (i) (mm), $\bar{V}_{available}(t)$ is the averaged available soil water content per layer within the overall rooted zone (mm), n is the number of rooted layers (-), $V_i(t)$ is the actual soil water content (mm), $V_{maxPV,i}$ is the volumetric soil water content of the maximal pore volume (%) and $V_{WP,i}$ is the volumetric soil water content up to the wilting point (%). The effective transpiration $\dot{V}_{T,i}(t)$ (mm) per layer (i) is derived from the relation between the residual potential evapotranspiration $\dot{V}_{ET,pot,rest}(t)$ (see eq. 5.2.5) and the transpiration of the rooted soil layers.

$$\dot{V}_{T,i}(t) = \dot{V}_{T,pot,rooted,i}(t) \cdot \frac{\dot{V}_{ET,pot,rest}(t)}{\sum_{i=1}^{n} \dot{V}_{T,pot,rooted,i}(t)} \tag{5.2.10}$$

The actual evapotranspiration is the sum of the losses from the interception storage (see eq. 5.2.8) and the sum of transpiration of the rooted zone.

$$\dot{V}_{ET}(t) = \sum_{i=1}^{n} \dot{\Delta} V_{I,S}(t) + V_{T,i}(t) \tag{5.2.11}$$

Computing the evaporation of open water surfaces $\dot{V}_{EW}(t)$. Open water evaporation $\dot{V}_{EW}(t)$ (mm) is computed solely for the topmost layer (i = 1) with the Penman approach described in DVWK [1996] (p. 30) and applied for stream segments, reservoirs and submerged flood prone areas.

Computing the influx $\dot{V}_{in}(t')$ on the temporal process-related micro scale. The sum of influx $\dot{V}_{(in,i=1)}(t)$ (in l/m^2 = mm) per unit area (m^2) and per time step t into the top layer (i = 1) is calculated with the following equation:

$$\dot{V}_{in,i=1}(t) = \dot{V}_{P,eff}(t) + \dot{V}_{inflow}(t) \tag{5.2.12}$$

where $\dot{V}_{P,eff}(t)$ is the effective precipitation per unit area at time step t (mm), t is the index of the time steps starting with 1 to the entity n (-), $\dot{V}_{inflow}(t)$ is the quantity of run-on flux or inflow flux in (mm) from linked elements (see for example page 62 figure 4.5 i/ii).

To compute the hydrological processes in permeable and thin layers, a time step size on the temporal process-related micro scale in seconds is required. The effective volumetric influx $\dot{V}_{(in)}(t')$ and the time step size $\Delta t'$ are computed according to the CFL-criterion described in section 4.2 (page 57 ff.). The algorithm to compute the process-related time step size ($\Delta t'$) depends on the following parameters: the actual volume of water feeding the substrate layers within the considered time step, the hydraulic conductivity of the media and the available retention capacity in the layer.

Water balance computation on the temporal process-related micro scale. The actual retained water content $V_i(t')$ in the layer is calculated with the following water balance equation per process-related time step size $\Delta t'$:

$$V_i(t') = V_i(t'-1) + \dot{V}_{inf,i}(t') - \dot{V}_{T,i}(t') - \dot{V}_{perc,i}(t') \tag{5.2.13}$$

where $V_i(t')$ is the actual water content per unit area and layer i in that process-related time step t' (mm), i is the index of the layers, $V_i(t'-1)$ is the retained water content in the previous time step (mm), $\dot{V}_{T,i}(t')$ is the actual transpiration per rooted soil layer (mm) (see equation (eq.) 5.2.10), $\dot{V}_{inf,i}(t')$ is the actual infiltration flux in the soil layer i (mm) (see eq. 5.2.18), and $\dot{V}_{perc,i}(t')$ is the actual percolation flux out of the layer i (mm) (see eq. 5.2.19).

Computing the in- and exfiltration processes per layer ($\dot{\mathbf{V}}_{\mathbf{inf,i}}$ and $\dot{\mathbf{V}}_{\mathbf{perc,i}}$). The method to compute the in- and outfluxes of each layer is based on the theoretical approach of the infiltration excess model (IEM) as described in section 3.2.3 (page 42 ff.). In the topmost layer, the quantity of precipitation which exceeds the infiltration capacity is defined as surplus water quantity, which is backed-up in the topmost layer to generate surface runoff. The advantage of the IEM approach is a computation of the dynamical filling and depletion of the reservoir storages of each layer with the index (i). The capacities of infiltration ($c_{in,i}$) and exfiltration ($c_{ex,i}$) depend on the hydraulic conductivity k_i and the hydraulic gradient which is derived from soil characteristics. A parametrisation of the soil using conceptual or empirical constants like in the Horton approach (see Hingray et al. [2014]) is not required in this method. Thereby, the number of potentially undefined input parameters is smaller in the applied approach in this work. The parametrisation is mainly based on physical-based soil characteristics which are available in literature for different soil classifications. For Germany, parameter values of soil characteristics are provided for example in Eckelmann et al. [2005].

The effective volumetric influx $\dot{V}_{(in,i)}(t')$ (in l/m^2 = mm) per process-related time step size $\Delta t'$ into the top layer (i = 1) is calculated with the equation 5.2.12. For deeper layers (i > 1), the actual infiltrated flux into the layer $\dot{V}_{inf,i}(t')$ and the actual percolated outflow of the layer $\dot{V}_{perc,i}(t')$ depend on the magnitude of the potential infiltration $\dot{V}_{inf,pot,i}(t')$ and potential percolation $\dot{V}_{perc,pot,i}(t')$ which are calculated with the infiltration capacity (c_{in}) and

exfiltration capacity (c_{ex}). The computation procedure is given in the following paragraphs. First the infiltration and percolation capacities are computed as follows:

$$c_{in,i} = \frac{k_i \cdot V_{maxPV,i}}{(V_{maxPV,i} - V_{WP,i})} \cdot F_{c,in,i} \tag{5.2.14}$$

$$c_{ex,i} = \frac{k_i \cdot V_{maxPV,i}}{(V_{maxPV,i} - V_{FC,i})} \cdot F_{c,ex,i} \tag{5.2.15}$$

where $c_{in,i}$ is the infiltration capacity (mm/s), k_i is the hydraulic conductivity (mm/s) (see eq. 5.2.20), $V_{maxPV,i}$ is the maximal pore volume (storage capacity) per unit area and layer (mm), $V_{WP,i}$ is the volumetric soil water content defining the wilting point per unit area (mm)[1], $F_{c,in,i}$ is an optional calibration factor of the infiltration capacity (-). $c_{ex,i}$ is the exfiltration capacity (mm/s), $V_{FC,i}$ is the volumetric soil water content of water defining the field capacity per unit area (mm) and $F_{c,ex,i}$ is an optional calibration factor of the exfiltration capacity (-). The calibration factors $F_{c,in,i}$ and $F_{c,ex,i}$ are by default equal to 1. An adjustment is done for soil material with deviating characteristics using a calibration procedure. The magnitude of the potential infiltration and percolation fluxes are calculated with the following equations:

$$\dot{V}_{inf,pot,i}(t') = c_{in,i} \cdot (1 - \frac{V_i(t')}{V_{maxPV,i}}) \tag{5.2.16}$$

$$\dot{V}_{perc,pot,i}(t') = c_{ex,i} \cdot (\frac{V_i(t') - V_{FC,i}}{V_{maxPV,i}}) \tag{5.2.17}$$

where parameters are defined per layer i and per process-related time step t', $\dot{V}_{inf,pot,i}(t')$ is the potential infiltration flux (mm/s), $V_i(t')$ is the actual water content (mm) and $\dot{V}_{perc,pot,i}(t')$ is the potential percolation flux according to the soil characteristics (mm/s). Further on, the effective infiltration and percolation fluxes depend on a differentiation between the layers ($i = 1$ to $i = n$) in the following form:

$$\dot{V}_{inf,i} = MIN \begin{cases} \dot{V}_{in,1}(t') & if\ i = 1 \\ \dot{V}_{perc,i-1}(t') & if\ i > 1 \\ \dot{V}_{inf,pot,i}(t') & if\ i > 1 \end{cases} \tag{5.2.18}$$

$$\dot{V}_{perc,i} = MIN \begin{cases} 0 & \textit{if layer i is sealed} \\ 0 & if\ V_i(t') < V_{FC,i} \\ V_{free,i}(t') = V_i(t') - V_{FC,i} & \\ \dot{V}_{perc,pot,i}(t') & \end{cases} \tag{5.2.19}$$

where $i = 1$ is the index of the topmost layer, $\dot{V}_{inf,i}(t')$ is the actual infiltration flux in the soil layer i (mm/s), $\dot{V}_{in,1}(t')$ is the effective influx in the topmost soil layer (mm/s), $\dot{V}_{perc,i-1}(t')$ is the percolation flux from the layer above (mm/s), $\dot{V}_{perc,i}(t')$ is the actual percolation flux

[1] The volume of water per unit area is given in litre per unit area (l/m^2) $\widehat{=}$ (mm). The value is divided per layer thickness to provide the volumetric soil water content in (mm/mm) or (%).

(mm/s), $V_i(t')$ is the actual soil water content (mm) and $V_{free,i}(t')$ is the actual drainable water quantity (mm).

Computation of the vertical directed hydraulic conductivity. The parametrisation and computation of the hydraulic conductivity is significant for modelling the soil water processes, but only few approaches are available. The discussion in section 3.2.3 (page 42) about theoretical approaches to model subsurface processes revealed the "hydraulic radius theory" (namely the Kozeny-Carman (KC) approach) as applicable for achieving the objectives of this work. It is based on the assumption that the porous soil is treated like a bundle of capillary tubes of equal lengths. Several modifications of the KC equation exist in literature and the following form is applied in this work:

$$k_i = c_0 \cdot \frac{g}{\nu_w} \cdot \frac{n^3}{(1-n)^2} \cdot (\frac{d_m}{6})^2 \tag{5.2.20}$$

where k_i is the hydraulic conductivity (mm/s), g is the acceleration of gravity ($9.81\,\mathrm{m/s^2} = 9810\,\mathrm{mm/s^2}$), n is the porosity of the soil (%), d_m is the mean particle size (mm) and ν_w is the kinematic viscosity of water (for a temperature of 15°C it is $1.15\,\mathrm{mm^2/s}$)[2]. The Kozeny's coefficient c_0 ranges between 0.500 to 0.167 (see Carman [1937]). As the porous material used within the structures of LSDMs may show differing hydraulic conductivities than the substrate of natural soil analysed by Carman [1937] (as described in Bear [1988]), this range is tested in laboratory studies and the results are presented in section 8.1.

5.3 Methods to model drainage features in LSDMs

The computation of LSDM drainage features is nested in the loop of process-related time steps as a third layer calculation routine (see figure 5.1, [c] on page 64). In this computational loop three processes are modelled. First, the micro scale runoff generation is calculated. Secondly, the horizontal and vertical drainage features in coupled layers are computed. Thirdly, the functions of control systems and rainwater harvesting are activated in this algorithm.

5.3.1 Computation of the horizontal processes in layered structures

A controlled flow routing among porous and storage layers within LSDMs improves the retention capacity. For example, the water is drained from a topmost storage layer to an underground storage layer as exemplified in figure 3.3 (page 46) for a swale-filter-drain system. The drainage from one layer into another layer is defined as coupled layer flow. It is computed if a coupled layer is defined and a saturation stage is reached. This case is true, when the actual water content in the layer reaches a defined saturation stage with the water level height h_{sat} in porous media or an overflow height in storage layers h_{ov} (see figure 5.1, [c]). The saturation stage or overflow height varies according to the design of the drainage layer.

[2] The KC equation is also known with the absolute dynamic viscosity of water (μ_w) with the ratio: $\nu = \frac{\mu_w}{\rho}$ where ν is the kinematic viscosity and ρ is the density of water.

As supplementary explanation, the method to compute h_{sat} on the basis of geometries is described in attachment B.2. The developed method supports the modelling of recently designed technologies which increase the retention time in LSDMs for instance by a higher roughness of applied materials or prolonged flow paths in the drainage layers.

In a LSDM structure with coupled layers, it is checked if the upper layer exceeds its saturation stage. In that case, the water is drained from that layer as exceedance flux to the receiving layer. The exceedance water flux from the source layer is drained to the receiving layer partly or completely according to the free storage volume in that time step. If the water can not be drained completely to the receiving layer, the rest remains in the actual layer and may create a backed-up water flux in the direction of the layers above.

The drainable water depends on the effective water level in the layer and the drainage attributes of the structure. For porous media the pore volume is taken into account to compute the effective water level. An overflow hight increases the retention capacity in the layer because the water is not drained directly but is retained to a certain quantity. The overflow hight is defined according to the geometry of the structure.

The flow routing processes in the drainage layer depend on the structure and retention characteristics. Two methods are defined to compute these processes. One method is developed to model the flow routing processes within a free storage layer made up of sealed materials (for example, plastic) which drains the water to an outlet. Another method is developed to compute the flow routing in a drainage layer made up of porous media, which is based on Darcy's law.

Computation of the flow routing processes in a free storage layer. The flow routing processes in a free drainage layer are computed for three cases. First, the flow over a crest height h_{ov} through an outlet is computed using the Poleni approach (see Bollrich [2013]; p. 397). Secondly, the maximal flow capacity is calculated with the Darcy-Weisbach approach by assuming a complete saturated stage. Thirdly, the flow through a drainage layer with retention characteristics is computed using the retention coefficient $k_{ret,drain,i}$. Because more than one of these cases may be present in a drainage layer at the same time, the actual flow ($Q_{drain,i}(t')$) is computed as minimum of these cases:

$$Q_{drain,i}(t') = MIN \begin{cases} \frac{2}{3} \cdot \pi \cdot D_{outlet,i} \cdot \mu \cdot \sqrt{2 \cdot g} \cdot (h_{w,i}(t'))^{\frac{3}{2}} & (Poleni\ approach) \\ \frac{\pi \cdot (D_{outlet,i})^2}{4} \cdot \sqrt{2 \cdot g \cdot I_{drain,eff,i} \cdot \frac{D_{outlet,i}}{\lambda_i}} & (Darcy - Weisbach\ approach) \\ \frac{h_{w,i}(t')}{k_{ret,drain,i}} \cdot A_{drain,i} & (Retention\ layer\ approach) \end{cases} \quad (5.3.1)$$

where $Q_{drain,i}(t')$ is the outflow (mm^3/s), $D_{outlet,i}$ is the diameter of the outlet (mm), $g = 9.81 \cdot 10^3$ (mm/s^2) is the standard acceleration due to gravity, $h_{w,i}(t')$ is the actual water level in the layer above an overflow crest height (mm), $k_{ret,drain,i}$ is the retention coefficient in the drainage layer (s) (see eq. 5.3.3), λ is the friction coefficient (-) (see eq. 5.3.4), $I_{drain,eff,i}$ is the effective gradient taking into account the actual water level and the gradient of the construction (-) and $A_{drain,i}$ is the drained area per outlet (mm^2). On the basis of the technical guideline in BWK [2009] three values for the overflow coefficient (μ) (-) are taken into account in this work. The values

are obtained from Bollrich [1996] and Knapp [1960] for a weir with rectangular form using the following conditions and equations:

$$\begin{aligned} &\textit{if overflow crest height } (h_{ov}) = 0: && \mu_i = 0.577 \\ &\textit{if } h_{ov,i} > 0 \textit{ and } h_{ov,i} > h_{w,i}(t') \cdot 0.167: && \mu_i = 0.61 \cdot (\tfrac{h_{w,i}(t')}{\pi \cdot h_{ov,i}})^{0.0544} \\ &\textit{if } h_{ov,i} > 0 \textit{ and } h_{ov,i} \leqslant h_{w,i}(t') \cdot 0.167: && \mu_i = 0.48 \end{aligned} \tag{5.3.2}$$

where $h_{ov,i}$ is the overflow crest height (mm). The retention coefficient in the drainage layer ($k_{ret,drain,i}$) is a derivative of the flow velocity ($v_{drain,i}$) which is calculated according to the Darcy-Weisbach approach (see eq. 5.3.3). The friction coefficient (λ_i) is computed with the Colebrook equation (see eq. 5.3.4).

$$k_{ret,drain,i} = \frac{L_{drain,i}}{v_{drain,i} \cdot 3600} \textit{ with } v_{drain,i} = \sqrt{\frac{1}{\lambda_i} \cdot g \cdot D_{drain,i} \cdot I_{drain,i}} \tag{5.3.3}$$

$$\frac{1}{\sqrt{\lambda_i}} = -2 \cdot log_{10} \cdot (\frac{R_{drain,i}}{D_{outlet,i} \cdot 3.71} + \frac{2.51}{Re \cdot \sqrt{\lambda_i}}) \tag{5.3.4}$$

where $L_{drain,i}$ is the longest flow path in the drainage layer (mm), $R_{drain,i}$ is the roughness in the drainage layer (mm), Re is the Reynolds number (-), $v_{drain,i}$ is the velocity of flow in the layer calculated according to the Darcy-Weisbach equation (mm/s), $D_{drain,i}$ is the diameter or height of the drainage layer (mm) and $I_{drain,i}$ is the gradient of the drainage layer (-). The term $\frac{2.51}{Re \cdot \sqrt{\lambda_i}}$ is approaching zero for turbulent flow conditions what is the case in the layered drainage structures considered in this work.

Computation of the flow routing processes in a porous drainage layer. The flow routing in a drainage layer made up of porous media is modelled with a concept based on the Darcy's law. Porous media is defined in this work by material with a pore volume less then 80 %, otherwise it is defined as a free storage layer. For the computation of flow in saturated soils the Darcy's law is applied in the following form:

$$Q_{drain,i}(t') = k_{f,substr,i} \cdot I_{drain,eff,i} \cdot (h_{w,i}(t') \cdot W_{drain,i}) \tag{5.3.5}$$

where $Q_{drain,i}(t')$ is the outflow of the drainage layer (mm^3/s) per process-related time step t' and layer i, $k_{f,substr,i}$ is the saturated hydraulic conductivity in porous media (mm/s) (see eq. 5.3.7), $I_{drain,eff,i}$ is the effective gradient taking into account the actual water level and the gradient of the construction (-), $h_{w,i}(t')$ is the effective water level in the layer above the overflow crest height (mm) and $W_{drain,i}$ is the width of the drainage area (mm). The hydraulic gradient is computed for an unsaturated stage (if $h_{w,i}(t') < h_{sat}$) and for a saturated stage (if $h_{w,i}(t') \geq h_{sat}$) with the following equations:

$$I_{drain,eff,i} = \begin{cases} I_{drain,i} + \frac{h_{w,i}(t')}{L_{drain,i}} & (\textit{if } h_{w,i}(t') < h_{sat}) \\ I_{drain,i} + \frac{(h_{w,i}(t'))^{f_{I,sat}}}{L_{drain,i}} & (\textit{if } h_{w,i}(t') \geq h_{sat}) \end{cases} \tag{5.3.6}$$

where $I_{drain,eff,i}$ is the effective gradient for the saturated flow computation (-), $I_{drain,i}$ is the gradient of the construction (-) and h_{sat} is the water level of the saturation stage in (mm) computed on the basis of the geometry of the structure (see attachment B.2). Exceedance flux is generated when the water level in the porous media reaches a saturation stage. At that point, the hydraulic head and thus the flow velocity is enlarged. The factor $f_{I,sat}$ is applied to model the increased flux. The value varies according to a change in the saturated flow behaviour which is caused by variations in density of the material. This approach is derived within this work and evaluated with physical model tests in laboratory. The results are presented in section 8.1 (page 117 ff.).

The hydraulic conductivity $k_{f,substr,i}$ in porous media is computed with a relation using the effective gradient $I_{drain,eff,i}$ and the flow path length $L_{drain,i}$ in the following form:

$$k_{f,substr,i} = t_{c,1} \cdot (I_{drain,eff,i})^{-t_{c,2}} \cdot L_{drain,i} / \Delta t' \tag{5.3.7}$$

where $k_{f,substr,i}$ is the saturated hydraulic conductivity for the horizontal flow velocity in the drainage layer (mm/s), $I_{drain,eff,i}$ is the effective hydraulic gradient taking into account the actual water level and the gradient of the construction (-), $L_{drain,i}$ is the longest flow path in the drainage layer (mm), $\Delta t'$ is the time step size (s) and the coefficients $t_{c,1}$ (=3.64) and $t_{c,2}$ (=0.37) are derived on the basis of results from the aforementioned physical model in laboratory testing.

5.3.2 Computation of unsteady loss rates of depressions on impervious surfaces

Water is retained in depressions on surfaces according to the topography and characteristic roughness. The retention takes place by filling local or micro reliefs on impervious surfaces with a percentage of precipitation. The retained water is subsequently evaporated and is considered as "depression loss" in the water balance computation. Exceeding inflow to a depression storage leads to overflow that can feed other depressions further downstream or contributes to the surface runoff reaching the outlet of the area. Depression storage capacities per unit area for different types of surfaces and varying slopes are summarised in Hingray et al. [2014] (p. 135). Although, knowledge is obtained in these parameters, the integration of unsteady methods in numerical models is hardly realised. Such a weakness existed as well in the hydrological numerical model which is applied in this work where a steady (time-independent) constant value was implemented to represent the depression storage and evaporation loss rate. Such a steady depression loss constant is not regarded as an up-to-date solution in hydrological catchment models.

In this work, a method is presented to use surface-related parameters such as the slope of the area, surface characteristics and a time-dependent filling and emptying rate of the depression storages on impervious surfaces. A method based on the approach of Kidd [1978], which is described in Hingray et al. [2014] (p. 135), is extended in this work. The maximum depression

storage is computed with the equation:

$$S_{D,max} = k \cdot I_0^{-0.5} \tag{5.3.8}$$

where $S_{D,max}$ is the maximal depression storage capacity (mm), I_0 the mean slope of the terrain and k (mm) is a depth coefficient that depends on the type of surface, for instance, 0.07 for an impervious surface and 0.28 for a permeable surface. The computation of the depression loss rate per time step is derived with the approach of Linsley et al. [1988] (p. 223):

$$\Delta S_D(t) = S_{D,max}(1 - exp(-\frac{\dot{V}_{in,eff}(t)}{S_{D,max}})) \tag{5.3.9}$$

where $\Delta S_D(t)$ is the quantity of water stored in depressions since the beginning of the event, $S_{D,max}$ is the maximal depression storage capacity (mm) and $\dot{V}_{in,eff}(t)$ is the effective influx (mm). A temporal duration defines the emptying rate after a storm event. The free space in the depression storage is filled up again during the following rainfall event. This method accomplishes a dynamic computation of depression loss rates to model several events in one simulation run. It is valid for the computation of loss rates from depression storages on surfaces of spatial structures on local (such as LSDMs) and meso scale subcatchments.

5.3.3 Modelling rainwater harvesting and drainage control functions

The retained water quantity in LSDMs comprises the infiltrated portion of the effective precipitation (such as in green roof structures), the water drained into the LSDM by linked areas such as in cisterns and the water flowing into the LSDM from linked streams (for example in case of backwater flooding). To mitigate the magnitude of flooding by uncontrolled exceedance flow over the surface, a cascade of several LSDMs with control functions is suggested. For example green roofs, cisterns and multifunctional areas in a backwater affected catchment are equipped with control valves as illustrated in figure 5.3. In that example, a low rainfall intensity is forecasted for subcatchment (1) and a high rainfall intensity is forecasted for subcatchment (2). The pre-emptying functions of the green roof structure and the multifunctional area are activated only for subcatchment (2) to enlarge the storage capacity before the rainfall event occurs. The valves in subcatchment (2) are closed before the storm event begins. A pre-emptying time duration defines the opening and closing functions. In subcatchment (1) the water storage content in LSDMs is retained for rainwater harvesting purpose, because it is not forecasted that the storages are filled up completely during that storm event.

The control functions for pre-emptying storages are driven by (forecasted) precipitation time series. The theoretical approach is described in section 3.3.2 (page 46). The precipitation data from weather or radar stations are intersected with the spatial data structures in the hydrological network. For continuous water supply, a minimum water level is retained in the rainwater harvesting devices. The developed algorithm to model this control function comprises a pre-processing of data which is performed for each cycle run. A cycle run is executed per event for shortterm or per year for longterm simulation runs. The input values

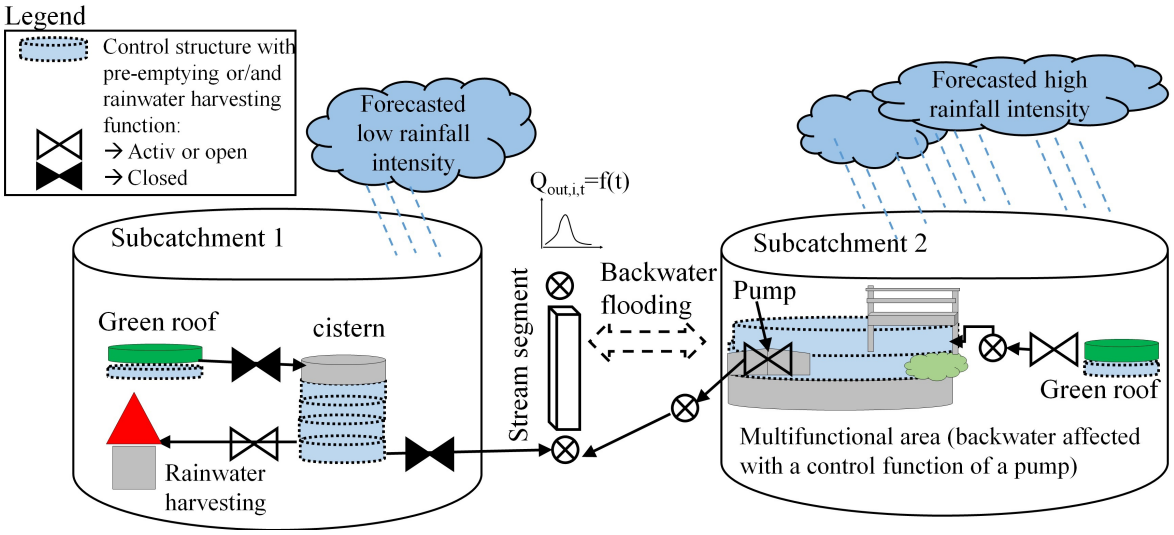

Figure 5.3: Scheme of the activated control functions in LSDMs. The control function settings are illustrated in the status before a storm event is forecasted with pre-emptying function.

are determined for "ideal yearly" rainwater harvesting time series. The advantage of an ideal yearly rainwater harvesting time series with a daily resolution is the differentiation of working and weekend days for different water utilizations. Pre-emptying functions and driver time series for operational retention systems are defined likewise as time series for storage roofs or multifunctional areas.

The activation of control functions is done in the data processing phase of the numerical model and depends on the control system criteria. In case of LSDMs, the drivers of a control function are primarily precipitation time series on spatial elements. Radar and weather station data are processed on the subcatchment (meso) scale. A control function is assigned per specified storage layer and labelled with a "key-name". The control function parametrisation using the "key-name" of the layer is set as parent part of the model data structure, while the individual LSDM and HRU data structures are checked for matching such key-names of layers. The flow chart to illustrate the method of the data pre-processing and the flow chart to explain the method to model rainwater harvesting as well as pre-emptying functions are given in attachment B.3.

The definition of control functions per layer with specified "key-names" facilitates a flexible data structure by using these layer functions in different types of LSDMs throughout the overall numerical model. An LSDM data structure is defined with multi-layers, whereas only the layers with the parameters of control functions, are activated for this computation. The parameters of the control functions are adjusted in a global manner by using the key-names of layers. In this way, the data pre-processing for the user to assign different control functions to LSDMs is kept small.

6. Methods to model flood routing and control systems in backwater affected catchments

In the third part of the methodology, the weaknesses and limitations of the required model features (8b) to (10) for computing the flood routing on local scale, control functions in streams and backwater effects are overcome. The specific objectives and theoretical approaches of the developed methods are summarised in table 3.4 on page 48.

The procedure to determine the magnitude and time of flow along a stream on the basis of the stream characteristics is defined as flood routing. It describes the propagation of discharge through streams, whereby translation and retention processes along the stream changes the shape of the hydrograph from an upstream to a downstream point. The literature review in chapter 2 revealed current weaknesses in state-of-the-art hydrological methods to model backwater effects and the local scale flood routing among LSDMs. These weaknesses and limitations are solved in this work. The developed methods are applicable for local as well as for meso scale hydrological numerical modelling and based on using the physical characteristics of the stream profiles to model the flood routing. A comparison of hydrological flood routing approaches in section 3.4 (page 47 ff.) pointed out, that the approach of Kalinin & Milyukov is applicable to be extended for achieving the objectives of this work. The developed flood routing method is described in the following section 6.1. Modelling control systems (for example, weirs, tide gates, retention or detention reservoirs) require the integration of control functions in the hydrological numerical model. These functions are described in section 6.2 with a focus on control structures in low lying (backwater affected) lands. The criteria of control functions depend on preset or process-related driver time series in the hydrological network. The output of the flood routing computation and the control system functions are used as well in the developed method for modelling backwater effects in streams and areas. This last part of the methodology is described in section 6.3. The developed methods accomplish the computation of backwater effects in streams and in spatial data structures (namely flood prone areas or LSDMs) on the local as well as meso scale.

6.1 Methods to model flood routing in free flow conditions

The flood routing in free flow conditions describes the flood wave propagation in streams which are not affected by downstream conditions. This means that an afflux of retained water in front of obstacles downstream of the considered stream segment is assumed to have no impact on the upstream segments. Under these assumptions no backwater effect is computed.

In numerical modelling, a stream segment is a linear data structure with a main flow direction from upstream to downstream. It can have a size of a ditch or pipe on local scale or a river stream segment on the meso scale. Each linear data structure is defined by one upstream and different downstream junction nodes as described in the first part of the methodology about the network generation in section 4.3 on page 60. Tributary stream segments drain from upstream into a junction node of a main stream segment. The results of linear data structures are given per downstream junction node. One cross section is defined per stream segment in the main flow direction from upstream to downstream point of view.

This work resolves shortcomings in flood routing computations of local and district scale linear streams (see figure 6.1 (a)). One objective is the definition of a parsimonious and applicable parametrisation for regional scale catchment modelling. The developed method uses the parameters of primary geometrical profiles (trapezoidal, rectangular or circular) with a low number of input parameters to model the directed flood routing among LSDMs with the approach of Kalinin-Milyukov (KM). Each stream segment is represented as a single reservoir and therefore this method is labelled as "KM1"-flood routing method and is described in the following section 6.1.1.

If natural and irregular profiles are present in stream segments and detailed profile data is available, another approach using an extended flood routing method is applicable which includes a different parametrisation of main channel and forelands. It results in a subdivision of each profile of a stream segment into five reservoirs. Therefore, the method is labelled as "KM5" flood routing method and is described in section 6.1.2.

For regional scale catchment modelling (>100 km^2) the integration of a detailed description of single sewer or drainage segments is still not feasible to model flood routing as described in Salvadore et al. [2015] (p. 72). For such large scale modelling, the data processing shall be limited to provide a parsimonious and applicable parametrisation. Therefore, a spatially aggregated method is applied to model the (piped) flood routing on the meso scale with a conceptual approach if no detailed parametrisation is applicable (see section 6.1.3).

The application cases of the KM1, KM5 and the spatially aggregated flood routing methods are depicted in figure 6.1 with the labels (a), (b) and (c). The sheet flow runoff routing over natural surfaces as well as inter- and baseflow runoff routing are modelled with a conceptual instantaneous unit hydrograph method combined with a time-area-function. These methods are described in a previous work (see for example Hellmers [2008]).

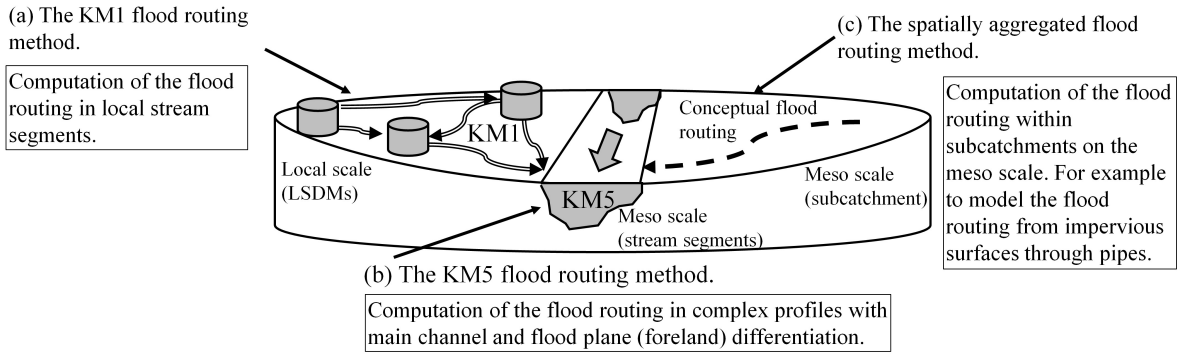

Figure 6.1: Overview of the defined flood routing methods and their designated scales for application.

6.1.1 The single reservoir flood routing method "KM1"

The KM1 flood routing method is based on the principle to define a quasi-stationary state with a waterlevel-volume-discharge-relation (WVQ-relation) per characteristic segment length L_c of the stream according to the approach of Kalinin and Milyukov [1957]. The theoretical approach is described in section 3.4.1 on page 48. Each stream segment is divided in a cascade of n reservoirs with a characteristic length L_c and the coefficient K_c. The WVQ-relations for different water levels in the stream segment are defined with an interpolation between supporting points of water level heights. This results in a division of the bankfull water level height H_{full} (m a.s.l) into (n_{wvq}) steps with a water level difference ΔH (m).

The input parameters in the KM1-method includes geometrical and roughness data. For a rectangular cross-section, the bed level width L_{bed} (m) and bank gradient I_{bank} (-) are required. For a circular cross-section, the diameter D_{stream} (m) needs to be given. When the method of geographical data mapping (see section 4.1 on page 55) is activated, the linear stream segment length L and slope of the stream I_S are derived on-the-fly from imported GIS-based data of the upstream and downstream junction nodes. Optionally, the length and gradient can be defined per stream segment manually. The stream segment length may comprise meandering prolongation which is taken into account by a factor f_L (-).

Three calculation routines are integrated in the KM1 flood routing method to compute the flow velocity in stream segments. The appropriate calculation routine is selected according to the stream segment's profile and data availability. In the first routine, stream segments with a circular profile are computed with the Darcy-Weisbach approach. Stream segments with rectangular or trapezoidal (angular) profiles are computed in the second routine likewise with the Darcy-Weisbach approach or in a third routine with the Manning-Strickler approach. The equivalent sand roughness k_s in (m) using the Darcy-Weisbach approach or the roughness K_{st} ($m^{1/3}/s$) using the Manning-Strickler approach are input parameters. Values of the equivalent sand roughness k_s in (m) are given in BWK [2009]. The Manning's roughness coefficients are discussed and provided in Arcement and Schneider [1989].

These three calculation routines in the algorithm of the KM1 flood routing method are illustrated in the flow chart in figure 6.2. The calculation routines compute the flood

routing in linear stream segments of rivers or among LSDMs where the flood routing occurs in "on-the-fly" created streams. The creation of these auxiliary streams on the local scale is described in the first part of the methodology in section 4.3 on page 60. The details of the calculation routines and formal parameters are described in the following paragraphs. A differentiation is done between actual input parameters (also known as arguments) and formal parameters. Formal parameters are processed as input and output in calculation routines in the algorithm. The computation of formal parameters in the algorithm for angular profiles is described first. Thereafter, formal parameters to model the flood routing in circular profiles are explained. Actual input parameters are the arguments given by the modeller to define specific characteristics of the structures to be modelled (for example geometry or material characteristics). A calculation routine which is repeated within an algorithm is named "computational loop".

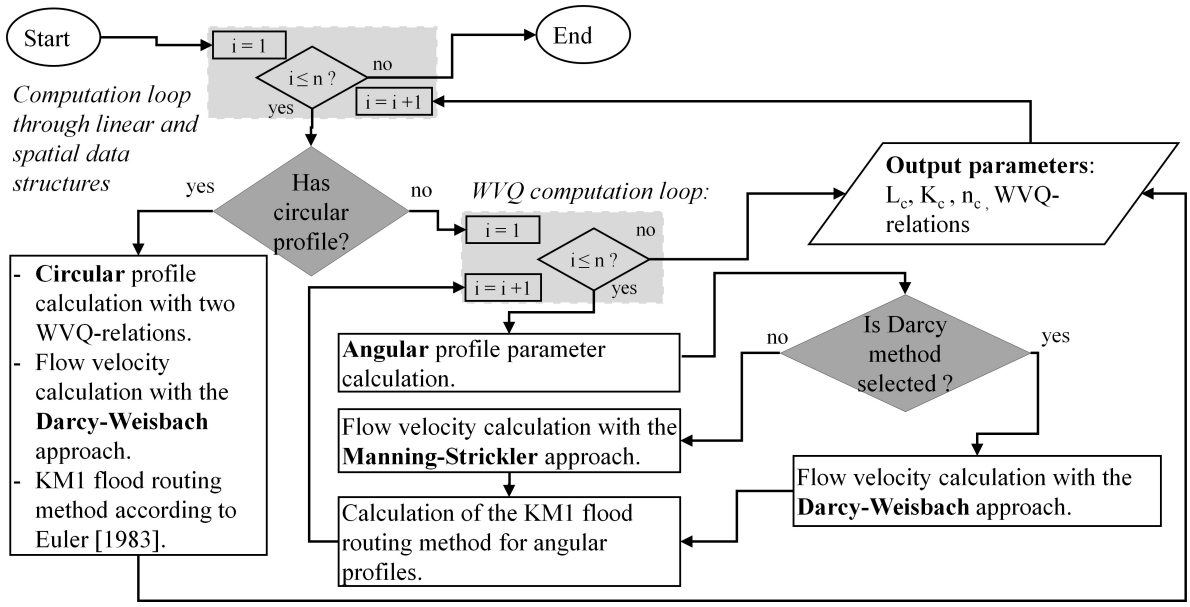

Figure 6.2: Flow chart of the algorithm to compute the flood routing parameters of the KM1-method. (The explanation of symbols is given in attachment B.1.)

Computation of the parameters to model the flood routing in angular profiles. For angular profiles the computation of the WVQ-relations starts with a minimum water level height which is increased step wise with ΔH (m a.s.l.) until reaching bankfull height. The computational loop begins with the index $i_{wvq} = 1$ and ends with $i_{wvq} = n_{wvq}$ to calculate the formal parameters of the WVQ-relations:

$$W_{wvq} = i_{wvq} \cdot \Delta H$$
$$V_{wvq} = L_s \cdot A_{wvq}$$
$$Q_{wvq} = v_{wvq} \cdot A_{wvq} \qquad (6.1.1)$$

where W_{wvq} is the water level (m a.s.l.), A_{wvq} is the wetted cross-section (m^2) (see eq. 6.1.2), V_{wvq} is the volume of water in the stream segment (m^3), Q_{wvq} is the discharge at the downstream

section (m^3/s) per supporting point i_{wvq} of the WVQ-relations, ΔH is the water level step size (m) between supporting points, L_s is the stream segment length (m) and v_{wvq} is the flow velocity (m/s) (see eq. 6.1.3 and eq. 6.1.7). Formal parameters of intermediate computations are the wetted cross-section A_{wvq} (m^2), the wetted perimeter P_{wvq} (m) and the hydraulic radius $R_{hyd,wvq}$ (m) which are calculated as follows:

$$\begin{aligned} A_{wvq} &= (L_{bed} + I_{bank} \cdot W_{wvq}) \cdot W_{wvq} \\ P_{wvq} &= L_{bed} + 2 \cdot W_{wvq} \cdot \sqrt{1 + (I_{bank})^2} \\ R_{hyd,wvq} &= A_{wvq} / P_{wvq} \end{aligned} \tag{6.1.2}$$

where L_{bed} is the bed level width (m) and I_{bank} is the bank gradient (-) of the angular profile. The flow velocity v_{wvq} in the stream is computed on the basis of the Darcy-Weisbach approach using the Colebrook-White's equation (see eq. 6.1.3) or using the approach of Manning-Strickler (see eq. 6.1.7).

Computation of the flow velocity using the Darcy-Weisbach approach. The flow velocity v_{wvq} (m/s) in stream segments is computed with the Darcy-Weisbach approach for angular profiles in the following form:

$$v_{wvq} = \sqrt{\frac{8 \cdot g \cdot R_{hyd} \cdot I_S}{\lambda}} \tag{6.1.3}$$

where I_S is the slope of the stream segment (-), g is the standard acceleration due to gravity ($\approx 9.81\,m/s^2$) and the friction factor λ (namely flow coefficient) is based on using the roughness approach of Colebrook & White with the equivalent sand roughness k_s in (mm) (see eq. 6.1.4). The basic equation by Colebrook & White is developed for pipe flows. It is rewritten by correlating the diameter of the closed stream (for example a pipe) D_{stream} to the hydraulic radius of an angular profile by $R_{hyd,wvq} = D_{stream}/4$ and using a shape coefficient f to compute the friction factor (BWK [2009]):

$$\begin{aligned} &\frac{1}{\sqrt{\lambda}} = -2.03 log\left(\frac{2.51}{f \cdot Re\sqrt{\lambda}} + \frac{k_s}{f \cdot 14.84 \cdot R_{hyd,wvq}}\right) \\ &\text{with: } Re = 4 \cdot v_{wvq} \cdot R_{hyd,wvq} / \nu \end{aligned} \tag{6.1.4}$$

where λ is the Darcy-Weisbach friction factor (-), ν is the kinematic viscosity of water ($\approx 1.3 \cdot 10^{-6}\ m^2/s$ at 10°C). The shape coefficients are computed according to the profile geometries (BWK [2009]):

$$\begin{aligned} f &= 1.0 && \text{for circular profiles} \\ f &= 0.9 - 0.38 \cdot e^{-5 \cdot W_{wvq}/b_{bed}} && \text{for rectangular profiles} \\ f &= 1.276 \cdot (W_{wvq}/b_{surf})^{3/20} && \text{for triangular profiles} \\ f &= 1.13 \cdot (R_{hyd}/b_{bed})^{1/4} && \text{for trapazoidal profiles} \end{aligned} \tag{6.1.5}$$

where b_{bed} (m) is the width of the stream segment at the bed level and b_{surf} (m) is the width of the stream segment at the bankfull level. The flow in the stream segments is characterised as turbulant flow ($Re > 2320$) and therefore, the first term in eq. 6.1.4 approaches to zero. The equation is applied in the following form:

$$\frac{1}{\sqrt{\lambda}} = -2.03 log(\frac{k_s}{f \cdot 14.84 \cdot R_{hyd}}) \tag{6.1.6}$$

Computation of the flow velocity using the Manning-Strickler approach. For angular profiles the Manning-Strickler approach is applied in the following form to compute the flow velocity in a stream segment:

$$v_{wvq} = K_{st} \cdot (R_{hyd,wvq})^{2/3} \cdot (I_S)^{1/2} \tag{6.1.7}$$

where K_{st} is the Manning-Strickler roughness ($m^{1/3}/s$), $R_{hyd,wvq}$ is the hydraulic radius (m) and I_S is the bed level gradient of the stream segment (-).

Computation of the characteristic length L_c for angular profiles. The characteristic length $L_{c,wvq}$ (m) per supporting point of each WVQ-relation is calculated with the approach of Kalinin & Milyukov. A differentiation is done here for angular and circular profiles of stream segments. For angular profiles the equation is as follows:

$$L_{c,wvq} = \frac{\Delta H \cdot Q_{wvq}}{I_S \cdot \Delta Q_{wvq}} \tag{6.1.8}$$

where ΔQ_{wvq} is the difference in discharge between the supporting points of the wvq-relation and ΔH is the difference in water level between the supporting points. ΔQ_{wvq} is computed for two cases with eq. 6.1.9 where the average discharge $\overline{Q}_{wvq}$ is calculated as an intermediate result among wvq-relations (see eq. 6.1.10).

$$\Delta Q_{wvq} = \begin{cases} \overline{Q}_{wvq} & \text{if } wvq = 1 \\ \overline{Q}_{wvq} - \overline{Q}_{wvq-1} & \text{if } wvq > 1 \end{cases} \tag{6.1.9}$$

$$\overline{Q}_{wvq} = \begin{cases} (Q_{wvq} + Q_{wvq+1})/2 & \text{if } wvq < \max \\ Q_{wvq} & \text{if } wvq = \max \end{cases} \tag{6.1.10}$$

The characteristic length L_c (m) of the stream segment is computed as an average over all single lengths $L_{c,wvq}$ of the WVQ-relations for the angular profile.

$$L_c = \frac{\Sigma L_{c,wvq}}{n_{wvq}} \tag{6.1.11}$$

Computation of the parameters to model the flood routing in circular profiles. The computation of the characteristic length for circular profiles assumes only an empty and a full pipe flow. Therefore, only two wvq-relations ($n = 2$) are calculated. The method is based on the Darcy-Weisbach approach using the Colebrook-White's equation with the equivalent sand roughness k_s for full pipe flow as input parameter. The intermediate formal parameters for circular profiles are computed as follows:

$$\begin{aligned} A &= (\pi/4) \cdot (D_{stream})^2 \\ P &= \pi \cdot D_{stream} \\ R_{hyd} &= 4 \cdot D_{stream} \end{aligned} \tag{6.1.12}$$

where A is the wetted cross-section (m^2), P is the wetted perimeter (m) and R_{hyd} is the hydraulic radius (m) of a full pipe flow. The computation of the flow velocity v (m^3/s) is done according to eq. 6.1.4. For circular profiles the approach of Kalinin & Milyukov can not be applied directly because of missing WVQ-relations over incremented water level states. Instead, the characteristic length to represent the quasi-stationary segment is computed using the approach of Euler [1983]. Euler derived a relation function between geometrical parameters and the discharge of a completely filled pipe. Euler concluded that the characteristic length of the stream segment L_c for circular profiles can be derived with the following equation.

$$L_c = 0.4 \cdot D_{stream} / I_S \tag{6.1.13}$$

where L_c (m) is the characteristic length of a quasi-stationary segment which corresponds to the approach of Kalinin & Milyukov, D_{stream} (m) is the diameter of the circular profile of the stream segment (such as a pipe) and I_S is the slope of the stream segment (-).

Computation of the Kalinin-Milyukov parameters $\mathbf{K_{km}}$ and $\mathbf{n_{km}}$. The Kalinin-Milyukov approach is based on the concept of a cascade of linear reservoirs (also known as "linear reservoir model"). The number of characteristic reservoirs is calculated as follows:

$$n_{km} = L_c / L_s \tag{6.1.14}$$

where L_c (m) is the characteristic length of the stream segment (see eq. 6.1.11 for angular and eq. 6.1.13 for circular profiles) and L_s is the topographic stream segment length (m). The KM-parameter $K_{c,km}$ for each reservoir with the length L_c is derived from the slope of the volume-discharge relations $S_{QV} = f(V(Q))$ as described in Maniak [2016] (p. 397 ff.) for angular profiles:

$$K_{c,km} = S_{QV} \tag{6.1.15}$$

For circular profiles the relation by Euler [1983] is applied:

$$K_{c,km} = 0.64 \cdot L_c \cdot \frac{(D_{stream})^2}{Q_{max}} \tag{6.1.16}$$

where the discharge Q_{max} in (m^3/s) is computed with $Q_{max} = v_{wvq=n} \cdot A_{wvq=n}$. The slope of the relation between the average discharge $\overline{Q}$ and the average volume $\overline{V}$ over the wvq-relations ($wvq = 1$ to n_{wvq}) is computed as follows:

$$\begin{aligned} \overline{V} &= \Sigma_1^{n_{wvq}}(V_{wvq}/n_{wvq}) \\ \overline{Q} &= \Sigma_1^{n_{wvq}}(Q_{wvq}/n_{wvq}) \\ S_{QV} &= \frac{\Sigma_1^{n_{wvq}}((Q_{wvq} - \overline{Q}) \cdot (V_{wvq} - \overline{V}))}{\Sigma_1^{n_{wvq}}((Q_{wvq} - \overline{Q})^2)} \end{aligned} \tag{6.1.17}$$

The retention coefficient K_{km} (s) for a stream segment with the length L_s is the product of the number of characteristic segments n_{km} and the characteristic retention constant $K_{c,km}$ (s):

$$K_{km} = K_{c,km} \cdot n_{km} \tag{6.1.18}$$

Computation of the flood routing discharge $Q_{out}(t)$ with a recursive function. A recursive computation is performed n_{km}-times to calculate the routed outflow $Q_{out}(t)$ at the downstream end of the stream element per time step t with the following equation according to the linear storage theory (see Maniak [2016], p. 310):

$$Q_{out}(t) = Q_{out}(t-1) + (Q_{in}(t-1) - Q_{out}(t-1) \cdot K_1 + (Q_{in}(t) - Q_{in}(t-1)) \cdot K_2 \tag{6.1.19}$$

where Q_{out} is the routed outflow of the characteristic stream segment (m^3/s), Q_{in} is the inflow into the stream segment (m^3/s), t is the index of the time step and $t-1$ is the previous time step. K_1 & K_2 are auxiliary (formal) parameters which are calculated as follows:

$$K_1 = 1 - e^{-\Delta t/K_{km}} \quad \text{and} \quad K_2 = 1 - \frac{K_{km}}{\Delta t} \cdot (1 - e^{-\Delta t/K_{km}}) \tag{6.1.20}$$

where K_{km} is the retention coefficient (s) and Δt is the time step size (s). This recursive computation is executed for each reservoir along the stream segment while the outflow from one reservoir is the inflow to the next one till reaching the downstream section. The outflow from the last reservoir in the cascade is the final routed discharge Q_{out} at the junction node of the stream element in (m^3/s).

6.1.2 The five reservoirs flood routing method "KM5"

The computation of the flood routing in stream segments on the meso scale with natural irregular profiles requires a separate parametrisation of main channel and flood plane areas. These profiles are subdivided into five reservoirs. Two reservoirs represent the characteristics

in the main channel, one reservoir is situated at the bankfull stage and two reservoirs are defined to model the flood routing on the foreland (see figure 6.3). Within each reservoir a derivative algorithm is executed which is based on the same approaches described for the KM1-method (see section 6.1.1). Because of the subdivision into five reservoirs, the concept is labelled as "KM5"-method in this work. To resolve the calculation routine through five reservoirs a "polynomial function" is required to compute the WVQ-relations and the Kalinin-Milyukov parameters. A partition factor α describes the fraction of flow which is routed through the main channel and the flood plane area. This fraction is $\alpha = 1$ as long as the water level is below the bankfull height. The fraction is reduced ($\alpha < 1$) when the water level exceeds the bankfull height and a percentage of water ($= 1 - \alpha$) flows over the flood plane area. The flood routing on the flood plane is computed using different roughness (R_{FP}) parameters as in the main channel ($R_{channel}$).

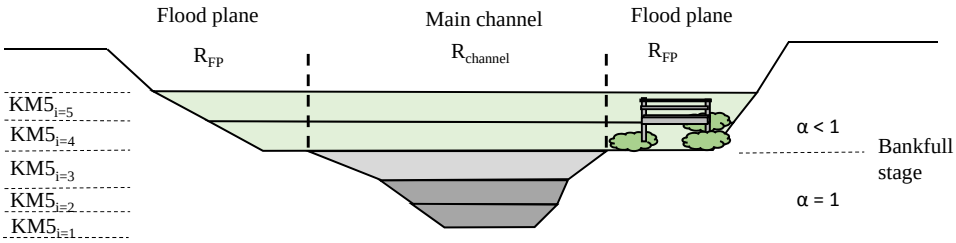

Figure 6.3: Scheme to separate a natural irregular profile into the flood plane (FP) area and the main channel to compute the flood routing along a stream with the KM5-method.

Such a model to compute WVQ-relations per profile with a polynomial function is described in Teschke [2003]. Both flood routing methods, the KM1- and the KM5-method, serve as basis to compute the backwater effects in stream segments in this work. For modelling the flood routing on the local scale among LSDMs, the KM1-method is explained in more detail. The methodology to compute backwater effects is described in section 6.3.

6.1.3 The meso scale spatially aggregated flood routing method

The flood routing computation of surface runoff from impervious areas on the meso scale is performed with a conceptual method. It is presented in this work as an alternative approach for the flood routing computation among LSDMs on the meso scale if the geographical location of LSDMs and the stream profiles are not known. The method is described in attachment B.4 and applied in the meso scale catchment model to compute the surface runoff routing from impervious areas. A comparison of results using this conceptual approach and the KM1-method for the flood routing computation among LSDMs in a meso scale catchment is presented in the application study in section 8.3.1.

6.2 Method to model control structures in streams on local and meso scale

A control structure implies features to model, for example, retention ponds, cisterns, multi-functional areas, (tidal) gates, pump stations, sluices and weirs. At these structures retention, drainage distribution or backwater effects occur in a hydrological network according to criteria. The criteria can be based on water level, discharge or precipitation intensity within hindcasted or forecasted driver time series. The theoretical approach to model control functions is described in section 3.3.2 (page 46). A control structure in streams is defined with drainage functions per time step to distribute the flow to target junction nodes. The functions are activated according to criteria, which are checked per time step and described in more detail in section 6.2.1. In figure 6.4 a control structure of a stream segment is illustrated with four flow distribution functions (f_c). In such a control structure the retained water can lead to backwater effects in upstream direction if an afflux of water occurs.

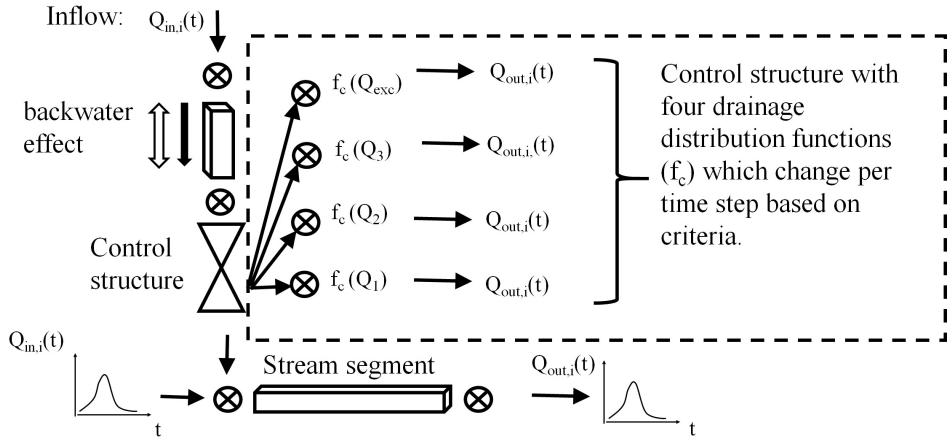

Figure 6.4: Scheme of a control structure with four flow distribution functions. (The explanation of symbols is given in attachment B.1.)

A control structure of a linear stream segment is defined with unsteady WVQ-relations and the flood routing is modelled with a storage indication method. In this work the modified Puls method is applied for this purpose and described in section 6.2.2.

6.2.1 The definition of criteria of control functions

Criteria of control functions are defined for three types of driver time series which are precipitation intensity, water level stages and discharge values. Hydrographs of water level stages and discharges are results given at junction nodes, while precipitation time series are part of spatial structures (namely subcatchments or LSDMs). Control functions are activated per time step during the execution of the numerical model. A differentiation is done for functions depending on preset (external pre-processed) or process-related (internal computed) driver time series. The control functions which depend on preset driver time series (for instance, precipitation or flow gauge measurements) are computed in the pre-processing phase of the

simulation run to set the configuration of a control system. This is described in the following paragraph labelled with (a). The control functions with criteria which depend on the output of computed formal parameters of the hydrological network (namely water level or discharge) are computed during the simulation run. This procedure depends on the condition that the driver elements are located upstream of the control structure and are not influenced by backwater effects. These conditions are described in more details in paragraph (b). If the criteria of a control structure depend on downstream conditions in an interactive system, a recursive calculation routine is started. Such a system is described in paragraph (c).

(a) Control functions based on criteria for preset "driver time series". In this case, control functions are defined on the local and meso scale using criteria of precipitation, discharge or water level time series which are pre-processed before the calculation routine is executed. For example, rainfall radar data is processed on the spatial scales of subcatchments. Values of observed water level and discharge time series are imported per junction node. Time series are checked for reaching a defined threshold value which corresponds to the criteria of the control function. This criteria can be an intensity of rainfall, a discharge threshold value or a water level threshold value exceeded over a specific duration of time. Setting a duration for each criteria prevents an unstable activation of control functions ("on/off-phenomena"). Flow charts of the developed algorithms to pre-process a driver time series to define the control functions per LSDM and the execution of the control functions per layer of LSDMs are given in attachment B.3. The algorithm to compute the control functions in linear structures like stream segments is developed likewise.

(b) Control functions based on criteria for computed "driver time series" of elements which are upstream located and not backwater affected. The hydrographs of any junction node in the hydrological network can be defined as driver time series for a criteria of a control function. The settings are defined according to control system category (a), as long as the driver elements are located upstream of the control structure and are not influenced by backwater effects. Otherwise the control function category (c) is activated.

(c) This procedure is the same as (b) but for interactive or backwater affected elements. Control systems within backwater affected catchments depend on interactive driver time series. This means that the control functions depend on the results of other structures within the system and may be located upstream or downstream of the considered control structure in the system. In this case, the explicit computation of elements from upstream to downstream require additional calculation loops. The algorithm of the interactive backwater system loop is based on nesting an internal spatial computational loop within a time loop which is further on nested in a backwater system loop as described in the following section 6.3.

6.2.2 Computation of the water storage volume and drainage functions

A control structure is defined in a similar manner as a stream segment (see section 6.1), but with variable water level, volume and drainage relations (WVQ-relations). The storage volume and the drainage functions of a control structure per time step are computed with the modified Puls method. This method is based on a storage continuity equation taking into account the finite difference in the storage volumes between time steps in the following manner (see for example Maniak [2016] p. 382):

$$[Q_{in}(t) + Q_{in}(t+1)]/2 - [Q_{out}(t) + Q_{out}(t+1)]/2 = [V(t+1) - V(t)]/\Delta t \tag{6.2.1}$$

where Q_{in} is the inflow in the control structure (m^3/s), $Q_{out}(t)$ is the outflow (m^3/s), V is the water volume in the storage (m^3), t is the current time step, $t+1$ is the next time step with the simulation time step size Δt in (s). If Δt is defined in a different unit than seconds (s), a transfer of the temporal scales into seconds is required. The input parameters represent the topography of the storage element and the outlet structure. The equation 6.2.1 is rewritten to compute the outflow $Q_{out}(t+1)$ and the storage volume $V(t+1)$ in the following form:

$$V(t+1)/\Delta t + Q_{out}(t+1)/2 = [Q_{in}(t) + Q_{in}(t+1)]/2 + V(t)/\Delta t - Q_{out}(t)/2 \tag{6.2.2}$$

In the modified Puls method a relation between the discharge $Q_{out}(t)$ and the storage volume $V(t)$ is derived: $[V(t)/\Delta t + Q_{out}(t)/2 = f(Q_{out}(t))]$, to compute $Q_{out}(t)$ (m^3/s) (see Maniak [2016]; p. 384 ff.). This approach is extended in this work to calculate $Q_{out}(t)$ and $V(t)$ from control functions based on unsteady WVQ-relations per time step.

The initial state in the control structure is represented with the formal parameters at the first time step (t = 1) including $Q_{in}(t = 1)$, $Q_{out}(t = 1)$ and $V(t = 1)$. These initial values are given as preset values or computed with a preceding longterm simulation run. Per time step the control functions are revised according to the criteria. The input parameters comprise the minimal water storage volume V_{min}, the maximal storage volume V_{max}, the initial water storage volume V_{ini} and the $Node - IDs$ for different target junction nodes. An example of a control system with a number of four different target nodes is illustrated in figure 6.4. Thereby, one downstream node, one exceedance flow node and different optional auxiliary junction nodes can be defined as targets. Another parameter is the storage line function for an allocatable array of WVQ-relations. The dimension of this array is specified during the execution of the computation. The storage line functions give a relation between the water level W (m a.s.l), the storage volume V (m^3), the discharge Q_{out} (m^3/s) and the ratios to the different target junction nodes. Additionally, the evaporation E (mm) of water from the storage volume is computed per time step. The developed algorithm is illustrated in the flow chart in figure 6.5. It is nested in a computational loop through the time steps. Control functions are called and revised according to the activated criteria per time step. In a first step, the potential outflow $[Q_{pot,out}(t)]$ is assumed from the available drainable water in the control structure of

the previous time step plus the inflow in that time step.

$$Q_{pot,out}(t) = [V(t-1) - V_{min}(t)]/\Delta t + Q_{in}(t) \tag{6.2.3}$$

If this potential outflow is smaller than the minimal outflow (wvq = 1) of the defined WVQ-functions $[Q_{pot,out}(t) < Q_{out,1}(t)]$ the storage volume is set to minimum $V_{min}(t)$ and the outflow $Q_{out}(t)$ is computed with:

$$Q_{out}(t) = Q_{in}(t) + V(t-1) - V_{min}(t)/\Delta t - V_{EW}(t)/\Delta t \tag{6.2.4}$$

where $V_{EW}(t)$ is the loss of water by open water evaporation which is computed with:

$$V_{EW}(t) = \dot{V}_{EW,pot}(t) \cdot A_{wvq} \tag{6.2.5}$$

where A_{wvq} is the water surface area (m^2) according to the current storage volume with the *wvq*-ordinal, $\dot{V}_{EW,pot}(t)$ is the computed potential flux of evaporation on the basis of the Penman approach for open water surfaces in (m^3/m^2) in the time step size Δt. Details about the computation of evaporation processes are described in section 5.2 on page 65 ff.

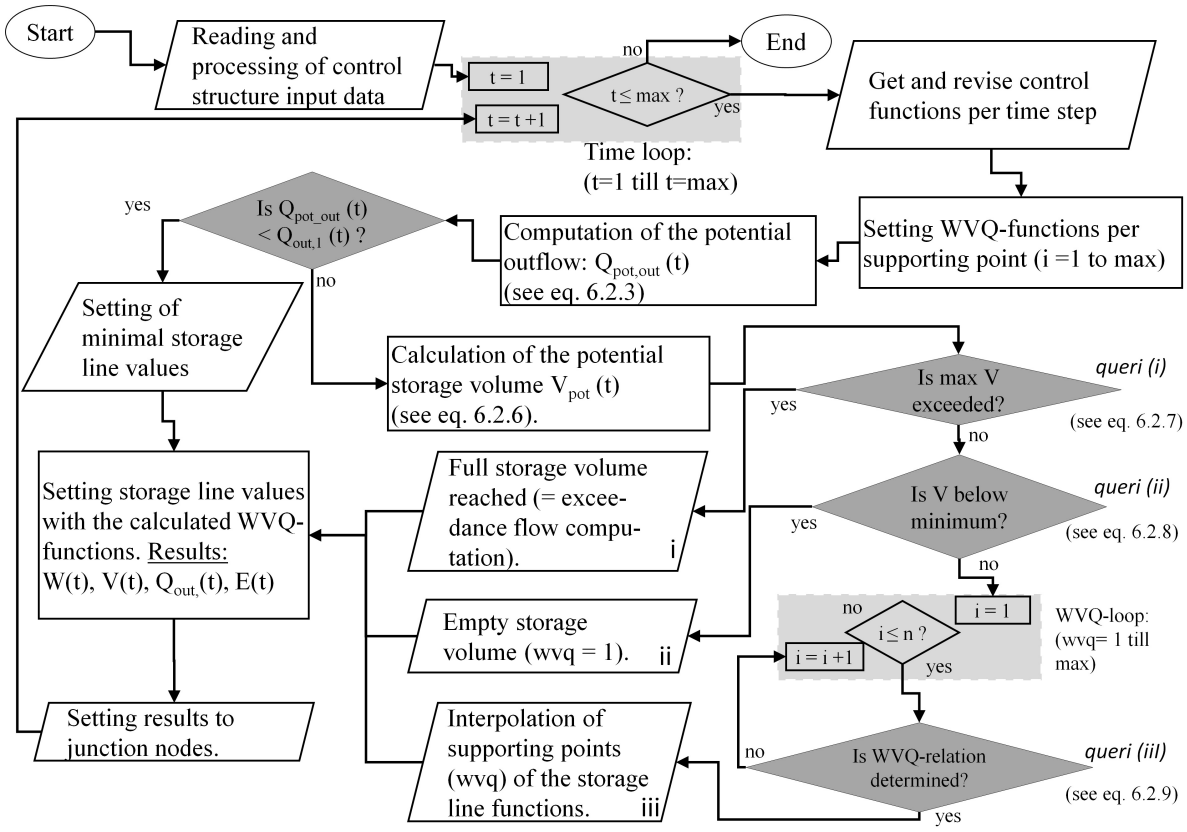

Figure 6.5: Algorithm to compute the water storage volume and drainage functions of a control structure.

If the potential outflow $Q_{pot,out}$ is larger than the minimal outflow $Q_{out,1}$, the calculation of the potential storage volume $V_{pot}(t)$ first assumes a retained volume based on the outflow of the

previous time step.

$$V_{pot}(t) = [Q_{in}(t-1) + Q_{in}(t)]/2 \cdot \Delta t + V(t-1) - Q_{out}(t-1) \cdot \Delta t - V_{EW}(t) \tag{6.2.6}$$

This relation is applicable for small simulation time step sizes ($\Delta t < 24\,\text{h}$) and as long as the following query is true: $[Q_{out}(t-1) < V(t-1)/\Delta t + \overline{Q}_{in}/2]$. Otherwise, the assumed outflow is reduced step wise to compute the first guess of the potential storage volume $V_{pot}(t)$. To compute the actual outflow $Q_{out}(t)$ and storage volume $V(t)$, three cases are differentiated. In the first case (i), (see figure 6.5, right side) the potential storage volume $V_{pot}(t)$ exceeds the maximal storage volume with $wvq = max$. The query (i) is defined as follows:

$$\text{Query (i): Is} \quad [V_{pot}(t) \geq V_{max} + Q_{out,max} \cdot \Delta t] \ ? \tag{6.2.7}$$

In a second case (ii), the potential storage volume V_{pot} is below the minimal storage volume with $wvq = 1$. The query (ii) is defined as:

$$\text{Query (ii): Is} \quad [V_{pot}(t) \leq V_1 + Q_{out,1} \cdot \Delta t] \ ? \tag{6.2.8}$$

In a third case (iii), the storage volume $V(t)$ and outflow $Q_{out}(t)$ are derived from an interpolation among the valid supporting points of the WVQ-functions. The valid wvq-functions are defined by a comparison with the potential storage volume $V_{pot}(t)$. The third query (iii) is as follows:

$$\text{Query (iii): Is} \quad [V_{pot}(t) \geq V_{wvq} + Q_{out,wvq} \cdot \Delta t] \ ? \tag{6.2.9}$$

According to the valid wvq-function per time step t, the results of the calculation routine are the time series of the storage volume $V(t)$, the water level $W(t)$, the evaporation losses of the water surface area $V_{EW}(t)$ and the outflow to the target junction nodes $Q_{out}(t)$. When for example, four target nodes are defined, the following time series are computed: $Q_{1,NodeID}(t)$ as the drainage to the downstream node of the control segment, $Q_{2,NodeID}(t)$ as the discharge to a second node, $Q_{3,NodeID}(t)$ as the discharge to a third node and $Q_{exc,NodeID}(t)$ as an exceedance flow drained optionally to another node.

6.3 Method to model backwater effects in streams and areas

The literature review revealed that hydrological numerical approaches to compute the flood routing neglect backwater effects up to now (see section 2.2.6, p. 24ff.). These flood routing approaches are referred to as "free" flood routing and one method is described in the previous section 6.1. When afflux conditions occur like in low lying lands, this free flood routing method needs to be extended.

An afflux of retained water in downstream segments leads to a rise of water level due to natural or artificial obstructions (for instance gates or weirs). The downstream directed flow is hindered and reversed in upstream direction as backwater, when the downstream water level is higher than upstream. One consequence of backwater effects is the flooding of upstream

areas (namely subcatchments or LSDMs). The current shortcoming in hydrological numerical models concerning the simulation of backwater effects is resolved in this work. The presented flood routing method (see sections (6.1) and control system computation (see section 6.2) are extended in such manner to model backwater effects.

Overview of the developed algorithm to compute backwater effects in streams and areas. The developed algorithm to compute backwater effects is illustrated in the flow chart in figure 6.6. The calculation routines are nested in computational loops as follows. A spatial loop of streams and areas is nested in a time loop. The time loop is again nested in a backwater system loop. The indicated calculation routines (i) to (iv) to compute the backwater effects are explained in the following sections 6.3.1 to 6.3.4. This paragraph describes the overall structure of the developed algorithm.

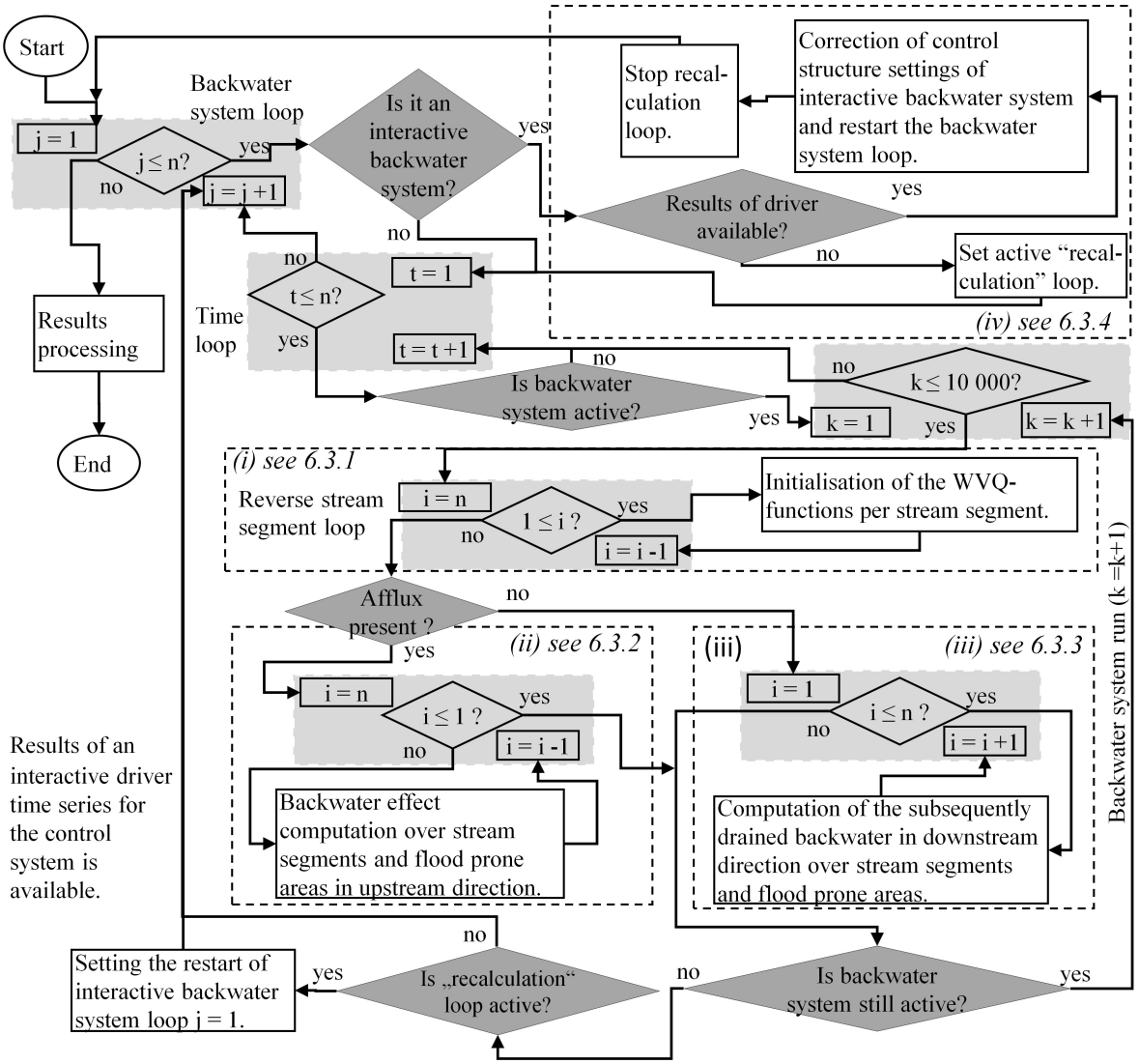

Figure 6.6: Algorithm to compute backwater effects in streams and flood prone areas.

Each backwater system includes linear structures (stream segments), spatial structures (subcatchments or LSDMs), junction nodes and at least one control structure at the downstream

section. Per backwater system and per time step a query checks if an interactive backwater system is defined. An interactive system depends on both, downstream and upstream conditions. In case of an interactive system, the flag for a "recalculation" loop is activated. The calculation routines in the stream segment loops (i) (explained in section 6.3.1) to (iii) (see section 6.3.3) are executed. These loops (i) to (iii) are running while at any element an afflux condition is present (see query: "Is backwater system active?" = yes). The final balanced stage is reached when in a backwater affected system the downstream water levels are not higher than the upstream water levels within a range of a minimum "tolerated" water level difference. The method demands to define a minimum difference (ΔW_{min}) according to the application purposes. In the evaluation study (see section 8.3) a water level difference of about 0.01 m gives sufficient results for meso scale stream segments. For local scale stream segments a difference of about 0.001 m gives adequate results. Indeed, a smaller tolerated water level difference increases the accuracy of computed water level results. At the same time, this increases the number of backwater computational runs ($k = k + 1$) before reaching a maximum number (currently: k = 10 000). This critical state prevents infinite calculation routines and a warning is provided if this limit is reached to check the input parameters which include an adjustment of the tolerated water level difference. Backwater effects are computed in open (angular) stream segments which are part of the defined backwater system. Circular (closed) stream segments (for instance pipes, culverts) are modelled to convey the backwater instantaneously to upstream segments or linked spatial structures (for example LSDMs or subcatchments).

When a control structure depends on criteria of a downstream backwater affected system, an interactive computational loop is activated (see figure 6.6, (iv)). In this case a "recalculation" loop is started and revises control structure settings if the results of the interactive backwater system are available. Then the recalculation loop restarts the computation of the loops (i) to (iii). This calculation routine (iv) is described in section 6.3.4.

The results of this developed algorithm to compute backwater effects are the time series of water levels (m a.s.l), discharges (m^3/s) and volumes (m^3) for stream segments and linked spatial data structures (namely subcatchments or LSDMs). Additionally, the activated control functions per control structure are given as time series for verification purposes.

6.3.1 Initialisation of the parameters for the backwater effect computation

For the computation of backwater effects, the formal parameters of each data structure are initialised. This includes, an initialisation of the water level, volume and discharge per time step. Discharges are computed with the flood routing methods described in the sections 6.1.1 and 6.1.2. The corresponding water levels and retained water volumes are derived from the calculated WVQ-relations per stream segment.

The initialisation of formal parameters of stream segments is nested in the computational loops per backwater system and per time step (as depicted in figure 6.6 (i)). The stream segments per backwater system are computed from downstream to upstream ordinal. The developed algorithm to initialise the formal parameters is illustrated in figure 6.7. The cal-

culation routine distinguishes between stream segments, control structures and areas. A first query decides, if it is the first computation run of the backwater system and which kind of formal parameters are initialised (KM1, KM5 or control structure parameters). In the initial computation run, the inflow into the control structures and the calculated WVQ-relations for control segments and stream segments are derived from the "free" flood routing computation output. If it is the first time step, these initial values are set directly. For time steps larger than 1, the volume and water level of the previous time steps are taken as basis to compute the actual WVQ-relations for each segment.

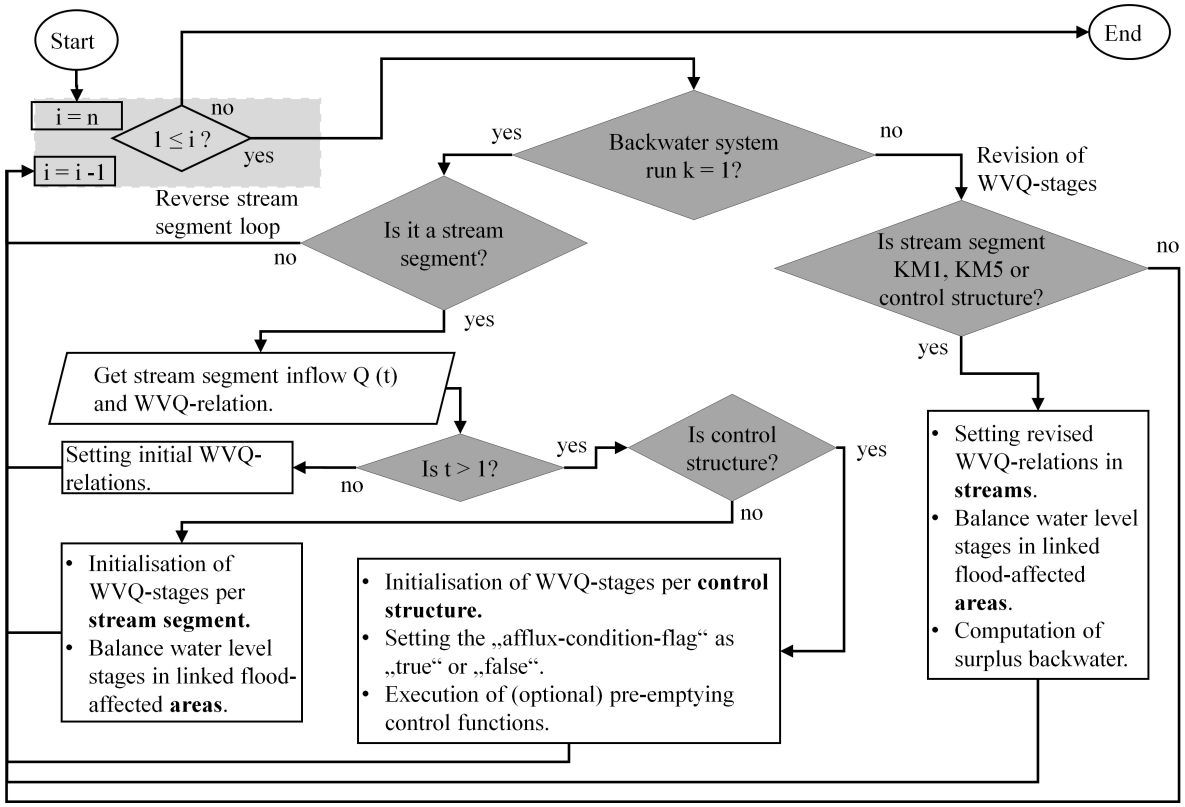

Figure 6.7: Algorithm to initialise WVQ-relations in streams, control structures and areas per backwater system computation. This corresponds to the calculation routine (i) in the algorithm in figure 6.6.

Initialisation of control structures per time step and executing the backwater system computation run (if k = 1). A control structure is the downstream element computed first per backwater system. In these structures, the active control function per time step is defined by the criteria which are based on water level, discharge or precipitation values. The volume in stream segments is computed with the following equation:

$$V(t) = V_{ini}(t) + \Delta V(t-1) + V_{exc}(t) \tag{6.3.1}$$

where $V_{ini}(t)$ is the initial water volume in the stream segments computed in free flood routing conditions. The difference in volume of the last time step $\Delta V(t-1)$ is computed according to a set of query functions described in the following paragraphs. The "surplus backwater"

$V_{exc}(t)$ is the backed up water quantity which exceeded the maximum storage volume in the last computation run and is processed subsequently in the following ones.

Setting the afflux conditions. When the volume in the control structure is increased ($V(t) > V(t-1)$), afflux is generated and the flag for afflux conditions is set to 'true'. The difference in volume between time steps ($\Delta V(t-1)$) is revised continuously during the following backwater computational loops (ii) and (iii). When the volume in the control system is decreased ($V(t) < V(t-1)$) or not changed ($V(t) = V(t-1)$) the flag for afflux conditions is set to "false" and the volume ($\Delta V(t-1)$) is reduced by the proportion of the changed volume ΔV which has been processed already in the time step before.

The upstream directed backwater routing is computed if the "afflux-conditions-flag" is set to "true". The downstream directed backwater routing is computed if the "afflux-conditions-flag" is set to "false". These computations are described in the computational loops (ii) and (iii) (see figure 6.6).

Setting additional pre-emptying control functions. The features of control structures comprise a pre-emptying of storage volumes in the developed algorithm. For example, when a forecasted storm event exceeds a rainfall intensity and duration, the water content in the storage is reduced until reaching a minimal water level by pre-emptying functions. The volume of water is drained to a receiving junction node in the hydrological network. This feature facilitates to model control functions for pre-pumping water from low lying areas by starting the pumping in advance of forecasted rainfall events. This feature is related to the pre-emptying function for cisterns, retention ponds and green roof storages with throttle valves (see section 5.3.3). An additional condition is taken into account when a minimal water level stage is kept stable by external criteria. For example a sluice or retention pond gate is controlled at the downstream section to keep the water level stable at a minimum.

Initialisation of stream segments per time step and executing the backwater system computation run (if k = 1). The computation of initial volumes in stream segments is done with equation 6.3.1. Additionally, the initialisation stage of stream segments takes into account linked flood prone areas (subcatchments or LSDMs). The water level in these areas (spatial structures) interact directly with the stream segment water level $W(t)$ and the volume $V(t)$. When the overflow height of the spatial structure is exceeded by the stream segments water level, a fraction of water flows into the spatial structure until the water level in the stream segment and the spatial structure reach an equilibrium. The water level in the stream segment is reduced according to the volume which flows into the area (spatial structure). This method is especially important for modelling flood prone areas on the local, district but as well on the meso scale. The results of this calculation routine are time series of the water level $W(t)$ in m.a.s.l., discharge $Q(t)$ in m^3/s, volume $V(t)$ in m^3 and the afflux condition for the stream segments.

Revision of stages in control structures and stream segments per backwater system computation run (if k > 1). After the initialisation phase, the following backwater computation runs (k > 1) take into account 'surplus backwater' $V_{exc}(t)$, which is temporary retained and processed during the following time steps. According to the change in storage volume, the respective water level and discharge are revised. The interpolation between the formal parameters of the WVQ-relations is done with the basic equation:

$$y = \frac{y_0(x_1 - x) + y_1(x - x_0)}{x_1 - x_0} \tag{6.3.2}$$

where y is the interpolated target value and x the given source value. For water level interpolations the referenced water levels in (m a.s.l) are transferred to netto differences in water levels.

6.3.2 Computation of upstream directed backwater effects

The backwater effect computational loop in upstream direction is activated, while afflux conditions are present in the backwater system (see figure 6.6, (ii)). The calculation is done per stream segment in a computational loop starting at the downstream element (i = n). If the difference in water levels between the actual and the upstream segment is larger than the defined tolerated water level difference ΔW_{min}, an algorithm to compute the backwater effect is activated. The equalization of water levels over stream segments by rebalancing water volumes is illustrated in a scheme in figure 6.8. The scheme shows the afflux of water at a downstream control structure. This volume of water is retained at the downstream section before computing the backwater effects. In the developed algorithm, this volume of water initiates the backwater effect computation in the system over several linear (stream segments) and linked spatial data structures (namely flood prone areas or LSDMs).

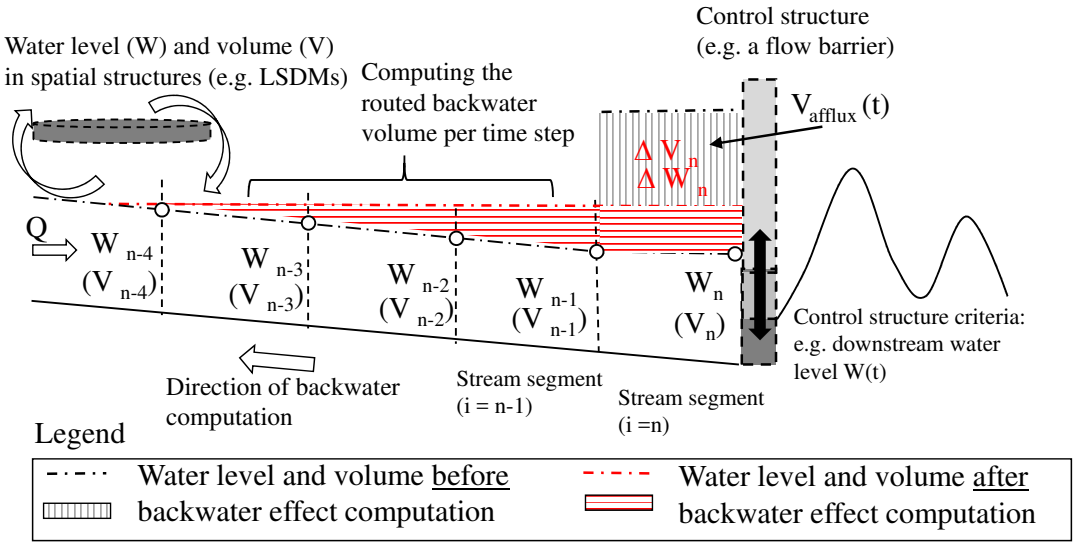

Figure 6.8: Scheme of afflux generation at a control structure and backwater effects in upstream direction.

On the local and district scale the backwater quantity derived from an afflux at the down-

stream segment, is routed to the upstream segments. Along the streams spatial structures are linked (for example, LSDMs) where the water is retained or causes backwater flooding. This developed concept is illustrated in the scheme in figure 6.9. In part (a) the backwater effect computation between stream segments with linked spatial structures (areas) is illustrated. The formal parameters of the WVQ-relations of the current (i) and the upstream (i-1) segment are processed. The computation is done in three calculation routines (namely A,B and C) to compute the water level and volume stages.

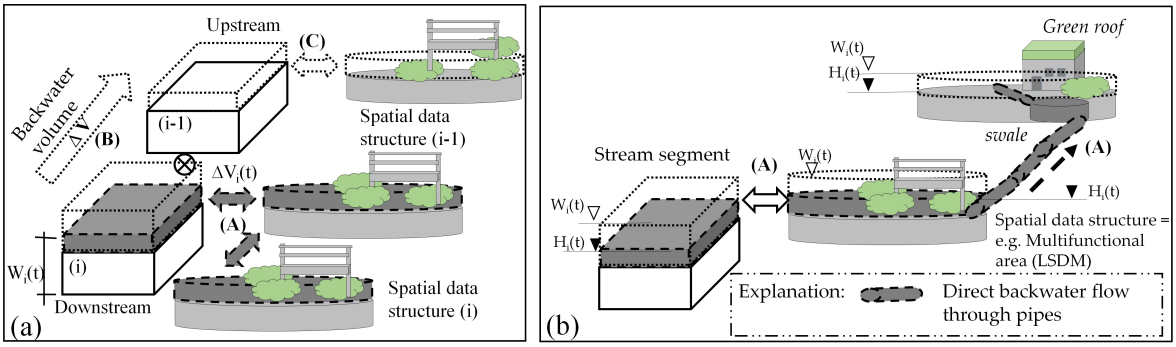

Figure 6.9: Scheme of the calculation routines (A), (B) and (C) to compute the backwater effects in (part a) for stream segments and linked flood prone areas and in (part b) for a stream segment with linked local scale areas (for example, LSDMs).

Explanation of the calculation routine (A). In case of linked spatial data structures, a portion of water flows from the stream segment (i) into the respective linked areas (i). The inflow continues until the water level in the stream $W_i(t)$ is equalised with the water level in the linked spatial data structures $W_{i,areas}(t)$. The result is a changed difference in volume $\Delta V_i(t)$ to be routed to the upstream segment (i-1).

Explanation of the calculation routines (B) and (C). The computed backwater effect in the calculation routine (B) describes, how the water volume $\Delta V_i(t)$ is added to the upstream linear data structure $V'_{i-1}(t) = V_{i-1}(t) + \Delta V(t)$, whereupon the water level is derived from the WVQ-relations. If the upstream segment is linked with another spatial data structure as illustrated in figure 6.9 (a) (case C), the equalisation of water level and volume is done respectively to the procedure in (A).

Explanation to calculate backwater effects. The algorithm to compute the upstream directed backwater effects is illustrated in figure 6.10. If the following queries are true, the upstream backwater effect computation is executed. These queries are called at the beginning of the calculation routine (see: "Are afflux conditions present?" in figure 6.10):

$$\begin{aligned} &is\ W_i(t) - W_{i-1}(t) > \Delta W_{min}\ ? \\ &is\ V_i(t) > V_{i,free}(t)\ ? \end{aligned} \tag{6.3.3}$$

where the water level $W_i(t)$ (m a.s.l.) and volume $V_i(t)$ (m^3) are defined by the WVQ-relation per stream segment with the index i. ΔW_{min} is the tolerable backwater affected water level rise given for the stream segments (m) in the backwater system. $V_{i,free}(t)$ is the water volume in the segment without backwater effects, which is computed with the flood routing method.

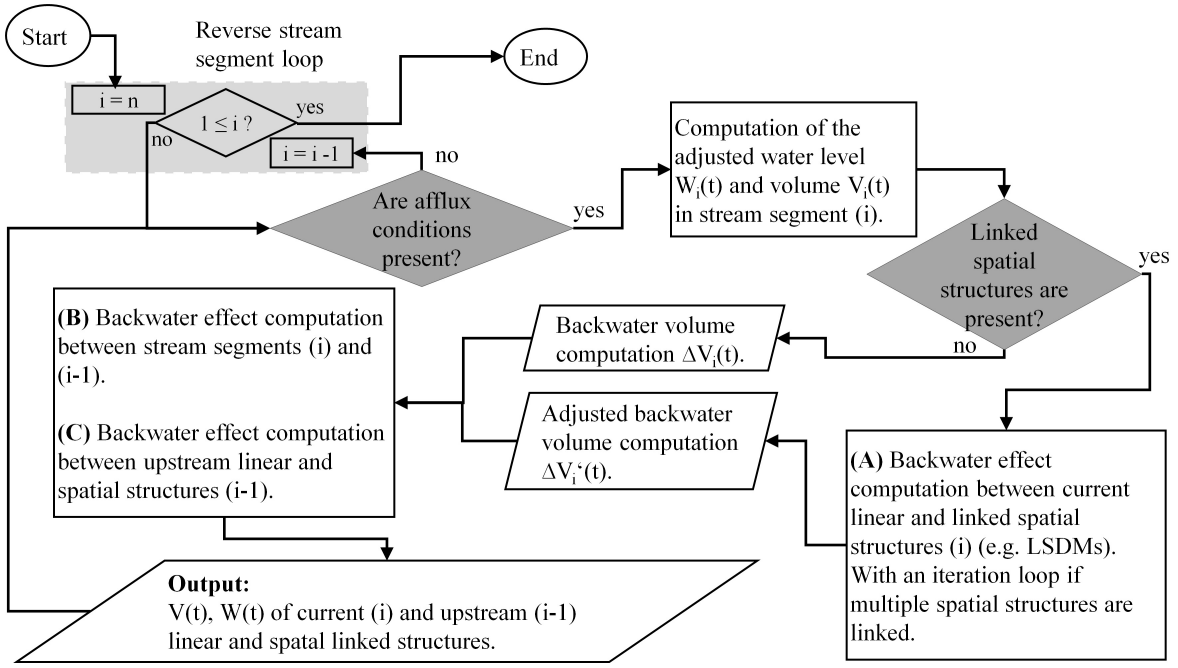

Figure 6.10: Scheme of the upstream directed backwater effect computation over stream segments and linked flood prone areas. This illustrates the calculation routine (ii) in the algorithm in figure 6.6.

While afflux conditions are present, the water level in the current stream segment (i) is reduced by the minimum water level difference ΔW_{min}. The adjusted storage volume of the stream segment $V_i'(t)$ is defined accordingly by the WVQ-relation. The adjustment of the stream segment (i) is done with the following equations:

$$\begin{aligned} W_i'(t) &= W_i(t) - \Delta W_{min} \\ V_i'(t) &= f(W_i'(t)) \rightarrow \text{Derivation of the WVQ-relations} \\ \Delta V_i(t) &= V_i(t) - V_i'(t) \end{aligned} \tag{6.3.4}$$

where i' indicates the adjusted stages in the stream segment (i). This results in a difference of volume $\Delta V_i(t)$ which is routed to a linked spatial data structure (for example a LSDM). This calculation routine is indicated with (A). Otherwise, the backwater is directly routed to the upstream linear data structure ($i-1$). These calculation routines are indicated as (B) and (C) in figure 6.9.

The output of the backwater computation. The output parameters of the calculation routine are the water levels $W_i(t)$ and volumes $V_i(t)$ of the linear and linked spatial data structures. The

topmost upstream linear structure of a backwater system is computed likewise with a linked spatial data structure. The backwater effect computation is finalised when the backwater level difference in all linked structures is less than the tolerable water level difference (meaning: $W_i(t) - W_{i-1}(t) < \Delta W_{min}$) for that specific backwater system.

Computation of the local scale backwater effects. The developed flood routing method KM1 (see section 6.1.1) comprises the computation of open streams (using the Manning-Strickler approach) as well as circular profiles using the approach of Darcy-Weissbach. For the developed method to compute backwater effects it is defined that circular profiles like storm water pipes are utilized by the maximum capacity during storm events. Stream segments with circular profiles are not considered to have free storage capacity for backwater volumes, but the backwater volume is routed directly to the next upstream segment or local spatial data structure (such as a flood prone area). The local scale streams with open trapezoidal profiles are computed with the same algorithms as presented in figure 6.10.

6.3.3 Computation of subsequently drained backwater in downstream direction

The backwater volume is routed downstream, if the afflux conditions at the downstream segment of the backwater system is not present anymore, for instance by the opening of a gate or starting additional pumping. The computation is done in the indicated stream segment loop (iii) in figure 6.6. The water level and storage volume in the stream segments are reduced per time step until free flow conditions are reached. In the developed calculation routine the drainage process of the backed up water volume is calculated. The stream segments are computed in the order from upstream (i = 1) to downstream (i = n). The algorithm for the computation of the subsequently drained backwater in downstream direction is related to the upstream directed computation, which is explained in the previous section. In contrast, the computations of water levels and volumes are done step wise with the current (i) and the downstream (i+1) data structures. The description and the flow chart of this calculation routine is given in the attachment B.5.

6.3.4 Computation of an interactive backwater system with control structures

An interactive backwater system is present when criteria of upstream control structures are based on the results of downstream segments, which are at the same time backwater affected and influenced by the inflow from upstream segments. The criteria defines the opening or closing of upstream control structures (for instance gates or sluices) to prevent backwater effects in the upstream segments. The ordinal number of backwater systems is taken into account for computing these constraints starting with the lowest number at the downstream section. The flow chart in figure 6.6 (see: "iv") illustrates the check for the interactive backwater system. As long as the driver time series for the criteria of the control structure is not available, a "recalculation" loop is activated. An example of an interactive backwater system is presented in attachment B.6.

7. Implementation of the methods in a hydrological numerical model

Implementing the developed methods into a target software is done for evaluation and application purposes. The software architecture[1] provides the basis and, at the same time, gives constraints to realise the implementation of the methods. One decisive point is the manner, how to provide the values of actual parameters (also known as arguments) for the execution of the model. On the one hand, the actual parameters are determined in form of text files, for instance in the format of the American Standard Code for Information Interchange (ASCII). On the other hand, the parameters are pre-processed by a software with a graphical user interface. In ASCII files each byte represents one character according to the ASCII code. This is in contrast to a binary file, in which there is no one-to-one mapping between bytes and characters (see Levi and Rembold [2003]). Models with a history of development over several decades in the past are primary based on text files. One of the first numerical models of the early 1960s is the Stanford Watershed Model (SWM) which used text files to structure the input parameters and the source code is written in the programming language Fortran[2] (see Crawford and Linsley [1966]; Donigian and Imhoff [2006]). For such models, the text-based structure still provides a larger degree of flexibility for additional implementations of calculation routines and for maintenance. But writing and processing the input parameters in text files is not straightforward with regard to the usability of the model in practice. A supplementary graphical user interface provides more support to the modeller with a workflow[3] to pre-process the input and analyse the output parameters. However, programming platforms with graphical user interfaces are likely more expensive to be built up and require higher maintenance, both in terms of manpower and time. In this work, it is decided to realise the implementation of the extended methods in a numerical model with an ASCII file based

[1] A software architecture comprises the software components and properties as well as relations between them.

[2] Fortran is an early created programming language originally invented by IBM (International Business Machines Corporation), which itself encompasses a development over the decades from basic Fortran (1950's), later Fortran 77, Fortran 90, Fortran 95, Fortran 2003, Fortran 2008 and currently Fortran 2018. Fortran is mainly developed and used in scientific and engineering fields (see Chivers and Sleightholme [2005]).

[3] A workflow gives a systematic organisation of the actual parameters to built and maintain a model as well as to analyse the results.

structure to pre-process the input and to write output parameters. Nonetheless, a numerical model is chosen which is operated already with a software platform providing a graphical user interface. Integrating the preprocessing of additional input parameters into the existing graphical user interface is an outlook of this work. This corresponds with the defined objective in chapter 3 according to the SMART-principle to realise the implementation of the methods in-time of this work for evaluation and application purposes.

The extended numerical model in this work supports to answer specific questions about the hydrological processes and the performance of LSDMs in backwater affected catchments. This is demonstrated with application studies, which are presented in the following chapter 8. The computed outputs are used for evaluation studies of the developed and implemented methods.

7.1 The hydrological catchment model KalypsoNA

The review in chapter 2 revealed appropriate categories of hydrological catchment models to reach the objectives of this work. The required model category is specified as a semi-distributed, deterministic, multi-layered and combined conceptual-physical based model (see section 2.2.8 page 26). The numerical model KalypsoNA[4] fulfils these criteria and is used for the implementation of the developed methods in this work. The model supports the simulation of hydrological processes on the meso scale such as surface runoff, infiltration, snow, evapotranspiration, soil moisture, interflow, base flow and groundwater recharge (see Pasche [2003]).

The processing of input as well as output parameters and the execution of the calculation code are integrated in the existing and in practice well approved software module Kalypso-Hydrology (see Belger et al. [2009], Lippert et al. [2009] and Hellmers et al. [2015]). Among others, this module provides a graphical user interface with a workflow view. It is part of the open source project Kalypso[5], which is an application for geospatial and hydrological as well as hydrodynamic-numerical modelling. The outline of the Kalypso project is illustrated in figure 7.1 with details of the hydrological module. Further modules are KalypsoHydrodynamic (1D2D & WSPM), KalypsoFlood and KalypsoRisk. Additional non-public modules include KalypsoEvacuation (see Lippert et al. [2009]) and the "Prognosesystem" Kalypso (see Schröder and Lippert [2006]). The pre-processing of input parameters for the execution of the calculation code is done with ASCII files. To assure the compatibility with previously released Kalypso versions in public[6], the additional input parameters are written in ASCII files within an extension folder.

The source code of the model KalypsoNA is based on the model BCENA, first developed by Björnsen Consulting Engineers (BCE) and renamed as well as given over to the institute of river and coastal engineering of the Hamburg University of Technology (TUHH) in the years

[4]The acronym "NA"-model stands for "Niederschlag-Abfluss"-Model (in German) and means rainfall-runoff model.

[5]Available under: https://sourceforge.net/projects/kalypso/.

[6]The most recent Kalypso version 18.2. was released in March 2018.

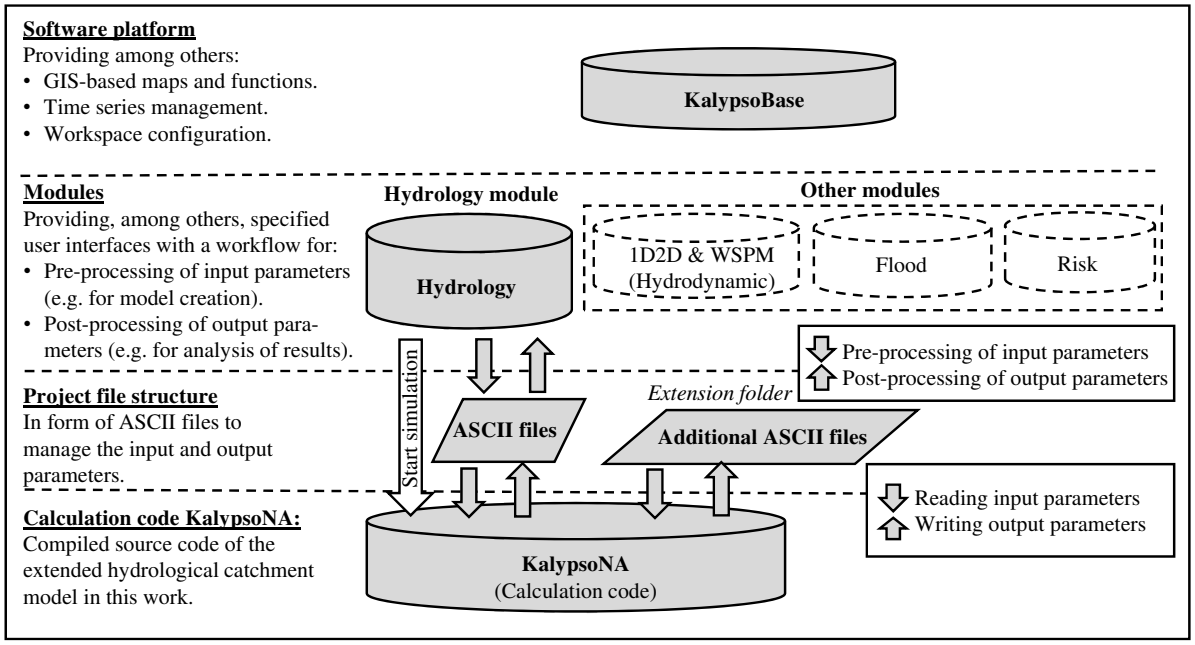

Figure 7.1: Outline of the Kalypso project with an overview of public modules and details of the module KalypsoHydrology as well as the operated calculation code (KalypsoNA). Input and output parameters are processed in ASCII files within an extension folder.

around 2000. It is an open source code under the license LGPL[7] and written in the programming language Fortran 95. The continuous development is driven by research demands and serves for application purposes in practice. Further details about the development history and basic features of the model KalypsoNA are available in TUHH-WB [2014], Hellmers [2010] and Pasche [2003]. A supplement description of the Kalypso project is given in attachment C.

7.2 Revision of algorithms in the hydrological catchment model

The algorithms in the source code KalypsoNA are revised for the integration of the developed methods to model the processes in LSDMs and backwater effects. An algorithm is made up of calculation routines which organise a sequence of numerical instructions and functions. These routines can be executed from different positions in an algorithm. A hydrological numerical model comprises algorithms in the form of time loops executed within a spatial tree structure (time-before-space algorithm) or spatial calculation routines are executed within a time loop (space-before-time algorithm). The differentiation is described in the theoretical approach in section 3.1.3 on page 39. Both approaches are integrated in the extended algorithm in the source code of KalypsoNA as illustrated in figure 7.2.

A time loop nested in a spatial loop accomplishes the simulation of the downstream data structures (such as subcatchments, stream segments, junction nodes or LSDMs) on the basis of the overall results of the upstream data structures. This means that the data structures are

[7] LGPL is the Lesser General Public License as published by the Free Software Foundation, version 2.1.

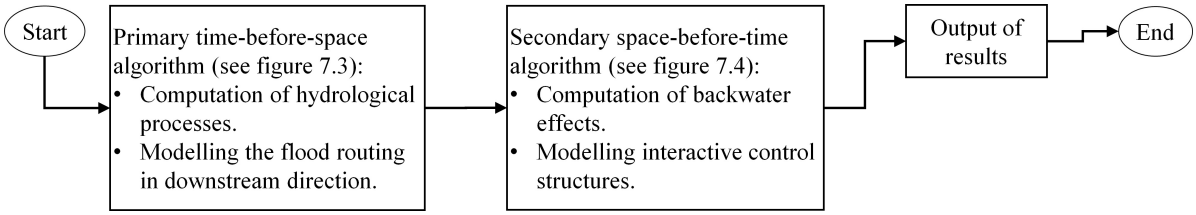

Figure 7.2: Flow chart of the implemented primary and secondary algorithm in the source code of KalypsoNA.

computed for the whole simulation period consecutively in the order given in the hydrological network from upstream to downstream. This provides actual time-dependent results of data structures to set control functions or drainage criteria in the hydrological network. This method is applied in the extended algorithm to model processes in LSDMs such as the soil water balance and the downstream directed flood routing. This implementation is realised with a time-before-space algorithm and described in section 7.2.1 (figure 7.3).

Additionally, a second algorithm is implemented within the scope of this work where spatial calculation routines are nested in time loops. This secondary algorithm provides the overall results of a backwater affected system per time step before computing the next time step. The time loop is additionally nested in a backwater system loop. In that calculation routine the backwater effects in streams and areas are computed. This implementation is labelled as space-before-time algorithm and explained in more detail in section 7.2.2 (figure 7.4).

7.2.1 Implementation of the primary time-before-space algorithm

The implementation of the first and second part of the methodology (see chapters 4 and 5) is realised in the primary time-before-space algorithm of the source code KalypsoNA. The developed methods comprise first, a flexible spatio-temporal scaling and secondly, to model local scale hydrological processes. In the algorithm, the simulation of hydrological processes for any spatial and linear data structure are completed for all time steps prior to moving on to the next data structure in downstream direction. The implementation of this primary algorithm with the extended methods is illustrated in figure 7.3.

The algorithm starts to call the linear data structures (stream segments) in an explicit order from upstream to downstream. The spatial data structures (such as linked subcatchments and LSDMs) drain into the downstream junction nodes of stream segments and are computed in the respective order. To model local scale drainage processes in LSDM data structures, a query is implemented to check for specific drainage features in the parametrisation (see "Is LSDM set?" in figure 7.3). The spatial local and meso scale parameters are defined according to the data mapping method presented in section 4.1 and section 4.3. Parameters of different temporal scales (here: longterm, seasonal, shortterm and process scale) are required for the numerical calculations. Each local and meso scale spatial data structure consists of at least one Hydrological Response Unit (HRU) and at least one layer. The calculation routines to model the developed LSDM features are integrated in the algorithm to compute the soil water

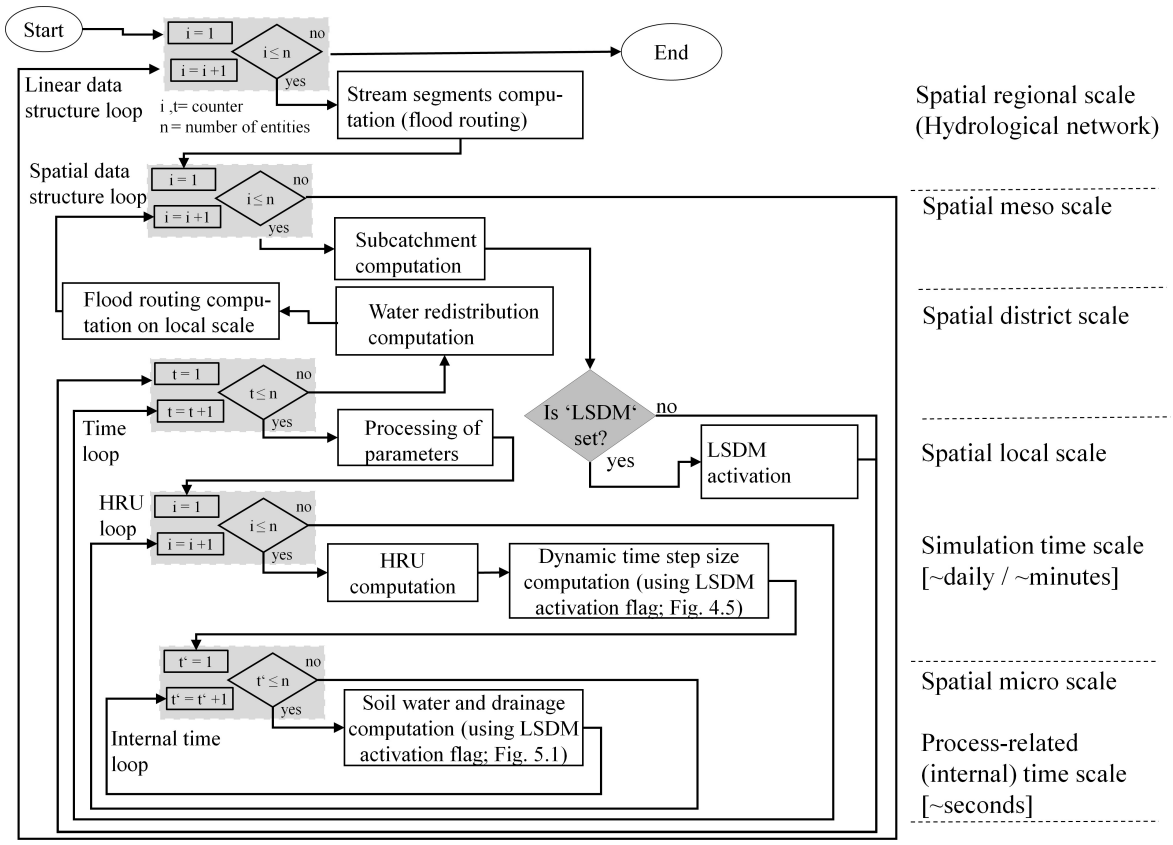

Figure 7.3: Flow chart of the implemented time-before-space algorithm to model the hydrological processes as well as the downstream directed flood routing on the regional, meso, district, local as well as micro scales. The definition of scales are illustrated in figure 3.1 on page 36 (adopted from Hellmers and Fröhle [2017]).

balance and drainage processes per layer on the micro scale. This is implemented in the developed calculation routine of process-related (internal) time steps which is described in section 4.2. The methods to compute the hydrological processes are explained in detail in chapter 5. After completing this primary algorithm a secondary one is activated to compute backwater effects and control systems (see next section).

7.2.2 Implementation of the secondary space-before-time algorithm for modelling backwater effects

The implementation of the third part ot the methodology (see chapter 6) to model backwater effects and control systems in stream segments as well as areas is realised with a secondary space-before-time algorithm. This implemented algorithm is illustrated in figure 7.4. The data structures (such as stream segments, control structures, spatial structures and junction nodes) are part of a backwater system. An active backwater system is present when afflux conditions at a downstream segment causes a backwater effect in upstream direction. The backwater system calculation routine starts with the downstream data structures and computes the backwater affected water level and storage volumes per time step for each data structure before

moving on to the next time step. Interactive backwater systems are computed which depend on downstream and upstream stages as described in the previous chapter 6.3. Additionally, the subsequent hydrological processes in submerged LSDMs or flood prone areas are modelled.

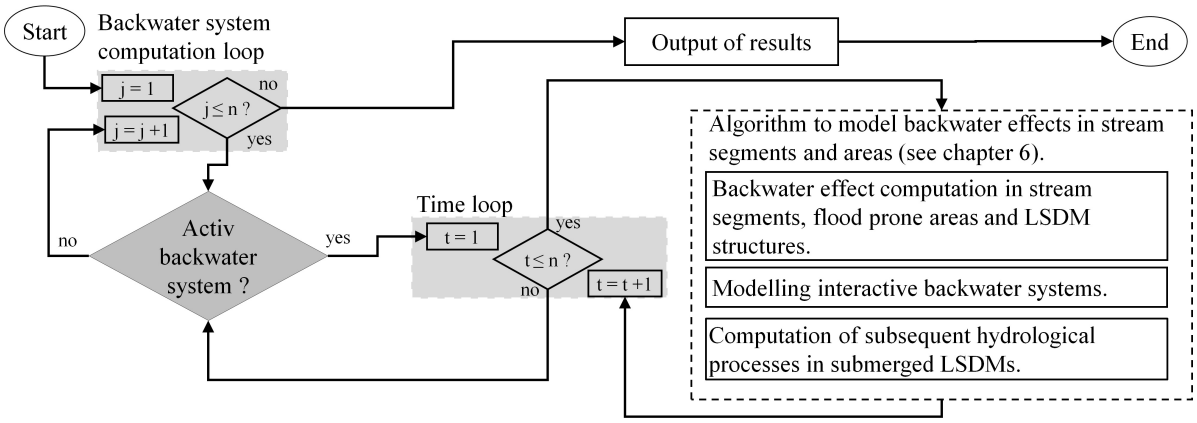

Figure 7.4: Flow chart of the implemented space-before-time algorithm for modelling backwater effects and control structures per backwater system.

7.3 Implementation of the parametrisation

For the execution of the developed model, the input parameters need to be defined and organised. The required level of complexity in the parametrisation depends on the temporal and spatial resolution to answer the specific questions as described also by Obled et al. [2009]. Along with the growth of complexity, the number of input parameters to be measured or estimated increases. A differentiation is done between actual input parameters (also known as arguments) and formal parameters. The last ones are processed during the execution of the numerical model as input and output among calculation routines. Actual parameters are the arguments given by the modeller to define specific characteristics of the structures to be modelled (for example geometry or material descriptions). In practice of hydrological numerical model development, described for example in Vaze et al. [2012], it is an aim to keep the number of estimated input parameters low and effective (namely sensitive) to define a parsimonious model. The complexity of the model, with regard to the number of parameters, is only suitable as far as respective detailed data is available (see Perrin et al. [2001]). Otherwise, over-parametrisation caused by unsuitable data sources for parameter estimation and calibration leads to uncertainties and unreliable model results as described by Petrucci and Bonhomme [2014]. More details about model uncertainty derived by over-parametrisation is given in attachment A.

The values of input parameters are provided in the form of ASCII files to describe the hydrological structure to be modelled. These parameters are used in the implemented methods to compute the hydrological processes, for example infiltration, retention and flood routing. The developed hydrological catchment model expects those actual parameters to be defined on different scales. Hence, more physical-based parameters are applied in the calculation routines to model local scale than meso scale processes. The reason is the difficulty

to estimate physical-based actual parameters on the meso scale according to their inherent nature and heterogeneity in space as well as time. On the meso scale, parameters are derived from regionalised field observations and other information sources (for instance thematic maps), because the data is subject to large spatial variability within the discretized elements. Whereas on the local scale of drainage constructions (namely LSDMs), the input parameters to describe material properties are more likely known by the suppliers.

A parameter which is estimated differently on meso than on local scale is, for example, the hydraulic conductivity in soil material. On meso scale, the hydraulic conductivity of the soil is derived from thematic maps describing the soil with empirical data. In contrast, on local scale the hydraulic conductivity is computed with the developed method described in section 5.2 on page 71 by applying the Kozeny-Carman approach using the particle size as input parameter. Further input parameters describe the characteristics of the following data structures on different scales:

- Spatial data structures on local scale (LSDMs) or meso scale (subcatchments).
- Linear data structures (stream segments) on local or meso scale.
- Junction data structures (junction nodes) on local or meso scale.
- Control data structures on local scale (for example, cisterns) or on meso scale (such as tide gates and pumping stations).

The input parameters of these data structures are described in this section with focus on those who are derived in this work. These parameters are organised and pre-processed in additional ASCII files in an extension folder (see table 7.1). The ASCII files which provide input parameters per individual data structure of the model are labelled with a "name".
By providing these additional ASCII files, the implemented methods in this work are activated during the execution of the numerical model KalypsoNA version 4.0[8]. When the ASCII files are not provided, the calculation routines of the afore released version 3.1 (published in 2016) are activated and an information is written in the output files. This distinction to activate or deactivate the developed methods supports to apply and test the extended calculation code KalypsoNA continiously in combination with the released module KalypsoHydrology. The implementation of the organisation and pre-processing of input parameters in the graphical user interface of KalypsoHydrology are not within the scope of this research work, but considered as an outlook (see section 9.4).

7.3.1 Input parameters to model hydrological processes on local scale

The input parameters for modelling multi-layered structures like LSDMs are defined in a modular way for each layer. Exemplified structures illustrate the usability as shown in attachment C. For the definition of input parameter values on the local scale (here LSDMs), the examples of laboratory-confirmed physical models of green roof structures are studied. A multi-layered and a single layer structure are exemplified with two different green roof installations. To define the values of the input parameters a calibration and validation procedure is

[8]The calculation code is available under: http://www.kalypso.wb.tu-harburg.de.

Table 7.1: List of additional ASCII files to organise and pre-process input parameters for the execution of the extended numerical model KalypsoNA.

ASCII file	Description of input parameters
minTimeStepSizes.dat	Minimal time step size (for example 0.1 seconds) to prevent infinite computations in process-related time loops.
runoffLossRate.dat	Input parameters to compute depression loss rates based on surface slope, roughness and duration for evaporating retained water from impervious surfaces.
lsdm.param	Additional input parameters to model hydrological and drainage processes in LSDMs.
overlay.ctrl	Configuration of criteria for control structures of spatial data structures ("overlays": LSDMs) and linear data structures (streams).
strands.ctrl	
overlay.kami	Input parameters for the flood routing computation in streams among LSDMs on local scale and in stream segments on meso scale.
strands.kami	
"lsdm-name".q	Ideal yearly rainwater harvesting time series in (l/m²/day) for 365 days and for 366 days for leap years (= "sj").
"lsdm-name".q.sj	
strands.topo	Input parameters to describe stream profiles.
"node-name".w	Time series of water levels (e.g. of gauging stations) for defined junction nodes.
"strand-name".wvq	(Optional) input parameters of the computed WVQ-relations (for example from a polynomial computation) when using the KM5-method.
nodes.xyz	Geographical location defined by the coordinates x (longitude), y (latitude) and z (height) for junction nodes or LSDM structures.
overlay.xyz	

* all ASCII files contain a header with a description of the input parameters and units.

performed. The procedure and results are given in section 8.1. The derived parameter values obtained by the calibration and validation procedures for exemplified green roof structures are transferable to other LSDM structures. The parameters which describe the geometry of LSDMs and hydrological soil characteristics are obtained by measurements (see table 7.2). The input parameters to model the hydrological processes of a vegetated cover are listed in table 7.3. Optional input parameters for the calibration procedure using measurements in laboratory on the local scale are summarised in table 7.4[9]. The coefficients for the computation of the subsurface flow retention time ($t_{c,1}$ and $t_{c,2}$) in permeable materials are derived from laboratory results and given in table 7.5.

Adjustment factors are introduced to model a change in drainage behaviour if compaction (settlement) takes place which increases the density of the material or clogging of the outlet occurs. The saturation stage height h_{sat} and the exceedance flux $\dot{V}_{sat}$ are influenced and calibration parameters (namely $f_{h,sat}$ and $f_{\dot{V},sat}$) are defined. The Kozeny-Carman coefficient is determined by literature to be in the range of 0.05 to 0.166, but requires calibration for the permeable materials in LSDMs. Additionally, a factor $f_{I,sat}$ to calibrate the saturated darcy flow is introduced. The input parameters in the additional ASCII files include the possibility to set a minimal time step size according to shortterm and longterm computation runs (for example 0.1 seconds). In this way, infinite computational loops are prevented and computing times

[9]Optional input parameters are by default set as empty text = " ", as factor equal to 1.0 or as value equal to 0.0 for addition or subtraction.

are reduced if the derived dynamical time step size is unreasonable small (see section 4.2 for details). The input parameters are provided in the additional files "lsdm.param" per layer and the file "minTimeStepSizes.dat".

The input parameters to model the depression and evaporation losses from impervious surfaces are given in the ASCII file "runoffLossRate.dat". The computation of the unsteady depression loss rate requires the definition of the surface slope (m/m) and a coefficient for the surface type, for example 0.07 for impervious surfaces (mm) according to Hingray et al. [2014]. The time duration to evaporate the water in the depressions is given as input parameter and the computed open water evaporation with the Penman approach can be adjusted optionally with a factor (by default = 1.0).

Table 7.2: Input parameters which describe the physical form of spatial data structures with drainage features of LSDMs per layer.

Physical form parameter	Unit	Description	Physical form parameter	Unit	Description
H	(mm)	Thickness of layer	L_{seal}	(-)	Sealed layer (yes/no)
D	(mm)	Diameter of the outlet	WP	(%)	Wilting point
R	(mm)	Roughness	FC	(%)	Field capacity
L	(m)	Flow path length to outlet	PV	(%)	Pore volume
I	(%)	Inclination of the structure	d_m	(mm)	Average particle size
h_{ov}	(mm)	Overflow crest height	$L_{coupled}$	(-)	Indication of a coupled layer
A_{outlet}	(m^2)	Drained area per outlet			

Table 7.3: Parameters to describe the vegetated cover of spatial data structures. Values are determined from literature (see DVWK [1996]) or measurements if available.

Ideal year parameter	Unit	Description	Ideal year parameter	Unit	Description
$S_{I,max}$	(mm)	Maximal interception storage capacity	R	(-)	Monthly defined crop coefficient for specific vegetation types
H_{root}	(mm)	Root depth per unit area			

Table 7.4: Optional input parameters for the calibration procedure to model the clogging or changes in density in the drainage materials of LSDMs.

Calibration parameter	Unit	Description	Calibration parameter	Unit	Description
$f_{H,sat}$	(%)	Factor of the saturation state height (default = 1.0).	c_0	(-)	Kozeny-Carman coefficient (range 0.05 - 0.166).
$f_{V,sat}$	(%)	Factor of the saturation state volume (default = 1.0).	$f_{I,sat}$	(-)	Factor of the saturated darcy flow (default = 1.0).

Table 7.5: Parameters to model the micro scale subsurface drainage fluxes per layer.

Empirical parameter	Unit	Description	Value
$t_{c,1}$	(-)	Coefficients of the subsurface flow retention time.	0.001
$t_{c,2}$	(-)		0.369

7.3.2 Input parameters to model control structures

Control structures are implemented on the local and meso scale with different input parameters. On the local scale, control functions are parametrised for spatial data structures (for instance cisterns or green roofs). On the district and meso scale, control functions are parametrised for modelling linear data structures (for example pumping stations, retention ponds or tide gates in rivers). The local scale control functions are defined in the text file "overlay.ctrl" while the meso scale control functions are defined in the file "strands.ctrl". The input parameters are summarised in table 7.6.

Table 7.6: Input parameters to model control functions in spatial data structures (for example, LSDMs) and linear data structures (such as stream segments) on local and meso scale.

Parameters	Unit	Description	Scale of the control structure
"name"	(-)	Name of the control structure.	Local and meso scale
Driver*-type	(-)	Type of driver data time series: precipitation, discharge or waterlevel.	
Driver "name"	(-)	Name of the driver data structure.	
Value (start / end)	(-)	Criteria of values to activate or end control functions.	
Duration (start / end)	min	Duration to fullfil the criteria to activate or end the control function.	
Time period of an advanced start of a control function	min	Duration to start the control function in advance of the reached threshold (such as for pre-emptying a cistern in advance of a forecasted rainfall intensity).	
Target value	(m)	Target value in water level for advanced emptying or pumping of a storage volume.	
Control function file name	(-)	The control function data series provide the rainwater harvesting or emptying values of LSDMs for an ideal year with a daily resolution.	Local scale
Flag for preset or computed driver time series	true or false	True or false flag to differentiate between preset or computed driver time series for the control functions of streams.	Meso scale

*A driver time series to activate a control function can be derived from any element in the hydrological network.

To model rainwater harvesting control functions, input parameters in the form of ideal yearly time series with daily time step sizes are provided in input files with the format: date, time, value. Per day the values are variable according to working or weekend day definitions. Varying time series for different land use classes (namely building types) can be defined. A

research study about possible ideal yearly rainwater harvesting time series is given for instance in Sverdlova [2015][10].

7.3.3 GIS-based input parameters

For the purpose to meet the needs of city planners, public agencies in practice and research demands, different structures of the same local scale drainage measure (for example, extensive and intensive utilised green roofs) need to be modelled within one (sub-)catchment. To import and process shape files with the location of different LSDM structures, GIS-based processing functions (such as intersection or aggregation) are applied in the Kalypso platform. The features in Kalypso support a project setup, import data management and visualisation of GIS-based data.

In addition to the already implemented meso scale data processing in the Kalypso platform, more detailed information about the geographical location of the local scale data structures (LSDMs) are required to compute the developed flood routing methods on the local scale. The extended geographical input parameters are written in the file "overlay.xyz" for spatial data structures (namely LSDMs) and in the file "nodes.xyz" for junction nodes. The applied coordinate system to define the input parameters in the additional ASCII files need to correspond to the settings of the coordinate system in the workspace of the Kalypso platform. A visualisation of the GIS-based data processing is exemplified in attachment C.

Spatial mapping of rainfall radar data. Using rainfall radar data with a high spatial resolution for hydrological numerical modelling of urban areas is presented with good results in Hellmers, Strehz, et al. [2016]; Jasper-Tönnies et al. [2018] and Hellmers and Fröhle [2020] (in press). Detailed radar data nowcasts with a spatial resolution of 1 km^2 are distributed on the spatial elements in the hydrological numerical model (KalypsoNA) by an analysis of proximity and neighbourhood. The precipitation is assigned to each spatial data structure as an area weighted mean of overlying radar raster cells. In this way, a detailed GIS-based integration of the precipitation data into the hydrological catchment model is achieved.

7.3.4 Input parameters for the generation of the hydrological network

The hydrological network is created with an algorithm based on graph theory which prevents the definition of closed loops. This algorithm is a function of the module KalypsoHydrology to write the resulting hydrological network into an ASCII file. The network structure explicitly defines the order of elements in the model. The order is given according to the stream segments from upstream to downstream. Additional virtual junction nodes and stream segments are added to the network structure on-the-fly to fulfil the explicit order with complemented LSDM linkages. Each stream segment is defined with one start and at least one end node. Spatial

[10] Sverdlova, L. (2015). Reference values to estimate the efficiency of sustainable drainage systems - Development by using hydrological modelling; supervised Masters Thesis by Sandra Hellmers (TUHH) & Nils Petersen (BWS); Examinors: Prof. Peter Fröhle & Prof. Ralf Otterpohl. Hamburg University of Technology, Hamburg, Germany.

elements on the meso scale (for example, subcatchments) and on the local scale (for example, LSDMs) are defined optionally and linked to linear data structures. The implementation of the methodology into the user interface of the module KalypsoHydrology has been done by the author in cooperation with Björnsen Consulting Engineers (see Hellmers, Belger, et al. [2016]). The created network fulfils the following requirements:

- Linear data structures (stream segments) always have one start and at least one end node.
- Spatial data structures (subcatchments or LSDMs) are always linked to linear data structures. Hence, the location of each subcatchment in the network plan is explicitly defined by a stream segment.
- The information about water distribution functions is given per junction node. Several junction nodes can be linked to one downstream junction node.

The percentage distribution of drainage flow among source and target LSDM structures is defined per junction node in the network (see section 4.1, page 53 ff). The module Kalypso-Hydrology includes a graphical representation and configuration of the main hydrological network elements. Supplementary network elements are integrated on-the-fly using drainage criteria during the execution and are not visualised in the graphical user interface, but written in the ASCII files. Thus, illustrating only the main elements and adding the supplementary ones in an on-the-fly processing, is especially required for the usability (user-friendliness) of the graphical presentation and configuration of large complex networks where there is a high information density.

7.3.5 Input parameters to model flood routing and backwater effects

The input parameters, to model the local scale flood routing with the KM1-method, comprise the profile data of stream segments on different scales. The parameters are given in the files: "overlay.kami" and "strands.kami". In the file "overlay.kami" the parameter values of local scale and in the file "strands.kami" the parameter values of district and meso scale streams are written. Both files comprise the following data: profile bed width (m), bank gradient (m), Manning-Strickler roughness k_{st} ($m^{1/3}/s$), bankfull height (m), hydraulic diameter (m), equivalent sand roughness k_s (m), number of interpolation steps (-) for the KM1-method, cross section form (circular or rectangular), minimal longitudinal gradient (m/m) and a choice of the computational approach (Manning-Strickler or Darcy Weisbach). According the chosen approach (Manning-Strickler or Darcy-Weisbach) and the cross section (circular or rectangular) the mandatory input parameters are specified.

The topographical data of stream segments and the input parameters for the backwater effect computation are given in the file "strands.topo". The stream length (m) and gradient (-) are computed with the geographical data of the upstream and downstream junction nodes or can be provided as user defined input values. A flow path prolongation factor is given optionally per data structure in the hydrological network. The stream segment input parameters comprise: the lowest bed level (m a.s.l), the minimal water level (m a.s.l.) and the number of

supporting points of the WVQ-function.

For calibration purposes an adjustment of the WVQ-functions per stream segment profile is provided (optionally) in the input files in the form of a percentage factor for the discharge (default = 1.0), a water level variance value (default = 0.0 m) and a cross-section adjustment using a variance value (default = 0.0 m^2). The stream segments are part of different backwater systems which are defined with an ordinal number (1 to n) from downstream to upstream. The tolerable backwater level difference is defined in (m) per stream segment, whereas larger values are suggested for streams with wider profiles than for narrow ones. Examples are given in the application study in section 8.2.1. Another input parameter in the file (here: "strands.topo") gives the number of linked spatial data structures (for example, subcatchments or LSDMs). The indexes of the linked spatial data structures are listed in the input file with an overflow height in m a.s.l. When the water level of a stream segment reaches this overflow height, water is flowing into the free storage volume of the linked spatial structure. This model feature is explained in chapter 6.3 (page 90 ff).

7.4 Output parameters for evaluation and application studies

The output parameters of the calculation code KalypsoNA are written in ASCII files. These files are post-processed with the module KalypsoHydrology to analyse the results (namely hydrographs of discharges and storage volumes) of the meso scale data structures. Additional output parameters of the implemented methods, are written in ASCII files of the defined extension folder (see the outline in figure 7.1 on page 101). The output parameters are processed for the purpose of model evaluation and application. In the following paragraphs, the extended output parameters are explained first, with regard to the output parameters of hydrological processes in LSDMs and secondly, concerning the output parameters of the flood routing computation with and without backwater effects.

(1) Output parameters of the implemented methods to model hydrological processes in LSDMs.
For each layer of a spatial data structure on the local scale (namely LSDM) the soil moisture balance equations are solved with the developed calculation routines as described in chapter 5. The following output parameters are written as time series per time step (t), with the time step size (Δt) and per unit area (m^2) of the LSDM structures in *.dat-format (date, time and value). For evaluation purposes the results with and without backwater effect computation are given.

- Influx (mm/Δt) per LSDM structure.
- Rainwater harvesting outflux (mm/Δt) per LSDM structure. The potential and the actual rainwater harvesting time series are given[11].
- Pre-emptying outflux (mm/Δt) per LSDM structure.

[11] After longer periods without rainfall, the potential rainwater harvesting demand is not served completely by the storage volume in the LSDM structure. In that case, the actual rainwater harvesting values are smaller than the potential rainwater harvesting demand.

- Water (drainage) outflux per layer and sum of drainage outflux per LSDM structure (mm/Δt).
- Exceedance outflux (mm/Δt) per LSDM structure.
- Evapotranspiration (mm/Δt) per LSDM structure.
- Interception storage volume (mm/Δt) per LSDM structure.
- Water volume per layer and sum of water volume in the LSDM structure without and with backwater effect computation (mm/Δt).

The following output parameters are written as aggregated sum of out- and influxes as well as changes in the storage volumes per simulation run and per spatial data structure (namely LSDM or subcatchment):

- Sum of influx in form of precipitation (mm).
- Sum of influx from linked LSDMs (mm).
- Sum of interception storage volume (mm).
- Sum of potential and actual evaporated water (mm).
- Sum of infiltrated water into the permeable material of the top layer (mm).
- Sum of transpired water over all layers in the root zone (mm).
- Sum of exceedance flow of the topmost layer and surface runoff (mm).
- Sum of lateral drainage fluxes of each layer (mm).
- Sum of actual rainwater harvesting (mm).
- Sum of actual controlled pre-emptying drainage fluxes (mm).
- Sum of percolation into the groundwater reservoir (mm).
- Sum of depression losses from impervious surfaces (mm).
- Change in water storage during the simulation run (mm) = ΔV.
- Area (m^2) per spatial data structure.

For each spatial data structure the water balance computation in the form of mass-balance is calculated for evaluation purpose in the following form:

$$\text{if} \quad V_{in} - V_{out} - \Delta V \neq 0 \quad \rightarrow \quad \text{A warning and the error value is given.} \tag{7.4.1}$$

where V_{in} is the influx (mm), V_{out} is the outflux (mm) and ΔV is the change in water storage (mm).

(2) Output parameters of the implemented method to model flood routing with and without backwater effects. The output parameters of flood routing computations are the formal parameters and the WVQ-relations before and after the calculation of backwater effects with the KM1- and KM5-method. A comparison of the inflow and outflow hydrograph volumes per stream segment is provided for evaluation purpose. Additionally, the time series with a temporal resolution of Δt for the following output parameters per stream segment and control structure are given:

- Storage volume before and after backwater effect computation (m^3).
- Water level before and after backwater effect computation (m a.s.l.).
- Control system settings per time step (-).
- Discharge per junction node (m^3/s).
- Evaporation rates from open water surfaces ($mm/\Delta t$).
- Exceedance flow of reservoir stream segments (m^3/s).

For evaluation purposes in the form of mass-conservation and for checking the calculated flood routing parameters, the following output is given per linear data structure:

- Total inflow hydrograph volume (m^3).
- Total outflow hydrograph volume (m^3).
- Change in water storage per simulation run (m^3).
- Computed (formal) parameters of the KM1-method:
  - Retention coefficient K_{km} (s).
  - Characteristic length L_c (m).
  - Number of characteristic lengths n (-).
- Computed (formal) parameters of the hydraulic capacity per stream segment (in the form of WVQ-relations):
  - Water level (m).
  - Volume (m^3).
  - Discharge (m^3/s).
  - Wetted cross section (m^2).
  - Hydraulic radius (m).
  - Flow velocity (m/s).

8. Model evaluation with application studies

In this chapter, the developed and implemented model to simulate required features of LSDMs and backwater effects is evaluated. The ten previously missing features in current hydrological numerical models are revealed in the review in chapter 2 (table 2.1 on page 14). For the model evaluation, five parameters are introduced according to the SMART-principle within the scope of work in chapter 3. These parameters are explained in the following paragraphs and applied to evaluate the implemented methods in application studies. These studies present an analysis of computed output parameters of the numerical model. First, observed data of local scale green roof installations in laboratory and secondly, observed data of gauging stations on the regional scale of a backwater affected catchment are applied to evaluate the numerical model results. The objective of the model evaluation is to determine the reliability of the numerical model results to be in a sufficient range of accuracy for the application purpose.

Objectives of the numerical model evaluation. For model evaluation, different perceptions of the terms "model verification" and "model validation" exist in research and practice. In this work, model verification aims to test the functional correctness of the numerical model implementation in a closed system as described in Oberkampf and Roy [2010]; Refsgaard and Henriksen [2004] and Sargent [2014]. For that purpose, verification tests are carried out to analyse the mass-conservation between influx and outflux processes, to test the accuracy in spatial data mapping and to check the correctness in hydrological network generation according to criteria.

A validation of the extended model KalypsoNA is performed by comparing the results of the numerical model with observed data of physical models in laboratory testing and of gauging station data on the regional scale of a catchment. The term "validation" indicates a weaker objective of testing the model reliability than a "verification". It aims for testing if the model results are within a sufficient range of accuracy for the designated but as well limited field of application (see Law [2008]; Oberkampf and Roy [2010]; Refsgaard and Henriksen [2004] and Sargent [2014]). The evaluation results of the developed and implemented methods in the numerical model KalypsoNA are presented in four sections as outlined in table 8.1.

Table 8.1: Outline of presented results and tested features of the extended model KalypsoNA in verification and validation studies by using evaluation parameters.

Section	Presented results	Solved features	Tested features of the extended model KalypsoNA	Applied evaluation parameters
8.1	Results of computed retention and drainage processes in LSDMs.	(1) to (6)	Physical-based parametrisation to model processes in LSDMs.	Validation of computed results by a comparison with observed data and analysing the sensitivity of parameters with studies (i, iv) .
			Computation of local scale retention and drainage processes.	
8.2	Results of GIS-based parameter processing and computation performance.	(1) to (4)	Testing the spatial resolution and data processing with a GIS-based local data mapping.	Verification by using the mass-conservation criteria and verification of the data processing (ii, iii) .
			Checking the explicit (on-the-fly) network generation.	Verification of the data processing (iii).
			Testing the model performance.	Testing the computation time to be short and the parametrisation to be parsimonious (v).
8.3	Results of local, district and meso scale flood routing and backwater effect computations.	(8) to (10)	Setting and processing of control functions in interactive backwater systems.	Verification of data processing and analysing the sensitivity of parameters with studies (iii, iv).
			Computation of backwater effects in streams and areas.	Verification of the mass-conservation criteria and validation with observed gauging station data (i,ii).
8.4	Results of computed hydrological processes in LSDMs as parts of meso scale and backwater affected catchments.	(1) to (10)	Computation of runoff, run-on and backwater effects in LSDMs.	Verification of the mass-conservation criteria, the data processing and analysing the sensitivity of parameters with studies (ii, iii, iv).
			Modelling local scale hydrological processes with process-related time steps.	
			Modelling LSDM technologies and local scale control functions.	

*Note: the resolved features to model LSDMs and backwater effects are summarised in the review table 2.1 on page 14.

In section 8.1, simulated results of local scale retention and drainage fluxes are validated by using observed data of a physical model in laboratory testing. This includes the calibration and validation of input parameters to provide a range of values which are valid in the application studies presented in this work. In section 8.2 the processing of input parameters to create a numerical model of the backwater affected regional scale catchment "Dove-Elbe" (175 km^2) in Hamburg, Germany is tested. The catchment comprises a tide gate as well as several sluices, weirs and low lying lands drained by pumping stations. One part of this area, namely the low lying backwater affected urban district scale catchment "Moorfleet" (8.42 km^2), is analysed with a focus to study the performance of LSDMs. The verification and validation results of the backwater effect computations are described in section 8.3. The numerical model

results of the local scale hydrological processes in LSDMs are verified with the method of mass-conservation as described in section 8.4.
The following five evaluation parameters (i) to (v) are introduced for the verification and validation of the numerical model within the scope of this work.

(i) Validation of the numerical model results by comparing them with observed data of physical models in laboratory testing or gauging station measurements in nature.

(ii) Verification of the mass-conservation between input, storage and output parameters of computed processes.

(iii) Verification of the functional correctness, including the accuracy in geographical data processing and hydrological network generation.

(iv) Analysing the sensitivity of parameters by varying the values of the structures and boundary conditions in the local and meso scale models.

(v) Testing the criteria to provide short computing times and a model structure with a parsimonious parametrisation. The execution of the implemented local scale methods shall not considerably increase the computing times of the primary meso to regional scale hydrological catchment model. This means a computing time of five minutes per simulation run of several days shall not be exceeded for operational application of the regional scale model (>100 km^2).

8.1 Evaluation of the methods to model hydrological processes in LSDMs

The computed output parameters of hydrological processes in multi-layered structures on the local scale are validated by comparing the simulated results with measurements of physical models in laboratory testing. In a first step, the calibrated values of input parameters are tested to be in a determined range for the computation of local scale hydrological processes. In a second step, the simulated results of the extended model KalypsoNA are validated by using additional measurements of physical models in laboratory testing. A requirement to perform the model calibration and validation is the definition of a "closed system" with defined conditions of time, space and boundaries. To validate the local scale infiltration, percolation, drainage and retention processes in particular, it has been determined that the conditions of a closed system can be sufficiently obtained in laboratory, where initial and boundary conditions are operated for a sequence of experiments. A local scale structure is defined here as a unit with technical specifications of material, layer composition and layer thickness.

The experiments are performed in the laboratory using the example of green roof installations with single and multi-layered structures. Different green roof structures with and without specified drainage layers are representative to analyse the hydrological processes for multi-layered LSDMs in a more general point of view. It gives transferable results for the considered hydrological behaviour of multi-layered systems of other LSDM types described

in this work. The processes of backed up water and exceedance flux generation among several layers are analysed. For this purpose, detailed observed and simulated outputs for each layer of the overall system are required. It is the first time that the drainage and retention processes of each separate layer are measured, modelled and analysed in such detail as published previously in Hellmers and Fröhle [2017].

Calibration and validation objectives with evaluation criteria. Five evaluation criteria are defined for the calibration and validation procedure: (1) Conformance in outflux hydrographs with regard to retention time before water is drained by the LSDM structure ("lag time"); (2) conformity in the time duration to reach the peak flux ("time to peak"); (3) Difference in peak flux values being less than 10 %; (4) the Root Mean Square Difference (RMSD) between the observed and simulated time series of values to be below 10 % of the input rainfall intensity and (5) the coefficient of determination R^2 in the scatter plot comparison between observed and simulated hydrographs to be larger than 90 %.

The RMSD gives a value of the spread of the observed values about the simulated values. It is computed with the following equation:

$$RMSD = \sqrt{(1/n \sum_{(i=1)}^{n} (\hat{\gamma}_i - \gamma_i)^2} \tag{8.1.1}$$

where RMSD is the root mean square difference given in the unit of the values γ, i is the index of ordered pairs of values, n is the entity of pairs of values (-), $\hat{\gamma}$ is the observed value and γ is the simulated value. The RMSD indicates how well the simulated entity of values of the numerical model fit to the observed entity of values in the respective unit. The evaluation parameters and criteria to validate the extended model KalypsoNA by a comparison between observed laboratory-confirmed and simulated model results on the local scale are summarised in table 8.2.

Table 8.2: Evaluation parameters and criteria to validate the implemented methods to model local scale retention and drainage processes.

Implemented methods	Scale	Evaluation parameters	Evaluation criteria
Methods to model the hydrological processes per layer on the local scale (see section 5.1 & 5.2.).	Spatio-temporal micro and local scale.	Validation by using observed physical model data and analysing the sensitivity of parameters (i,v).	• Conformity in lag time and time to peak in hydrographs (< 2 min). • Difference in maximal outflux < 10 %. • Root Mean Square Difference (RMSD) < 10 %. • Coefficient of determination R^2 > 90 %.

8.1.1 Description of the physical model setup in laboratory

Different installations of green roofs in laboratory are tested with the Rainfall-Simulator of the Hamburg University of Technology (RS-TUHH) developed by colleagues of the institute

of river and coastal engineering, Justus Patzke and Giovanni Palmaricciotti, in the years 2014 to 2015. The system geometry, performance and characteristics of the rainfall simulator are described in Palmaricciotti et al. [2014, 2015].

The RS-TUHH consists of a lightweight aluminium structure with a pressure valve, water distribution and irrigation device. An outline of the setup in laboratory is given in figure 8.1. The RS-TUHH can reproduce uniform rainfall with intensities between 3 to 300 mm/h over the testing area of about 6 m^2. The drop height is about 2.5 m and drops with an average fall velocity of 1.8 to 2.6 m/s are generated. The size of drops can be varied between 0.4 to 0.65 mm by adjusting different meshes.

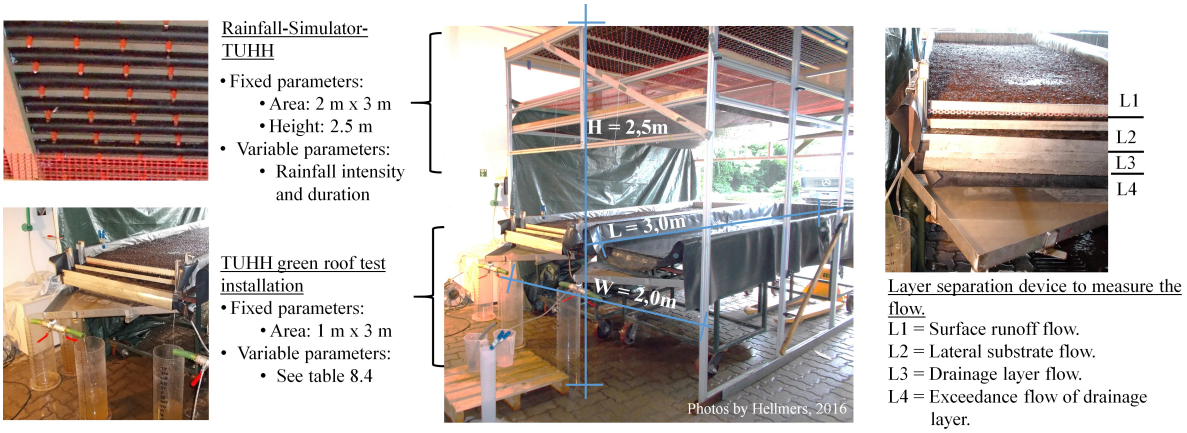

Figure 8.1: Outline of the physical model setup with the Rainfall-Simulator of the Hamburg University of Technology (RS-TUHH) and two green roof test installations in laboratory (adopted from Hellmers and Fröhle [2017]).

The results of two exemplified green roof installations are applied for the numerical model evaluation in this work. The first installation is made up of a single layer structure using the substrate HansePor of the company HanseGrand (Selsingen, Germany) and the second is a multi-layered structure using the Extensive-Substrate Typ E, a filter nonwoven geotextile and a patented drainage system (Meander 30) of the company OptiGrün (Krauchenwies-Göggingen, Germany). The soil hydrological input parameters of the HansePor and Extensive-Substrate Typ E ("Esubstr") are summarised in table 8.3. The values are given as volumetric soil water content in (%). The hydrological parameters (wilting point WP, field capacity FC and maximal pore volume PV) are obtained by laboratory studies (see attachment page D1).

Table 8.3: Soil hydrological parameters of the two sorts of substrate materials. The values are given as volumetric soil water content (%).

	Wilting point (WP)	Field capacity (FC)	Pore volume (PV)	Mean particle size distribution (d_m)
	(%)	(%)	(%)	(m)
Esubstr	12.00	39.90	58.26	0.002
HansePor	12.00	30.00	45.00	0.002

The meander 30 panels with a thickness of 30 mm prolong the flow path in the drainage layer. Details of the product are available in Optigrün international AG [2015]. The materials are

provided by these companies for research purposes.

The green roof installations are equipped with a layer separation device for the specific purpose to measure the outflow of each layer. In this manner, studying retention and drainage processes in each layer separately is enabled. The flow separation device is shown in figure 8.1 (right) for a green roof installation with drainage and substrate layer. The device is made up of water resistant membrane, which lies about 5 cm horizontally in depth of the layers. The device consists of different tubes conveying the flow from the separate layers: tube 1 (L1) = surface runoff (overflow), tube 2 = lateral substrate layer flow, tube 3 = outflow of the drainage layer, tube 4 = flow of the exceedance water volume from the drainage layer. The horizontal outflow is quantified for each layer using measuring cylinders. The tubes have a diameter of about 1.2 cm and are installed at the outlets of the layer separation device.

The measured data of 22 different experimental runs is analysed in this work. Each experiment with specified parameters is defined in this work as "run". The variable parameters for the different experimental runs of the green roof structures are summarised in table 8.4.

Table 8.4: Overview of variable parameters to define the 22 analysed experimental runs for the calibration and validation of the numerical model with evaluation criteria.

Variable input parameters per experimental run:	**Purpose of the 22 analysed runs:**	**Evaluation criteria:**
• Two different substrate materials. • Single or multiple layered structure. • Two gradients: 2 % or 6 %. • Two substrate thicknesses: 6 cm or 8 cm. • Three different rainfall durations and intensities (i, ii, iii see table 8.5)	• 7 runs are applied for the calibration of input parameter values. • 15 runs are analysed for validation purpose.	• Conformity in hydrographs with regard to difference in time (< 2 min). • $\Delta \dot{V}_{max}$ < 10 %. • RMSD < 10 %. • R^2 > 90 %.

The variable parameters of the green roof structures comprise different gradients, a variety in substrate thickness, varying types of materials and with or without a drainage layer. The variety in design rainfalls is created with different rainfall intensities ranging from 0.6 to 1.9 mm/minute and rainfall durations ranging from 15 to 90 minutes. These rainfall types correspond to statistical rainfall events with a probability of occurrence (T) of once in 100 years (T = 100 a)[1]. The applied rainfall types are summarised in table 8.5.

Table 8.5: Summary of the applied three rainfall types in the experimental runs.

Rainfall type	h_p (mm) for T = 100a*	Duration (minutes)	Intensity P mm/minute
i	27.9	15.0	ca. 1.9 ± 20%
ii	42.7	45.0	ca. 1.0 ± 20%
iii	50.9	90.0	ca. 0.6 ± 20%

* h_p = statistical precipitation height (mm). T = 100a is the return period of once in 100 years. According to KOSTRA-DWD 2010R (2017) for the Hamburg inner city region using data from January to Decembre (1951 to 2010) for a statistic. The tolerance in rainfall intensity generation with the RS-TUHH is about ± 20%.

Each experiment is carried out 24 hours (h) after full saturation of the substrate layer and

[1] According to KOSTRA 2010 R these rainfall intensities and durations represent storm events with a return period of once in 100 years for the Hamburg inner city region with a tolerance of ± 20 %.

without the influence of vegetation. The measurement of the outflow per layer is done in an interval of 30 seconds. The experimental runs are carried out with colleagues and students from the Hamburg University of Technology (TUHH). The reports of the laboratory works are referenced in the attachment on page D1.

8.1.2 Description of the numerical model setup

The numerical model is created by pre-processing input parameters with the module Kalypso-Hydrology and writing additional local scale parameters in ASCII files of the extension folder. The module and the structure of the additional ASCII files are described in chapter 7. The simulation runs are executed with KalypsoNA version 4.0 which is extended and compiled within the scope of this work. Two green roof structures are modelled: (1) a single layered structure and (2) a multi-layered structure with a drainage system. The area of each green roof structure is 1 m wide and 3 m long. Gradients along the length and thickness of layers are variable.

The single layer structure consists of a topmost free storage layer (L1) with a thickness of 14.0 cm and a substrate layer (L2) with a thickness of 6.0 cm or 8.0 cm (see figure 8.2: design 1).

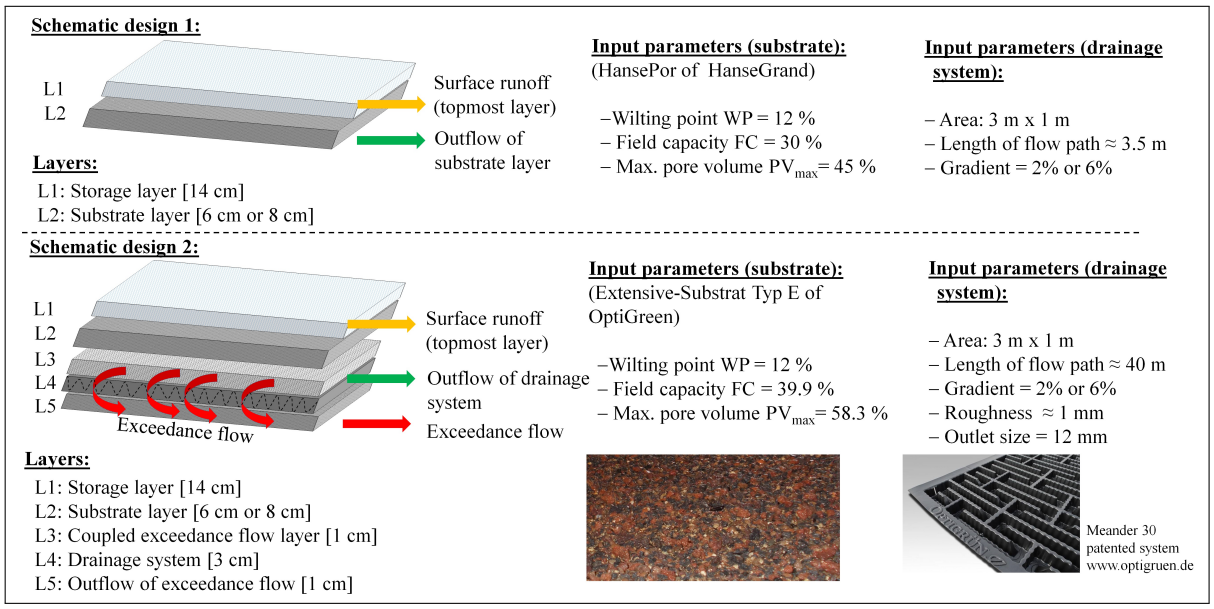

Figure 8.2: Schematic design and input parameters for the numerical model setup (adopted and extended from Hellmers and Fröhle [2017]).

The numerical model of the multi-layered structure consists of 5 layers (see figure 8.2: design 2). The first layer (L1) is a free storage layer with a thickness of 14.0 cm. The second layer (L2) is modelled with the soil hydrological parameters of the Extensive-Substrate Typ E with a thickness of 6.0 cm or 8.0 cm. The third layer (L3) is a virtual storage layer of the exceedance flow of the drainage layer. The forth layer (L4) is modelled as drainage layer (namely the Meander 30 structure) with a thickness of 3.0 cm. The exceedance flow begins when a saturation stage in the drainage system is reached. The third layer (L3) is coupled with the bottom layer (L5) under the drainage system and drains the exceedance water to the outlet of the green

roof structure. The input parameters for the single layer structure are summarised in table 8.6 and for the multi-layered structure in table 8.7.

Table 8.6: Input parameters of the single layer green roof structure.

Layer description	Height (H)	Outlet	Rough-ness	Length	$I_{Gradient}$	L_{coupl}	$A_{drained}$	Layer sealing (yes/no)
	(cm)	(m)	(m)	(m)	(%)	(-)	(m²)	(-)
(L1) Storage	14.0	1.0	0.005	3.5	2.0 or 6.0	-	3.0	no
(L2) HansePor	6.0 or 8.0	1.0	0.005	3.5	2.0 or 6.0	-	3.0	Yes

Table 8.7: Input parameters of the multi-layered green roof structure.

Layer description	Height (H)	Outlet	Rough-ness	Length	$I_{Gradient}$	L_{coupl}	$A_{drained}$	Layer sealing (yes/no)
	(cm)	(m)	(m)	(m)	(%)	(-)	(m²)	(-)
(L1) Storage	14.0	1.0	0.005	3.0	2.0 or 6.0	-	3.0	no
(L2) Esubstr	6.0 or 8.0	1.0	0.005	3.0	2.0 or 6.0	-	3.0	no
(L3) Ex_Mean	1.0	1.0	0.001	3.0	2.0 or 6.0	L5	3.0	no
(L4) Meander	3.0	0.0012	0.001	30.0	2.0 or 6.0	-	3.0	yes
(L5) Ex_Drain	1.0	0.0012	0.001	3.0	2.0 or 6.0	-	3.0	yes

The input parameters of the drainage system (namely the Meander30 structure of OptiGreen) are described in the data sheets of the product and are complemented by laboratory measurements. The flow path length in the meander system is about 40 m. The material roughness for the horizontal subsurface routing computation in the substrate layer is about 5 mm and in the drainage layer about 1 mm. The results of the model setup with a gradient of the green roof structure of 2 % and 6 % are presented in this work. The particular soil hydrological input parameters for the two kinds of substrate materials are summarised in table 8.3 on page 119. The hydraulic conductivity k_f in (mm/s) is computed using the Kozeny-Carman equation with the input parameter of the mean particle size (d_m). The particle size distribution is defined on the basis of laboratory tests of the porous media. The distribution curves and the references to the laboratory reports are given in the attachment on page D1.

Rainfall (in mm/minute) and temperature (here about 15°C) are input parameters of the boundary conditions. Further climatic input parameters (such as wind, sunshine duration, relative humidity) are neglected for these studies because of the assumption of a closed system in the laboratory. No vegetation is considered in the numerical and physical model runs. Thus, no losses due to evapotranspiration are analysed in this part of the evaluation studies. The initial soil moisture at the beginning of each experimental run is measured and ranges between 22 to 36 % of the volumetric soil water content. Because a focus is set on analysing the retention and drainage behaviour during the experimental runs, the initial soil moisture variation is defined as an input parameter for each numerical model run. The rainfall intensity is controlled by a pressure valve of the RS-TUHH. Setting the rainfall intensity is subject to adjustments per run because of external impacts derived by a fluctuating pressure in the water supply system. These parameters are reported for each calibration and validation

run as described in the following sections. For the numerical simulation runs, the analysed duration is 3 hours and the time step size is set to 1 minute. According to the developed dynamic time step size computation method, the smallest internal time step size is calculated to be about 1 s. The internal time step size ($\Delta t'$) depends on the Courant-Friedrichs-Lewy (CFL) criterion based on the influx magnitude per layer thickness (see section 4.2, page 57 ff). In this manner, the soil water balance computation is performed 60 times per simulation time step to compute the hydrological processes (such as infiltration, percolation and backed up water fluxes).

8.1.3 Procedure and results of the numerical model calibration

The calibration procedure aims to obtain the range of parameter values which represent the observed physical-based characteristics in the limited field of application in this work. These values are determined by comparing the numerical model results with observed data in laboratory testing. The input parameters are described in the following paragraph. The output of four different experimental runs of the single layer structure and the output of three different runs of the multi-layered structure are analysed in the calibration procedure. The difference in the runs is defined by changes in input parameters which are summarised in table 8.4 on page 120. With the obtained range of calibrated parameter values, the model is applicable for further model computations within the scope of this work. This is tested with 15 additional experimental runs in the validation phase as described in section 8.1.4.

Description of the parameters for the calibration procedure. During the experimental runs in the laboratory an accumulation of fine materials at the drainage layer outlet (having a size of 3 mm · 12 mm) and a compaction of the substrate materials took place. These effects change the retention and drainage behaviour of the structure over time. Four calibration parameters are used to simulate these effects. A reduced saturation height ($f_{H,sat} < 1$) and volume ($f_{V,sat} < 1$) indicate a larger outflow rate because of an increased density of the material (compaction) and a clogging of the drainage layer. A factor of the saturated darcy flow $f_{I,sat}$ (> 1.0) simulates less retention potential in the substrate layer. In these cases a larger proportion of exceedance flux is generated. The Kozeny's coefficient c_0 is expected to be up to 0.166 as proposed by Carman [1937] and described in Bear [1988]. For very porous materials the value of the coefficient c_0 can be 1/3 lower as illustrated by the experimental results of Chapuis and Aubertin [2003] and Urumović and Urumović Sr. [2016]. The method is described in section 5.2 (page 71). Variations in this value illustrate likewise changes of the material in density and behaviour throughout the experiments. Thus, input parameters for calibration purpose in the numerical model are:

- $f_{H,sat}$: Factor of the saturation hight in the drainage layer (by default = 1.0).
- $f_{V,sat}$: Factor of the saturation volume which exceeds the storage capacity of the layer (by default = 1.0).
- c_0: The Kozeny-Carman constant (by default 0.166).

- $f_{I,sat}$: Factor to adjust the saturated Darcy flow above the saturation stage (by default = 1.0).

Additionally, a correlation between the gradient of the structure and the retention coefficient in porous material is defined. The retention coefficient is computed per meter of the flow path length of the structure. The coefficients $t_{c,1}$ = 3.64 and $t_{c,2}$ = 0.37 are determined in this work by analysing the measurements of the physical models in laboratory testing. The method is described in section 5.3.1 (page 73).

Results of the calibration procedure. For each experimental and numerical model run specific input parameters are defined according to the structural differences. The experimental runs are numbered with an index and labelled to differentiate the different structures as follows: type of structure (single layer = SL or multi-layer = ML), substrate layer height H (cm) and the gradient I (%). The physical model runs in laboratory are done three times and the fluctuations of the observed values are smoothed over five points for the analysis. The results are visualised in attached diagrams and scatter plots with specified scales (see page D2 ff). Selected diagrams are illustrated in this chapter to explain the main findings.

For the runs [1] to [6], hydrographs of the drainage and exceedance fluxes are given in figure 8.3. On the left side (see a,c,e), the runs with a gradient of 6 % and a substrate thickness of 8 cm are given. On the right side (see b,d,f), the runs with 2 % gradients and substrate thickness of 6 cm are illustrated. In the single layer structure, a subsurface flux occurs in the substrate layer during run [2] and [4] (see hydrographs (b) and (d)). Thus, for the runs with a lower gradient (here 2 %) and lower substrate thickness an exceedance flux and an overall higher peak flow is generated in a single layered structure. For a higher gradient (here 6 %) and higher substrate thickness no or only a small quantity of exceedance flux is generated. Further runs are analysed in the validation procedure to examine if the gradient or the substrate thickness has a larger influence on the drainage behaviour.

Different rainfall types (i) and (ii) are analysed using the single layer structure as illustrated in figure 8.3. The precipitation intensities P (in mm/minute) and durations D (in minutes) are defined in table 8.5 on page 120. A comparison of the hydrographs [1] & [2] to the hydrographs [3] & [4] illustrates lower peak flux rates for lower rainfall intensities. The peak flux is reached after 15 minutes for the more intensive rainfall (i) and after about 10 minutes for the runs with less intensive rainfall (ii). An exception is the observed slower rising limp in run [3] for rainfall type (ii) and a single layer structure, where the peak flux is reached after 45 minutes. The hydrographs show conformity in the peak flux being reached later for a larger gradient and larger substrate thickness, while for a structure with lower gradient and smaller substrate thickness the peak flux is reached earlier. In contrast to the conventional roof hydrographs, all green roof model runs show a good potential to retain more water by increased lag time and lower peak flux rates especially for events with shorter rainfall duration (see grey stripped line in figure 8.3). The values of the calibrated input parameters are summarised in table 8.8.

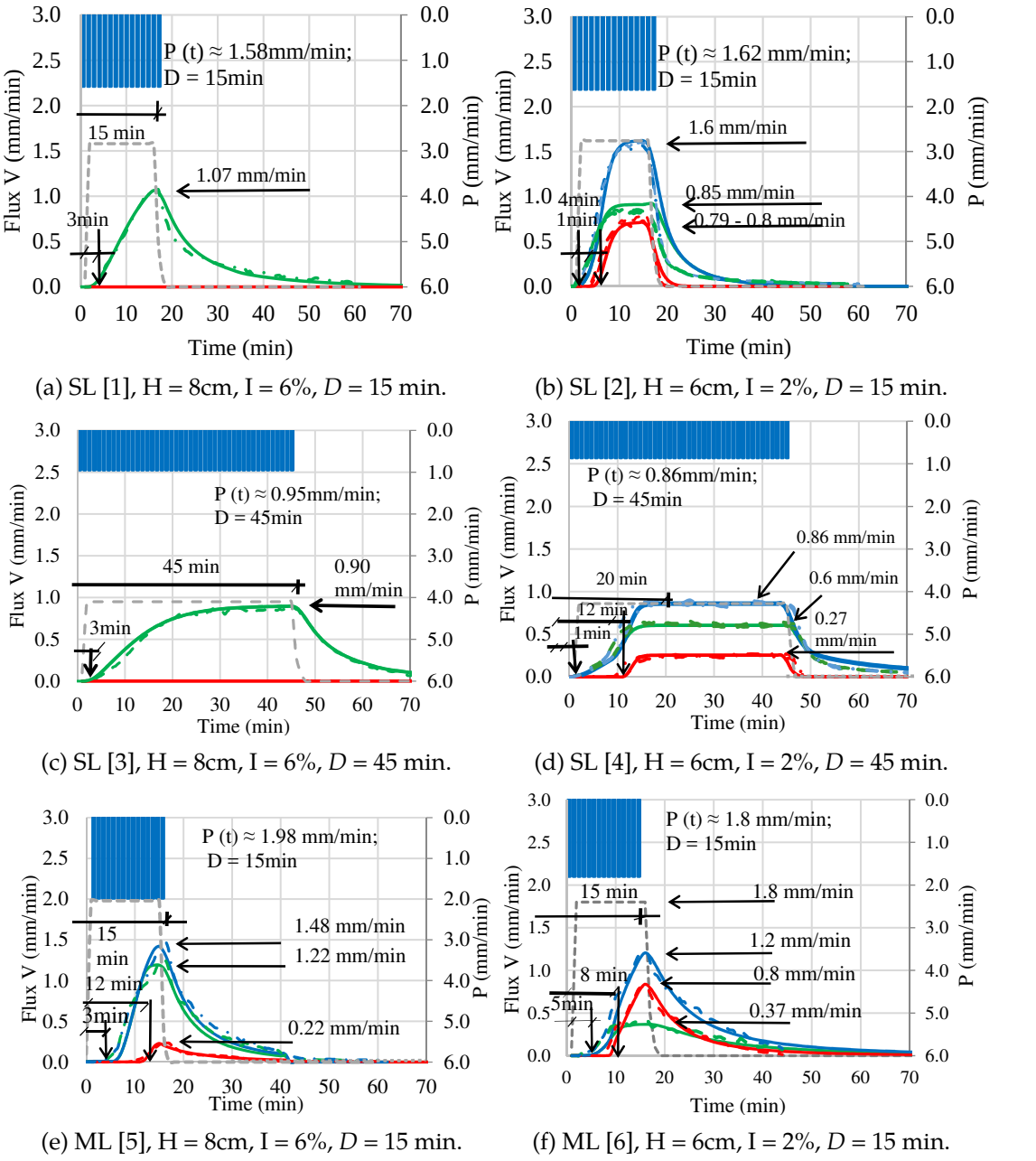

(a) SL [1], H = 8cm, I = 6%, D = 15 min.

(b) SL [2], H = 6cm, I = 2%, D = 15 min.

(c) SL [3], H = 8cm, I = 6%, D = 45 min.

(d) SL [4], H = 6cm, I = 2%, D = 45 min.

(e) ML [5], H = 8cm, I = 6%, D = 15 min.

(f) ML [6], H = 6cm, I = 2%, D = 15 min.

Figure 8.3: Composite of hydrographs of the single layered runs [1] to [4] and the multi-layered runs [5] & [6] of green roof structures. The legend of fluxes and scales is applied in all diagrams and scatter plots of local scale green roof studies. SL = Single Layer structure, ML = Multi-Layered structure, [x] = index of experimental run, H = height of the substrate layer (cm), I = gradient of the structure (%), D = Duration of precipitation (minutes) and P = precipitation intensity (mm/min).

Table 8.8: Summary of the input parameters, calibration values and evaluation criteria results for the calibration runs.

Rainfall type:		(i)		(ii)		(i)		(ii)
Structure type:		Single layer (SL) - structures				Multi-layered (ML) - structures		
Structure details:		[1] SL H=8cm I=6%	[2] SL H=6cm I=2%	[3] SL H=8cm I=6%	[4] SL H=6cm I=2%	[5] ML H=8cm I=6%	[6] ML H=6cm I=2%	[7] ML H=8cm I=6%
Input parameters (of boundary conditions):								
P (t); D*	(mm/min)	1.58mm/min; 15min	1.62mm/min; 15min	0.95mm/min; 45min	0.86mm/min; 45min	1.98mm/min; 15min	1.8mm/min; 15min	0.97mm/min; 45min
V_{ini}	(%)	30.5	31.8	29.7	30.6	22.6	35.6	25.6
Calibration values:								
$f_{H,sat}$	(-)	-	0.49	-	0.84	1.10	-	0.80
$f_{V,sat}$	(-)	-	0.45	-	-	-	-	-
c_0	(-)	0.05	0.16	0.05	0.08	0.08	0.08	0.08
$f_{I,sat}$	(-)	1.34	1.80	1.34	1.34	1.34	1.34	1.34
Results of the evaluation criteria:								
lag time (Δ)	(min)	3min (< 1 min)	1min (< 1 min)	3min (< 1 min)	1min (< 1 min)	3min (+2 min)	1min (< 1 min)	6min (< 1 min)
time to peak (Δ)	(min)	15 min (< 1min)	14 min (< 1 min)	44min (<1min)	38min (≈1min)	15 min (< 1 min)	15 min (< 1 min)	43min (+ 2min)
max. peak flux (Δ)	(mm/min)	1.07 mm/min (+0.6%)	1.6 mm/min (+1.6%)	0.90 mm/min (+2.6%)	0.86 mm/min (-4.4%)	1.48 mm/min (-4.1%)	1.2 mm/min (+1.08%)	0.95 mm/min (+1.1%)
RMSD	(mm/min)	0.06 (3.5%)	0.08 (4.9%)	0.05 (5.3%)	0.06 (7%)	0.09 (4.5%)	0.08 (4.4%)	0.06 (6.2%)
R^2	(-)	>0.95	>0.95	>0.95	>0.90	>0.95	>0.95	>0.95

*P (t) = Rainfall intensity (mm) per minute (min); D = duration in minutes; RMSD = root mean square deviation as total value and (%) deviation of input flux; R^2 = coefficient of determination from the scatter plots; positve delta Δ = overestimation of simulated values; negative delta Δ = understimation of simulated values; "-" means no adjustment of the default value for the model calibration.

The table 8.8 itemizes the specifications of the varying rainfall intensities and the initial soil moisture conditions after 24 hours drying period of a full saturation stage. The initial soil moisture conditions V_{ini} are measured for all runs. It ranges between 22 to 35 (%) of volumetric soil moisture content. For a multi-layered structure, with a drainage layer of OptiGreen (Meander 30), the hydrographs are illustrated for run [5] and run [6] in figure 8.3 (e) and (f). In run [5], with a larger gradient of 6 % and larger substrate layer of 8 cm the main flux proportion is drained by the meander panel and only a small proportion is drained by exceedance flow. In run [6], a multi-layered structure with a gradient of 2 % and a smaller substrate layer thickness of 6 cm is analysed. Here, a larger exceedance flow is generated and less water is drained through the meander panel. Another multi-layered green roof model run [7] with similar setup as run [5] is analysed for the calibration purpose and gives comparable results to run [5]. Additional scatter plots and the overall diagrams are given in the attachment on page D2.

The experiments are performed over several weeks, where settling of material and clogging of outlets by fine material influence the drainage behaviour. To model the clogging and changes in the saturation stages during the experimental series, two adjustment factors are introduced in this work: the factor $f_{H,sat}$ for adjusting the overflow height and $f_{V,sat}$ for adjusting the exceedance volume flux rate. The factor for the volumetric stage $f_{V,sat}$ has a range between 0.5 to 0.8 when clogging in the drainage layer is present.[2] The adjustment of the factors $f_{H,sat}$ and $f_{V,sat}$ is partly required as indicated in the table 8.8. Only in run [2] for the single layer structure the overflow height is reached already at 50 % of the geometrical overflow height and the peak flux rate reaches 1.6 mm/minute after 14 minutes which is higher compared to the other runs with the same rainfall type. Here, the green roof structure illustrated less retention potential. The difference in the single layer run [1] with a higher gradient of 6 % and higher substrate thickness (8 cm) shows a fast subsurface flux rate through the porous material. The single layer run [2] with a lower gradient of 2 % and lower thickness of the substrate layer illustrates a faster generation of surface runoff and the subsurface flux is lower.

The Kozeny's coefficient c_0 is in the range of 0.05 to 0.16. The proposed values by Carman [1937] are described in Bear [1988] and are tested by Chapuis and Aubertin [2003] as well as Urumović and Urumović Sr. [2016] to be approximately $c_0 = 0.2$. The lower values in these studies are explained by the different form and shape of the drainage material in comparison to natural soils. The computed hydraulic conductivity for the infiltration capacity is overestimated when using the parameter value ($c_0 = 0.2$) as in natural soils. The calibration factor $f_{I,sat}$ is applied to adjust the computed subsurface flux using the equation of Darcy (see section 5.3.1, page 73). In most runs the value of $f_{I,sat}$ is set to 1.34. Only in the experimental run [2] a faster flow velocity is observed. Here, an adjustment value of $f_{I,sat} = 1.8$ is determined. This experimental run [2] presents a lower retention by reaching the saturation state earlier. The larger value for $c_0 = 0.16$ shows that the infiltration capacity is higher and the saturation

[2] Installed roofs will suffer from clogging of the drainage layer outlet with a slot size of 3 mm in width and 12 mm in height after a period of time and may react likely as a "clogged meander" roof experiment with a reduced value of $f_{H,sat}$.

state is reached earlier. In consequence, a larger portion of surface runoff is observed.

Sensitivity of gradient and substrate thickness on the drainage processes. In the experimental runs [2,4,6] a surface runoff is generated, when using structures with a small gradient (I = 2 %) and substrate thickness of 6 cm. In other runs [1,3,5,7] a larger subsurface flux is observed, when using structures with higher gradient (6 %) and larger substrate thickness of 8 cm. The full saturation stage is reached faster for small gradients of 2 % and smaller substrate thickness. With a higher gradient and larger substrate thickness the subsurface flow velocity is larger. Thus, more water is drained through subsurface flow paths. The sensitivity of changes in substrate thickness (6 cm and 8 cm) or the gradient (2 % and 6 %) is discussed in the validation results in section 8.1.4 by comparing 15 additional runs.

Summary of calibrated values. The calibrated values of input parameters are summarised in table 8.9. The factors of the overflow height $f_{H,sat}$ and overflow volumetric flux $f_{V,sat}$ are below 1 when the drainage layer is influenced by clogging or compaction of the substrate. The Kozeny's coefficient c_0 to compute the hydraulic conductivity and the factor to compute the saturated flow $f_{I,sat}$ are differentiated. Both values are lower when the substrate layer is influenced by lower infiltration rate and lower saturated flow velocity. This may be caused by higher compaction. In this way, the calibration parameter values are given in a range according to the physical conditions of the materials and structure during the experiments. For the validation runs, the unclogged stage is always set first as default (see table 8.9 "Default value") and adjusted if clogging of the material is present. For computing the infiltration capacity a lower parameter value $c_0 = 0.05$ is set as default and the saturated flow factor $f_{I,sat}$ is set to 1.34.

Table 8.9: Range of values of the calibrated input parameters representing clogging or differences in compaction rates of the porous material.

Parameter	Default value	Range of values to model clogging		Parameter	Default value	Range of values to model the change in hydraulic conductivity	
$f_{H,sat}$	1.0	< 1	with clogging	c_0	0.05	0.05	lower infiltration capacity
		≈ 1.0	no clogging			0.16	higher infiltration capacity
$f_{V,sat}$	1.0	< 1	with clogging	$f_{I,sat}$	1.34	1	lower saturation flow velocity
		≈ 1.0	no clogging			2	higher saturation flow velocity

Summary of evaluation criteria for the calibration results. The evaluation criteria comprise the difference between outflux hydrographs with regard to retention time before water drains from an LSDM structure ("lag time") and the time duration to reach the peak flux ("time to peak"). For both evaluation criteria the time difference remains below 2 minutes for all runs. Thus, the hydrographs illustrate a good conformity with regard to the temporal drainage behaviour. The peak flux shows an underestimation of up to 4.4 % and an overestimation of up to 2.6 %. This fulfils the evaluation criteria that the difference shall be less than 10 %.

The Root Mean Square Difference (RMSD) of the observed and simulated results is below 0.1 mm/minute and fulfils the criteria to be less than 10 % of the applied rainfall intensity in mm/minute. The coefficient of determination R^2 in the scatter plot comparison between measured and simulated hydrographs ranges between 0.92 to 0.99 and presents a good fit (see scatter plots in the attachment on page D2 ff.).

8.1.4 Procedure and results of the numerical model validation

In the procedure of the model validation, the determined parameter values of the calibration procedure (see table 8.9) are applied for additional 15 different green roof model runs with varying rainfall types. For the validation procedure, all three different rainfall types are applied: a rainfall intensity of about 1.9 mm/minute for a duration of 15 minutes (i), a rainfall intensity of about 1.0 mm/minute for a duration of 45 minutes (ii) and a rainfall intensity of about 0.6 mm/minute for a duration of 90 minutes (iii).

Validation results of runs with single layered structures [run 8 to 15]. Eight validation runs of single layered structures are labelled according to the order of different rainfall types. Run [8 & 9] are performed with rainfall type (i), run [10 & 11] with rainfall type (ii) and the runs [12 to 15] with rainfall type (iii). The analysis of the resulting hydrographs confirm that the difference of the drainage and retention fluxes is influenced mainly by the gradient of the structure. In the four runs with a low gradient of 2 % an exceedance flux is generated. The results for these runs [9,11,14 & 15] are given on the attached pages D6 ff. In the other four runs [8,10,12 & 13], a larger subsurface flux is generated when a higher gradient of 6 % is installed. Hence, with a larger gradient the subsurface flow velocity is larger. Thus, more water is drained by subsurface flow and less exceedance flux is generated. This is exemplified in figure 8.4 using a comparison between the hydrographs of the runs [3] and [11]. In both runs the substrate thickness is 8 cm, but the gradient varies. Run [3] is performed with a gradient of 6 %, while run [11] is performed with a gradient of 2 %. Varying the thickness of the substrate layer within the runs, while keeping the gradient constant, has no significant influence on the hydrograph output. This is shown, for example, by comparing the hydrographs of the runs [14] and run [15] (see attachment on page D9 ff.). In the runs performed with the rainfall types (ii) and (iii) the peak flux reaches the magnitude of the rainfall intensity in all runs because of full saturation stage which is reached after a duration of about 40 to 45 minutes. The hydrographs, scatter plots and tables to summarise the input parameters as well as the evaluation criteria are given in the attachment on the pages D6 ff. The values of the evaluation criteria show a good congruency between the observed and numerical model results. The differences lie in a similar range as described for the calibration results.

Validation results of the runs with multi-layered structures [run 16 to 22]. The indexes [16 to 22] of the validation runs of multi-layered structures are defined again according to the order of rainfall types: run [16 & 17] are performed with rainfall type (i), run [18 & 19] with rainfall type (ii) and the runs [20 to 22] with rainfall type (iii). The analysis of the output hydrographs

shows that a difference in substrate layer thickness from 6 cm to 8 cm has almost no impact, while a change of the gradient from 2 % to 6 % has a larger influence on the retention and drainage behaviour. The diagrams and tables are given in the attachment on page D6 ff. For example, run [5] and run [16] only differ in a varying substrate thickness as input parameter and show almost no difference in the output. A comparison of the impact in changing only the gradient from 6 % to 2 % is illustrated in figure 8.4 (c) [run 16] and (d) [run 6]. With a lower gradient, the saturation state is reached earlier causing a higher exceedance flow of the meander drainage layer. At the same time, the drainage flux peak is still lower for the 2 % gradient than for the 6 % gradient structure.

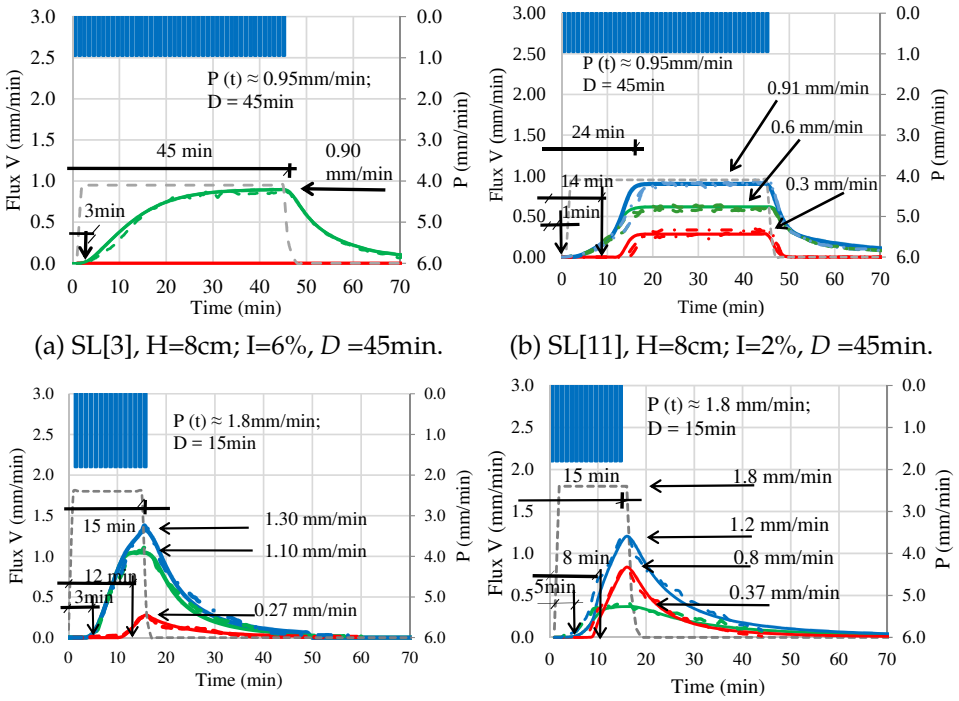

(a) SL[3], H=8cm; I=6%, D =45min.

(b) SL[11], H=8cm; I=2%, D =45min.

(c) ML[16], H=6cm; I=6%, D =15min.

(d) ML[6], H=6cm, I=2%, D =15min.

Figure 8.4: Composite of the hydrographs of the validation runs for single layered (in a, b) and multi-layered green roof structures (in c, d). The legend is given in figure 8.3.

The overall hydrographs, scatter plots, parameter tables and evaluation criteria of run [16] to [22] show a good congruency of the observed and numerical model data. The results are within the defined range of accuracy of the five evaluation criteria given in table 8.4 (page 120).

Comparison of simulated and measured soil moisture. For a limited set of laboratory experiments of the multi-layered structures (runs [16], [17], [20] & [21]) additional soil moisture measurements are analysed. The observed data is compared with the numerical model output of the volumetric soil water content in the substrate layer. For the three rainfall types and a multi-layered structure with a layer thickness of 6 cm and a gradient of 6 % the results are illustrated (see page D14 ff). The initial soil moisture is around 25 % at the beginning of the runs. The soil moisture reaches a level above the field capacity of > 34 %, while at the same time a subsurface flux is observed. The observed and numerical model data show a good

conformity with respect to soil moisture values and timing. For the larger intensity of rainfall in type (i) the largest soil moisture is reached earlier (here after 3 minutes) compared to the run with rainfall (type iii) (here after 6 minutes). After 24 hours the initial soil moisture is reached again and the next experimental run is performed.

When comparing the soil moisture measurements of a 6 cm and 8 cm substrate thickness for the same rainfall type (here iii, with 90 minutes duration), the initial soil moisture and soil moisture hydrographs vary only slightly. These results point out that the thickness of the substrate layer has a small influence on the drainage behaviour.

8.2 Evaluation of the data processing and computation performance of a regional scale model

The developed and implemented methods to model hydrological processes in LSDMs and backwater effects are evaluated on the local, district and meso scale of a tidal influenced catchment area (here: "Dove-Elbe" in Hamburg, Germany). The output of the GIS-based local data mapping, the explicit network generation and the computation performance of the numerical model are tested and described in this section 8.2.

Afterwards, a validation of the methods to compute the backwater effects and control structures is performed by using observed time series of gauging stations on meso scale stream segments. The validation results are explained in section 8.3.

For the evaluation of the developed and implemented methods to model hydrological processes in LSDMs, different scenarios with LSDM installations in a district scale catchment area (here: Moorfleet, Hamburg) are analysed in section 8.4. The district scale catchment area Moorfleet has a size of 8.42 km^2 and is part of the regional scale catchment area "Dove-Elbe" (175 km^2).

8.2.1 Description of the regional scale catchment "Dove-Elbe"

The regional scale catchment area "Dove-Elbe" has a size of 175 km^2 and is located in the South-East of Hamburg, Germany. The river segment Dove-Elbe is a stream of 18 km in length and is a tributary of the tidal influenced river Elbe. Further tributary streams which drain into this main river segment are the Gose-Elbe, Schleusengraben, Brookwetterung and a downstream segment of the Bille. These streams are part of the analysed regional scale catchment as well. The soil is mainly peat and clay with a varying spatial distribution and thickness. Another regional scale catchment (namely of the river "Bille") with a size of about 337 km^2 drains into the regional scale study area "Dove-Elbe". Thus, an overall catchment area of about 512 km^2 is drained trough the tide gate "Tatenberger Deichsiel". The downstream situated water level in front of the tide gate is affected by a mean tidal range of about 3.7 m (see Nehlsen [2017] p. 49). The Mean Low Water (MLW)[3] is at about -1.5 m a.s.l. and the

[3] MLW corresponds to MTnw (in German: "Mittleres Tideniedrigwasser ") and MHW corresponds to MThw (in German: Mittleres Tidehochwasser).

Mean High Water (MHW) is at about 2.2 m a.s.l. The tide gate closes when a water level of about 0.9 m a.s.l is exceeded in the Elbe river. During the closure period of the tide gate, water is retained in the Dove-Elbe stream segments leading to an afflux of water which causes backwater effects. The catchment border and backwater affected streams are indicated in the map in attachment D.2.1 on page D17. Additionally, the locations of eight gauging stations and seven control structures are given.

These control structures comprise gates, weirs, pumping stations and a tide gate. The numerical model includes 75 subcatchments, 75 junction nodes and 75 meso scale stream segments. The numerical model of the backwater affected catchment "Dove-Elbe" is created by the author as part of the work in the project "StucK" ("Long term drainage management of tide-influenced coastal urban areas with consideration of climate change")[4].

8.2.2 Description of the urban district scale catchment "Moorfleet"

The urban catchment area Moorfleet is located at the downstream section of the backwater affected catchment Dove-Elbe, in Hamburg. The area has a size of about 8.42 km^2. Low lying areas are situated in the upstream parts (also known as "Moorfleeter Wanne") of the catchment. This upstream area is characterised with a mixed urban and rural landuse. It has a size of about 1.57 km^2, with an impervious area of about 0.45 km^2. A map of surface sealing rates, the location of subcatchments and a topographical map of the area Moorfleet are given in the attachment on page D20. A church and detached houses are located in that low lying area. Flood prone areas are mostly green fields situated on a ground surface level of about -0.4 m a.s.l up to 0.1 m a.s.l. A documentation of fire brigade services in the past pointed out the occurrences of flooding in this area "Moorfleeter Wanne". The downstream areas are elevated artificially by deposit of dredged material. An industrial area "Allermöhe" with a size of 4.31 km^2 is situated downstream of the subcatchment "Moorfleeter Wanne". This area is characterised progressively by highly sealed industrial and business areas since the last two decades. The surface runoff from the industrial areas is drained directly to open water streams. The impervious surfaces in the industrial areas of this subcatchment have a size of about 1.17 km^2 with a sealing rate of up to 90 %.

The pumping station at the outlet ("Eichbaum") drains water from the district streams in Moorfleet to the main channel Dove-Elbe. The water level in the district scale streams is maintained on a level of about -0.8 m a.s.l. by this pumping station. It has a capacity of three pumps with 1.15 m^3/s each. The pumping is started according to the water levels at the downstream segments of Moorfleet. When the water level reaches -0.85 m a.s.l one pump is running. When the water level exceeds -0.80 m a.s.l. another pump is started and all three pumps are running when a water level of -0.75 m a.s.l. is exceeded. During storm events with high rainfall intensity and return periods larger than once in 30 years (like for the

[4] The projekt StucK (www.stuck-hh.de) is a joint project in the framework "Regional Water Resources Management for Sustainable Protection of Waters in Germany" (ReWaM) financed by the German Federal Ministry of Education and Research (BMBF). The project started in May 2015 and finishes in September 2019 (see Hellmers and Fröhle [2020], in press).

event in August 2002) the capacity of the pumping station is not sufficient to drain the surface water from the Moorfleeter stream segments. An afflux at the downstream pumping station is generated and leads to backwater effects in the upstream segments. The reversed flow in upstream direction reaches the low lying land in the subcatchment "Moorfleeter Wanne" and causes backwater flooding. For example, high water levels were reported after the storm event in August 2002 where an increase of 0.47 m led to a water level of up to -0.33 m a.s.l. in the streams. Hence, the 2002 summer event induced a number of fire brigade services in the area of "Moorfleeter Wanne" to drain the water from cellars and streets.

8.2.3 Description of the input parameters for the numerical modelling

The input parameters for the numerical modelling are summarised with respect to model the flood routing, functions of control structures, backwater effects and spatial hydrological processes in subcatchments as well as LSDMs.

Input parameters to model stream segments and control structures. The control structures in the backwater affected Dove-Elbe stream segments are indicated in the attached map on page D17 and are defined with parameters in the attachment on page D18 ff. The control functions are ordered according to their activation criteria from the lowest to the highest water level. The functions comprise the opening as well as closure of gates and sluices or starting of pumps according to defined criteria.

The stream segments are differentiated according to the scale and available data of profiles. Three different categories are defined to compute the flood routing in the streams: (1) district and local scale streams which are computed with the developed KM1-method, (2) meso scale complex profiles with large forelands where the flood routing is modelled with the KM5-method and (3) derived meso scale profiles with smaller forelands where the KM5-method is likewise applied. The stream profiles on the district scale of the Moorfleet study area for a river length of about 9 km are defined with trapezoidal geometries. These are determined as profile category (1). The locations of these profiles are shown in the attached map on page D18. The stream profiles are defined as open water trapezoidal profiles with a bottom width of about 5 m, bank gradients of about 0.5 (-), bankfull height of about 2 m, bank gradients between 0.004 % to 0.1 % and a Manning-Strickler roughness of 25 to 30. The geographical location, length and averaged gradient are exported from a digital elevation model. The Kalinin-Milyukov parameters for these strands are computed with the implemented KM1 flood routing method described in section 6.1.1 (p. 79 ff.).

The backwater affected river segments in the Dove-Elbe with a length of about 12.5 km are characterised with wide profiles (width >100 m) and wide flood prone areas (width >200 m) on the meso scale. For the computation of the flood routing, the KM5-method is applied. The profiles in these stream segments correspond to category (2) which are marked in the attached map on page D18. The profiles of the category (3) are derived from upstream river profiles. A river stream segment length of about 8 km is modelled with category (3) profiles and the KM5-method. For the computation of the KM5-method the WVQ-relations

are calculated on the basis of a polynomial function which is applied in a hydrodynamic model (here KalypsoWSPM) in the pre-processing phase. The method is described in section 6.1.2 (see page 84 ff.).

Input parameters to model the hydrological processes per subcatchment including LSDMs. The subcatchment (namely watershed) border lines are defined according to the stormwater drainage system and topographical maps. Hydrological processes are computed on the spatial scale of Hydrological Response Units (HRUs) which are generated by intersecting the data of pedology, geology, land use, existing LSDMs and watershed border lines. The pedology data is derived from punctual soil investigations of the State Ministry for Urban Development and Environment of Hamburg (BUE), which has been processed to areal information. The preprocessed land use data describes the areal drainage fractions to the stormwater drainage systems of each property. Additionally, ATKIS[5] landuse data is used to derive the vegetated surface cover information. In this way, a detailed landuse description is created with a high spatial resolution of HRUs. For example, by GIS-based intersection of pedological, geological, landuse and watershed data, a number of 585 HRUs are created in the subcatchment "Moorfleeter Wanne" (1.57 km^2) and 606 HRUs are created in the industrial area (Allermöhe) (4.31 km^2). Further input parameters for the model creation are described in Hellmers and Fröhle [2020] (in press).

8.2.4 Definition of scenario studies to model LSDMs and backwater effects

Different scenario studies are defined to model the performance of LSDMs in a backwater affected catchment. In the first scenario, estimated climate change (CC) impacts are analysed. An increased rainfall intensity leads to a higher impact of backwater flooding in the low lying lands. In the second scenario, LSDMs are installed only in the low lying lands which are affected by backwater flooding and in the third scenario LSDMs are installed additionally in the downstream located industrial areas to analyse the impact on the magnitude of backwater flooding in the low lying lands. The second and third scenario are modelled as well with the increased rainfall intensity to simulate the effectiveness of LSDMs to reduce flooding.

Scenario 1: Precipitation intensities are increased by estimated climate change "CC" impacts

The numerical model is applied to quantify the effects on discharges and water levels in streams caused by estimated climate change impacts on the intensity of storm events. For this purpose, an increase of 15 % is defined as add-on to the observed storm event in August 2002. This add-on value is defined in the project 'StucK' as possible climate change (CC) impact for the near future 2035. Details to the derivation of the scenario are described in the final report of the project (Hellmers and Fröhle [2020], in press). The duration of the event is about one hour and the maximal precipitation intensity is increased from 10.6 to 12.2 mm/5minutes. In this way, the rainfall sum is increased from 48.3 mm/h to 55.6 mm/h. According to the statistical

[5] ATKIS = Amtliches Topographisch-Kartographisches Informationssystem.

report published as KOSTRA-DWD 2010R [2017] over rainfall intensities, this precipitation event has a return period of once in 30 to 40 years in the region of Hamburg, Germany.

Scenario 2: LSDMs are installed only in the upstream backwater affected low lying lands

In the upstream subcatchment "Moorfleeter Wanne" a number of six green roofs (GRs), three cistern systems (Cs) and two multifunctional areas (MFAs) are installed. The locations of these LSDMs are illustrated in figure 8.5. The green roofs have a total area of 118 540 m^2 which are coupled to cisterns with a total area of 920 m^2 and multifunctional areas which have a total area of 8990 m^2.

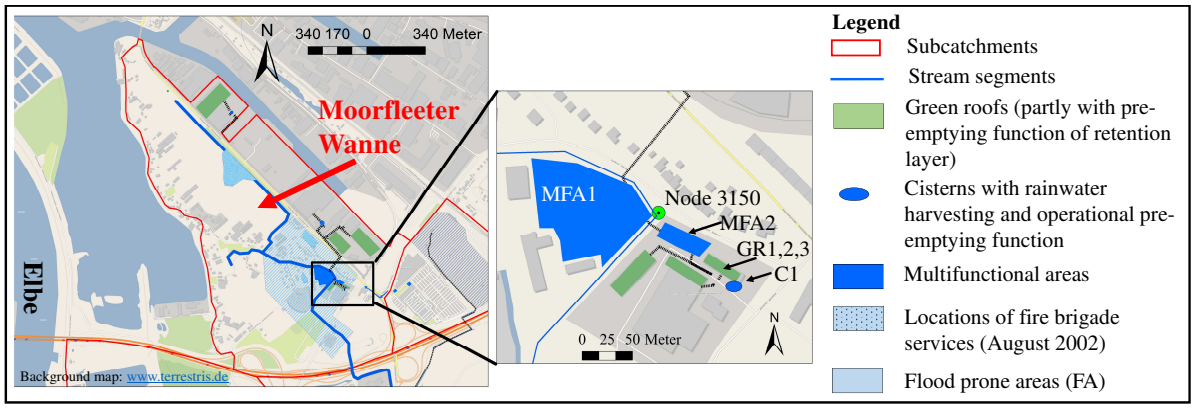

Figure 8.5: Map of installed LSDMs in the upstream subcatchment "Moorfleeter Wanne" (left) and the location of exemplified LSDMs for the verification studies (right).

The MFA1 is installed in the backwater affected flood prone area in the subcatchment "Moorfleeter Wanne". The ground level of this LSDM structure is on -0.85 m a.s.l. which is 5 cm below the operated water level in the district stream (-0.80 m a.s.l.). A weir with a crest height at -0.45 m a.s.l. provides a storage volume of about (1335 m^3) in the MFA1. A pump is installed to drain the retained water after a flood event. The illustrated LSDMs in figure 8.6 are studied in more detail for the numerical model evaluation in this work. These LSDMs comprise green roofs with a retention layer and control valve (GR1) having a size of 764 m^2, a detention roof with a "meander 30" structure (GR2) having a size of 367 m^2 and a single layer green roof structure (GR3) with a size of 448 m^2. Further on, several cisterns are defined with a total area of 58 m^2 (= cistern system C1). In addition, a multifunctional area (MFA1) having a size of 3337 m^2 and MFA2 having a size of 828 m^2 are modelled.

In the subcatchment "Moorfleeter Wanne" another three green roofs (GR4, GR5 and GR6) with a vegetated cover and substrate layer of 8 cm are implemented with an underlying retention layer system of 85 mm and an operational valve system to pre-empty the retention layer in advance to forecasted storm events. The pre-emptying function is activated operationally 12 hours before a forecasted event. The threshold value of the precipitation intensity to activate the pre-emptying function is adjusted to 4.8 mm/minute for this specific study.

Further retention measures comprise the installation of three cistern systems with a depth of about 3 m for industrial and business usage. The size of the cistern areas is designed according to the drained roof areas with the condition, that 1 m^2 cistern area is installed per

100 m² drained roofs area. This relation is adjustable and serves for demonstration purposes. When larger storm events are forecasted, the exceeding water of the cistern storages is drained to the multifunctional areas. The flood routing among measures is computed with the KM1-method using Darcy-Weisbach for circular pipes (as described in section 6.1 on page 78). The adaptation scenario 2 (and as well scenario 3) are modelled in combination with the increased precipitation intensity which is estimated to be derived by climate change impacts (see scenario 1).

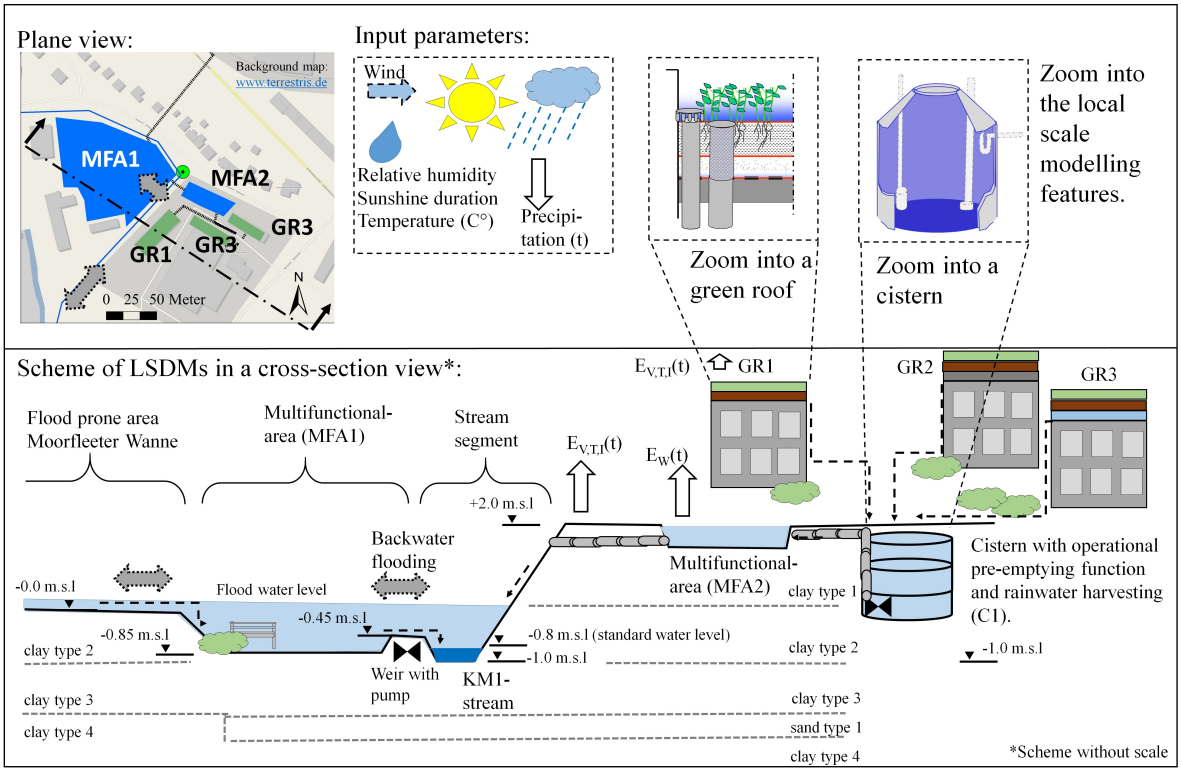

Figure 8.6: Plane view and cross-section as scheme of the modelled LSDMs in the backwater affected case study area "Moorfleeter Wanne".

Scenario 3: LSDMs are installed additionally in the downstream located industrial area "Allermöhe". In the third scenario, the LSDMs comprise 24 green roofs, 23 cistern systems and 7 multifunctional areas. A number of 18 green roofs with a vegetated substrate layer of 8 cm are installed additionally to the described ones in scenario 2. The cistern systems are defined likewise as in scenario 2. The added multifunctional areas are situated on a ground surface level of about 2.0 m a.s.l. The attributes and locations of the installed LSDMs are desribed in the attachment on page D20 ff. The area of green roofs is increased to a total area of 274 840 m² which are coupled to cisterns (total area of 5376 m²) and multifunctional areas with a total extent of 47 814 m².

8.2.5 Evaluation results of local scale data processing and the computation performance

The developed and implemented methods for data processing on the local scale and the computation performance of the numerical model are verified with evaluation criteria. The following four model features of KalypsoNA are tested. First, the accuracy of the GIS-based mapping to integrate the local scale data structures by so called "overlays" into the meso scale numerical model. Secondly, the correctness of the explicit hydrological network generation including LSDMs. Thirdly, the parametrisation of the numerical model to be parsimonious and fourthly, the computing time of a simulation run to be reasonable short for operational applications (< 5 minutes). The evaluation parameters and criteria are summarised in table 8.10. As supplementary information, the reference to the section of the described methods and the specific scales per model feature are given.

Table 8.10: Evaluation parameters and criteria to verify the data processing for creating a hydrological catchment model including LSDMs.

Evaluated model feature	Implemented methods	Scale	Evaluation parameters	Evaluation criteria
Detailed GIS-based local data mapping	Processing of spatial data to create LSDM data structures (section 4.1 and 4.2).	Local scale	Verification of the spatial congruency after data processing.	Spatial congruency in data mapping with a difference smaller than 1%.
"On-the-fly" network generation	Explicit hydrological network generation including LSDMs (section 4.2 and 4.3).	Local and meso scale		Prevention of infinit computation loops (circular computations).
Parsimonious parametrisation	Flexible spatial resolution and dynamical time step size computation (section 4.3).		Evaluating the complexity of parametrisation and duration of computing times.	Number of input parameters to be less than 100.
Short computing time of simulation runs				Computing time with and without LSDMs to be shorter than 5 min for a regional scale catchment model (>100km²) over a 10 days event simulation.

GIS-based mapping to integrate local scale data structures into the meso scale model. The developed method of the GIS-based local scale data mapping computes the geographical intersection of local scale data with the meso scale (namely subcatchment) data while preventing any loss or superimposition of spatial data[6]. The GIS-based model features are implemented in the software platform Kalypso (see chapter 7). The pre-processed parameters are written in ASCII files and serve as input data for the execution of the numerical model (here the cal-

[6]Loosing spatial data occurs when gaps are generated during the GIS-based mapping process. Superimposed spatial data is generated when spatial data is not correctly intersected and increases the areal magnitudes.

culation code KalypsoNA). Three tests are performed to verify this model feature. First, the intersection of thematic maps including data of pedology, geology, land use and watershed data is performed. Secondly, an additional intersection with the data of building shapes is executed. Thereby, intersecting the land use data with the building shape files requires a correction procedure to revise the information about permeable and impervious spatial fractions per HRU. In this way, required landuse data for LSDM mapping is created. Finally, an intersection with LSDM data structures is realised. The resulting GIS-based data source provides for example green roofs on buildings with geographical location and its connection to the drainage system. The evaluation criteria for this model verification is a spatial difference to be less than 1 % in all outputs of the spatial data intersections which is fulfilled in all three test cases. The verification procedure and results are described in the attachment on page D21.

Evaluation of the network generation based on drainage criteria including LSDMs. The hydrological network is created on the basis of drainage criteria to ensure an explicit computational order from source to target elements as described in section 4.3 (page 60 ff). The network order ensures that the water balance computations of the source elements are completed before the calculation of target (sink) elements is started. The network is generated on-the-fly based on drainage criteria for adding supplementary junctions of streams and spatial data structures. The input parameters and criteria are described in section 7.3.5 on page 110. An attached example on page D23 of a generated hydrological network for the Moorfleet study area with and without LSDMs illustrate the functional correctness. The evaluation criteria verify that no infinite or closed loops are generated. The supplementary junction nodes and streams are not shown in the user interface of the module KalypsoHydrology to facilitate the visualisation of complex networks. Instead, the source and target drainage criteria with flow distribution fractions to create such a hydrological network are determined.

Evaluation of the parametrisation to be parsimonious. A differentiation between simple, parsimonious and complex parametrisations is presented in the literature review in section 2.2.7 (p. 25). In this work, thirty input parameters are defined to model the hydrological processes in LSDMs and sixteen input parameters are defined to model the extended flood routing as well as backwater effects (see section 7.3, p. 104). Seven calibration parameters are defined: four parameters are used for modelling the hydrological processes in LSDMs and three parameters are provided to adjust the computed backwater effects in streams. These parameters are processed in the extension folder with additional ASCII files and do not increase the input parameters of the meso scale hydrological catchment model. The developed method brings into focus the parameters and processes where detailed data is available. This is regarded as "a zoom into" processes. On the other hand, the method accomplishes to zoom out of the processes where meso scale parameters are to be applied. With this adjustable input parameter structure, the number of parameters remains below 100 for a meso scale model and fulfils the criteria to define a parsimonious parametrisation. The application studies on local and meso scale demonstrate the input parameters to be effective and sensitive.

Evaluation of the computation performance To evaluate the computation performance, the computing times with and without LSDMs in the regional scale hydrological catchment model Dove-Elbe with a size of 175 km^2 are compared. In the presented application studies a standard computer with i7-5600U CPU and 2.6 GHz is applied. The computing time without LSDMs is 110 seconds and with LSDMs (in scenario 3) it is 140 seconds for a simulation run covering 10 days with a simulation time step size of 5 minutes. Both simulation durations are below 5 minutes (300 seconds) and fulfil the evaluation criteria. The hydrological processes in the LSDMs are computed with a time step size of 1 second, while the meso scale processes are computed with the simulation time step size of 5 minutes.

8.3 Evaluation of the flood routing and backwater effect computation

A flood routing method is extended within the scope of this work to model local scale streams among LSDMs and backwater effects. The computation takes into account the geographical locations of the source and target (sink) elements. Details are described in section 6.1 (p. 78 ff). The implementation in the numerical model KalypsoNA is explained in chapter 7.

The flood routing method is based on the approach of Kalinin & Milyukov using the input parameters of the flow path length, gradient and stream profile data. Because each profile is modelled as a single reservoir, the flood routing approach is labelled as KM1-method. In another approach, each profile is modelled with five reservoirs and labelled as KM5-method. The source and sink elements are not only junction nodes along river segments, but as well the drained subcatchments as well as LSDMs. For evaluation purposes, the mass-conservation of inflow and outflow hydrographs are checked. Further on, the results of a district scale flood routing are compared with outputs of another numerical model.

By means of modelling the existing numerous control structures of gates and pumping stations in the Dove-Elbe catchment, the developed and implemented functions of control structures (see section 6.2, on page 86 ff.) are evaluated.

The method to extend the aforementioned flood routing approach for the computation of backwater effects is described in section 6.3 (see page 90 ff.). A validation of this method is done by comparing the numerical model results with a limited set of gauge measurements along the river stream segments of the backwater affected catchment Dove-Elbe. The measurements of six gauging stations in the Dove-Elbe stream segments are available for one event and the measurements of three gauging stations are available for another two events. For a sufficient validation of the Dove-Elbe catchment model the measurements of more events (likely over at least a whole year) are required. The validation presented in this work fulfils the specific objective of evaluating the developed and implemented methods, but does not present a validation of the overall numerical catchment model Dove Elbe.

Evaluation parameters and criteria to verify and validate the results in the flood routing methods are summarised in table 8.11. Supplement information in the table provides the section where the developed method is described and the applicable scale for the method.

Table 8.11: Evaluation parameters and criteria to verify and validate the methods to compute the flood routing and backwater effects in streams and areas.

Model feature of KalypsoNA	Implemented methods	Scale	Evaluation parameters	Evaluation criteria
Local scale flood routing method KM1.	Computation of formal parameters and output of the KM1-method (section 6.1.).	Local scale	Verification of mass-conservation in computed processes and testing the sensitivity of input parameters.	Influx and outflux balance $\Delta < 0.1\%$. Sensitivity of parameters when changing locations and flood routing characteristics.
		District scale	Verification of mass-conservation in computed processes and comparison with limited results of another numerical model.	Influx and outflux balance $\Delta < 0.1\%$. Deviation in simulated outputs to be less than 10%.
Computation of control structures in stream segments.	Computation of control functions (section 6.2).	Local, district and meso scale	Verification of data processing.	Confirmation in criteria fulfilment and control function activation per time step (time shift smaller than 1s).
	Computation of an interactive backwater affected system (section 6.3).		Verification of mass-conservation in computed processes and validation with limited gauging station data.	Deviation in water levels between observed and simulated output to be smaller than 10% of observed fluctuation range of water table.
Computation of backwater effects in streams and areas.	Backwater effect computation (section 6.3).			
	Modelling hydrological processes in backwater affected areas (chapter 5 & 6).		Verification of mass-conservation in computed processes .	Deviation in water levels between stream segments and LSDMs to be less than the tolerated minimum water level difference (min ΔH).

8.3.1 Evaluation of the KM1-method to model the flood routing

To model the flood routing among LSDMs and in stream segments on the local scale, it is required to provide a parsimonious parametrisation and data processing within meso to regional scale catchment modelling (>100 km^2). The basis data is provided by drainage criteria and the geographical location of LSDMs. Using this parametrisation for an on-the-fly hydrological network generation is described in section 4.3 (page 60). On the local scale, the flow path length L (m) and the flow path gradient I_s (%) are computed along with the network generation on the basis of the geographical location of the source and the target (sink) elements. The source and target elements are spatial data structures (LSDMs) or junction nodes. The input parameters for the flood routing method KM1 are defined per source data structure.

An example is given in the attachment on page D26 for the LSDM structures in the Moorfleet study area.

The flood routing from green roofs to cisterns and cisterns to multifunctional areas is modelled with pipes (circular closed streams) using the approach of Darcy Weisbach. The flood routing from a multifunctional area to the receiving stream is done with open water trapezoidal profiles using the approach of Manning-Strickler.

The verification of mass-conservation criteria in the flood routing method is done by computing the difference between total volume of inflow (m^3) and outflow (m^3) which shall be less than 0.1 %. The local scale flood routing computation on the district scale using the geographical location of the elements is a new method implemented in the hydrological catchment model KalypsoNA within the scope of this work.

To illustrate the sensitivity of the local scale flood routing method, the input parameters are changed and a comparison with a meso scale runoff routing method is presented. The results show that using the meso scale instantaneous unit hydrograph (IUH) method and neglecting the geographical location of source and target elements leads to on overestimation of the retention effects on the local scale (see attachment page D28). The developed method in this work presents a solution to tackle this weakness in meso scale hydrological catchment modelling.

Results of the flood routing computation in streams on the district scale. In the Moorfleet study area stream profiles are defined as open water trapezoidal cross-sections with bed level gradients between 0.04 % to 0.1 % and with a Manning-Strickler roughness coefficient between 25 to 30. The details of the input parameters per stream segment are provided in the attachment on page D27. The output of the computed WVQ-relations with the KM1-method are compared with the output of a numerical model published in the report by Krob et al. [2000]. The results of the comparison are attached on page D30 and confirm the evaluation criteria of a difference to be less than 0.1 %.

A verification of the flood routing method is done by comparing the inflow and outflow total volume of the hydrographs for the upstream strand in the Moorfleet catchment. A bias of about 0.01 % in the mass-conservation criterion is computed (see page D30). This fulfils the criteria of this evaluation parameter.

8.3.2 Evaluation of the method to model backwater affected control structures

Control functions of tide gates, sluices and pumping stations depend on water tables upstream or downstream of the structures. Changes in control functions are activated with criteria using thresholds of water levels for different junction nodes in the hydrological network. One example is illustrated in figure 8.7 for the opening and closing function of the tide gate according to water levels at the downstream gauging station "Schöpfstelle"[7] in the Elbe river. The tide gate closes when a water level of 0.9 m a.s.l. is exceeded at the downstream gauging

[7] The location of the tide gate is indicated in the map in the attached figure D.30 (A) and the gauging station "Schöpfstelle" is indicated with index (1).

station "Schöpfstelle". In the illustrated example of February 2002, the tide gate remained closed two times during low tide periods because of too high water levels at the downstream sections (>0.9 m a.s.l.). The long closure times generated a larger afflux and consequently larger backwater effects in the upstream segments. The simulated and observed water levels show a difference of only 0.02 m. This difference is analysed in more detail in the following section 8.3.3. The observed precipitation data is obtained from the station "Wettermast" of the University of Hamburg. This station is about 0.5 km north of the Moorfleet study area as indicated in the attached map on page D17. A summary of the other control structures in the study area is given in the attachment on page D19.

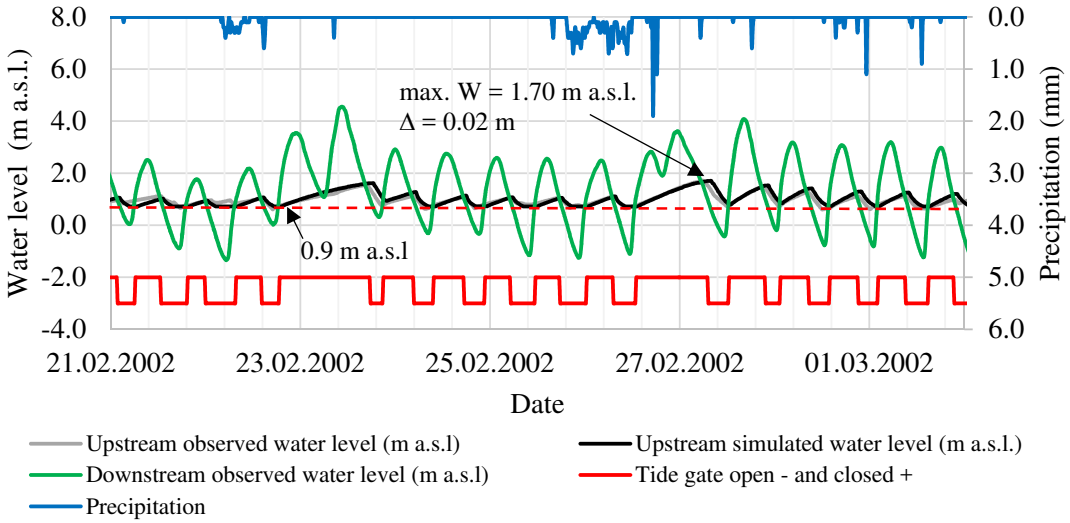

Figure 8.7: Closure and opening state of the tide gate "Deichsiel Tatenberg" per time step as well as simulated and observed water levels upstream and downstream of the gate for the event February 2002. The simulated and measured water levels depict a difference of only 0.02 m in a stream with a water table fluctuation of about 1 m. (The location of the tide gate is given in the attached map on page D17 (A).)

Further results of the events February 2002, February 2011 and August 2002 for the control structures ("Tatenberger Schleuse", "Reitschleuse" and "Dove-Elbe Schleuse") are given in the attachment on the pages D32 ff. An interactive control system is present for the structures "Reitschleuse" and "Dove Elbe Schleuse" which depend on the downstream water levels in the Dove-Elbe stream segments. In this case, the method to model interactive control systems is applied and verified. The method is described in section 6.3 (page 90).

8.3.3 Evaluation of the method to compute backwater effects in streams

The flood routing method and the computation of backwater effects are validated with observed water levels at six gauging stations. The locations are illustrated in the attachment on page D17 with the indexes 2 to 7. The water levels in the stream segments depend on the correct activation of the control functions according to the defined criteria. For each junction node the observed water level (m a.s.l.), the simulated water level (m a.s.l.) and the control system settings (open = "-" or closed = "+") are plotted in the attached diagrams on

the pages D32 ff. The maximum observed and simulated water level values are indicated in the diagrams and listed in the following table 8.12. The average difference in observed and simulated water level peaks is about 0.05 m. This difference is about 5 % in relation to the 1 m large fluctuation range of the water table in these stream segments. The results show a good reliability of the computed flood routing and backwater effects in streams. The method is applied on the meso scale and for open water streams on the district as well as on the local scale. The difference in scales is taken into account by adjusting the tolerable backwater affected water level difference which is larger in meso scale streams (here: 1 cm) as on the district scale of the Moorfleet study area (here: 0.1 mm).

Table 8.12: Summary of simulated and observed maximal water levels of stream segments in the Dove-Elbe catchment. Locations of gauging stations are given in the attached figure on page D17 and diagrams of results are attached on the pages D32 ff.

Gauging station	Event	Max. water level (W) in m a.s.l.		ΔW
		Computed	Observed	(m)
Gauge node Allermöher Deich	Feb 02	1.70	1.72	0.02
	Aug 02	1.11	1.20	0.09
	Feb 11	1.42	1.42	0.00
Eichbaum pump station	Aug 02	-0.33	-0.33	0.00
Downstream Krapphof sluice	Feb 11	1.47	1.54	0.07
Upstream Krapphof sluice	Feb 11	2.04	2.15	0.11
Upstream Sehrran weir	Feb 11	3.29	3.17	0.12
Gauge Möörkenweg	Feb 11	4.73	4.72	0.01
			∅ =	0.05 m

Results of computed backwater effects in flood prone areas. Two areas of the district scale study area "Moorfleet" are affected by backwater flooding. The upstream area is located in the low lying lands of the "Moorfleeter Wanne" and the second one is situated in a downstream rural area. Both areas are situated on surface levels of -0.4 m a.s.l. The locations of these areas are indicated in the attached map on page D21.

Observed water levels are not available for the stream segments or the flood prone areas. Therefore, the results are analysed with respect to the topographical situation and the criteria of mass-conservation of flow volume into and out of these areas. The computation results of backwater affected flood prone areas and LSDMs are analysed in the following section in more detail on the basis of scenario simulations. These results are depicted in diagrams on the attached pages D37 ff.

8.4 Evaluation of the methods to model hydrological processes and backwater effects in LSDMs

To achieve the specific objectives of this work to model hydrological processes on the local scale with a meso scale numerical model, the computations are required to be performed on flexible spatio-temporal scales. For this purpose, additional methods are developed and

implemented. On the local scale, methods are developed to model the hydrological processes in multi-layered drainage structures which include exceedance flow, rainwater harvesting and pre-emptying functions. The processes on local scale comprise interception, evaporation, transpiration, infiltration and percolation in vegetated and submerged surfaces. In table 8.13 the evaluation parameters and criteria to verify the methods to model hydrological processes in LSDMs are summarised. A variation in the input parameter values of LSDM structures is analysed in scenario studies to illustrate the sensitivity of the parametrisation. The flood routing of exceedance flow from a source LSDM to a receiving LSDM is verified with mass-conservation criteria. The features to model local scale control structures are tested like rainwater harvesting of cisterns and pre-emptying control functions for retention layers of green roofs as well as cisterns.

Table 8.13: Evaluation parameters and criteria to verify the methods to model hydrological processes in LSDMs.

Model feature of KalypsoNA	Implemented methods	Scale	Evaluation parameters	Evaluation criteria
Modelling hydrological processses in LSDMs.	Computation of hydrological processes in multiple layered structures (namely LSDMs) (section 5.1 & 5.2).	Local scale	Verification of mass-conservation, data processing and testing the parametrisation with sensitivity studies (ii, iii, iv).	Mass-conservation in influx, outflux and change in storage to be less than 1% .
	Computation of exceedance flow routing among LSDMs (chapter 6.1).			
	Local scale rainwater harvesting and pre-emptying features (section 5.3).			Correct control function activation per time step (time shift smaller than 1s).

8.4.1 Performance of LSDMs to reduce peak discharge and water levels in streams

For the evaluation of the numerical model and to illustrate the performance of LSDMs, three scenarios are defined. In scenario 1 ("CC" = climate change) the precipitation intensity is increased from 48.3 mm to 55.6 mm for the studied hourly event. Consequently, the computed water level rises by about 16 cm (from -0.33 m a.s.l. to -0.17 m a.sl.) and the discharge increases from 1.33 m^3/s to 1.79 m^3/s in the streams of the Moorfleet catchment area. The input parameters are described in section 8.2.4 (p. 134). Results are illustrated for the downstream pumping station "Eichbaum" and the upstream segment which drains a flood prone area (see attachment page D37 ff). For a comparison, the results of the status quo simulations are presented on the attached pages D36 ff.

In scenario 2, LSDMs are defined in the upstream subcatchment "Moorfleeter Wanne" and modelled with climate change impacts like in scenario 1. The results show that the implementation of LSDMs can compensate the increase in peak discharge caused by climate change impacts. The maximal discharges and water levels are summarised in table 8.14. A backwater affected flooding in the MFA1 occurs when only the LSDMs in the subcatchment

"Moorfleeter Wanne" are installed (see the attached diagram D.50, p. D38). This local scale backwater affected flooding and the hydrological processes in the other LSDMs are described in the following section 8.4.2 for verification purpose of the developed methods. The computed water levels in the streams of Moorfleet show that a compensation of the climate change impact is achieved. But the main discharge is still drained with a short lag time from impervious areas of the industrial downstream area "Allermöhe". This drainage volume contributes significantly to the generation of the backwater effect and high water levels.

Table 8.14: Results of water levels and peak discharges in the Moorfleet study area for the analysed scenarios. The hydrographs are depicted on the attached pages D37 ff.

Stream segment	Water level / Discharge	Status Quo		Scenario 1 "CC"	Scenario 2 "CC_LSDM _in parts"	Scenario 3 "CC_LSDM _all"
		Observed	Computed			
Moorfleeter Wanne	W (m a.s.l.)	--	-0.33	-0.24	-0.30	-0.51
	Q (m³/s)	--	1.32	1.79	1.35	1.29
Downstream outlet	W (m a.s.l.)	-0.33	-0.33	-0.24	-0.30	-0.64
	Q (m³/s)	--	6.84	7.96	7.45	3.94

In scenario 3, LSDMs are additionally implemented in the industrial area "Allermöhe" and climate change impacts are added. Overall, 22 green roofs are defined with a retention layer of 85 mm in height and an operational valve system to pre-empty the retention layer in advance of forecasted storm events. The locations of these LSDMs are indicated in the attached map on page D21. The pre-emptying function is activated automatically 12 hours before a forecasted event with an intensity above 4.5 mm/minute. When installing LSDMs in all subcatchments, the backwater flooding in the upstream segments is mitigated. The results of the reduced peak discharges and water levels are given in table 8.14. The water level hydrographs are depicted in the attached figure D.51 (page D38). The peak discharge at the pumping station Eichbaum is reduced from 6.8 m^3/s to 3.9 m^3/s as shown in the hydrograph in the attached figure D.52. In comparison to the results illustrated in scenario 2, no backwater flooding occurs in the upstream low lying land "Moorfleeter Wanne" in scenario 3. The storage area of the multifunctional area MFA1 is drained about 15 hours earlier as compared to the situation if backwater affected flooding occurs like in scenario 2.

8.4.2 Results of the computed hydrological processes and backwater effects on local scale

The hydrographs of six LSDMs are studied in more detail to evaluate the following points. First, to verify the mass-conservation in influx, outflux and change in storage to be smaller than 1 %. Secondly, to evaluate the conformance of outflux according to influx hydrographs with respect to the flow time. These studied measures comprise two multifunctional areas (MFA1 and MFA2), three different green roofs (GR1, GR2, GR3) and one cistern system (C1). The locations are given in figure 8.5 on page 135. The hydrograph results illustrate the fulfilment of the evaluation criteria and are attached on the page D40 ff. while the mass-conservation

results are attached on the pages D44 ff.

The computed results for the multifunctional area 1 (MFA1) of scenario 2 are analysed in more detail for the evaluation study. The area has a size of about 3337 m^2 and is situated on a ground level of -0.85 m a.s.l. The output hydrographs of the computed hydrological processes are illustrated in figure 8.8. Backwater flooding into this LSDM occurs by a rise of water level of about 550 mm in the linked downstream river segment. In consequence, a water volume of 330 l/m^2 flows into the area within a short duration of about 15 minutes. The water is retained, until the water level in the river segment is lowered by the downstream pumping station "Eichbaum". During the retention period, evaporation of the open water surface takes place. The water is subsequently drained from the MFA by pumps.

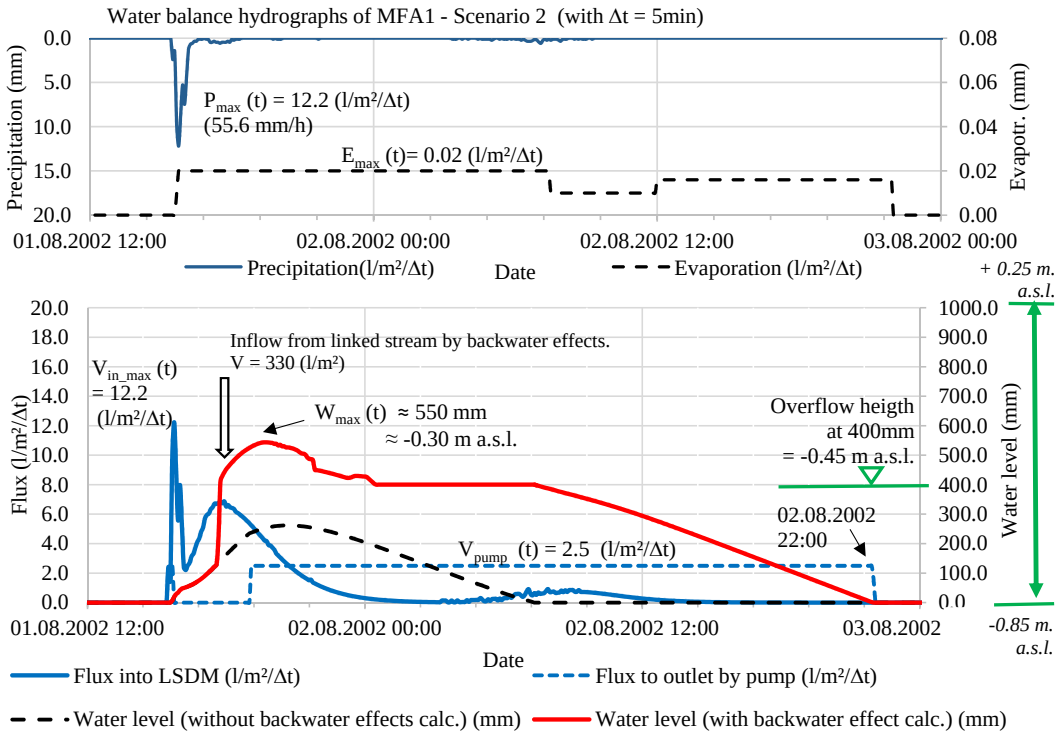

Figure 8.8: Results of the computed hydrological processes in the multifunctional area (MFA1) which is affected by backwater flooding in scenario S2.

Results of the computed hydrological processes of the other LSDMs are attached on the pages D40 ff. The timing of hydrological processes with regard to water retention, evapotranspiration, rainwater harvesting, pre-emptying control functions of cisterns and control valves in retention green roofs are illustrated in these attached diagrams. The hydrographs are analysed with regard to in- and outflux interaction as well as points of time in peak fluxes. The analysed water balance graphs point out reliable results of the implemented methods. The hydrographs of the different green roof types GR1 (with a control valve), GR2 (with a "meander30" retention layer) and GR3 (with a single layered substrate structure) illustrate the sensitivity of different layered structures. The input parameters are derived from the experimental runs of green roof structures in the laboratory testing as presented in section 8.1. The highest retention performance is shown by the GR1 structure and the lowest by the GR2

structure. Antecedent moisture conditions are computed with a longterm simulation run, which embraces several event based runs. The method is explained in section 4.2 (p. 57).

8.4.3 Evaluating the mass-conservation in computed processes on local scale

The computed graphs of the hydrological processes in LSDMs are analysed with respect to mass-conservation criteria. The results of green roofs (here: GR1, GR2, GR3) and further roof areas of about 4300 m^2 are drained to the cistern system (here: C1).[8] First the run-on and inflow fluxes in the system are checked. The inflow into a receiving (target) LSDM depends on the outflow of the drained (source) LSDM. The results of the green roof GR1, cistern system C1 and MFA2 are described in this section to demonstrate the computation of in- and outflux per unit area. The other results are summarised in the attachment on page D44. In a first step, the total outflow of the source elements (here: Σ of GR1, GR2 & GR3) is given per areal unit in l/m^2. The runoff flux is transferred into a run-on flux in l/m^2 of the target (sink) area (here: C1) by multiplying it with the areal ratio in the following manner:

$$\dot{V}_{target,in} = \dot{V}_{source,out} \cdot A_{source} / A_{target} \tag{8.4.1}$$

where $\dot{V}_{target,in}$ (l/m^2) is the influx into the target LSDM, $\dot{V}_{source,out}$ (l/m^2) is the outflux of the source LSDM, A_{source} (m^2) is the area of the source LSDM and A_{target} (m^2) is the area of the target LSDM.

The outflow from the green roof GR1 comprises the pre-emptied outflow of 36.5 l/m^2 and the drainage from the layers of 27.9 l/m^2. This flux quantity is reduced by depression losses on impervious surfaces and evaporation of 8.9 l/m^2. The outflow of 55.6 l/m^2 is transferred to the area of the cistern (= 55.6 l/m^2 · 763.9 m^2 / 58.1 m^2) and results in an influx of 730.6 l/m^2. Further on, the outflow from C1 into MFA2 is multiplied with the areal ratio (= 58.1 m^2 / 828.2 m^2). The result is an influx of 332.4 l/m^2 into MFA2.

The results of the mass-conservation studies are summarised in the attached tables on page D44 and D45. In the first table the sum of inflow fluxes is compared with the outflow fluxes of each LSDM which is transferred to run-on fluxes. Additionally, the outflow of the LSDM depends on storage control systems (for instance rainwater harvesting) and evaporation processes. The difference in the outflow mass-balance is between 0 % to 2 %.

The outflow plus the difference in water storage is balanced with the inflow in each LSDM. The computed difference in water storage corresponds to the water volume stored or lost in the LSDM after the simulation period. This verification procedure illustrates that the runoff (outflow), run-on and inflow fluxes are correctly computed with regard to mass-conservation criteria.

[8] The implementation of one large cistern system comprises several smaller once at the building scale. The spatial distribution on the plot scale is aggregated close to the source.

8.5 Summary of complementary application studies

The extended hydrological catchment model KalypsoNA was applied for further research projects and case studies in the last decade by the author of this work. The findings and results of the following research projects and publications present the broad field of application of the developed numerical model to compute the performance of LSDMs.

The first development and application study was done for a small urban catchment (2 km^2) in Garforth, West Yorkshire in England in the year 2008. The focus of that study was to prove the conformity of the water balance computations of LSDMs. First results were presented in Hellmers [2008] and Pasche et al. [2009]. Further implementations in the source code were realised in the second case study of the Krückau catchment area (274 km^2) in Northern Germany to analyse the performance of green roofs, swales and swale-filter-drain systems to mitigate discharge peak flows in streams. The outcomes showed promising results to mitigate flood peak discharges and were described in Hellmers [2010]; Hellmers and Pasche [2011a]; Hellmers and Pasche [2011b]. The third case study focused on the urban catchment Wandse (88 km^2) in Hamburg, Germany. That case study was analysed in detail within the German Research Project KLIMZUG-NORD (2009-2014). Within the scope of that project, the module KalypsoHydrology (version 13) was enhanced to support a GIS-based import function of overlays and the definition of different LSDM types per subcatchment (see section 4.1). Three urban growth and adaptation scenarios for Hamburg were created to quantify the effectiveness of LSDMs (namely green roofs linked with multifunctional areas) to reduce flood peak discharges in streams and water levels in flood prone areas. For that purpose, the model was enhanced with the functionality to drain the exceedance water from one element to another (see section 4.3). The hydrological numerical model was applied in combination with the modules KalypsoWSPM, KalypsoFlood and KalypsoRisk. The results demonstrated the potential to mitigate the flood risk and related damage costs (in €/a) of specific flood events by implementing LSDMs in an urban catchment area (see Hellmers [2016]; Hellmers et al. [2015] and Hellmers, Manojlović, et al. [2016]). In the project KLEE (2013–2016) ("Adaption to climate change in the Este catchment") an integrated approach for the Este river catchment (365 km^2) was developed, which covered the overall catchment and aimed to mitigate effects from climate change impacts (KLEE Verbund [2016]). Thus, the effectiveness of LSDMs was analysed on a regional scale. The results of that project pointed out that the performance of LSDMs to mitigate flood peak discharges depends significantly on the catchment characteristics. Implementing green roofs in downstream located urban areas led to an increase in lag times of hydrographs. These retained peak discharges superimpose with the hydrograph peak flows from the natural areas and generated even higher peak discharges in the downstream segments. In the recently published study (Hellmers and Fröhle [2017]), the validation results of the micro scale hydrological processes in LSDMs were presented using measurements of green roof installations in laboratory as described in section 8.1. Supplementary results of the developed functions to model backwater affected streams and areas will be published in the project report "StucK" in Hellmers and Fröhle [2020] (in press).

9. Discussion of findings and results

Findings of the developed methods and results of evaluation studies are discussed in this chapter. It points out the achievements and limitations in accomplishing the objectives of this work. The specific objectives and the scope of work are described in chapter 3 according to the SMART-principle including the definition of evaluation parameters for verification and validation purposes of the developed and implemented methods. The developed model features, (1) to (10), resolve weaknesses and limitations in current hydrological numerical models (see table 2.3 on page 28). The results in modelling LSDMs and backwater effects with these ten features are compared in this chapter to related study results in literature. The discussion is structured in three sections according to the objectives for solving the defined limitations and weaknesses in current hydrological models as follows:

9.1 Resolved model features (1) to (4): Discussion of the developed methods to provide the required detailed spatio-temporal resolutions and support a hydrological network generation including LSDMs, while facilitating an applicable parsimonious parametrisation in a meso scale hydrological numerical model.

9.2 Resolved model features (5) to (8a): Discussion of findings in the developed methods and parametrisation to model the hydrological processes and control functions (technologies) in LSDMs.

9.3 Resolved model features (8b) to (10): Discussion of the integrated methods for modelling control structures in local scale streams, the flood routing among interlinked LSDMs and modelling backwater effects, which were missing in hydrological numerical models until now.

Key aspects of findings ("key findings") are summarised within each section according to the integrated model features. The chapter concludes in section 9.4 with a description of limitations of the developed methods and an outlook provides a basis for further research in this topic.

9.1 Discussion of methods to model a flexible spatio-temporal scaling and a local scale network generation

The developed methods facilitate to zoom into the hydrological processes (physically, spatially and temporally) where reasonable values of parameters in practice are available based on knowledge from investigations in nature and laboratory. At the same time, it supports to zoom out of the processes to apply conceptual approaches on the meso scale. To integrate this developed first part of the methodology (chapter 4), a semi-distributed model approach is extended in this work. In comparison to a fully distributed model, the benefits of a semi-distributed approach lie in a smaller effort for data processing while still enabling a spatial detailed discretization based on hydrological response units (HRUs). The achieved objectives in the revised (semi-distributed) catchment model includes a detailed spatial discretization of LSDMs, a flexible temporal resolution to facilitate a dynamical time step size computation, an on-the-fly network generation based on drainage criteria, short computing times and a revision of the parametrisation for a parsimonious data structure for meso scale modelling. A parsimonious parametrisation aims to define parameters on the critical scales and differentiates in this work between meso and local scale parameters. The required and now integrated model features are numbered from (1) to (4) in the review (see table 2.1 on page 14).

The developed methods facilitate a GIS-based local data mapping in meso scale catchment modelling and an explicit on-the-fly network generation based on drainage criteria. The methods are described in chapter 4.1 and tested in an application study in section 8.2.5. The results of GIS-based spatial intersections to integrate LSDMs in meso scale catchments illustrate good conformity with less than 1 % in spatial difference after data processing. The geographical location of LSDMs is given per centre of area. The network generation prevents circular linkages and integrates the flood routing computation among LSDMs as well as meso scale data structures. The on-the-fly data processing is executed during the simulation run of the module KalypsoHydrology on the basis of drainage criteria. This method is verified and shows good results (see section 8.2.5). Digitised thematic maps of cartographic real land utilisation can be imported. Thereby, building shapes with the attribute of flat roofs are processed and serve for computing the performance of potential green roof installations. LSDM data structures are still in connection with the data structures of the surrounding meso scale subcatchments. The spatial location and additional drainage attributes are integrated in the parametrisation of local scale data structures, while the data processing of meso scale subcatchments remains conceptual. In this way, a parsimonious parametrisation is generated for the computation of structures on different spatio-temporal scales.

Discussion of findings in comparison to related research studies in literature. The review of hydrological numerical models applied for LSDM modelling revealed the model SWMM as a widely-applied tool in research and practice (for example in Aryal et al. [2016]; Eric et al. [2013]; Krebs [2016]; Palla and Gnecco [2015]; Scherer et al. [2018]; Versini, Jouve, et al. [2014]; Versini et al. [2015]). To model the flood routing among LSDMs in a related detailed way with

the model SWMM, requires the modeller to create individual links for each single LSDM as it has been done by Krebs [2016]. Alternatively, LSDMs are defined as spatial percentages per subcatchment as described in Versini et al. [2015]. The first approach demands for an expensive data processing when applying it for regional scale catchment modelling (>100 km^2). With the second option, the geographical location and flood routing computation among LSDMs with flow paths is not possible. In SWMM the areas for modelling LSDMs are substracted from the subcatchment as spatial percentage and the discharges computed from the contributing LSDMs are added directly to the total subcatchment response (see Versini et al. [2015]). The geographical location, spatial distribution of LSDMs and distance to the outlet of a surrounding subcatchment are neglected in that approach. This means, that the flood routing (namely flow concentration) is assumed from the subcatchment scale. An alternative is the integration of the stormwater drainage network in the form of a hydrodynamic-numerical model, while decreasing the size of subcatchments on building scale and, in turn, increasing the model parametrisation. This leads to a significant increase of computational costs as well as data processing effort for regional scale hydrological modelling (>100 km^2).

In contrast, the developed methods in this work facilitate a hydrological flood routing computation using the flow path length between source and sink elements (such as LSDMs or junction nodes) within the subcatchments. The input parameters comprise a shape of geographical data of LSDMs, geometry descriptions of profiles and roughness's along the flow paths per category of LSDMs. The hydrological network is then created on-the-fly without user interventions. Neither of the approaches in SWMM fulfil the defined objectives of modelling LSDMs with respect to meso scale catchment applications (>100 km^2) using such an on-the-fly hydrological network generation.

With regard to the categorisation of Salvadore et al. [2015], there is a tendency that regional hydrological catchment models (>100 km^2) apply a fixed rough spatial and temporal scale, while models for small urban catchments (<10 km^2) use a fixed detailed spatial discretization combined with a more detailed temporal scale. This more or less established categorisation is revised in a more flexible way in this work. In the presented numerical model of the Dove-Elbe catchment, the smallest HRU has a size of less than $1 \cdot 10^{-3}$ m^2 and the largest has a size of $1 \cdot 10^4$ m^2. Detailed landuse data including the information of property fractions being drained by stormwater pipe system or surface runoff (provided by HamburgWasser in the project "StucK", see Hellmers and Fröhle [2020], in press) were successfully processed with the GIS-based platform Kalypso on a catchment scale of 175 km^2. However, time step sizes of minutes are supported for the simulation runs on the meso scale, while time step sizes of seconds are applied to model processes in LSDMs. The developed methods accomplish short computation times below five minutes per simulation run of about 10 days for this regional scale catchment model (175 km^2).

Key findings of the developed spatial discretization and on-the-fly network generation. The developed and implemented method of the spatial discretization and hydrological network generation uses a data processing of the geographical location of each LSDM individu-

ally within meso scale subcatchments. In contrast to recent models, like SWMM, the linkages among source and sink elements (such as LSDMs or junction nodes) within meso scale subcatchments are generated on-the-fly based on drainage criteria and geographical location. This supports the applicability of the developed tool for regional scale modelling. The GIS-based method facilitates the aggregation of spatial data according to congruence criteria to reduce the required computational resources for data processing on the meso scale.

Discussion of the method to facilitate a flexible time step size computation. To model the hydrological processes in thin layers of multi-layered LSDMs, which are exposed to large influx rates[1], small time step sizes are required. The developed method in section 4.2 takes into account the Courant-Friedrichs-Lewy (CFL) criterion (see Courant et al. [1928]) to compute dynamical time step sizes for the modelling of hydrological processes in LSDMs. According to the CFL-criterion, the time step size is a function of the spatial dimension (here: layer thickness) and the speed with which the water can flow within the spatial element. The flux depends on the hydraulic conductivity of the soil or material. The local scale method is successfully implemented in the meso scale model without enlarging the computational resources of the meso scale model. This approach supports the definition of a time step size of several minutes on the meso scale and still ensures a process-related minimum time step size (in seconds) on the local scale. This prevents oscillations in the water fluxes, which occur when the entering water volume into the regarded layer in one time step is larger than the available storage volume. This results in an "on-off" phenomenon, where in one time step a surplus of water enters the layer and in the following time step it may drop to zero.

Recently, an approach switching between 10 minutes, 1 hourly and 1 daily time step intervals is presented by Leistert et al. [2018]. That approach is based on an analysis of the rainfall data and switches to shorter times step sizes when rainfall intensities increase. In this way, the presented model computes longterm periods (for example 30 years) and overcomes the task of calculating antecedent moisture conditions. The model is a distributed detailed model with computing times of several hours up to one day for one simulation run. Such long computation times are not feasible in forecast and operational modelling which is in contrast, supported with the extended model in this work. Additionally, the provided time step sizes in this model are even smaller for process-related computations in LSDMs.

Key findings in the flexible time step size computation. A flexible time step size computation is implemented in the extended model KalypsoNA. The sizes of time steps vary between daily and minutes for simulations on the meso scale, while providing processes-related time step sizes in seconds for modelling drainage and soil water processes which have a fast response time. In that manner, a detailed process-related simulation and at the same time, short computing times are accomplished in this work. Examples of computing times are presented in the application study. A computing time of only 2:20 minutes is required for a simulation run over ten days of the tidal influenced catchment model Dove-Elbe (175 km^2) including

[1] Derived by effective precipitation on that area and additional inflow from linked areas.

backwater affected flood routing, seven control systems and about 50 LSDM structures (see section 8.2.1). The short computing times of the presented model in this work support the successful application for operational and real-time forecast simulations in practice. Another application study of the presented model (KalypsoNA) is presented in Jasper-Tönnies et al. [2018] and Hellmers and Fröhle [2020] (in press). The extended model KalypsoNA is applied as an operational hydrological forecast model of an urban catchment in Hamburg (33 km^2) which computes ten ensemble forecast members within an actualisation period of 15 minutes since April 2017. The applied meso scale hydrological model KalypsoNA is designed for simulation runs, which cover a defined number of time steps per "cycle". Such a cycle covers a time interval of one year within longterm simulation run. For event based simulation runs, a cycle covers a time period of 2880 time steps[2]. An allocatable number of time steps per simulation run is regarded as an optimisation issue, but not a constraint in the developed model of this work. The objectives of this work are obtained in the implemented method to compute flexible time step sizes in a defined length of the simulation runs, while keeping the computing times reasonable short.

Discussion of the implemented parametrisation The literature review of hydrological numerical models revealed the demand for parsimonious parametrisation and applicable data structures. A so called parsimonious model aims to define a balance between the available input parameters, computational resources and representing the physical behaviour of the processes. The demand for parsimonious models is stated for example in Beven [2012]; Perrin et al. [2001] and Pechlivanidis et al. [2011]. A differentiation between simple, parsimonious and complex models is given with a categorisation in literature. The distinction criteria comprise the number of input parameters and the risk of over-parametrisation. To model local scale hydrological processes in LSDMs thirteen input parameters based on the geometry of the structures, two parameters to describe the subsurface fluxes, three parameters describing the vegetated cover and four (optional) parameters for calibration purposes of the micro scale soil moisture computation are defined. The control functions are implemented with eight parameters. The input parameters of the flood routing computation include geometrical profile data (such as bed width, bank gradient and roughness). The gradient along the main flow path and the length are computed optionally via geographical data. For computing backwater effects, a minimum tolerance in difference of water levels and optional adjustment parameters for the WVQ-relations are defined. Overall, a number of 30 effective parameters are implemented in this work. The input parameters are explained in section 7.3. Further on, the input parameters of the basic meso scale hydrological catchment model consists of about 50 parameters. According to the categorisation presented in the review in section 2.2.7 this model with less than 100 parameters is defined with a moderate risk of over-parametrisation and is regarded as a parsimonious model. In contrast, a fully-distributed physically based model with up to 1000's of parameters is defined as a complex model with a larger risk of over-parametrisation.

[2]The number of time steps per simulation run is independent from the number of process-related time steps.

Key findings of the implemented parametrisation. The enhanced model KalypsoNA is categorised as a semi-distributed model using conceptual and physical-based hydrological approaches. It is a parsimonious and applicable model in practice and research. The number and kind of input parameters are available by using digitised cartography data sources or physical-based data on local scale. The risk of over-parametrisation is considered to be moderate in comparison to a physical-based fully-distributed hydrological numerical model.

9.2 Discussion of methods to model the processes in LSDMs

In the second part of the methodology in chapter 5, the developed methods to integrate the simulation of processes in LSDMs in meso scale hydrological models are explained. This comprises a physical-based parametrisation, an extension of methods to model local as well as micro scale hydrological processes and methods to model local scale drainage technologies.

The method of the infiltration excess model using a dynamic time step size (see section 5.2), the computation of the hydraulic conductivity using the Kozeny-Carman approach (see section 5.2), and the flow routing through drainage layers using the Darcy-Weisbach approach (see section 5.3) are some of the extended and implemented methods within this work. The behaviour of retention and drainage processes among different layers in LSDMs is analysed in a physical model in laboratory with a multi-layered green roof structure. The measurements with a layer separation device provided observed data to study the drainage flux of each individual layer. This measuring device of separated layered flow described in this work (section 8.1.1) is an approach first time applied and presented in Hellmers and Fröhle [2017]. With the detailed results of the drainage and retention behaviour of different layers, the physical-based parametrisation in the developed methods is calibrated and validated.

The evaluation of methods is performed with a verification of the mass-conservation in computed processes, a validation using the measurements in laboratory and a limited number of sensitivity studies by varying structures and boundary conditions. Physical-based parameters take into account the geometry, sizes and material characteristics. Four calibration parameters are defined which describe the changes in compaction of the material or clogging of the drainage structure. The comparison of simulated with observed results of green roof structures proved a good conformity in seven calibration and fifteen validation runs. Root mean square differences (RMSDs) between physical model measurements and simulated model outputs of the drainage flux hydrographs are less than 10 %. The time lag and occurrence of the peak flux show a good congruency with a differentiation of maximal two minutes during the experiments of 15 to 90 minutes in length of time. Additionally, the sensitivity of the defined parameters is studied by varying the type of structures and boundary conditions (namely the precipitation intensities). The input parameters to model LSDMs are listed and explained in section 7.3.1. Different values of input parameters are given in section 8.1 for the example of green roof structures and in section 8.2 for a regional scale numerical model (namely the Dove-Elbe catchment).

Evapotranspiration from vegetated structures is computed with the approach of Penman-

Monteith. The vegetation parameters of the root depth, a vegetation crop factor and the interception storage are applied to compute the evapotranspiration. A method to model the evaporation from submerged surfaces is developed and implemented in this work. Such open water surfaces exist in open stream segments of rivers, retention ponds, submerged flood prone areas and LSDMs. Test results of the numerical model of the Dove-Elbe in section 8.4 illustrate a good conformance of the mass-conservation criteria of the computed processes and a good conformity in the temporal sequences of the computed hydrological processes. The differences in mass-conservation between the processes are less than 0.1 %.

Discussion of findings in comparison to studies in literature. A comparison between simulated and observed drainage results of green roof installations are given in the following publications. Monitored measurements of a green roof in Portland (Oregon) over three years are presented by She and Pang [2010]. Versini et al. [2016] studied measurements of green roof test fields in Paris (France) from a nine months period of time. Locatelli et al. [2014] analysed measurements of smaller green roof installations in Denmark over two years. Szota et al. [2017] presented monitored data of green roof test bed installations over a period of four months in Melbourn (Australia) and De-Ville et al. [2017] analysed measurements of green roof test fields covering a period of five years in Sheffield (United Kingdom). In a comparable study by Vesuviano et al. [2014] a rainfall simulator is used to analyse the impacts on the green roof retention performance using different rainfall intensities over specified durations. The observed measurements are compared with simulated numerical results. The studies by De-Ville et al. [2017]; Versini et al. [2016]; Vesuviano et al. [2014] and Stovin et al. [2015] used a conceptual numerical approach published previously in Zimmer and Geiger [1997]. This conceptual approach of Zimmer and Geiger is based on the linear reservoir theory with the parameters n (-) and k (h) to model the drainage flux through the substrate media. The parameter n describes the number of (conceptual) reservoirs within a substrate layer. The parameter k is an empirical derived storage coefficient. These reservoir routing parameters are adjusted during a calibration procedure (see for example in Stovin et al. [2015]), but are lacking a physical-based description of the applied materials. In Vesuviano et al. [2014] an additional "delay" factor is applied to fit the numerical model results with the observed field monitoring data. The conceptual approach by Zimmer and Geiger is lacking the differentiation of free drainage layers which behave differently than subsurface flux through permeable substrate. The conceptual approaches described in Versini et al. [2016]; Vesuviano et al. [2014]; Zimmer and Geiger [1997] and Stovin et al. [2015] are applied to model hydrological processes on the local scale until now, but are not integrated in meso scale numerical models yet.

In Locatelli et al. [2014] the conceptual approach using the parameters n and k is compared to monitored green roof drainage measurements and compared to MIKE Urban numerical model results. In the MIKE Urban model, the conceptual hydrological model NAM (= Nedbor Afstromnings Model) by the Danish Hydraulic Institute (DHI) is implemented. The NAM model input parameters were calibrated by trial and error. A physical-based description of the input parameters for LSDM modelling is missing. Both results of the numerical models

show good congruency with monitored green roof drainage measurements after a calibration of the parameters, but a transfer of the calibrated values to other case studies is not possible.

Modelling LSDMs with the numerical model SWMM is done by using a modified version of the module "bio-retention cell" (see Alfredo et al. [2010]; She and Pang [2010] and Versini et al. [2015]). In this module, each layer is modelled as a reservoir. The saturated hydraulic conductivity is defined as an input parameter. The drainage of the different layers is routed with a transfer function. This function is based on the Manning-Strickler approach using a roughness coefficient and the relation between width and drainage area as input values. A possible prolonged flow path length is not considered. A modified pulse method is applied to compute the storage content in each layer reservoir. In Versini et al. [2015] the parameters of porosity, field capacity, saturated hydraulic conductivity and roughness are calibrated for each test run. The comparison of monitored and simulated drainage hydrograph results show a sufficient congruency. But the input values of soil characteristics with a physical-based meaning are changed significantly. For example the measured field capacity of 0.4 mm is changed to 0.21 mm and the physically assumed saturated hydraulic conductivity is calibrated from 1158 mm/h to 2 mm/h. The adjustment of these values is not reproducible and therefore regarded as non-transferable to other green roof structures.

In contrast to that studies, in this work the Kozeny-Carman approach (also known as the "hydraulic radius theory") is applied to compute the saturated hydraulic conductivity for subsurface fluxes in permeable substrate and the runoff routing in "free" storage layers is computed by using the Darcy-Weisbach approach taking into account the flow path length and the roughness of the material. The Kozeny-Carman approach is based on using the average particle size (d_m in mm) as input parameter. It is based on modelling the porous soil like a bundle of capillary tubes of equal length. The computation of the outflow includes the size of the outlet by using the approach of Poleni to compute a flow over a weir. With this method, the parametrisation of the drainage behaviour of subsurface flux is computed in a more physical-based way in comparison to the conceptional approach of Zimmer and Geiger [1997]. If clogging by fine material or subsequent compaction of the material is taken place, an adjustment with calibration parameters is provided. The results are presented and described in section 8.1.4. A comparison of the results for a green roof structure with a slope of 2 %, a substrate thickness of 10 cm and a free drainage layer described in Vesuviano et al. [2014] for a rainfall type with an intensity of 0.6 mm/minute is given in the attachment E. The resulting hydrographs of that study are comparable to the results described in this work, but the parameter values of this developed method is transferable to other case studies because of a physical-based description.

Limitation and outlook in the presented case study results of modelling hydrological processes in LSDMs. In this work, it is shown that the installation of linked LSDMs can support to reduce peak discharges and water levels in streams as well as flood prone areas. The model output is analysed with a focus on verifying the developed methods. For implementation surveys, more details about the constructions of the selected flat roofs have to be utilised. The

developed methods are validated with physical model measurements in laboratory. Further tests with measurements from implemented LSDMs over longer periods of time including several vegetated periods and for more different structures are not covered in the scope of this work. The variation in (in-situ) substrate compaction as well as the changes in vegetated cover over time are important factors not comprised completely in laboratory results yet (Szota et al. [2017]). The objectives of this work are achieved with respect to validate the developed methods with physical model measurements in laboratory and a regional scale model application study. The presented results illustrate a good reliability in the model to be applied for further research tasks and for follow-up comparisons with in-situ roof installations.

Discussion of findings of the methods to model LSDM technologies Limitations in hydrological numerical models are resolved in this work with respect to model multi-layered structures. This includes the drainage of exceedance flow between linked layers, rainwater harvesting functions and (real-time) control features for pre-emptying LSDM storages based on outputs of rainfall forecast models.

The aforementioned widely-applied conceptual approach with the parameters n and k (see Zimmer and Geiger [1997]) lack the computation of exceedance flow routing from upper layers to underground storage layers. This coupled flow has not yet been modelled or studied in the reviewed literature. This limitation is resolved in this work with the method described in section 5.1. A parametrisation describes the exceedance flow routing of any layer in a structure to another underlying layer, when an overflow height or a saturation state is exceeded.

Current tools in research and practice apply constant values for modelling rainwater harvesting features, while neglecting the variation of work- and weekdays as well as seasonal differences for the water utilization (see M. Burns et al. [2010]). The water demand from rainwater harvesting is often estimated as an average based on the storage capacity of the structure. Ignoring the variability in user behaviour leads to discrepancies in estimated water quantities as shown for example in M. Burns et al. [2010]. These approaches are not sufficient to model rainwater harvesting functions over longer periods of time as reported also in Li et al. [2017]. This weakness of current numerical models is solved in this work by enabling the definition of an "ideal yearly" rainwater harvesting time series for normal and leap years. It provides values on daily resolution to differentiate between working and weekend days. The seasonal differentiation varies per month. The rainwater harvesting functions are assigned to the layers of data structures. In that way, the control functions can serve several LSDM data structures in the numerical model (for example, industrial or household usage). The ideal yearly parametrisation provides a flexible data structure for longterm simulations over several decades (see section 5.3.3). The verification studies in section 8.4.3 illustrate the functional correctness in mass-conservation and data processing when running the LSDM simulation with pre-emptying and rainwater harvesting features in a regional scale catchment model.

In the study of Keser and Mietzel [2012, 2014], a control structure for rainwater harvesting is modelled with a conceptual reservoir approach using the numerical model Simba-

Simulink (see ifak[3]). The results demonstrate that daily rainfall forecasts are not precise enough for modelling control systems on the local scale. High spatial resolution of radar data with a small temporal resolution are required, but this is not realised in the reviewed studies up to now. This weakness of current models is resolved in this work and the related project "StucK", where the model KalypsoNA is extended to run as "operational model"[4] since 2017 with ensemble forecast simulations in an actualising interval of 15 minutes (see Hellmers, Strehz, et al. [2016] and Jasper-Tönnies et al. [2018]). The implemented control functions are more flexible and comprise additional criteria of rainfall intensities as well as water levels and discharges at different elements in the hydrological network (see section 5.3.3).

Limitation and outlook of the presented case study results in rainwater harvesting. The sizing of the cisterns in the presented application study serves primarily demonstration purposes according to the following relation: an area of $100\,m^2$ is drained to $1\,m^2$ of a cistern system which has a height of 3 m. More detailed studies are presented by Kuller et al. [2016] and Ward et al. [2010] to derive relations between drained areas and rainwater harvesting demands. The size of the cistern is limited because of bacteria breeding. In the presented study, the larger cistern systems (tanks) are considered to be separated for implementation planning in that areas. An example is given in Ward et al. [2010], where a roof area of a business building with a size of $1500\,m^2$ is connected to storage tanks having a total volume of $25\,m^3$ and are designed for a rainwater usage rate of $5.19\,m^3$ per working day and $0.36\,m^3$ per holiday using the tool RainCycle developed by Ashley & Co. That knowledge about rainwater harvesting supports the requirement to apply the developed tool in this work for further studies. The evaluation studies with differently assumed relations between drained area and cisterns show reliable results of the model application.

Key findings of the developed methods to model hydrological processes and techniques in LSDMs. The created physical-based parametrisation to model hydrological processes on local scale is transferable among different types of LSDMs and application studies. This parametrisation and the developed methods resolve limitations and weaknesses in comparison to the widely-applied conceptual approach, which is presented in Kasmin et al. [2010]; Versini et al. [2016, 2015]; Vesuviano et al. [2014]; Zimmer and Geiger [1997] and Stovin et al. [2015]. The effective parametrisation of LSDMs is sufficiently evaluated using the example of green roofs in the scope of this work from a practical point of view. The developed and implemented methods to model hydrological processes on the local and micro scales are successfully validated and verified with evaluation criteria. Subsequent hydrological processes such as evaporation and controlled drainage of backwater affected LSDMs are computed and the developed methods show appropriate results in the application studies. Further on, the extended and implemented control functions in the hydrological numerical model are applicable to compute rainwater harvesting systems, pre-emptying functions and exceedance flow

[3] www.simba.ifak.eu

[4] An operational numerical model executes simulations automatically in a specified time interval.

management. The fulfilment of the evaluation criteria for testing the implemented methods, show good results and promote the application of the developed model for further studies in this research field.

9.3 Discussion of methods to model flood routing, control systems and backwater effects

Extended methods to compute the flood routing on local scale among LSDMs and control functions are developed and implemented in the scope of this work. These methods are included in the third part of the methodology (see chapter 6). Modelling backwater effects with hydrological approaches was rarely possible in hydrological numerical models until now. This limitation is resolved in this work. The findings of modelling the flood routing, control structures and backwater effects are described and discussed in comparison to related study results from literature in the following three paragraphs. Each section concludes with a summary about the key findings.

Discussion of findings to model interlinked flood routing on local scale. The developed method to compute the flood routing among LSDMs is indicated as "KM1"-method (see section 6.1.1). It uses a hydrological and physical-based approach which is related to the Kalinin-Miljukov concept and defines each stream segment as one reservoir. Profile data of (circular) pipes or (trapezoidal) open water profiles are included in the parametrisation. For the flow velocity computation, the approach of Manning-Strickler for open water profiles and of Darcy-Weisbach for modelling circular as well as trapezoidal profiles are implemented. The roughness properties (k_s = equivalent sand roughness and k_{st} = Manning-Strickler coefficient) are input parameters. The method is less data demanding than a hydrodynamic approach, while it still applies a physical-based parametrisation with geometrical profile data and routing characteristics per stream segment. The evaluation of the accuracy of the method is done with sensitivity studies and mass-conservation tests of computed flood routing output among LSDMs as described in section 8.3.1 and 8.4.3. The results show good conformity in the evaluation criteria with a mass difference of less than 1.0 %.

This method resolves prevailing weaknesses in modelling the flood routing in an interlinked drainage network of LSDMs within meso scale catchments. The geographical location of LSDMs is applied to calculate the flow path length and gradient for the flood routing computation on-the-fly. The developed method to generate hydrological networks ensures that an explicit computational order among source and target (sink) LSDMs is created. The simulations of hydrological processes are executed after the LSDMs receive the respective run-on water from linked source elements. This method accomplishes a detailed computation of the flood routing for regional scale studies (>100 km^2) based on drainage criteria.

To obtain a comparable detailed model with SWMM, a more exhaustive data processing needs to be done. A related detailed model is presented for example in Krebs [2016], where an area of 0.06 km^2 is discretized into 690 individual subcatchments which represent either 100 %

pervious, 100 % impervious or 100 % LSDM areas. Each of these areas required a user defined inlet in the sewer system as well as a parametrisation. In that way, the computation of the flood routing among LSDMs is done with the hydrodynamic-numerical calculation routines in SWMM, but this approach ends up with a very data exhaustive and complex model. The application of this approach using the model SWMM (see Krebs [2016]) on the regional scale (>100 km^2) is not considered to be feasible in practice.

Key findings of the method to model the flood routing on local scale. The developed KM1-method to model the flood routing on the local scale is applicable in regional scale catchment models (>100 km^2) and accomplishes the modelling of the flood routing among LSDMs using physical-based flow path characteristics and drainage criteria. The implemented methods discretise "on-the-fly" the LSDMs with geographical location according to drainage criteria and define automatically the links (namely stream segments) among the created source and target (sink) elements.

Key findings to model control functions. In the literature review in chapter 2.2, hydrological numerical models are described with control functions which are based on using the water level or volume within the control element as criteria to set a steady WVQ-relation[5]. These control functions are applied to model retention ponds, detention basins or hydro dams, but are not sufficient to model control functions in LSDMs like cisterns or multifunctional areas. The application of control criteria like precipitation intensities within a forecast system is not implemented in these hydrological numerical catchment models up to now. The limitations in enabling the application of more divers control criteria and the missing functions for modelling control functions in LSDMs is resolved in this work. A development of additional and more flexible functions for different structures is realised. The extended criteria for control structures comprise precipitation intensities, water levels and discharges as functions of time of varying drivers in the hydrological network. The developed method is described in section 6.2 and the parameters of the control criteria are listed in section 7.3.2. The evaluation of results in application studies of the complex and tidal influenced catchment Dove-Elbe (175 km^2) illustrate good conformance in the simulated control functions of tide gates, sluices, pumping stations and LSDMs (namely cisterns, retention roofs and multifunctional areas).

Summary of findings to model backwater effects. In low lying lands, backwater effects and backwater induced flooding of areas are an important issue. The literature review revealed that modelling backwater effects is not or rarely implemented in hydrological numerical models up to now. This weakness of current models is resolved in the scope of this work.

The developed, implemented and evaluated method for modelling backwater effects is based on a hydrological flood routing approach and a backwater volume routing according to the water level slope described in section 6.3. A relation between the water level, volume and discharge (namely a WVQ-relation) is derived per stream segment in the extended flood

[5]Water level, Volume, Discharge-relation (WVQ-relation).

routing method. The input parameters comprise data of the stream profiles, gradients and roughness along the flow path. The gradient and length can be given as input values or are computed "on-the-fly" using the geographical locations of the inlet and outlet junction nodes. This hydrological model approach uses physical-based parameters and is therefore transferable to other application studies. The input parameters are described in section 7.3.5. The verification and validation results of the methods to compute the backwater affected water levels in stream segments give only small differences of 0.02 m to 0.10 m within streams, which have a backwater affected water level variation larger than 1 m. The differences are determined by comparing observed gauge station measurements (in nature) and numerical model results. The rising and falling limps of the backwater affected water level hydrographs illustrate a good conformity in comparison of simulation results with gauge station measurements.

The developed method for modelling the backwater induced flooding of areas (such as LSDMs or flood prone areas) is implemented and computes the water levels per time step for these affected areas. The methods accomplish the computation of the run-on routing into LSDMs, the subsequent drainage and the evaporation from open water surfaces. Evaluation tests of this method show a good conformance in the mass-conservation criteria with deviations less than 1 %.

Key findings in modelling control functions within interactive backwater affected systems. An interactive backwater system is computed, when a control structure (such as a gate) depends on downstream water levels which are at the same time backwater affected. The developed methodology in this work (see section 6.3) facilitates to model such interactive systems, but demands the modeller to define the order of the interactive components. With this confirmation of an interactive system, the computational loop is restarted at that element when the driver results of the control criteria are available. In the presented application study ("Dove-Elbe") this calculation routine is activated for two tributary gates which depend on the downstream segments in front of a tide gate. A suggested outlook of this implemented method is the automatic ordering of such multiple computational loops. This outlook improves the user friendly application of the model in practice, but does not diminish or enlarge the reliability in the model results presented in this work.

Discussion of modelling backwater effects in comparison to related research studies in literature. Only few related studies are available with respect to model backwater effects in meso scale catchments with hydrological approaches, while non of the reviewed studies analysed the retention potential of LSDMs for backwater induced flooding. Four related approaches are discussed in this paragraph.

The hydrological model "ArcEGMO" (by the "Büro für Angewandte Hydrologie", Berlin) takes into account backwater effects by hindering the downstream flood routing when the water level at the downstream section is higher than the upstream one (Pfützner [2018]). This method calculates a retained flood rooting, but neither computes backwater volume being routed into upstream sections by a reverse flow direction nor the backwater induced flooding

of adjacent areas. The method presented by Szilagyi and Laurinyecz [2014] applies a discrete linear cascade model to account for backwater effects in flood routing by adjusting a storage coefficient of the cascade. This method calculates a retained flood rooting (as in the ArcEGMO model) and likewise neither computes backwater volume being routed into upstream sections by a reverse flow direction nor the backwater induced flooding of adjacent areas.

In the study by Messal [2000], backwater effects among river streams and the subsurface flow in river banks are modelled. It applies a proportional relationship between upstream and downstream elements for calibration purposes. The model serves well for the specific studied catchment, but the parameter values are non-transferable to other catchment studies because of a lack in physical descriptions. This approach is not applicable for meso scale model applications and does not take into account unsteady changes at the downstream section (for example, by the closure and opening of tide gates).

Another approach is presented by Riedel [2004] to model the backwater effects among river streams. The approach uses the reservoir cascade theory including the input parameters of the roughness coefficient by Manning-Strickler and geometric descriptions of the profiles for the flood routing computation. The river is modelled as a cascade of reservoirs (namely a NASH-cascade), while the water level from the previous time step of the downstream sections are taken into account to compute the flood routing. A time step shift in the computational approach is accepted by Riedel [2004] because he reduced the simulation time step size to one minute. The model computes a reservoir cascade on the basis of a defined boundary condition at the downstream section. The simulation of backwater flooding of flood prone areas or LSDMs is not included.

These reviewed hydrological methods compute backwater effects in a more or less conceptual way with the described weaknesses and limitations. Non of these studies analysed the backwater induced flooding of adjacent areas or in this specific case, of LSDMs. Consequently, non of the studies accomplish to model a controlled retention of backwater in such areas and a subsequent drainage as well as the computation of the evaporation from submerged areas. Further on, most studies do not apply physical-based parameters to transfer any validated values and knowledge from one catchment to other studies.

Key findings of the method to model backwater effects. The developed method in this work uses physical-based parameters, which facilitate the transfer of the parametrisation to other study areas. In comparison to hydrodynamic-numerical approaches, the developed method computes the backwater effects in two steps. First, the inflow from subcatchments and the non-backwater affected flood routing processes are computed. Secondly, the afflux conditions are computed which cause backwater effects in upstream direction. Afflux conditions occur mainly at tributary inlets or control structures (for example, tide gates, weirs, retention ponds or sluices). For that purpose, each of the these structures indicate a backwater affected system in the developed algorithm. Setting boundary conditions according to measured water levels is possible, but not a prerequisite for the simulation of the model. To prevent infinite computational loops, a minimum tolerated water level difference (for example:

1 mm) can be set as boundary condition to compute backwater effects.

In contrast to hydrodynamic-numerical approaches, the developed hydrological model does not compute velocity fields within streams and water levels represent average values per stream segment. This hydrological flood routing method is appropriate to accomplish the objectives of this work to model regional scale backwater affected catchments (>100 km^2) with the requirement to keep the computing times small and with a parsimonious parametrisation. It does not replace the demand to model two or three-dimensional velocity fields and to compute the distribution of water levels within streams or submerged areas by the use of hydrodynamic-numerical models for specific research questions.

Another advantage of the developed method is the direct computation of hydrological processes in backwater affected areas. For example, the evaporation of water from submerged areas is modelled. Temporary detained water in LSDMs is drained by pumps after water levels in streams are lowered in consequence of a flood event. The verification results with mass-conservation criteria of these computed processes proved a good conformance with a difference below 1 %.

9.4 Context, limitation and outlook of presented findings in this work

The developed methods to integrate the modelling of LSDMs and backwater effects resolve current shortcomings in state-of-the-art hydrological numerical models. The presented findings contribute to related studies in flood risk management as given for example in Hellmers et al. [2015]. In that study, the mitigation of flood risk (here in form of computed damage values in flood prone areas) by the implementation of LSDMs is analysed, among others, with the extended model of this work. Tools to model the performance of LSDMs on the catchment scale support to motivate and encourage public agencies for the implementation of decentralized drainage measures in urban areas, because the evaluation of their performance depends on regional scale catchment characteristics. Hence, these tools facilitate the design of local drainage measures, are applicable for educational purposes and support the decision-making process in polity. A supplementary outlook of this work is to facilitate a parameter pre-processing with the user interface of the module KalypsoHydrology to increase the user friendly application. This will replace the writing of additional parameter values in ASCII files in an extension folder (see figure 7.1 on page 101).

A holistic study about the procedure of decision-making and, among others, the adoption of LSDMs into flood management plans is described in Vojinović [2015]. Related study results about decision-making processes and multi-criteria analysis of how to choose an effective combination of LSDMs are given for example in Alves et al. [2016] and Chow et al. [2014]. Economic aspects are important in the implementation phase of LSDMs in urban planning. Case studies which analyse the economic benefits of LSDMs are presented for instance in USEPA [2013], Ashley et al. [2016, 2018] and Alves et al. [2019]. The recent publication by Alves et al. [2019] takes into account co-benefits (such as water savings, air quality improvement and energy savings) in the decision making processes. The paper illustrates results

of a cost-benefits analysis to compare "green", "blue" and "grey" (conventional pipe systems) concerning flood risk mitigation as well as the aforementioned co-benefits. A discussion about the difficulty in the economical analysis by taking into account the manifold benefits as well as drawbacks is given by Amos et al. [2016] and calls for a standardized method. A broader review of regulations, degree of applications and pitfalls in the implementation of rainwater harvesting systems is presented in Campisano et al. [2017]. An overview of further decision-making tools, including the performance of LSDMs, is published in Lerer et al. [2015].

The implementation of LSDMs by regulations and how to promote adaptation and perception of LSDMs in practice are not dealt with in this work, but are described for instance in Hoang and Fenner [2015]; Kuller et al. [2017]; Petrucci et al. [2013] and T. Schütze [2013]. Learning action alliances (see Ashley et al. [2012]) are considered here as an important step to raise the awareness to implement LSDMs.

In this work a hydrological flood routing method is extended to model exceedance flow among LSDMs and backwater effects in regional scale catchments (<100 km^2). For using instead a hydrodynamic-numerical model, information about the application and functionality is given for example in Price and Vojinović [2011] as well as Vojinović and Abbott [2012]. In contrast to hydrodynamic-numerical models, the developed hydrological model does not compute velocity fields within streams and the output of water levels represent average values per stream segment. Therefore, the developed hydrological model does not replace the demand for hydrodynamic-numerical models to compute two or three-dimensional velocity fields and the spatial detailed distribution of water levels within streams or areas for specific research questions. Nonetheless, for the objectives in the scope of this work (see section 3.4), the developed and implemented hydrological model is proved to be appropriate.

This work focuses on water quantity issues from the hydrological point of view. Additionally to the benefits by LSDMs on the changes in the flow regime by retention and detention processes, the purification by vegetation and filter materials in LSDMs has an impact on the water quality of the stormwater drained into receiving streams. A study about the reduction in suspended solids, nitrogen and phosphorus by rain gardens and bioretention basins is published in Gagrani et al. [2014]. An additional recent demand in research is the monitoring of the performance of LSDMs on the catchment scale with measurements in nature over longer periods of time as explained in Li et al. [2017] (p. 636). Neither that report, nor this study contributed to that open requirement for a catchment wide monitoring of measurements in nature.

These aforementioned issues put the findings in this work into a wider context of actual topics in research and practice. Especially in low lying (coastal) regions the concern to mitigate backwater induced flooding is and will be an important request with regard to predicted mean sea level rise, change in magnitude as well as probability of storm events and changes in urbanisation. The developed and implemented model shows good results to be applied as tool for further studies in research and practice to quantify the performance of LSDMs to mitigate flooding in backwater affected meso scale catchments.

10. Summary and conclusion

This work resolves prevailing limitations and weaknesses in modelling local scale drainage measures (LSDMs) in backwater affected catchments with an extended hydrological numerical model. The review in chapter 2 revealed limitations in the required high spatio-temporal resolutions in the computational methods. A parametrisation to model the processes in LSDMs was not yet defined on physical-based parameters which represent measurements in nature or laboratory. For modelling multiple and interlinked layered systems, physical-based approaches were missing. Hydrological methods to compute the exceedance and runoff flood routing among LSDMs within regional scale catchments were not applicable. Further on, approaches to model control systems and backwater effects on the local and meso scale with hydrological numerical models were unavailable. The review pointed out that a semi-distributed, deterministic, combined conceptual-physical based approach with a flexible spatio-temporal resolution and with the requirement of a parsimonious parametrisation is an applicable model category to be extended in this work to resolve these aforementioned limitations and weaknesses.

The scope of this work comprises objectives and theoretical approaches which are explained in chapter 3 using the SMART-principle. The specific objectives are distinguished with measurable evaluation parameters, applicable numerical approaches, relevant extensions for current hydrological numerical modelling and prerequisites for an in-time achievement within the scope of this work. The defined theoretical approaches are applied in the methodology of this work to create extended methods for hydrological numerical modelling. The methodology is subdivided into three consecutive parts and comprises several methods. First, methods are explained in chapter 4 to model a flexible spatio-temporal scaling and an on-the-fly network generation. Secondly, methods are developed and specified in chapter 5 to compute local scale hydrological processes and technologies in LSDMs. Thirdly, extended and new methods to model the flood routing among LSDMs, control systems in streams and backwater effects in streams as well as areas are described in chapter 6.

One strength of the developed methods is the application of parameters and numerical approaches on different spatio-temporal scales. The methods accomplish to zoom into the processes (physically, spatially and temporally) where reasonable values of parameters in practice

are available and detailed computation is required. At the same time, the methods enable to zoom out of the processes where lumped conceptualized approaches are applied. Calculation routines to model hydrological processes on the local and micro scale are successfully integrated in the algorithm of the meso scale numerical model. The methods provide a dynamic time step size calculation and accomplish a detailed computation on the spatio-temporal micro scale. Flexible spatial discretization of different types of LSDMs in a subcatchment is realised by a GIS-based mapping. This method uses so called overlays to create spatial local scale data structures with specific drainage attributes. The method offers the simulation of several different designs of LSDMs of the same type per subcatchment. For example, different structures of green roofs or different kinds of cisterns with rainwater harvesting functions are integrated per subcatchment. The generated hydrological network consists of data structures which are spatial (like subcatchments, HRUs or LSDMs), linear (like river stream segments) and punctiform (like junction nodes). Not only punctiform, but as well spatial data structures function now as source and target (sink) elements. Exceedance flow management is an important issue in decentralised storm water management. This is modelled with a flexible on-the-fly net generation to compute the flood routing among data structures on the meso and local scale. A method for modelling the hydrological processes in multi-linked layers on a detailed temporal and spatial scale is developed, implemented and validated with measurements of a physical model in laboratory. Upcoming technologies in LSDMs like the real-time control of storages in cisterns or retention roofs is modelled with extended control functions. These functions are based on criteria of precipitation intensities, water levels and discharges as functions per time. In this way, technologies which are connected to operational forecast systems with radar rainfall data described for example in Hellmers, Strehz, et al. [2016] and Jasper-Tönnies et al. [2018] are computed. Additionally, the developed methods facilitate to model the features of (tide) gates, sluices, retention ponds and pump stations on the basis of water level stages or discharges which are situated upstream or downstream of the control structure. For the computation of the flood routing on the meso scale, the results of the micro and local scale data structures are aggregated according to their contributing inlet in the network structure of the model. The flood routing method applies physical-based parameters to characterise stream segments. The method distinguishes between the need to model irregular profiles with flood plane delineation or simplified geometric shape. A single-reservoir approach using the Kalinin-Miljukov theory (named as "KM1-method") is applied to model the flood routing among LSDMs with simplified geometric shapes. Flood routing in irregular river stream profiles is modelled with a five-reservoirs approach (named as "KM5-method"). In low lying lands, an afflux which is generated by retained water leads to a rise in downstream water levels, which in turn causes backwater effects in upstream direction. Both, the KM1- and KM5-method, are extended to compute such backwater effects within the hydrological network. Finally, the methods accomplish to compute backwater effects in streams, flood prone areas and LSDMs. Additionally, subsequent open water evaporation from submerged backwater affected areas and controlled drainage of LSDMs are calculated.

The methods developed in this work are implemented in the open-source hydrological numerical model KalypsoNA which is operated by the module KalypsoHydrology. The model and the implementation procedure are presented in chapter 7. The applicability of the model in research as well as in practice depends among others on an available, physical-based but parsimonious parametrisation. Providing additional features like a user interface, enabling GIS-based functions and supportive information (for instance in the form of manuals) facilitate the applicability. These requirements for subsequent usability and applicability in practice as well as research are provided by the model KalypsoNA which is revised and extended in the scope of this work.

For the evaluation of the implemented methods, different application studies are analysed in chapter 8 on the local scale with laboratory experiments and on the regional scale with the backwater affected catchment "Dove-Elbe" (175 km^2) in Hamburg, Germany. The results are evaluated with criteria in mass-conservation of simulated processes, tested with respect to functional correctness in data processing and validated by using measurements of gauging stations as well as physical models in laboratory. The evaluation parameters are introduced within the SMART-principle in chapter 3 and used in chapter 8 to prove the reliability of the developed and implemented methods. The comparison between simulated and observed model results from laboratory comprised seven calibration and fifteen validation runs of different green roof installations. The root mean square differences between the observed and simulated results are about 6 %. Lag time and peak flux rate differences are less than 1 %. Hence, the simulated and observed hydrographs are in good agreement. Methods to model LSDM techniques like exceedance flow among layers, rainwater harvesting and operational control functions are developed and tested for functional correctness. With the regional scale hydrological model "Dove-Elbe" (175 km^2), the computation of backwater effects is evaluated. The criteria in mass-conservation and a comparison of the simulated results with water level measurements at gauging stations in the backwater affected streams, demonstrate a good conformance. The difference in observed and simulated peak water levels is only about 0.02 m to 0.10 m within river streams where the variability of the backwater affected water level range has a size of about 1 m. For the application of the model in practice within flood-forecast systems short computing times are required. In the presented application studies a standard computer with i7-5600U CPU and 2.6 GHz is applied. A computing time of only 2:20 minutes is observed for a simulation run over ten days of the tidal influenced catchment model Dove-Elbe (175 km^2) including backwater affected streams, seven control systems and about 50 LSDMs. The short computing times of the presented model in this work facilitates the application for operational and real-time forecast simulations in practice.

The application study results of modelling LSDMs in a backwater affected catchment area demonstrate good potential in flood peak reduction and subsequent reduction of backwater induced flooding in low lying lands. In the study area "Moorfleet" with a size of about 8.42 km^2, the peak discharge is reduced by 50 % (from a maximum of 7.97 m^3/s to 3.94 m^3/s) and backwater induced flooding is prevented by the implementation of green roofs having a

size of 0.28 km^2 (meaning 3.3 % of the total catchment area) which are coupled to cisterns having a size of 0.06 % (0.005 km^2) of the total catchment area and multifunctional areas having a size of 0.6 % (0.05 km^2) of the total catchment area. The evaporation from vegetated surfaces (namely green roofs) is increased and stormwater is retained in cisterns and retention roofs. The reduction of surface runoff is improved by a pre-emptying control function of retention roofs and cisterns with the criteria of forecasted precipitation intensities.

The discussion of findings in the developed methods and results of the evaluation studies in chapter 9 points out the achievements and limitations of this work in comparison to related study results in literature. One key finding of the developed method to model hydrological processes in LSDMs is the effective physical-based parametrisation. In contrast to a widely-applied conceptual approach, the created parametrisation in this work is transferable to other LSDM structures and case studies. The developed on-the-fly network generation, which uses drainage criteria and geographical location of LSDMs, provides required features to model the performance of linked LSDMs within regional scale catchments. This is a benefit in comparison to current hydrological numerical models which rely on manual linkages or use conceptual routing approaches among LSDMs. The current numerical hydrological models are not applicable to model large scale catchments (>100 km^2) with a detailed flood routing computation among LSDMs. Although small process-related time step sizes in the range of seconds are used to compute the hydrological processes in LSDMs, the computing time of a simulation run over about ten days remains below five minutes for a regional scale model. These computing times are smaller than of related numerical models which apply detailed time step size computations. In contrast to related hydrological models, the extended control functions in this work cover a wider field for application in real-time control management. The discussion of the developed hydrological method, to compute backwater effects in meso scale catchments, shows benefits in using physical-based parameters and the possibility to compute backwater effects among streams and flood prone areas (or LSDMs).

Upcoming challenges in preparing drainage systems in urban areas for an uncertain range of mean sea level rise, change in magnitude as well as probability of storm events and changes in urbanisation require reliable and applicable tools. Especially in low lying lands, the concern to mitigate backwater induced flooding is and will be an important task. The input parameters of the developed methods to model the features of LSDMs and backwater effects in streams and areas are part of a physical-based (parsimonious) parametrisation using geometry and material characteristics. This parametrisation facilitates the application of the model and knowledge for further catchment studies. It is proved, with a sufficient exactness from a practical point of view, that the developed and implemented model is an appropriate instrument to analyse the hydrological performance of LSDMs on the meso scale in backwater affected catchments.

References

Abbaspour, A., Tanyu, B. F., Aydilek, A. H., & Dayioglu, A. Y. (2018). Methodology to evaluate hydraulic compatibility of geotextile and RCA in underdrain systems. *Geosynthetics International*, *25*(1), 67–84. doi: 10.1680/jgein.17.00034

Ahiablame, L. M., Engel, B. A., & Chaubey, I. (2012). Effectiveness of low impact development practices: literature review and suggestions for future research. *Water Air Soil Pollut. (Water, Air, & Soil Pollution)*, *223*(7), 4253–4273. doi: 10.1007/s11270-012-1189-2

Alamdari, N., Sample, D. J., Liu, J., & Ross, A. C. (2018). Assessing climate change impacts on the reliability of rainwater harvesting systems. *Resources, Conservation and Recycling*, *132*, 178–189. doi: 10.1016/j.resconrec.2017.12.013

Alfredo, K., Montalto, F., & Goldstein, A. (2010). Observed and Modeled Performances of Prototype Green Roof Test Plots Subjected to Simulated Low- and High-Intensity Precipitations in a Laboratory Experiment. *Journal of Hydrologic Engineering*, *15*(6), 444–457. doi: 10.1061/(ASCE)HE.1943-5584.0000135

Allen, R., Smith, M., Perrier, A., & Pereira, L. (1994). An Update for the Definition of Reference Evapotranspiration. *ICID Bulletin (International Commission on Irrigation and Drainage)*, *43*(2), 1–34.

Allen, R. G., Pereira, L. S., Raes Dirk, & Smith, M. (1998). *Crop evapotranspiration: Guidelines for computing crop water requirements* (Repr ed., Vol. 56). Rome: FAO - Food and Agriculture Organization of the United Nations.

Alves, A., Gersonius, B., Kapelan, Z., Vojinovic, Z., & Sanchez, A. (2019). Assessing the Co-Benefits of green-blue-grey infrastructure for sustainable urban flood risk management. *Journal of environmental management*, *239*, 244–254. doi: 10.1016/j.jenvman.2019.03.036

Alves, A., Sanchez, A., Gersonius, B., & Vojinovic, Z. (2016). A Model-based Framework for Selection and Development of Multi-functional and Adaptive Strategies to Cope with Urban Floods. *Procedia Engineering*, *154*, 877–884. doi: 10.1016/j.proeng.2016.07.463

Amerman, C. R. (1965). The use of unit-Source watershed data for runoff prediction. *Water Resources Research*, *1*(4), 499–507. doi: 10.1029/WR001i004p00499

Amos, C. C., Rahman, A., & Gathenya, J. M. (2016). Economic Analysis and Feasibility of Rainwater Harvesting Systems in Urban and Peri-Urban Environments: A Review of the Global Situation with a Special Focus on Australia and Kenya. *Water*, *8*(4), 149. doi: 10.3390/w8040149

Anacostia Waterfront Trust. (2017). *The Holy Hill is Going Green this Thursday!* Washington, DC, United States. Retrieved 14.12.2018, from https://www.anacostiatrust.org/anacostia-trust/2017/5/9/the-holy-hill-is-going-green-this-thursday

Arcement, G. J., & Schneider, V. R. (1989). *Guide for selecting Manning's roughness coefficients for natural channels and flood plains* (- ed.) (No. 2339). Denver, CO, USA.

Aryal, S. K., Ashbolt, S., McIntosh, B. S., Petrone, K. P., Maheepala, S., Chowdhury, R. K., ... Gardiner, R. (2016). Assessing and Mitigating the Hydrological Impacts of Urbanisation in Semi-Urban Catchments Using the Storm Water Management Model. *Water Resources Management*, *30*(14), 5437–5454. doi: 10.1007/s11269-016-1499-z

Ashley, R. M., Blanskby, J., Newman, R., Gersonius, B., Poole, A., Lindley, G., ... Nowell, R. (2012). Learning and Action Alliances to build capacity for flood resilience. *Journal of Flood Risk Management*, *5*(1), 14–22. doi: 10.1111/j.1753-318X.2011.01108.x

Ashley, R. M., Digman, C. J., Horton, B., Gersonius, B., Smith, B., Shaffer, P., & Baylis, A. (2016). Using the multiple benefits of SuDS tool (BeST) to deliver long-term benefits. In *Proceedings of Novatech 9th International Conference.* Lyon, France.

Ashley, R. M., Gersonius, B., Digman, C., Horton, B., Bacchin, T., Smith, B., ... Baylis, A. (2018). Demonstrating and Monetizing the Multiple Benefits from Using SuDS. *Journal of Sustainable Water in the Built Environment*, *4*(2), 05017008. doi: 10.1061/JSWBAY.0000848

Askarizadeh, A., Rippy, M. A., Fletcher, T. D., Feldman, D. L., Peng, J., Bowler, P., ... Grant, S. B. (2015). From Rain Tanks to Catchments: Use of Low-Impact Development To Address Hydrologic Symptoms of the Urban Stream Syndrome. *Environmental science & technology*, *49*(19), 11264–11280. doi: 10.1021/acs.est.5b01635

Bach, M. (2011). *Integrierte Modellierung für Einzugsgebiete mit komplexer Nutzung* (Dissertation, Darmstadt University of Technology, Darmstadt, Germany). Retrieved 14.12.2018, from http://tuprints.ulb.tu-darmstadt.de/2413/

Bach, P. M., Rauch, W., Mikkelsen, P. S., McCarthy, D. T., & Deletic, A. (2014). A critical review of integrated urban water modelling – Urban drainage and beyond. *Environ. Model. Softw.*, *54*, pp. 88–107. doi: 10.1016/j.envsoft.2013.12.018

Balmforth, D., Digman, C., Kellagher, R., & Butler, D. (2006). *CIRIA C635 - Designing for exceedance in urban drainage: Good practice* (Vol. C635). London: CIRIA.

Bear, J. (1988). *Dynamics of Fluids in Porous Media* (1st ed.). New York, N.Y.: Dover.

Behörde für Stadtentwicklung und Umwelt (BSU). (2013). *Regenwasserhandbuch SBH und RISA: Ganzheitlicher Umgang mit Niederschlag an Hamburger Schulen: Das Projekt RISA – RegenInfraStrukturAnpassung.* Retrieved 28.11.2018, from http://www.hamburg.de/contentblob/4106776/data/d-regenwasserhandbuch.pdf

Behörde für Umwelt und Energie (BUE). (2015). *Auf die Dächer - Fertig- Grün! Hamburger Gründachförderung: Mehr Gründächer für Hamburg.* Retrieved 07.07.2018, from https://www.hamburg.de/contentblob/4599638/baf6f2302bfa9162490113babe005269/data/d-broschuere.pdf

Belger, G., Haase, M., Jung, T., & Lippert, K. (2009). A GIS-based Platform for Environmental and Water resources Modeling - Kalypso Open Source. *geoinformatics*, *2009*, 36–39. Retrieved 17.12.2018, from http://www.bjoernsen.de/uploads/media/geoinformatics_2009.pdf

Bergström, S. (1992). *THE HBV MODEL - its structure and applications.* Norrköping, Sweden. Retrieved 15.12.2018, from https://www.smhi.se/polopoly_fs/1.83592!/Menu/general/extGroup/attachmentColHold/mainCol1/file/RH_4.pdf

Beven, K. (1993). Prophecy, reality and uncertainty in distributed hydrological modelling. *Advances in Water Resources*, *16*(1), 41–51. doi: 10.1016/0309-1708(93)90028-E

Beven, K. (2007). Towards integrated environmental models of everywhere: Uncertainty, data and modelling as a learning process. *Hydrology and Earth System Sciences*, *11*(1), 460–467. doi: 10.5194/hess-11-460-2007

Beven, K. (2012). *Rainfall-Runoff Modelling: The Primer, Second Edition*. Chichester, UK: John Wiley & Sons, Ltd. doi: 10.1002/9781119951001

Beven, K., & Freer, J. (2001). Equifinality, data assimilation, and uncertainty estimation in mechanistic modelling of complex environmental systems using the GLUE methodology. *Journal of Hydrology*, *249*(1-4), 11–29. doi: 10.1016/S0022-1694(01)00421-8

Beven, K., & Germann, P. (1982). Macropores and water flow in soils. *Water Resources Research*, *18*(5), 1311–1325. doi: 10.1029/WR018i005p01311

Beven, K., & Germann, P. (2013). Macropores and water flow in soils revisited. *Water Resources Research*, *49*(6), 3071–3092. doi: 10.1002/wrcr.20156

Björnsen Consulting Engineers GmbH (BCE). (2018). *Kalypso.* Koblenz, Germany. Retrieved 15.12.2018, from https://kalypso.bjoernsen.de/

Björnsen Consulting Engineers GmbH (BCE), & Institute of River & Coastal Engineering (WB-TUHH). (2018). *Kalypso.* Retrieved 15.12.2018, from www.sourceforge.net/projects/kalypso

Blair, P., & Buytaert, W. (2016). Socio-hydrological modelling: A review asking 'why, what and how'? *Hydrology and Earth System Sciences*, *20*(1), 443–478. doi: 10.5194/hess-20-443-2016

Blöschl, G., & Sivapalan, M. (1995). Scale issues in hydrological modelling: A review. *Hydrological Processes*, *9*(3-4), 251–290. doi: 10.1002/hyp.3360090305

Bollrich, G. (1996). *Technische Hydromechanik (Bd. 1; Grundlagen)* (4., durchges. Aufl. ed.). Berlin u.a.: Verl. für Bauwesen. Retrieved from https://external.dandelon.com/download/attachments/dandelon/ids/DE001ACCEBB132CA1AAABC12575BE002948A0.pdf

Bollrich, G. (2013). *Technische Hydromechanik (1; Grundlagen)* (7. Auflage ed.). Berlin Wien Zürich: Beuth Verlag GmbH. Retrieved from http://www.beuth.de/cmd?level=tpl-langanzeige&websource=vlb&smoid=169443777

Bos, R., Hoffmann, L., Juilleret, J., Matgen, P., & Pfister, L. (2006). *Conceptual modelling of individual HRU's as a trade-off between bottom-up and top-down modelling, a case study.* Belvaux, Grand-Duchy of Luxembourg. Retrieved 15.12.2018, from http://former.iemss.org/sites/iemss2006//papers/s12/9_vandenBos_3.pdf

Bozovic, R., Maksimović, C., Mijic, A., Smith, K. M., Suter, I., & van Reeuwijk, M. (2017). *Blue Green Solutions: A system approach to sustainable, resilient and cost-efficient urban development*. London, United Kingdom. Retrieved 15.12.2018, from http://www.climate-kic.org/wp-content/uploads/2017/10/BGD-Guide.compressed.pdf

Brears, R. C. (2018). *Blue and Green Cities: The Role of Blue-Green Infrastructure in Managing Urban Water Resources*. London: Palgrave Macmillan UK. doi: 10.1057/978-1-137-59258-3

Bulatewicz, T., & Cuny, J. (2005). *Interface - based Support for Model Coupling: Spatial Representation and Compatibility Issues.* Oregon, Eugene. Retrieved 15.12.2018, from http://www.geocomputation.org/2005/Bulatewicz.pdf

Bund der Ingenieure für Wasserwirtschaft, Abfallwirtschaft und Kulturbau e.V. (BWK). (2009). *Hydraulische Berechnung von naturnahen Fließgewässern - Teil 1, Stationäre Berechnung der Wasserspiegellinie unter besonderer Berücksichtigung von Bewuchs- und Bauwerkseinflüssen* (3rd ed.). Sindelfingen, Germany: Fraunhofer IRB Verlag.

Burns, M., Fletcher, T. D., Hatt, B. E., Ladson, A. R., & Walsh, C. J. (2010). Can allotment-scale rainwater harvesting manage urban flood risk and protect stream health? In B. Chocat & J.-L. Bertrand-Krajewski (Eds.), *Proceedings of the 7th International Conference on Sustainable Techniques and Strategies in Urban Water Management* (pp. 1–10).

Burns, M. J., Fletcher, T. D., Walsh, C. J., Ladson, A. R., & Hatt, B. E. (2012). Hydrologic shortcomings of conventional urban stormwater management and opportunities for reform. *Landscape and Urban Planning*, *105*(3), 230–240. doi: 10.1016/j.landurbplan.2011.12.012

Butler, D., & Davies, J. (2011). *Urban Drainage* (3rd Edition ed.). New York, NY, USA: Spon Press.

BWS GmbH. (2011). *Erweiterter Vergleich von Planungsvarianten zur Verbesserung des Binnenhochwasserschutzes im Bereich der Vier- und Marschlande Hydraulische Untersuchungen im Einzugsgebiet der Dove-Elbe/Bille: Dok. 7: Bauwerksverzeichnis und Steuerungsrandbedinungen*. Hamburg, Germany.

Campisano, A., Butler, D., Ward, S., Burns, M. J., Friedler, E., DeBusk, K., ... Han, M. (2017). Urban rainwater harvesting systems: Research, implementation and future perspectives. *Water research*, *115*, 195–209. doi: 10.1016/j.watres.2017.02.056

Carman, P. C. (1937). Fluid flow through granular beds. *Transactions of the Institution of Chemical Engineers*, *1937*(15), 155–166. doi: 10.1017/S0021859600051789

Caseri, A., Ramos, M.-H., Javelle, P., Leblois, E., Lang, M., Klijn, F., & Samuels, P. (2016). A space-time geostatistical approach for ensemble rainfall nowcasting. *3rd European Conference on Flood Risk Management*, *7*, 1–5. doi: 10.1051/e3sconf/20160718001

Casper, M. C., Herbst, M., Grundmann, J., Buchholz, O., & Bliefernicht, J. (2009). Einfluss der Niederschlagsvariabilität auf die Simulation extremer Abflüsse in kleinen Einzugsgebieten: Influence of rainfall variability on the simulation of extreme runoff in small catchments. *Hydrologie und Wasserbewirtschaftung*, *2009*(HW 53. 2009, H.3), 134–139.

Chapuis, R., & Aubertin, M. (2003). *Predicting the coefficent of permeability of soils using the Kozeny-Carman equation*. Montréal, Canada: (Technical Report) EPM-RT-2003-03.

Chivers, I., & Sleightholme, J. (2005). *Introduction to Programming with Fortran: With coverage of Fortran 2003, 95, 90 and 77* (1. ed. ed.). Goldaming: Springer London. doi: 10.1007/b137984

Chow, J.-f., Savić, D., Fortune, D., Kapelan, Z., & Mebrate, N. (2014). Using a Systematic, Multi-criteria Decision Support Framework to Evaluate Sustainable Drainage Designs. *Procedia Engineering*, *70*, 343–352. doi: 10.1016/j.proeng.2014.02.039

CIRIA. (2018). *Construction industry research and information association.* London, United Kingdom. Retrieved 15.12.2018, from www.ciria.org

Clark, M. P., Slater, A. G., Rupp, D. E., Woods, R. A., Vrugt, J. A., Gupta, H. V., ... Hay, L. E. (2008). Framework for Understanding Structural Errors (FUSE): A modular framework to diagnose differences between hydrological models. *Water Resources Research*, *44*(12), W00B02. doi: 10.1029/2007WR006735

Clarke, R. T. (1973). A review of some mathematical models used in hydrology, with observations on their calibration and use. *Journal of Hydrology*, *19*(1), 1–20. doi: 10.1016/0022-1694(73)90089-9

Climate Innovation Window (CIW). (2018). *The Hydroactive Smart Roof System : HYDROVENTIV: Climate Innovation Window Project - Brigaid.* Netherlands. Retrieved 15.12.2018, from https://climateinnovationwindow.eu/innovations/hydroventiv

Conradt, T. (2013). *Challenges of regional hydrological modelling in the Elbe River basin: Investigations about model fidelity on sub-catchment level* (Dissertation, Universität Potsdam, Potsdam, Germany). Retrieved 15.12.2018, from https://publishup.uni-potsdam.de/opus4-ubp/frontdoor/index/index/year/2013/docId/6285

Courant, R., Friedrichs, K., & Lewy, H. (1928). Über die partiellen Differenzengleichungen der mathematischen Physik. *Math. Ann. (Mathematische Annalen | Journal)*, *100*(100), 32–74.

Crawford, N. H., & Linsley, R. K. (1966). *Digital Simulation on Hydrology: Stanford Watershed Model IV: Technical Report No. 39* (Vol. 1966). Stanford University, Palo Alto, CA: Department of Civil and Environmental Engineering.

Cunge, J. A. (1969). On The Subject Of A Flood Propagation Computation Method (Muskingum Method). *Journal of Hydraulic Research*, *7*(2), 205–230. doi: 10.1080/00221686909500264

Department of Planning and Local Government (DPLG). (2010). *Water Sensitive Urban Design Technical Manual for the Greater Adelaide Region: WSUD Chapter 15.* Adelaide, Australia. Retrieved 15.12.2018, from https://www.sa.gov.au/__data/assets/pdf_file/0020/15059/WSUD_chapter_15.pdf

Deutsche Vereinigung für Wasserwirtschaft, Abwasser und Abfall (DWA). (2016). *Grundsätze zur Bewirtschaftung und Behandlung von Regenwetterabflüssen zur Einleitung in Oberflächengewässer (Entwurf): Arbeitsblatt DWA-A 102/BWK-A 3.* Hennef, Germany: Deutsche Vereinigung für Wasserwirtschaft, Abwasser und Abfall.

Deutscher Verband für Wasserwirtschaft und Kulturbau e.V. (DVWK). (1996). *Ermittlung der Verdunstung von Land- und Wasserflächen* (Vol. 238). Bonn, Germany: Wirtschafts- und Verlagsgesellschaft Gas und Wasser.

Deutsches Institut für Normung e. V. (DIN). (2002). *DIN 1989-1:2002-04: Regenwassernutzungsanlagen - Teil 1: Planung, Ausführung, Betrieb und Wartung / Rainwater harvesting systems Part 1: Planning, installation, operation and maintanance.* Berlin: Beuth Verlag GmbH.

Devia, G. K., Ganasri, B. P., & Dwarakish, G. S. (2015). A Review on Hydrological Models. *Aquatic Procedia*, *4*, 1001–1007. doi: 10.1016/j.aqpro.2015.02.126

De-Ville, S. (2017). *Hydrological Performance Evolution of Extensive Green Roof Systems* (Dissertation, The University of Sheffield, Sheffield). Retrieved 15.12.2018, from http://etheses.whiterose.ac.uk/17718/1/DeVille_S_Thesis_Final.pdf

De-Ville, S., Menon, M., Jia, X., Reed, G., & Stovin, V. (2017). The impact of green roof ageing on substrate characteristics and hydrological performance. *Journal of Hydrology*, *547*, 332–344. doi: 10.1016/j.jhydrol.2017.02.006

Digman, C. J., Ashley, R. M., Balmforth, D. J., Balmforth, D. W., Stovin, V. R., & Glerum, J. W. (2012). *CIRIA C713 - Retrofitting to manage surface water.* London. Retrieved 16.12.2018, from https://www.ciria.org/Resources/Free_publications/Retrofitting_manage_surface_water.aspx

Donigian, A. S., JR., & Imhoff, J. C. (2006). Chapter 2: History and Evolution of Watershed Modeling: Derived from the Stanford Watershed Model (SWM). In CRC Press (Ed.), *Watershed models* (pp. 21–45). Boca Raton: Taylor & Francis Group. Retrieved 16.12.2018, from http://www.aquaterra.com/resources/pubs/pdf/donigian-2006.pdf

Dooge, J. C. I. (1959). A general theory of the unit hydrograph. *Journal of Geophysical Research*, *64*(2), 241–256. doi: 10.1029/JZ064i002p00241

Dooge, J. C. I. (1973). *Linear theory of hydrologic systems: Tech. Bul., No. 1468.* Washington, DC, United States. Retrieved 16.12.2018, from http://ageconsearch.umn.edu/bitstream/160041/2/tb1468.pdf

Doran, G. T. (1981). There's a S.M.A.R.T. way to write management's goals and objectives. *Management Review*, *1981*(70.11), 35–36. Retrieved 25.03.2019, from https://community.mis.temple.edu/mis0855002fall2015/files/2015/10/S.M.A.R.T-Way-Management-Review.pdf

Dorp, M., Loch, E., & Rothe, B. (2017). *Modellierung von Rückstau, Fließrichtungswechsel und Abflussaufteilung.* Retrieved 16.12.2018, from https://www.hydrotec.de/n-a-modell-modelliert-dynamische-systeme/

Eckelmann, W., et al. (Eds.). (2005). *Bodenkundliche Kartieranleitung. KA5.* Stuttgart, Germany: Schweizerbart Science Publishers. Retrieved from http://www.schweizerbart.de//publications/detail/isbn/9783510959204/Bodenkundliche_Kartieranleitung_5_Aufl

Einfalt, T., Arnbjerg-Nielsen, K., Golz, C., Jensen, N.-E., Quirmbach, M., Vaes, G., & Vieux, B. (2004). Towards a roadmap for use of radar rainfall data in urban drainage. *Journal of Hydrology*, *299*(3-4), 186–202. doi: 10.1016/j.jhydrol.2004.08.004

Elliott, A. H., & Trowsdale, S. A. (2007). A review of models for low impact urban stormwater drainage. *Environ. Model Softw. (Environmental Modelling & Software)*, *22*, 394–405. doi: 10.1016/j.envsoft.2005.12.005

(EPA) United States Environmental Protection Agency. (2018a). *Green Infrastructure.* Retrieved 16.12.2018, from www.epa.gov/green-infrastructure

(EPA) United States Environmental Protection Agency. (2018b). *Storm Water Management Model (SWMM).* Retrieved 16.12.2018, from https://www.epa.gov/water-research/storm-water-management-model-swmm

Eric, M., Fan, C., Joksimovic, D., & Li, J. Y. (2013). Modeling low impact development potential with hydrological response units. *Water Science and Technology*, *68*(11), 2382–2390. doi: 10.2166/wst.2013.502

Euler, G. (1983). Ein hydrologisches Näherungsverfahren für die Berechnung des Wellenablaufs in Kreisrohren. *Wasser und Boden*, *1983*(2).

European Commission (EC). (2000). *Water Framework Directive: Directive 2000/60/EC of the European Parlament and the council - of 23 October 2000 - establishing a framework for Community action in the field of water policy.* Official Journal of the European Communities. Retrieved 27.12.2018, from http://eur-lex.europa.eu/resource.html?uri=cellar:5c835afb-2ec6-4577-bdf8-756d3d694eeb.0004.02/DOC_1&format=PDF

European Commission (EC). (2007). *EU Floods Directive: Directive 2007/60/EC of the European Parlament and the council - of 23 October 2007 - on the assessment and management of flood risks.* Retrieved 16.12.2018, from http://eur-lex.europa.eu/legal-content/EN/TXT/PDF/?uri=CELEX:32007L0060&from=EN

European Commission (EC). (2013). *The EU Strategy on adaptation to climate change: Strengthening Europe's resilience to the impacts of climate change.* Retrieved 16.12.2018, from https://ec.europa.eu/clima/sites/clima/files/docs/eu_strategy_en.pdf

eWater. (2012). *Evolving water management - About Us.* Bruce, ACT, 2617, Australia. Retrieved 16.12.2018, from www.ewater.org.au/about-us/

eWater. (2018). *MUSIC - Software Release Version 6* (6th ed.). Retrieved 16.12.2018, from http://www.toolkit.net.au/Tools/MUSIC

Fenicia, F., Kavetski, D., Savenije, Hubert H. G., & Pfister, L. (2016). From spatially variable streamflow to distributed hydrological models: Analysis of key modeling decisions. *Water Resources Research*, 1–36. doi: 10.1002/2015WR017398

Fenicia, F., McDonnell, J. J., & Savenije, Hubert H. G. (2008). Learning from model improvement: On the contribution of complementary data to process understanding. *Water Resources Research*, *44*(6), 1–13. doi: 10.1029/2007WR006386

Fletcher, T. D., Andrieu, H., & Hamel, P. (2013). Understanding, management and modelling of urban hydrology and its consequences for receiving waters: A state of the art. *Advances in Water Resources*, *51*, 261–279. doi: 10.1016/j.advwatres.2012.09.001

Fletcher, T. D., Shuster, W., Hunt, W. F., Ashley, R., Butler, D., Arthur, S., ... Viklander, M. (2014). SUDS, LID, BMPs, WSUD and more – The evolution and application of terminology surrounding urban drainage. *Urban Water J. (Urban Water Journal)*, *12*(7), 525–542. doi: 10.1080/1573062X.2014.916314

Freie und Hansestadt Hamburg, Umweltbehörde (FHH). (2000). *Dezentrale naturnahe Regenwasserbewirtschaftung*. Hamburg, Germany.

Gaborit, E., Muschalla, D., Vallet, B., Vanrolleghem, P. A., & Anctil, F. (2013). Improving the performance of stormwater detention basins by real-time control using rainfall forecasts. *Urban Water Journal*, *10*(4), 230–246. doi: 10.1080/1573062X.2012.726229

Gagrani, V., Diemer, J. A., Karl, J. J., & Allan, C. J. (2014). Assessing the Hydrologic and Water Quality Benefits of a Network of Stormwater Control Measures in a SE U.S. Piedmont Watershed. *JAWRA Journal of the American Water Resources Association*, *50*(1), 128–142. doi: 10.1111/jawr.12121

García, L., Barreiro-Gomez, J., Escobar, E., Téllez, D., Quijano, N., & Ocampo-Martinez, C. (2015). Modeling and real-time control of urban drainage systems: A review. *Advances in Water Resources*, *85*, 120–132. doi: 10.1016/j.advwatres.2015.08.007

Gentine, P., Troy, T. J., Lintner, B. R., & Findell, K. L. (2012). Scaling in Surface Hydrology: Progress and Challenges. *J. Contemp. Water Res. Educ. (Journal of Contemporary Water Research & Education)*, *2012*(147), 28–40. doi: 10.7916/D84M9FP7

Gersonius, B., Ashley, R., Pathirana, A., & Zevenbergen, C. (2013). Climate change uncertainty: building flexibility into water and flood risk infrastructure. *Climatic Change*, *116*(2), 411–423. doi: 10.1007/s10584-012-0494-5

Gessner, M. O., Hinkelmann, R., Nützmann, G., Jekel, M., Singer, G., Lewandowski, J., . . . Barjenbruch, M. (2014). Urban water interfaces. *Journal of Hydrology*, *514*, 226–232. doi: 10.1016/j.jhydrol.2014.04.021

Gleeson, T., & Paszkowski, D. (2013). Perceptions of scale in hydrology: What do you mean by regional scale? *Hydrol. Sci. J. (Hydrological Sciences Journal)*, *59*(1), 99–107. doi: 10.1080/02626667.2013.797581

Goncalves, M. L. R., Zischg, J., Rau, S., Sitzmann, M., & Rauch, W. (2018). Modeling the Effects of Introducing Low Impact Development in a Tropical City: A Case Study from Joinville, Brazil. *Sustainability*, *10*(3), 728. doi: 10.3390/su10030728

Grayson, R., & Blöschl, G. (2001a). Chapter 1: Spatial Processes, Organisation and Patterns. In R. Grayson & G. Blöschl (Eds.), *Spatial Patterns in Catchment Hydrology.* Cambridge u.a.: Cambridge Univ. Press.

Grayson, R., & Blöschl, G. (2001b). Chapter 3: Spatial Modelling of Catchment Dynamics. In R. Grayson & G. Blöschl (Eds.), *Spatial Patterns in Catchment Hydrology.* Cambridge u.a.: Cambridge Univ. Press.

Haase, D. (2009). Effects of urbanisation on the water balance – A long-term trajectory. *Environmental Impact Assessment Review*, *29*(4), 211–219. doi: 10.1016/j.eiar.2009.01.002

Hamburger Stadtentwässerung AöR (HSE), & Behörde für Umwelt und Energie (BUE). (2015). *RISA Strukturplan Regenwasser 2030: Ergebnisbericht des Projektes RISA – RegenInfraStrukturAnpassung.* Hamburg, Germany. Retrieved 16.12.2018, from https://www.risa-hamburg.de/fileadmin/risa/Downloads/BUE_HSE_2015_RISA_Strukturplan_Regenwasser_2030.pdf

Hamel, P., & Fletcher, T. D. (2013). The impact of stormwater source-control strategies on the (low) flow regime of urban catchments. In *Novatech 8th International Conference.* Lyon, France.

Hellmers, S. (2008). *Sustainable Concepts of Urban Drainage in the UK and Assessment Methods of their Effectiveness* (Project Work at the Institute of River and Coastal Engineering). TU Hamburg-Harburg, Hamburg, Germany. In Cooperation with the University of Sheffield, England.

Hellmers, S. (2010). *Hydrological impacts of climate change on flood probability in small urban catchments and possibilities of flood risk mitigation* (No. 13). Hamburg: Hamburger Wasserbau-Schriften. Re-

trieved 15.12.2018, from http://www.tuhh.de/t3resources/wb/Publikationen/wb-schriften/Wasserbauschrift_Band13.pdf

Hellmers, S. (2016). Abbildbarkeit mehrfach vernetzter heterogener dezentraler Maßnahmen in NA-Modellen. In Casper, M., Gronz, O (Ed.), *Räumliche Heterogenität - Erkennen, Abbilden, Validieren oder Ignorieren?* (Vol. 36.16, pp. 75–84). Trier, Germany: Forum für Hydrologie und Wasserbewirtschaftung. doi: 10.14617/for.hydrol.wasbew.36.16

Hellmers, S., Belger, G., & Fröhle, P. (2016). Mapping of multiple linked green infrastructure systems in rainfall-runoff models. In NCKU (Ed.), *Proceedings 12th International Conference on Hydroscience & Engineering: 6–10 November 2016.* Tainan, Taiwan.

Hellmers, S., & Fröhle, P. (2017). Integrating local scale drainage measures in meso scale catchment modelling. *Water (Special Issue: Hydroinformatics and Urban Water Systems)*, *2017*(9,71). Retrieved 16.12.2018, from doi:10.3390/w9020071

Hellmers, S., & Fröhle, P. (2020). Hydrologie und Flächenmanagement: Arbeitspaket 2. In LSBG, TUHH, UHH, HWWI, & hydro meteo GmbH&Co.KG (Eds.), *BMBF-Projekt STUCK: Abschlussbericht 2015-2019; Sicherstellung der Entwässerung küstennaher, urbaner Räume unter Berücksichtigung des Klimawandels.* Hamburg, Germany.

Hellmers, S., Manojlović, N., Palmaricciotti, G., & Fröhle, P. (2016). Modelling decentralised systems for urban drainage and flood mitigation. *Journal of Applied Water Engineering and Research*, 1–9. doi: 10.1080/23249676.2015.1128368

Hellmers, S., Manojlović, N., Palmaricciotti, G., Kurzbach, S., & Fröhle, P. (2015). Multiple linked sustainable drainage systems in hydrological modelling for urban drainage and flood risk management. *J. Flood Risk Manag. (Journal of Flood Risk Management)*, S5-S16. doi: 10.1111/jfr3.12146

Hellmers, S., & Pasche, E. (2011a). Hydrologische Wirkungsanalyse des Klimawandels und Anpassungsmaßnahmen auf der Grundlage von hochaufgelösten Klimadaten. In G. Blöschl & R. Merz (Eds.), *Hydrologie & Wasserwirtschaft - Von der Theorie zur Praxis.* Wien, Austria: Forum für Hydrologie und Wasserbewirtschaftung.

Hellmers, S., & Pasche, E. (2011b). Quantification of climate change impacts on flood probability in urban areas and adaptation measures using climate model data with a high spatial resolution and a semi-distributed rainfall runoff model. In Acqua Alta (Ed.), *Proceedings of the Exhibition and International Conference on Climate Impact, Flood Protection and Hydraulic Engineering.* Hamburg, Germany.

Hellmers, S., Strehz, A., Leese, N. S., Einfalt, T., & Fröhle, P. (2016). Optimisation of Rainfall-Runoff Modelling for Urban Flood Management with Ensemble Radar Nowcasts. In *Proceedings of Novatech 9th International Conference* (Vol. 9). Lyon, France.

Henonin, J., Russo, B., Mark, O., & Gourbesville, P. (2013). Real-time urban flood forecasting and modelling – a state of the art. *Journal of Hydroinformatics*, *15*(3), 717–736. doi: 10.2166/hydro.2013.132

Hingray, B., Picouet, C., & Musy, A. (2014). *Hydrology - A Science for Engineers* (1st ed., Vol. 1). Boca Raton, FL, USA: CRC Press. doi: 10.1201/b17169

Hoang, L., & Fenner, R. A. (2015). System interactions of stormwater management using sustainable urban drainage systems and green infrastructure. *Urban Water Journal*, 739–758. doi: 10.1080/1573062X.2015.1036083

Hong, Y., Hsu, K.-L., Moradkhani, H., & Sorooshian, S. (2006). Uncertainty quantification of satellite precipitation estimation and Monte Carlo assessment of the error propagation into hydrologic response. *Water Resources Research*, *42*(8), 1147. doi: 10.1029/2005WR004398

Huong, H. T. L., & Pathirana, A. (2013). Urbanization and climate change impacts on future urban flooding in Can Tho city, Vietnam. *Hydrology and Earth System Sciences*, *17*(1), 379–394. doi: 10.5194/hess-17-379-2013

Hydrotec. (2018). *Hydrologische Modellierung mit NASIM.* Retrieved 16.12.2018, from https://www.hydrotec.de/software/nasim/

Ichiba, A., Gires, A., Tchiguirinskaia, I., Schertzer, D., Bompard, P., & ten Veldhuis, M.-C. (2018). Scale effect challenges in urban hydrology highlighted with a distributed hydrological model. *Hydrology and Earth System Sciences*, *22*(1), 331–350. doi: 10.5194/hess-22-331-2018

Institute of River and Coastal Engineering (TUHH-WB). (2014). *KALYPSO - Modelltheorie: Niederschlag-Abfluss-Modell.* Hamburg, Germany.

IPCC. (2013a). Long-term Climate Change: Projections, Commitments and Irreversibility: 12. In T. F. Stocker et al. (Eds.), *Climate Change 2013: The Physical Science Basis. Contribution of Working Group I to the Fifth Assessment Report of the Intergovernmental Panel on Climate Change* (pp. 1029–1136). Cambridge, United Kingdom and New York, NY, USA: Cambridge University Press. Retrieved from www.climatechange2013.org doi: 10.1017/CBO9781107415324.024

IPCC. (2013b). Near-term Climate Change: Projections and Predictability: 11. In T. F. Stocker et al. (Eds.), *Climate Change 2013: The Physical Science Basis. Contribution of Working Group I to the Fifth Assessment Report of the Intergovernmental Panel on Climate Change* (pp. 953–1028). Cambridge, United Kingdom and New York, NY, USA: Cambridge University Press. Retrieved from www.climatechange2013.org doi: 10.1017/CBO9781107415324.023

IPCC. (2013c). Sea Level Change: 13. In T. F. Stocker et al. (Eds.), *Climate Change 2013: The Physical Science Basis. Contribution of Working Group I to the Fifth Assessment Report of the Intergovernmental Panel on Climate Change* (pp. 1137–1216). Cambridge, United Kingdom and New York, NY, USA: Cambridge University Press. Retrieved from www.climatechange2013.org doi: 10.1017/CBO9781107415324.026

Jacob, D., Petersen, J., Eggert, B., Alias, A., Christensen, O. B., Bouwer, L. M., ... Yiou, P. (2014). EURO-CORDEX: new high-resolution climate change projections for European impact research. *Regional Environmental Change*, *14*(2), 563–578. doi: 10.1007/s10113-013-0499-2

Jajarmizad, M., Harun, S., & Salarpour, M. (2012). A Review on Theoretical Consideration and Types of Models in Hydrology. *Journal of Environmental Science and Technology*, *5*(5), 249–261. doi: 10.3923/jest.2012.249.261

Jasper-Tönnies, A., Hellmers, S., Einfalt, T., Strehz, A., & Fröhle, P. (2018). Ensembles of radar nowcasts and COSMO-DE-EPS for urban flood management. *Water Science and Technology*, *2017*(1), 27–35. doi: 10.2166/wst.2018.079

Jayasooriya, V. M., & Ng, A. W. M. (2014). Tools for Modeling of Stormwater Management and Economics of Green Infrastructure Practices: A Review. *Water, Air, & Soil Pollution*, *225*(8), 2055. doi: 10.1007/s11270-014-2055-1

Jing, X., Zhang, S., Zhang, J., Wang, Y., Wang, Y., & Yue, T. (2018). Analysis and Modelling of Stormwater Volume Control Performance of Rainwater Harvesting Systems in Four Climatic Zones of China. *Water Resources Management*, *32*(8), 2649–2664. doi: 10.1007/s11269-018-1950-4

Kalinin, G. P., & Milyukov, P. I. (1957). O raschete neustanovivshegosya dvizheniya vody v otkrytykh ruslakh: On the computation of unsteady flow in open channels (in Russian): On Raschete Neustanovi. *Met. i. Gidrologiya Zhuzurnal. Leningrad, Russia*, *10*(10), 10–18.

Kampf, S. K., & Burges, S. J. (2007). A framework for classifying and comparing distributed hillslope and catchment hydrologic models. *Water Resources Research*, *43*(5), 1–24. doi: 10.1029/2006WR005370

Kasmin, H., Stovin, V. R., & Hathway, E. A. (2010). Towards a generic rainfall-runoff model for green roofs. *Water Sci. Technol. (Water science and technology : a journal of the International Association on Water Pollution Research)*, *62*(4), 898–905. doi: 10.2166/wst.2010.352

Keser, B., & Mietzel, T. (2012). New strategies for decentralized stormwater storage by controlled cisterns. In *Procedings of Stormwater Conference 15.-19. Oktober 2012* (Vol. 2012). Melbourne, Australia. Retrieved 17.12.2018, from http://www.stormwater.asn.au/images/Conference_Papers/Stormwater12/Keser_Benjamin_and_Mietzel_Thorsten_-_Non_Refereed_Paper.pdf

Keser, B., & Mietzel, T. (2014). *Entlastung von Abwasserkanälen durch den Einsatz gesteuerter dezentraler Regenwasserspeicher: 13. RegenwasserTage 2004 (01.-02. Juli 2014) - Vortrag*. Dresden.

Kidd, C. (1978). *Rainfall-runoff processes over urban surfaces. Proceedings of an International Workshop. p, Report No. 53.* Wallingford, UK.

KLEE Verbund. (2016). *Perspektiven für die Este von Morgen – Bausteine für die Anpassung an den Klimawandel* (1st ed.). Hamburg. Retrieved 16.12.2018, from http://klee-este.de/wp-content/uploads/2013/05/KLEE_Perspektiven-Este_2016_online.pdf

Klemes, V. (1983). Conceptualization and scale in hydrology. *Journal of Hydrology*, *65*(1-3), 1–23. doi: 10.1016/0022-1694(83)90208-1

Klijn, F., de Bruijn, K. M., Knoop, J., & Kwadijk, J. (2012). Assessment of the Netherlands' Flood Risk Management Policy Under Global Change. *Ambio*, *41*(2), 180–192. doi: 10.1007/s13280-011-0193-x

Knapp, F. H. (1960). *Ausfluss, Überfall und Durchfluss im Wasserbau: Eine angewandte Hydraulik auf physikalischer Grundlage*. Karlsruhe: Braun.

KompetenzNetzwerk. (2010). *Regenwassermanagement für Hamburg.* Hamburg, Germany. Retrieved 15.12.2018, from https://www.risa-hamburg.de/fileadmin/risa/Downloads/Abschlussberichte/100216_Abschlussbericht%20RWM%20im%20KHW_Druck.pdf

Koussis, A. D. (2009). Assessment and review of the hydraulics of storage flood routing 70 years after the presentation of the Muskingum method. *Hydrological Sciences Journal*, *54*(1), 43–61. doi: 10.1623/hysj.54.1.43

Kouwen, N., Soulis, E. D., Pietroniro, A., Donald, J., & Harrington, R. A. (1993). Grouped Response Units for Distributed Hydrologic Modeling. *Journal of Water Resources Planning and Management*, *119*(3), 289–305. doi: 10.1061/(ASCE)0733-9496(1993)119:3(289)

Kozeny, J. (1927). Über kapillare Leitung des Wassers im Boden: Aufstieg, Versickerung und Anwendung auf die Bewässerung. *Akad. Wiss. Wien*, *136*, 271–306. Retrieved 16.12.2018, from http://www.zobodat.at/pdf/SBAWW_136_2a_0271-0306.pdf

Kraft, P. (2012). *A hydrological programming language extension for integrated catchment models* (Dissertation, Justus-Liebig-Universität Giessen, Giessen). Retrieved 16.12.2018, from https://pdfs.semanticscholar.org/0ed6/5b453aa74dc86a3f47aa1d870669c04e4cc2.pdf

Krebs, G. (2016). *Spatial Resolution and Parameterization of an Urban Hydrological Model: Requirements for the Evaluation of Low Impact Development Strategies at the City Scale* (Dissertation, Graz University of Technology, Graz, Austria). doi: 10.13140/RG.2.2.33118.84800

Krob, L., Widrinka, F., Beister, D., & Oberländer, N. (2000). *Hydrologisch-wasserwirtschaftliche Untersuchungen zum Entwässerungsgebiet Moorfleth: Phase 1: Grundlagenermittlung und hydrologisch-wasserwirtschaftliche Bestandsaufnahme: Zwischenbericht*. Hamburg, Germany.

Kuller, M., Bach, P. M., Ramirez-Lovering, D., & Deletic, A. (2017). Framing water sensitive urban design as part of the urban form: A critical review of tools for best planning practice. *Environmental Modelling & Software*, *96*, 265–282. doi: 10.1016/j.envsoft.2017.07.003

Kuller, M., Dolman, N. J., Vreeburg, J., & Spiller, M. (2016). Scenario analysis of rainwater harvesting and use on a large scale – assessment of runoff, storage and economic performance for the case study Amsterdam Airport Schiphol. *Urban Water Journal*, *14*(3), 237–246. doi: 10.1080/1573062X.2015.1086007

Law, A. M. (2008). How to Build Valid and Credible Simulation Models. In S. J. Mason, R. R. Hill, L. Mönch, O. Rose, T. Jefferson, J. W. Fowler (Ed.), *Proceedings of the 2008 Winter Simulation Conference* (pp. 1–10). Piscataway, N.J.: IEEE Service Center. Retrieved 15.12.2018, from https://www.informs-sim.org/wsc09papers/003.pdf doi: 10.1109/WSC.2008.4736054

Law, A. M., & Kelton, W. D. (1991). *Simulation modeling and analysis* (2. ed. ed.). New York: McGraw Hill.

Le Prieuré. (2018). *Hydroventiv - Système de toiture hydroactive connectée.* Moisy, France. Retrieved 17.12.2018, from http://www.toiture-hydroactive-connectee.com/

Leistert, H., Steinbrich, A., Schütz, T., & Weiler, M. (2018). Wie kann die hydrologische Komplexität von Städten hinreichend in einem Wasserhaushaltsmodell abgebildet werden? In N. Schütze, Müller, Uwe, Schwarze, Robert, T. Wöhling, & J. Grundmann (Eds.), *M^3 - Messen, Modellieren, Managen in Hydrologie und Wasserressourcenbewirtschaftung* (p. 18). Dresden, Germany: Fachgemeinschaft Hydrologische Wissenschaften. Retrieved 17.12.2018, from https://tu-dresden.de/bu/umwelt/hydro/ihm/hydrologie/ressourcen/dateien/tdh2018/TdH_2018_Abstractband.pdf?lang=de

Lerer, S., Arnbjerg-Nielsen, K., & Mikkelsen, P. (2015). A Mapping of Tools for Informing Water Sensitive Urban Design Planning Decisions—Questions, Aspects and Context Sensitivity. *Water*, *7*(3), 993–1012. doi: 10.3390/w7030993

Levi, P., & Rembold, U. (2003). *Einführung in die Informatik für Naturwissenschaftler und Ingenieure* (4., aktualisierte und überarb. Aufl. ed.). München: Hanser. Retrieved 17.12.2018, from http://www.hanser-elibrary.com/isbn/9783446219328

Li, C., Fletcher, T. D., Duncan, H. P., & Burns, M. J. (2017). Can stormwater control measures restore altered urban flow regimes at the catchment scale? *Journal of Hydrology*, *2017*(549), 631–653. doi: 10.1016/j.jhydrol.2017.03.037

Lian, J. J., Xu, K., & Ma, C. (2013). Joint impact of rainfall and tidal level on flood risk in a coastal city with a complex river network: A case study of Fuzhou City, China. *Hydrology and Earth System Sciences*, *17*(2), 679–689. doi: 10.5194/hess-17-679-2013

Liguori, S., & Rico-Ramirez, M. A. (2014). A review of current approaches to radar-based quantitative precipitation forecasts. *International Journal of River Basin Management*, *12*(4), 391–402. doi: 10.1080/15715124.2013.848872

Linsley, R. K., Kohler, M. A., & Paulhus, J. L. H. (1988). *Hydrology for engineers* (S.I Metric edition ed.). London: McGraw-Hill.

Lippert, K., Jung, T., Belger, G., Haase, M., & Schrage, N. (2009). Kalypso: Ein Open Source Modellierungssystem für die Wasserwirtschaft. In *Wasserstandsinformationsdienste der BfG für die Bundeswasserstraßen.* Koblenz, Germany. Retrieved 25.01.2018, from https://kalypso.bjoernsen.de/fileadmin/kalypso/template/images/Veroeffentlichungen/BfG_01_2009.pdf

Locatelli, L., Mark, O., Mikkelsen, P. S., Arnbjerg-Nielsen, K., Bergen Jensen, M., & Binning, P. J. (2014). Modelling of green roof hydrological performance for urban drainage applications. *J. Hydrol. (Journal of Hydrology)*, *519*, 3237–3248. doi: 10.1016/j.jhydrol.2014.10.030

Ludwig, K., & Bremicker, M. (2006). *The Water Balance Model LARSIM: Design, Content and Applications* (No. 22). Freiburg, Germany. Retrieved 18.12.2018, from http://www.larsim.info/fileadmin/files/Dokumentation/FSH-Bd22-Bremicker-Ludwig.pdf

Maksimović, Č., Kurian, M., & Ardakanian, R. (2015). *Rethinking Infrastructure Design for Multi-Use Water Services*. Cham: Springer International Publishing. doi: 10.1007/978-3-319-06275-4

Maniak, U. (2016). *Hydrologie und Wasserwirtschaft: (in German)*. Berlin, Heidelberg: Springer Berlin Heidelberg. doi: 10.1007/978-3-662-49087-7

McAlister, T., Mitchell, G., Fletcher, T., & Phillips, B. (2006). Modelling Urban Stormwater Management Systems: Chapter 14. In T. H. F. Wong (Ed.), *Australian Runoff Quality* (pp. 14.1–14.14). Crows Nest, N.S.W: Engineers Media.

McGrane, S. J. (2016). Impacts of urbanisation on hydrological and water quality dynamics, and urban water management: A review. *Hydrological Sciences Journal*, *61*(13), 2295–2311. doi: 10.1080/02626667.2015.1128084

Mein, R. G., & Larson, C. L. (1973). Modeling infiltration during a steady rain. *Water Resources Research*, *9*(2), 384–394. doi: 10.1029/WR009i002p00384

Melville-Shreeve, P., Ward, S., & Butler, D. (2016). Rainwater Harvesting Typologies for UK Houses: A Multi Criteria Analysis of System Configurations. *Water*, *8*(4), 129. doi: 10.3390/w8040129

Merz, R., & Blöschl, G. (2004). Regionalisation of catchment model parameters. *Journal of Hydrology*, *287*(1-4), 95–123. doi: 10.1016/j.jhydrol.2003.09.028

Messal, Hilmar E. E. (2000). *Rückkopplungen und Rückwirkungen in der hydrologischen Modellierung am Beispiel von kontinuierlichen Niederschlag-Abfluß-Simulationen und Hochwasservorhersagen* (Dissertation, Technische Universität Berlin, Berlin, Germany). doi: 10.14279/depositonce-224

Mobilia, M., Longobardi, A., & Sartor, J. F. (2014). Impact of green roofs on stormwater runoff coefficients in a Mediterranean urban environment. In USCUDAR (Ed.), *Proceedings of the 5th International Conference on Urban Sustainability, Cultural Sustainability, Green Development, Green Structures and Clean Cars.* Retrieved 16.12.2018, from http://www.wseas.us/e-library/conferences/2014/Florence/USCUDAR/USCUDAR-13.pdf

Mulligan, M. (2004). Modelling Catchment Hydrology: Chapter 4. In J. Wainwright & M. Mulligan (Eds.), *Environmental modelling* (pp. 107–121). Hoboken, NJ: Wiley.

Myers, B., Beecham, S., & van Leeuwen, J. A. (2011). Water quality with storage in permeable pavement basecourse. *Proceedings of the Institution of Civil Engineers- Water Management - Water Management*, *164*(7), 361–372. doi: 10.1680/wama.2011.164.7.361

Nehlsen, E. (2017). *Wasserbauliche Systemanalyse zur Bewertung der Auswirkungen des Klimawandels für tidebeeinflusste Nebengewässer der Elbe* (Dissertation, Hamburg University of Technology, Hamburg, Germany). doi: 10.15480/882.1435

Novotry, V. (2009). Sustainable urban water management. In S. Feyen & M. Neville (Eds.), *Water and Urban Development Paradigms: Proceedings of the International Urban Water Conference, Heverlee, Belgium, 15-19 September, 2008* (pp. 18–31). Boca Raton, FL, USA: Taylor & Francis Group, London.

Oberkampf, W. L., & Roy, C. J. (2010). *Verification and validation in scientific computing*. New York: Cambridge University Press. doi: 10.1017/CBO9780511760396

Obled, C., Zin, I., & Hingray, B. (2009). Choix des pas de temps et d'espace pour des modélisations parcimonieuses en hydrologie des crues: Optimal space and time scales for parsimonious rainfall-runoff models (in French). *La Houille Blanche*(5), 81–87. doi: 10.1051/lhb/2009059

O'Driscoll, M., Clinton, S., Jefferson, A., Manda, A., & McMillan, S. (2010). Urbanization Effects on Watershed Hydrology and In-Stream Processes in the Southern United States. *Water*, *2*(3), 605–648. doi: 10.3390/w2030605

Optigrün international AG. (2015). *Retention Roof Meander 30.* London. Retrieved 16.12.2018, from https://www.optigreen.com/products/drainage-boards/meander-30/

Optigrün international AG. (2018a). *Optigreen Meander Retention Roof System.* Krauchenwies-Göggingen, Germany. Retrieved 18.12.2018, from https://www.optigreen.com/fileadmin/contents/img/English/Brochures/og_maeander_6seiter_GB_20120829.pdf

Optigrün international AG. (2018b). *Smart Flow Control 4.0.* Krauchenwies-Göggingen, Germany. Retrieved 18.12.2018, from https://www.optigreen.com/fileadmin/contents/Prospekte/England/Flow-Control-Retention-Roof.pdf

Ostrowski, M., Bach, M., DeSimone, S. V., & Gamerith, V. (2010). *Analysis of the time-step dependency of parameters in conceptual hydrological models: Report.* Darmstadt, Germany. Retrieved 18.12.2018, from http://tuprints.ulb.tu-darmstadt.de/2099/

Palla, A., & Gnecco, I. (2015). Hydrologic modeling of Low Impact Development systems at the urban catchment scale. *Journal of Hydrology*, *528*, 361–368. doi: 10.1016/j.jhydrol.2015.06.050

Palla, A., Gnecco, I., & Lanza, L. G. (2012). Compared performance of a conceptual and a mechanistic hydrologic models of a green roof. *Hydrological Processes*, *26*(1), 73–84. doi: 10.1002/hyp.8112

Palmaricciotti, G., Hellmers, S., Manojlovic, N., & Pasche, E. (2012). Adaptation measures to control exceedance flow in urban catchments. In *Proceedings of the 9th International Conference on Urban Drainage Modelling, UDM 2012.* Belgrad, Serbia.

Palmaricciotti, G., Patzke, J., Hellmers, S., Manojlović, N., & Fröhle, P. (2014). Rainfall Simulator TUHH (RS-TUHH) - Planning, Construction and Use. In BAW (Ed.), *Proceedings of the 11th International Conference on Hydroscience & Engineering.* Hamburg, Germany.

Palmaricciotti, G., Patzke, J., Hellmers, S., Manojlović, N., & Fröhle, P. (2015). Entwicklung und Umsetzung des Regensimulators RS-TUHH. In M. Evers & B. Diekkrüger (Eds.), *Aktuelle Herausforderungen im Flussgebiets- und Hochwassermanagement Prozesse, Methoden, Konzepte* (Vol. 35.15, pp. 101–110). Forum für Hydrologie und Wasserwirtschaft. Retrieved 18.12.2018, from https://www.fghw.de/download/forumsbeitraege/35.15_Gesamt.pdf

Paniconi, C., & Putti, M. (2015). Physically based modeling in catchment hydrology at 50: Survey and outlook. *Water Resources Research*, *51*(9), 7090–7129. doi: 10.1002/2015WR017780

Pasche, E. (2003). *Wasserbau – fünf Jahre: Alles fließt: Institute of River and Coastal Engineering – five years: everything flows.* Hamburg, Germany. Retrieved 16.12.2018, from https://www.tuhh.de/t3resources/wb/Publikationen/wasserbau_5-jahre.pdf

Pasche, E., Manojlovic, N., Brüning, C., Behzadnia, N., & Hellmers, S. (2009). Hydrologic Sensitivity Analysis - contribution to assessment of efficiency of SUDS in small urban catchments. In *Proceedings of the 33rd International Association of Hydraulic Engineering & Research - Water Engineering for Sustainable Environment: 9–14 August 2009.* Vancouver, BC, Canada.

Patzke, J., Hellmers, S., Schuyenburg, F., & Fröhle, P. (2017). Laboruntersuchungen an Gründachmodellen bei schichtweiser Erfassung von Niederschlagsabflüssen: Poster Beitrag. In M. C. Casper, O. Gronz, R. Ley, & T. Schuetz (Eds.), *Proceedings: Wie gehen wir mit Nichtstationarität in der Hydrologie um? - Konferenz: Tag der Hydrologie 23. u. 24. 03.2017.* Trier.

Pechlivanidis, I. G., Jackson, B. M., Mcintyre, N. R., & Wheater, H. S. (2011). Catchment scale hydrological modelling: A review of model types, calibration approaches and uncertainty analysis methods in the context of recent developments in technology and applications. *Global NEST Journal*, *2011*(13-3), 193–214. Retrieved 18.12.2018, from http://journal.gnest.org/sites/default/files/Journal%20Papers/193-214_778_Pechlivanidis_13-3.pdf

Perrin, C., Michel, C., & Andréassian, V. (2001). Does a large number of parameters enhance model performance? Comparative assessment of common catchment model structures on 429 catchments. *Journal of Hydrology*, *242*(3), 275–301. doi: 10.1016/S0022-1694(00)00393-0

Petrucci, G., & Bonhomme, C. (2014). The dilemma of spatial representation for urban hydrology semi-distributed modelling: Trade-offs among complexity, calibration and geographical data. *J. Hydrol. (Journal of Hydrology)*, *517*, 997–1007. doi: 10.1016/j.jhydrol.2014.06.019

Petrucci, G., Rioust, E., Deroubaix, J.-F., & Tassin, B. (2013). Do stormwater source control policies deliver the right hydrologic outcomes? *Journal of Hydrology*, *485*, 188–200. doi: 10.1016/j.jhydrol.2012.06.018

Pfützner, B. (2018). *ArcEGMO Dokumentation: Das Modul Q_KalMil.* Berlin, Germany. Retrieved 18.12.2018, from http://www.doku.arcegmo.de/?s=R%C3%BCckstau

Pinder, G. F. (2002). *Groundwater modeling using geographical information systems*. New York, NY, USA: Wiley.

Price, R. K., & Vojinović, Z. (2011). *Urban Hydroinformatics: Data, Models and Decision Support for Integrated Urban Water Management*. London: IWA Publishing.

Radhakrishnan, M. (2017). *Flexibility in adaptation planning: When, where and how to include flexibility for increasing urban flood resilience* (Dissertation, Delft University of Technology and UNESCO-IHE, Delft, Netherlands). doi: 10.4233/uuid:7ed71021-e0f6-4d65-92aa-791b3e9fa817

Refsgaard, J. C., & Henriksen, H. J. (2004). Modelling guidelines—-terminology and guiding principles. *Advances in Water Resources*, *27*(1), 71–82. doi: 10.1016/j.advwatres.2003.08.006

Riedel, G. (2004). *Ein hydrologisches Modell für tidebeeinflusste Flussgebiete* (Dissertation, TU Braunschweig, Braunschweig, Germany). Retrieved 18.12.2018, from https://publikationsserver.tu-braunschweig.de/receive/dbbs_mods_00001644

Rodriguez, F., Andrieu, H., & Morena, F. (2008). A distributed hydrological model for urbanized areas – Model development and application to case studies. *Journal of Hydrology*, *351*(3-4), 268–287. doi: 10.1016/j.jhydrol.2007.12.007

Rohrer, A. R., & Armitage, N. P. (2017). Improving the Viability of Stormwater Harvesting through Rudimentary Real Time Control. *Water*, *9*(6), 371. doi: 10.3390/w9060371

Rossman, L. A. (2015). *Storm Water Management Model: User's Manual Version 5.1.* Retrieved 18.12.2018, from https://nepis.epa.gov/Exe/ZyPDF.cgi/P100N3J6.PDF?Dockey=P100N3J6.PDF

Rujner, H., Leonhardt, G., Marsalek, J., & Viklander, M. (2018). High-resolution modelling of the grass swale response to runoff inflows with Mike SHE. *Journal of Hydrology*, *562*, 411–422. doi: 10.1016/j.jhydrol.2018.05.024

Rutter, A. J., Kershaw, K. A., Robins, P. C., & Morton, A. J. (1971). A predictive model of rainfall interception in forests, 1. Derivation of the model from observations in a plantation of Corsican pine. *Agricultural Meteorology*, *9*, 367–384. doi: 10.1016/0002-1571(71)90034-3

Salvadore, E., Bronders, J., & Batelaan, O. (2015). Hydrological modelling of urbanized catchments: A review and future directions. *Journal of Hydrology*, *529*, 62–81. doi: 10.1016/j.jhydrol.2015.06.028

Samaniego, L., Kumar, R., & Attinger, S. (2010). Multiscale parameter regionalization of a grid-based hydrologic model at the mesoscale. *Water Resources Research*, *46*(5). doi: 10.1029/2008WR007327

Sargent, R. G. (2014). Verifying and Validating Simulation Models. In A. Tolk, S. Y. Diallo, I. O. Ryzhov, L. Yilmaz, S. Buckley, and J. A. Miller (Ed.), *Proceedings of the 2014 Winter Simulation Conference* (pp. 118–131). Retrieved 18.12.2018, from http://simulation.su/uploads/files/default/2014-sargent.pdf

Savenije, H. H. G. (2009). HESS Opinions - The art of hydrology. *Hydrology and Earth System Sciences*, *13*(2), 157–161. doi: 10.5194/hess-13-157-2009

Scherer, I., Henrichs, M., & Uhl, M. (2018). Robuste Parametrisierung zur urban hydrologischen Modellierung grüner Infrastrukturen. In N. Schütze, Müller, Uwe, Schwarze, Robert, T. Wöhling,

& J. Grundmann (Eds.), *M*^{3} *- Messen, Modellieren, Managen in Hydrologie und Wasserressourcenbewirtschaftung.* Dresden, Germany: Fachgemeinschaft Hydrologische Wissenschaften.

Schröder, R., & Lippert, K. (2006). Parameternachführung im Hochwasservorhersagemodell Weiße Elster. *Veranstaltungen der Bundesanstalt für Gewässerkunde*, *2016*(3), 1–11.

Schröter, K., Llort, X., Velasco-Forero, C., Ostrowski, M., & Sempere-Torres, D. (2011). Implications of radar rainfall estimates uncertainty on distributed hydrological model predictions. *Atmospheric Research*, *100*(2-3), 237–245. doi: 10.1016/j.atmosres.2010.08.014

Schulla, J. (2017). *Model Description WaSiM: Water balance Simulation Model.* Zürich, Switzerland. Retrieved 18.12.2018, from http://www.wasim.ch/downloads/doku/wasim/wasim_2017_en.pdf

Schumann, A. H. (1993). Development of conceptual semi-distributed hydrological models and estimation of their parameters with the aid of GIS. *Hydrological Sciences Journal*, *38*(6), 519–528. doi: 10.1080/02626669309492702

Schütze, M., Pabst, M., & Haas, U. (2016). Urban Drainage Systems – Static throttle flows or real time control? A systematic approach to answer this. In *Proceedings of Novatech 9th International Conference.* Lyon, France.

Schütze, T. (2013). Rainwater harvesting and management - Policy and regulations in Germany. *Water Science & Technology: Water Supply*, *13*(13.2), 376. doi: 10.2166/ws.2013.035

She, N., & Pang, J. (2010). Physically Based Green Roof Model. *Journal of Hydrologic Engineering*, *15*(6), 458–464. doi: 10.1061/(ASCE)HE.1943-5584.0000138

Sherrard, J. A., & Jacobs, J. M. (2012). Vegetated Roof Water-Balance Model: Experimental and Model Results. *Journal of Hydrologic Engineering*, *17*(8), 858–868. doi: 10.1061/(ASCE)HE.1943-5584.0000531

Shreve, R. L. (1967). Infinite topologically random channel networks. *J. Geol. (Journal of Geology)*, *1967*, 178–186.

Shuster, W., & Rhea, L. (2013). Catchment-scale hydrologic implications of parcel-level stormwater management (Ohio USA). *Journal of Hydrology*, *485*, 177–187. doi: 10.1016/j.jhydrol.2012.10.043

Sieker, H., Helm, B., Krebs, P., Schlottmann, P., & Tränkner, J. (2008). Flexibility-a planning criterion for stormwater management. In *Proceedings of the 11th International Conference on Urban Drainage.* Edingburg, Scotland, UK.

Stovin, V., Vesuviano, G., & De-Ville, S. (2015). Defining green roof detention performance. *Urban Water Journal*, 1–15. doi: 10.1080/1573062X.2015.1049279

Sweet, W. V., Kopp, R. E., Weaver, C. P., Obeysekera, J., Horton, R. M., Thieler, E. R., & Zervas, C. (2017). *Global and Regional Sea Level Rise Scenarios for the United States: NOAA Technical Report NOS CO-OPS 083.* Silver Spring, Maryland, US. Retrieved 07.07.2018, from https://tidesandcurrents.noaa.gov/publications/techrpt83_Global_and_Regional_SLR_Scenarios_for_the_US_final.pdf

Szilagyi, J., & Laurinyecz, P. (2014). Accounting for Backwater Effects in Flow Routing by the Discrete Linear Cascade Model. *Journal of Hydrologic Engineering*, *19*(1), 69–77. doi: 10.1061/(ASCE)HE.1943-5584.0000771

Szota, C., Fletcher, T., Desbois, C., Rayner, J., Williams, N., & Farrell, C. (2017). Laboratory Tests of Substrate Physical Properties May Not Represent the Retention Capacity of Green Roof Substrates In Situ. *Water*, *9*(12), 920. doi: 10.3390/w9120920

Teschke, U. (2003). *Zur Berechnung eindimensionaler instationärer Strömungen von natürlichen Fließgewässern mit der Methode der Finiten Elemente* (Dissertation). Hamburg University of Technology, Hamburg, Germany.

Todini, E. (1991). Hydraulic and Hydrologic Flood Routing Schemes. In D. S. Bowles & P. E. O'Connell (Eds.), *Recent advances in the modeling of hydrologic systems* (pp. 389–406). Dordrecht [etc.]: Kluwer Academic Publishers.

Todini, E. (2007). Hydrological catchment modelling: Past, present and future. *Hydrol. Earth Syst. Sci.*, *11*, pp. 468–482. doi: 10.5194/hess-11-468-2007

Tromp-van Meerveld, H. J., & McDonnell, J. J. (2006). Threshold relations in subsurface stormflow: 2. The fill and spill hypothesis. *Water Resources Research*, *42*(2), 1–11. doi: 10.1029/2004WR003800

Umweltbundesamt. (2005). *Versickerung und Nutzung von Regenwasser: Vorteile, Risiken, Anforderungen.* Dessau, Germany. Retrieved 18.12.2018, from https://www.umweltbundesamt.de/sites/default/files/medien/publikation/long/2973.pdf

United Nations. Department of Economic and Social Affairs (UN DESA). (2014). *Population Division (2014). World Urbanization Prospects: The 2014 Revision, Highlights* (Vol. 352). New York, NY, USA: United Nations.

United Nations. Department of Economic and Social Affairs (UN DESA). (2018). *World Urbanization Prospects: The 2018 Revision. Key Facts. With assistance of Population Division, Department of Economic and Social Affairs.* New York, NY, USA. Retrieved 18.12.2018, from https://esa.un.org/unpd/wup/Publications/Files/WUP2018-KeyFacts.pdf

Unites States Environmental Protection Agency (USEPA). (2013). *Case Studies Analyzing the Economic Benefits of Low Impact Development and Green Infrastructure Programs: EPA 841 -R- 13- 004.* Retrieved 18.12.2018, from https://www.epa.gov/sites/production/files/2015-10/documents/lid-gi-programs_report_8-6-13_combined.pdf

Urban District and Flood Control District (UDFCD). (2014). *Rainwater Harvesting, real-time cistern control.* Retrieved 18.12.2018, from https://udfcd.org/services/research-test/rain-water-harvesting/

Urbonas, B. (2007). *Stormwater Runoff Modeling; Is It as Accurate as We Think? In Proceedings of the International Conference on Urban Runoff Modeling: Intelligent Modeling to Improve Stormwater Management.* Arcata, CA, USA. Retrieved from http://uwtrshd.com/assets/stormwater-runoff-modeling-accuracy-for-udfcd.pdf

Urumović, K., & Urumović Sr., K. (2016). The referential grain size and effective porosity in the Kozeny-Carman model. *Hydrology and Earth System Sciences*, *20*(5), 1669–1680. doi: 10.5194/hess-20-1669-2016

U.S. Department of Agriculture (USDA). (2018). *The Soil and Water Assessment Tool (SWAT).* Retrieved 18.12.2018, from https://swat.tamu.edu/

Vaché, K. B., & McDonnell, J. J. (2006). A process-based rejectionist framework for evaluating catchment runoff model structure. *Water Resources Research*, *42*(2), 1–15. doi: 10.1029/2005WR004247

Vaze, J., Jordan, P., Beecham, R., Frost, A., Summerell, G., & (eWater Cooperative Research Centre). (2012). *Guidelines for rainfall-runoff modelling: Towards best practice model application.* Bruce, Australia. Retrieved 18.12.2018, from http://ewater.org.au/uploads/files/eWater-Modelling-Guidelines-RRM-%28v1-Mar-2012%29.pdf

vegetal i.D. (2018). *Hydroventiv Specifications.* Batavia, NY, U.S.. Retrieved 19.12.2018, from http://www.vegetalid.us/green-roof-solutions/stormwater-management/300-hydroactive-smart-roof-specifications.html

Versini, P.-A., Gires, A., Abbes, J.-B., Giangola-Murzyn, A., Tchiguirinskaia, I., & Schertzer, D. (2014). Simulation of Green Roof Impact at Basin Scale by Using a Distributed Rainfall-Runoff Model. In ICUD (Ed.), *Proceedings of the 13th International Conference on Urban Drainage (ICUD),.* Sarawak, Malaysia.

Versini, P.-A., Gires, A., Tchinguirinskaia, I., & Schertzer, D. (2016). Toward an operational tool to simulate green roof hydrological impact at the basin scale: a new version of the distributed rainfall-runoff model Multi-Hydro. *Water Science and Technology*, *74*(8), 1845–1854. doi: 10.2166/wst.2016.310

Versini, P.-A., Jouve, P., Ramier, D., Berthier, E., & de Gouvello, B. (2014). Use of green roofs to solve storm water issues at the basin scale – Study in the Hauts-de-Seine County (France). *Urban Water Journal*, *13*(4), 372–381. doi: 10.1080/1573062X.2014.993993

Versini, P.-A., Ramier, D., Berthier, E., & de Gouvello, B. (2015). Assessment of the hydrological impacts of green roof: From building scale to basin scale. *Journal of Hydrology*, *524*, 562–575. doi: 10.1016/j.jhydrol.2015.03.020

Vesuviano, G., Sonnenwald, F., & Stovin, V. (2014). A two-stage storage routing model for green roof runoff detention. *Water Science and Technology*, *69*(6), 1191–1197. doi: 10.2166/wst.2013.808

Vesuviano, G., & Stovin, V. (2013). A generic hydrological model for a green roof drainage layer. *Water Science and Technology*, *68*(4), 769–775. doi: 10.2166/wst.2013.294

Vojinović, Z. (2015). *Flood Risk: The Holistic Perspective : From Integrated to Interactive Planning for Flood Resilience* (1st ed.). London: IWA Publishing (Intl Water Assoc).

Vojinović, Z., & Abbott, M. B. (2012). *Flood Risk and Social Justice: From Quantitative to Qualitative Flood Risk Assessment and Mitigation (Urban Hydroinformatics)* (1st ed.). London, United Kingdom: IWA Publishing (Intl Water Assoc).

Vrugt, J. A., ter Braak, C. J. F., Clark, M. P., Hyman, J. M., & Robinson, B. A. (2008). Treatment of input uncertainty in hydrologic modeling: Doing hydrology backward with Markov chain Monte Carlo simulation. *Water Resources Research*, *44*(12), 937. doi: 10.1029/2007WR006720

Wackermann, R. (1981). Eine Einheitsganglinie aus charakteristischen Systemwerten ohne Niederschlag-Abfluss-Messungen: A unit hydrograph developed from characteristic parameters without the aid of rainfall-runoff readings. *Wasser und Boden*, *1981*(1), 23–28.

Waldhoff, A., Ziegler, J., Bischoff, G., & Rabe, S. (2012). Multifunctional Spaces for Flood Management - an Approach for the City of Hamburg, Germany. *gwf Wasser und Abwasser*, *2012*(153), 84–88. Retrieved 20.12.2018, from http://ojs.di-verlag.de/index.php/gwf_wa/article/view/1250

Ward, S., & Butler, D. (2016). Rainwater Harvesting and Social Networks: Visualising Interactions for Niche Governance, Resilience and Sustainability. *Water*, *8*(11), 526. doi: 10.3390/w8110526

Ward, S., Memon, F. A., & Butler, D. (2010). Rainwater harvesting: Model-based design evaluation. *Water Science and Technology*, *61*(1), 85–96. doi: 10.2166/wst.2010.783

Webber, J. L., Gibson, M. J., Chen, A. S., Savic, D., Fu, G., & Butler, D. (2018). Rapid assessment of surface-water flood-management options in urban catchments. *Urban Water Journal*, *15*(3), 1–8. doi: 10.1080/1573062X.2018.1424212

Winston, R. J., Al-Rubaei, A. M., Blecken, G. T., Viklander, M., & Hunt, W. F. (2016). Maintenance measures for preservation and recovery of permeable pavement surface infiltration rate–The effects of street sweeping, vacuum cleaning, high pressure washing, and milling. *Journal of environmental management*, *169*, 132–144. doi: 10.1016/j.jenvman.2015.12.026

Wong., T., Allen, R., Brown, R., Deletić, A., Gangadharan, L., Gernjak, W., ... Walsh, C. (2013). *blueprint2013 - Stormwater Management in a Water Sensitive City.* Melbourne,Australia.

Woods Ballard, B., Wilson, S., Updale-Clarke, H., Illman, S., Scott, T., Ashley, R. M., & Kellagher, R. (2015). *The SuDS Manual (C753). CIRIA* (5th ed.). London, United Kingdom. Retrieved 18.12.2018, from https://www.ciria.org/Resources/Free_publications/SuDS_manual_C753.aspx

World Meteorological Organization (WMO). (2008). *Guide to hydrological practices* (6th ed., Vol. 168). Geneva, Switzerland: World Meteorological Organization. Retrieved 19.12.2018, from http://www.worldcat.org/oclc/525716390

World Meteorological Organization (WMO). (2011). *Manual on flood forecasting and warning* (Vol. 1072). Geneva: World Meteorological Organization. Retrieved 18.12.2018, from http://www.worldcat.org/oclc/778563632

Xu, W., Fletcher, T., Duncan, H., Bergmann, D., Breman, J., & Burns, M. (2018). Improving the Multi-Objective Performance of Rainwater Harvesting Systems Using Real-Time Control Technology. *Water*, *10*(2), 147. doi: 10.3390/w10020147

Yau, W., Radhakrishnan, M., Liong, S.-Y., Zevenbergen, C., & Pathirana, A. (2017). Effectiveness of ABC Waters Design Features for Runoff Quantity Control in Urban Singapore. *Water*, *9*(8), 577. doi: 10.3390/w9080577

Zeeberg, J. J. (2009). *Flood control in the Netherlands: A strategy for dike reinforcement and climate adaptation*. Leiden, Netherlands: Hoogheemraadschap van Rijnland. Retrieved 19.12.2018, from http://www.worldcat.org/oclc/637139008

Zevenbergen, C., Cashman, A., Evelpidou, N., Pasche, E., Garvin, S., & Ashley, R. (2011). *Urban flood management*. Boca Raton, Fla: CRC. Retrieved 19.12.2018, from http://www.worldcat.org/oclc/681533578

Zhang, X., Drake, N. A., & Wainwright, J. (2013). Spatial Modelling and Scaling Issues. In M. Muzlligan & J. Wainwright (Eds.), *Environmental Modelling: Finding Simplicity in Complexity, 2nd ed.* (pp. Chapter 5, 69–90). Chichester, UK: John Wiley & Sons, Ltd. doi: 10.1002/9781118351475.ch5

Zimmer, U., & Geiger, W. F. (1997). Model for the design of multilayered infiltration systems. *Water Science and Technology*, *36*(8-9), 301–306. doi: 10.2166/wst.1997.0683

Zoppou, C. (2001). Review of urban storm water models. *Environmental Modelling & Software*, *16*(3), 195–231. doi: 10.1016/S1364-8152(00)00084-0

List of Figures

List of Tables

Index

A. Supplementary information about hydrological numerical modelling

Developing and selecting an applicable numerical model for hydrological simulations depend on the objectives, availability of data and scale of the system being modelled. The scale varies, among others, between neighbourhood (urban districts), river reaches, reservoirs or regional river basins. Model selection criteria support to evaluate the applicability of numerical models for specific projects and modelling purposes in research or practice. The WMO [2008] suggests amongst others (such as in Vaze et al. [2012]) the following five questions to be relevant when selecting a model: (1) What are the specific hydrological objectives being modelled, for instance, event based design floods or low flow average discharges? (2) What is the spatio-temporal scale of the hydrological system? (3) What are the climatic and physiographic characteristics? (4) Which data is available with regard to type, resolution, length and quality and (5) which model simplicity, computational resources and ease of application are required?

Especially the criteria (4) and (5), about data availability and required model complexity, provoke a discussion about model uncertainties which is explained in the following section A.1. The issue of "over-parametrisation" and the demand for parsimonious models will be clarified for the limited scope of this work (see section A.2). In section A.3, the differentiation between hydrological, hydrodynamic-numerical and hybrid models is described, while a review about applied numerical models for simulating LSDMs is given.

A.1 The issue of uncertainty in hydrological numerical modelling

In hydrological modelling different sources of uncertainty exists which have a varying impact on the simulated results. These sources are ordered from higher to lower uncertainty impacts in the following way (according to Vaze et al. [2012]):

1. Uncertainty in the quality and quantity of data to describe input parameters, including "driving" input parameters like precipitation.
2. Uncertainty in model assumptions and conceptualisation of represented processes.
3. Uncertainty in the nature of the scientific approaches underlying the model.

4. Uncertainty in the coding including numerical approximations and undetected software bugs.

The order given by Vaze et al. [2012] goes along with the statements by Salvadore et al. [2015] as well as Petrucci and Bonhomme [2014], that the quality and quantity of available input data in the required spatio-temporal resolution is the main constrain. This is true, although remote sensed data technology and radar rainfall data increased the quantity and quality of available input data in recent years (see Hingray et al. [2014]). Consequently, models which depend mainly on the correctness and high resolution of input data (like fully-distributed physical-based models) reveal drawbacks in practical application compared to conceptual based models when respective data is not available. A review about required and available data is given by Hingray et al. [2014] including geographic as well as meteorological time series and historical related data.

To overcome uncertainties in data availability, a coarsening of the spatial model resolution is a practised response to the limited availability of spatial data. This results in a conceptualization which requires less detailed information (see Klemes [1983]). This approach is also known as regionalisation of parameters which is described by Blöschl and Sivapalan [1995]; Fenicia et al. [2016]; Gentine et al. [2012]; Merz and Blöschl [2004] to determine the parametrisation for large (regional) scale catchment modelling. The process of "parameter regionalisation" pursues to determine a relation between model parameters to observable catchment characteristics (see Fenicia et al. [2016]).

A significant source of uncertainty in the application of a hydrological numerical model is derived by a too rough or even wrong distribution of rainfall data (see Casper et al. [2009]; Hingray et al. [2014]; Urbonas [2007]). It is a logical consequence, that the uncertainty of estimated areal precipitation data increases when the density of the rain-gage network and the temporal resolution of the data decreases. A discussion about the benefits, limits, availability and quality of radar rainfall data is given in Casper et al. [2009]; Hingray et al. [2014]; Hong et al. [2006]; Jasper-Tönnies et al. [2018]; Liguori and Rico-Ramirez [2014].

Casper et al. [2009] compared the models NASIM (a semi-distributed model by Hydrotec [2018]), LARSIM (a large scale distributed hydrological model by Ludwig and Bremicker [2006]) and WaSiM-ETH (a fully-distributed physical-based model by Schulla [2017]) to determine the influence of rainfall variability on the simulation of extreme runoff in small catchments. The uncertainty in the models is analysed with 100 ensemble computation runs of rainfall realisations. The results demonstrate the semi-distributed model approach to be most sensitive to the spatial variability of rainfall data and showed the best extrapolation potential (Casper et al. [2009]). The distributed model WaSiM-ETH showed less sensitive results when heavy storm events are modelled than the semi-distributed model NASIM. The authors argument that the sensitivity of parametrisation could be a reason for these results.

Especially for flood forecasting a smaller temporal and spatial scale of rainfall forecast data is required (WMO [2011]). In the past two decades, the use of radar data with increasing spatial resolution (namely from $0.5\,\mathrm{km}^2$ to $4\,\mathrm{km}^2$) has become popular for estimating the rainfall (see Einfalt et al. [2004]; Hingray et al. [2014]; Jasper-Tönnies et al. [2018]). The

temporal resolution varies between 5 to 10 minutes as described in Hingray et al. [2014]. Using ensembles for forecast applications is a promising approach as presented by Jasper-Tönnies et al. [2018]; Schröter et al. [2011] and Caseri et al. [2016], but the uncertainty inherent in radar data partly propagates into hydrological predictions as studied by Schröter et al. [2011] (p. 238) and demands for further research. Additional sources of model uncertainty are derived by calibration, validation and the issue of equifinality, where different parameter sets and model structures can yield equally good results (see Beven and Freer [2001]; Pechlivanidis et al. [2011]; Todini [2007]). Reducing uncertainty in modelling tools is presented by Vrugt et al. [2008] using Markov chain Monte Carlo simulations to assess how much confidence can be placed in model predictions. Further information about the issue of uncertainties in hydrological catchment models is discussed in a number of publications like in Beven [2007, 2012]; Clark et al. [2008]; Pechlivanidis et al. [2011]; Perrin et al. [2001]; Petrucci and Bonhomme [2014]; Salvadore et al. [2015]; Savenije, H. H. G. [2009].

In this work, a semi-distributed approach is extended in a hydrological numerical model where uncertainties in input data are coped with by introducing a solution with radar rainfall data. In the project "StucK", the author of this work together with colleagues, coupled the extended numerical model KalypsoNA with an operational system using ensembles of forecasted rainfall radar data. In that way, the uncertainties derived by spatial inaccuracies by punctiform stationary data is reduced. The spatial resolution of the radar data is $1\,km^2$ and the temporal resolution is 5 minutes. The catchment model covers an area of $33\,km^2$ to simulate forecasted discharges and related water levels within an actualisation interval of 15 minutes for 10 forecast ensemble members. The model is running in the operational state since April 2017 (Hellmers and Fröhle [2020], in press).

A.2 The issue of over-parametrisation and the demand for parsimonious data models

Recent reviews in hydrological numerical modelling discuss the required complexity of the models to accomplish the simulation of hydrological processes. The complexity of the model, with regard to the number and kind of parameters, is only suitable as far as appropriate data is available (see for example Perrin et al. [2001]). Otherwise, over-parametrisation caused by unsuitable data sources for parameter estimation and calibration leads to uncertainties and unreliable model results as described by Petrucci and Bonhomme [2014]. Uncertainty in hydrological modelling derived by a lack of data availability for distributed models is stated in an early stage by Beven [1993] and is updated in Beven [2007] while giving approaches how to deal with the uncertainty. The study by Fenicia et al. [2008] presents an approach of a step wise adjustment of the model structure till reaching a point, where a balance between model complexity and data availability is reached with the aim to keep the model as simple as possible, but complex enough to explain the dynamics of the data. The objective is a parsimonious model approach. The study results by Perrin et al. [2001] and Fenicia et al.

[2008] pointed out that some parsimonious (likely conceptual) semi-distributed models can yield more promising results, whereas complex distributed models show more weaknesses in applications on large catchment scales.

To mitigate uncertainties by undefined parameters and to introduce a parsimonious parametrisation in this work, the developed methodology performs a "zoom into" processes (physically, spatially and temporally) where appropriate physical-based parameters are available and detailed computation is required. At the same time, the methods accomplish a "zoom out" of processes where lumped conceptualized approaches are applied. In this way, parameters to model features of LSDMs are defined on local scale without increasing the meso scale parametrisation. This solution mitigates the risk of over-parametrisation on meso scale and showed good applicability in modelling a regional scale catchment with a size of 175 km^2 including backwater affected streams and integrated LSDMs.

A.3 Differentiation of hydrological, hydrodynamic-numerical and integrated hybrid models

In urban storm water management with a focus on modelling the flow regime in centralised stormwater drainage networks or open channels, hydrodynamic-numerical models are applied because of the requirements in modelling flow rates and water level computations (see Butler and Davies [2011]; García et al. [2015]; Vojinović and Abbott [2012]). In hydrodynamic models the computation of water balance processes on or below the surfaces as well as the runoff generation are simplified to calculate the inflow hydrographs of streams. The level of detail incorporating hydrological processes vary from model to model.

In hydrological numerical models the water balance processes on or below the surfaces as well as the runoff generation are modelled in more detail while the flood routing methods in hydrological catchment models are mainly based on conceptual approaches (see Hingray et al. [2014]; Linsley et al. [1988]; Maniak [2016]) which neglect backwater effects and unsteady flow computations. In meso scale hydrological catchment modelling it is still not feasible to integrate a detailed description of sewers or drainage networks because of modelling the processes on a large scale as described in Salvadore et al. [2015] (p. 72). There is a tendency to comprise as well some hydrodynamic-numerical routing approaches as presented by Salvadore et al. [2015], but simpler routing methods like kinematic wave routing or conceptual reservoir cascade flood routing are considered to be sufficient in hydrological catchment models as long as backwater effects play a minor role like in lower reaches of a catchment as described by Elliott and Trowsdale [2007].

Two examples of coupled hydrodynamic-numerical with hydrological models are selected to demonstrate hybrid model types. SWMM (namely EPA's Stormwater Management Model) is a hydrodynamic-numerical and hydrological water quality model used for the simulation of runoff in urban and rural or semi-rural areas. It was first developed in 1971 and used for the simulation of conventional central stormwater systems in urban areas (EPA [2018]). It

is originally developed as hydrodynamic-numerical model, but was revised to model hydrological processes and LSDMs (here: low impact developments; LIDs). Another related hybrid model is the model MIKE Urban[1] which is likewise a hydrodynamic-numerical model and incorporates additional calculation routines to account for hydrological and LSDM modelling. It includes a model referred to as NAM (namely Nedbør-Afstrømnings-Model ≈ rainfall–runoff model), which is developed to compute the runoff from permeable areas. MIKE Urban is applied for instance by Locatelli et al. [2014] for LSDM modelling and is characterised as a deterministic lumped model based on the linear reservoir theory. These models incorporate limited calculation routines to model hydrological processes (see discussion in section 9.2).

Integrated model structures as presented and reviewed in M. Bach [2011]; P. M. Bach et al. [2014]; Blair and Buytaert [2016]; Bulatewicz and Cuny [2005] and Kuller et al. [2017] incorporating social, economic, 1D-2D flow models or 3D-groundwater model couplings (for example in Bulatewicz and Cuny [2005]) are not part of this work. OpenMP (Open Multi-Processing) approaches are presented by Kraft [2012]; Vaché and McDonnell [2006] and for the model Multi-Hydro in Versini, Gires, et al. [2014]. Although these hybrid, OpenMP and integrated models are very interesting from the urban drainage perspective, it can not be stated that these approaches provide a benefit and doing better when mainly water quantity issues are studied. The complex invention, implementation, testing and model structure handling is still not economical compared to "lightweight" hydrological numerical models as argued also by Kraft [2012]. This is also confirmed in recent reviews in literature of hydrological and hydrodynamic-numerical models which are applied for modelling the performance of LSDMs. A summary of the reviews is given in table A.1. The main focus of this work concentrates on resolving the weaknesses and limitations in modelling LSDMs in backwater affected catchments with a "stand-alone" meso scale hydrological numerical model.

Table A.1: Overview of selected reviews in literature of hydrological and hydrodynamic-numerical models applied for modelling the performance of LSDMs.

Reference in literature	Hydrological and/or hydrodynamic-numerical models reviewed for LSDM modelling
Ahiablame et al. [2012b] reviewed three models.	L-THIA-LID, SWMM and SUSTAIN.
DPLG [2010] reviewed eleven models.	MUSIC, EPA-SWMM, XP-SWMM, Water Cress, Drains, Hec-Ras, SWITCH, Switch2,PermPave, Raintank Analyser and E2.
Elliott and Trowsdale S. A. [2007] reviewed ten models.	MIKE Urban, MUSIC, P8-UCM, PURRS, RUN-QUAL, SLAMM, StormTac, SWMM, UVQ and WBM.
Jayasooriya and Ng [2014] reviewed ten models.	SWMM, WERF, CNT, SUSTAIN, MUSIC, P8, LINDRA, RECARGA, GI and WinSLAMM.
Kuller et al. [2017] reviewed four models.	MUSIC, PURRS, SWMM and WERF.
Li et al. [2017] reviewed eight models.	SWMM, MUSIC, StormNet, HEC-HMS, SWAT, SCS, SUSTAIN, SG WATER.
Lerer et al. [2015] reviewed twenty-four models.	e.g. SWMM, MIKE URBAN, MUSIC, Modflow, SUSTAIN, UHRU and SUDSLOC.

[1] MIKE URBAN is a one-dimensional hydrodyanmic-numerical model by the Danish Hydraulic Institute (DHI).

B. Supplementary materials of the developed methods

B.1 Explanation of applied symbols in flow charts to visualise the developed algorithms

The numerical model algorithms are visualised in flow charts using a specific set of symbols to illustrate terminals, flow lines, computation of processes, input or output of data, decision operations and calculation loops (see figure B.1). A unique visualisation scheme of algorithms supports a recognition of structures throughout the work, reduces the repetition of legends and increases the readability. Additional symbols and simplified illustrations are added in the flow charts of algorithms to visualise specific processes.

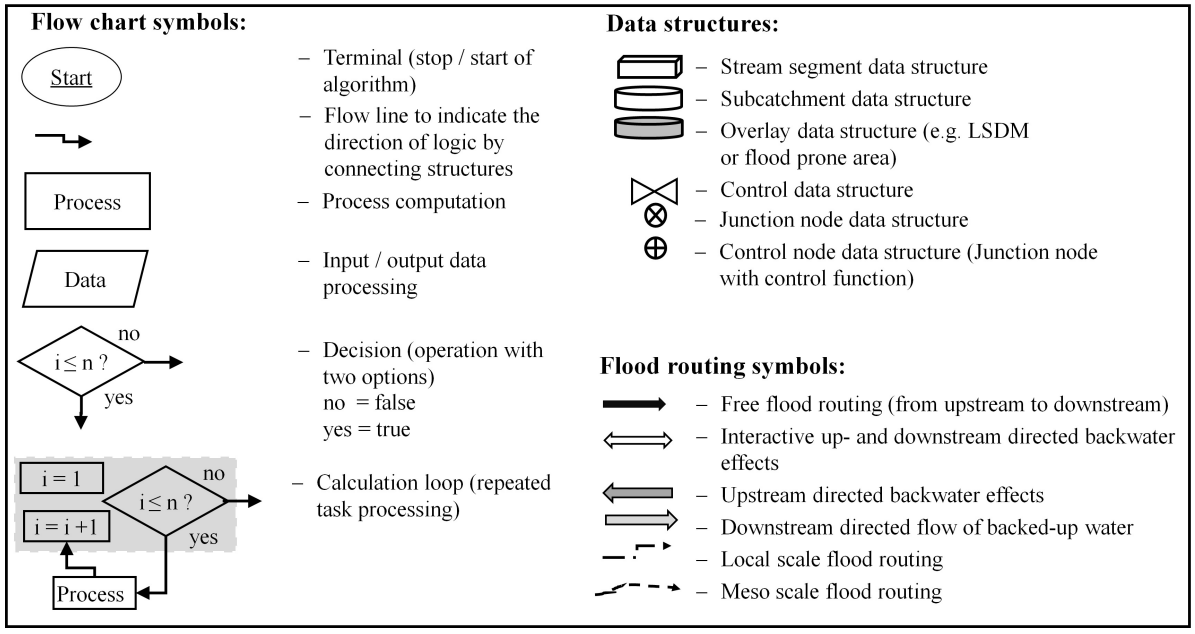

Figure B.1: Applied symbols in flow charts to visualise the developed algorithms.

Data structures combine different variables, data types or secondary data structures in one unit. The main data structures which are visualised with symbols throughout the work are

listed in figure B.1. Overlay data structures are described in section 4.1 (page 54) including spatial elements like LSDMs and flood prone areas. In contrast to the conventional free (unhindered) surface flood routing direction from upstream to downstream in hydrological catchment models, further flood routing directions are integrated in the developed methods. These directions are symbolised with arrows in different white, grey and black shades.

B.2 Supplementary notes about the micro scale soil water balance computation

Computation of the saturation stage (height) h_{sat}. In porous media the drainage flow is computed with the Darcy theory. A differentiation is done when the saturation state in the layer is exceeded (see section 5.3.1 page 73). This saturation stage depends on the inclination and the thickness of the layer. Two geometrical correlations are derived and tested with the physical model output of laboratory studies described in section 8.1. The first correlation describes a structure with a layer thickness h_L (mm) larger than the inclination height h_I (mm) over the length of the flow path $L_{drain,i}$. In this case, the saturation stage h_{sat} is computed with:

$$h_{sat} = (h_L - \frac{h_I}{2}) \cdot f_{h,sat} \tag{B.2.1}$$

where h_L is the layer thickness above an overflow crest height (mm), h_I is the inclination height with ($h_I = I_L \cdot L_{drain,i}$), I_L is the inclination of the layer (-), $L_{drain,i}$ is the flow path length of the drained area to the outlet (mm) and $f_{h,sat}$ is an adjustment factor for porous media described in the following paragraph (by default = 1.0). The parameters are illustrated in figure B.2 (a).

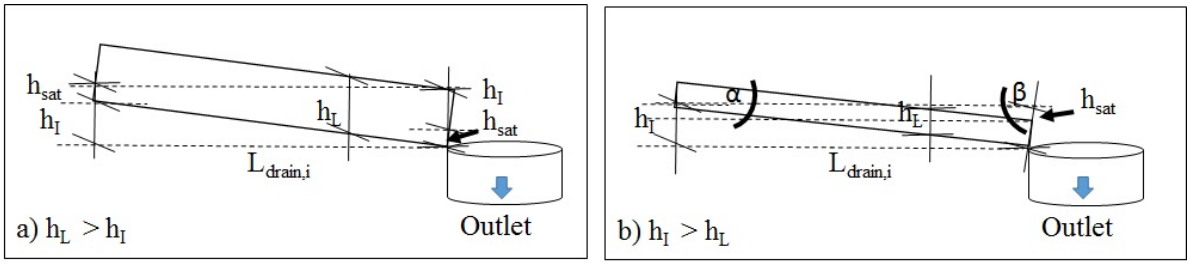

Figure B.2: Scheme of the saturation height h_{sat} in a layer with different relations between thickness and gradient.

The second correlation describes thin layers, where the layer thickness h_L (mm) is smaller than the inclination height h_I (mm) (see figure B.2 (b)), the exceedance water quantity and saturation stage h_{sat} are computed with the triangle area exceeding the layer thickness using the Pythagoras' theorem:

$$\alpha = arctangent(I_L)$$
$$\beta = 90 - \alpha$$
$$L_b = tangent(\beta) * h_L$$
$$A_{sat} = L_b * h_L$$
$$h_{sat} = \frac{A_{sat}}{L_{drain,i}} \cdot f_{h,sat} \quad \text{(B.2.2)}$$

where A_{sat} is the triangle area exceeding the layer thickness (mm^2), the angles α and β are illustrated in figure B.2, (b).

The adjustment factors of porous media $f_{h,sat}$ and $f_{V,sat}$. The illustrated approach in figure B.2 is true for layers with a defined border line and a free overflow (for example, a drainage layer made up of plastic). For drainage layers made up of porous media without a defined overflow height the saturation stage height h_{sat} (mm) is computed with an adjustment factor where $f_{h,sat} < 1$ (-). By default the factors are 1.0 for porous media with a free overflow. The factor is smaller by reaching 0.5 when the media is dense or settled.

In porous media the retention capacity of the layer has an influence on the retained and drained water proportions. For the adjustment of the exceedance flux $\dot{V}_{sat}$ a calibration parameter $f_{V,sat}$ is defined to adjust the retention characteristics of porous media. The methodology to compute the drainage processes in LSDMs is described in section 5.3 (page 71 ff).

B.3 Supplementary flow charts of the developed algorithm to model control functions

Control functions use different criteria to activate, change or stop drainage from a layer in an LSDM or stream segment. The criteria are based on precipitation intensities, water levels or discharges as functions per time of different elements in the hydrological network. These criteria of "driver" time series activate or deactivate a control function in the algorithm. For local scale control functions based on precipitation thresholds, the driver can be the individual local data structure which is affected by local rainfall or any pre-defined spatial data structure. A query is developed to distinguish between the different driver types. The query of a control function is illustrated in the flow chart in figure B.3.

If the driver is pre-defined for all data structures, the driver input time series are read and pre-processed directly. If the driver time series are to be processed individually for each data structure, all subcatchments and LSDM data structures are checked if these include active control layer functions to be computed in recursive calculation routines. In this way, the spatial pre-processed precipitation for each data structure is applied as individual driver time series. For local heavy (convective) storm events this spatial differentiation is significant. The results of the algorithm in figure B.3 are time series of active control functions per layer of each (LSDM) data structure.

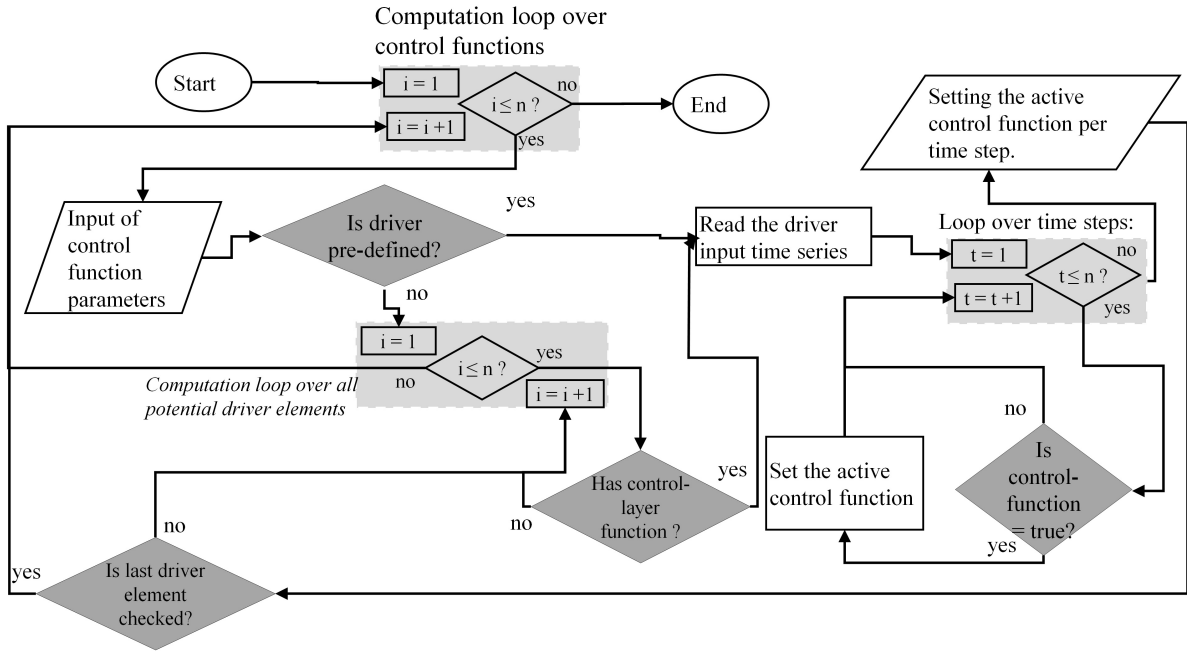

Figure B.3: (a) Pre-processing of the driver time series to define the control functions per data structure.

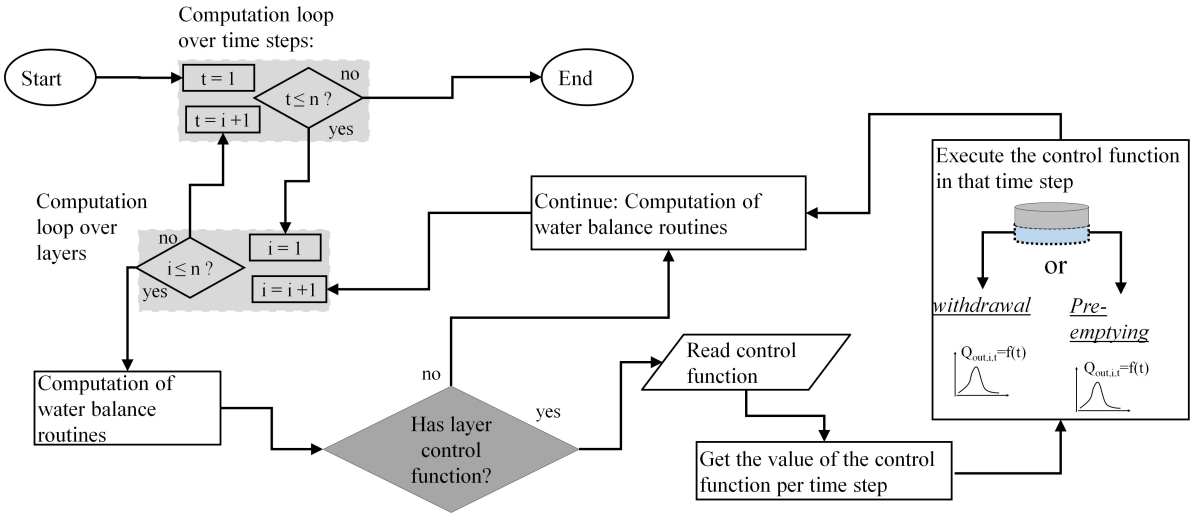

Figure B.4: (b) Execution of the control functions per layer within the soil moisture balance calculation routine.

The execution of the control function per layer is nested in the time step loop and the water balance calculation routines. This algorithm is illustrated in figure B.4. If the LSDM structure is computed with a control function, the water balance computation is extended with an additional calculation routine to execute the control functions. It is distinguished between a withdrawal or a pre-emptying control function. The computation of the water balances and the drainage processes are described in chapter 5.

B.4 Explanation of the meso scale spatially aggregated flood routing method

For the computation of the flood routing through conventional drainage systems (piped flow) on the meso scale a conceptual hydrological approach is applied based on the linear reservoir concept. In this approach, a unit impulse function is computed. It requires the definition of a retention constant k (h) and the number of reservoirs n. The basic theory of the unit hydrograph is described, for example in Dooge [1959], which is applied by Wackermann [1981] to model the flood routing through stormwater drainage pipes. The equation to compute the system response function $u(t)$ is applied in the following form:

$$u(t) = \sum_{i=1}^{m} \frac{(t_m)^{n-1}}{(n-1)! \cdot k^n} \cdot e^{-t_m/k} \cdot \Delta t/m \tag{B.4.1}$$

where the following parametrisations are derived to compute the conceptual flood routing from impervious areas (namely piped flow in urban areas) on the meso scale. A fixed number of three storages $n = 3$ is defined like suggested by Wackermann [1981] and applied later in different models (for instance in BlueM.Sim (M. Bach [2011]) and KalypsoNA (TUHH-WB [2014]). Δt is the simulation time step size in hours (h). k is the retention constant of the storage cascade (h), m is the number of $u(t)$-functions which is fixed to $m = 5$ and t is the index of the time step in the hydrograph. t_m is the step size of each unit function and is computed with the following equation:

$$t_m = (t-1) * \Delta t - \Delta t/10 + \sum_{i=1}^{m} (\Delta t/m) \tag{B.4.2}$$

A transfer of the unit impulse function to an instantaneous unit impulse function ($u \rightarrow iuh$) is done with the following equation:

$$iuh(t) = \frac{u(t) + u(t+1)}{2} \cdot \frac{1}{\sum_{\tau=1}^{\tau_{max}} u(\tau) \cdot \Delta t} \tag{B.4.3}$$

where $iuh(t)$ is the instantaneous unit impulse function ($1/\Delta t$), τ is the convolution step index per unit impulse function, τ_{max} is the maximal number of the convolution steps, Δt is the time step size of the simulation (h). The maximal number of convolution steps τ_{max} depends on the flow duration D_{flow} of the unit impulse function and the time step size Δt of the simulation as

follows:

$$\tau_{max} = D_{flow} / \Delta t \tag{B.4.4}$$

For a retention constant (k=0.5h) the resulting instantaneous unit impulse functions are plotted for different time step sizes Δt with the condition $\Delta t \leq k$ in figure B.5 The flow duration D_{flow} is 5 hours and $\Delta t = \Delta \tau$. When the time step size is close or even larger to the retention coefficient $\Delta t \geq k$ the hydrograph exceeds the flow duration (> 5 hours) because of a mathematical convolution with a too large time step size for this retention constant. Examples are given in figure B.6. The current procedure is a definition of a reasonable small time step size (for example, Δt < 5 minutes) for this conceptual approach on the meso scale to agree with the criteria $\Delta t \leq k$. The normalisation of the impulse function provides a time step size independent *iuh*-function as long as the criteria is fulfilled, otherwise the retention behaviour is overestimated.

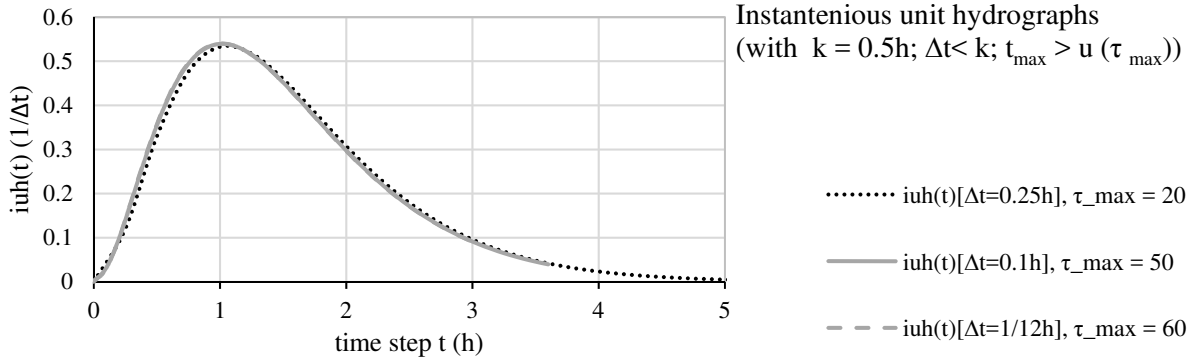

Figure B.5: Plotted instantaneous unit hydrograph (*iuh*(t)) functions with a retention constant k = 0.5 h and varying time step size Δt (h) with the condition $\Delta t < k$.

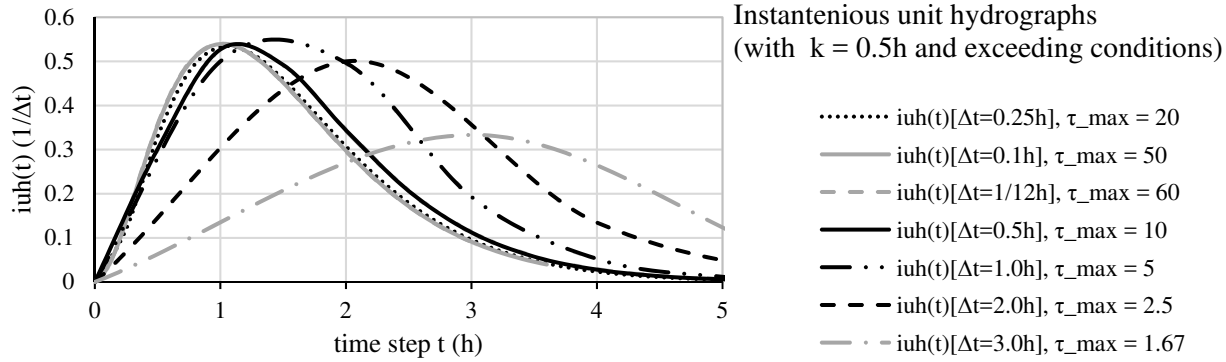

Figure B.6: Plotted instantaneous unit hydrograph (*iuh*(t)) functions with a retention constant k = 0.5 h and varying Δt (h) to illustrate the deviation when $\Delta t > k$.

To compute the retention constant k different approaches are applicable to derive the concentration time t_c in the subcatchments as summarised in Maniak [2016]. For example the approaches of Kirpich, kinematic wave or the SCS-lag-equation are suggested. An alternative is the application of the physical-based Darcy-Weisbach approach with the Colebrook-White equation and a summation of the flow times in the pipes along the longest flow path with $k \approx t_c = t_A + \sum_{i=1}^{n} t_i$ (TUHH-WB [2014]). Where t_A is the flow time till reaching the inlet in

the pipe systems (h) and t_i is the flow time in each pipe segment along the longest flow path. For each pipe segment the flow time is computed with $t_i = l_i / v_i$ where l_i (m) is the length of the pipe segment and the velocity v_i is computed with eq. 5.3.3 on page 73. A conceptual approach to compute the retention coefficent is suggested earlier by Wackermann [1981] with the relation:

$$k = \frac{a \cdot t_c}{(n-1)} \tag{B.4.5}$$

where $n = 3$ is the number of storages in the reservoir-cascade for piped flow routing. a is an empirical parameter derived by Wackermann [1981] with the relation between time to peak t_p and concentration time t_c ($t_p = a \cdot t_c$). For piped flow the parameter a is set to 0.5 as described by Wackermann [1981]. The concentration time t_c is computed using the approach of Kirpich in the following form:

$$t_c = 0.0663 \cdot L_s^{0.77} \cdot I_s^{-0.385} \tag{B.4.6}$$

where L_s is the longest flow path of the streams (m) in the subcatchment and I_s is the averaged slope of the drainage system (-).

The routed flow is computed by using a convolution of the unit step input load (($Q_{in}(\tau)$) with the unit impulse response $u(t - \tau + 1)$ over the time steps:

$$\begin{aligned} Q_{out}(t) &= \sum_{\tau=1}^{\tau_{max}} Q_{in}(\tau) \cdot u(t - \tau + 1) \\ \text{with } Q_{in}(\tau) &= (P_{eff}(\tau) + Q_{run-on}(\tau))/1000 * A * \Delta t/3600 \end{aligned} \tag{B.4.7}$$

where $Q_{out}(t)$ is the routed flow to the target (sink) data structure (m^3/s), u is the system function (see eq. B.4.1), τ is the convolution step index of the unit impulse function, t is the time step index of the simulation run, P_{eff} is the effective precipitation flux on the impervious area ($mm/\Delta t$) reduced by depression and evaporation losses (see section 5.3.2, page 74 ff), Δt is the simulation time step size which is transformed to seconds (s), A is the area of the spatial data structure (m^2) and Q_{run-on} is the run-on flux into the area by linked spatial data structures ($mm/\Delta t$) (for instance in case of linked LSDMs). The target of the flood routing can be any junction node, LSDM or other subcatchments in the hydrological network. This conceptual flood routing method depends on the defined time step size Δt which is an input value in eq. B.4.2. The condition $\Delta t < k$ is required to be checked by the simulation settings. The method is affected by the issue described in Ostrowski et al. [2010], where the dependency between time size and behaviour of hydrological parameters is discussed. Here, the $u(\tau)$-function is limited by the condition $\Delta t < k$. This conceptual approach is valid for retention constants defined for piped flood routing in meso scale catchments. Using this conceptual approach for the flood routing among LSDMs on the local scale leads to an overestimation of the retention when the flow path length is small in comparison to the subcatchment scale. A comparison of results using this conceptual approach and the developed KM1-method for flood routing of LSDMs in a meso scale catchment is given in section 8.3.1 (page 140).

B.5 Explanation of the method to compute subsequently drained backwater in downstream direction

A supplementary flow chart is described in this section to explain the developed method to compute subsequently drained backwater in downstream direction. The method is introduced in section 6.3.3 (page 98). The algorithm to model the downstream directed drainage of backwater volume is related to the algorithm to compute upstream directed backwater effects. The difference lies in balancing the water level and volumes of the current data structures (i) with the downstream (i+1) data structures. The first pre-condition for downstream directed drainage of backwater is the presence of a backwater volume in the current stream segment (i) within that time step (t) ($V_i(t) > V_{i,free}(t)$). The second pre-condition is, that the difference in water levels between the current stream segment (i) and the downstream segment (i+1) is larger than the defined minimum tolerated water level difference. With that conditions the calculation routine to model the downstream directed backwater flow is restarted. An outline of the developed algorithm to compute these effects is given in figure B.7. The flag for the active backwater system re-computation is set to 'true', hence the method parts (i) to (iv) are repeated. In the calculation routine (iii), the subsequently drained backwater in downstream direction is computed with the algorithm in figure B.8.

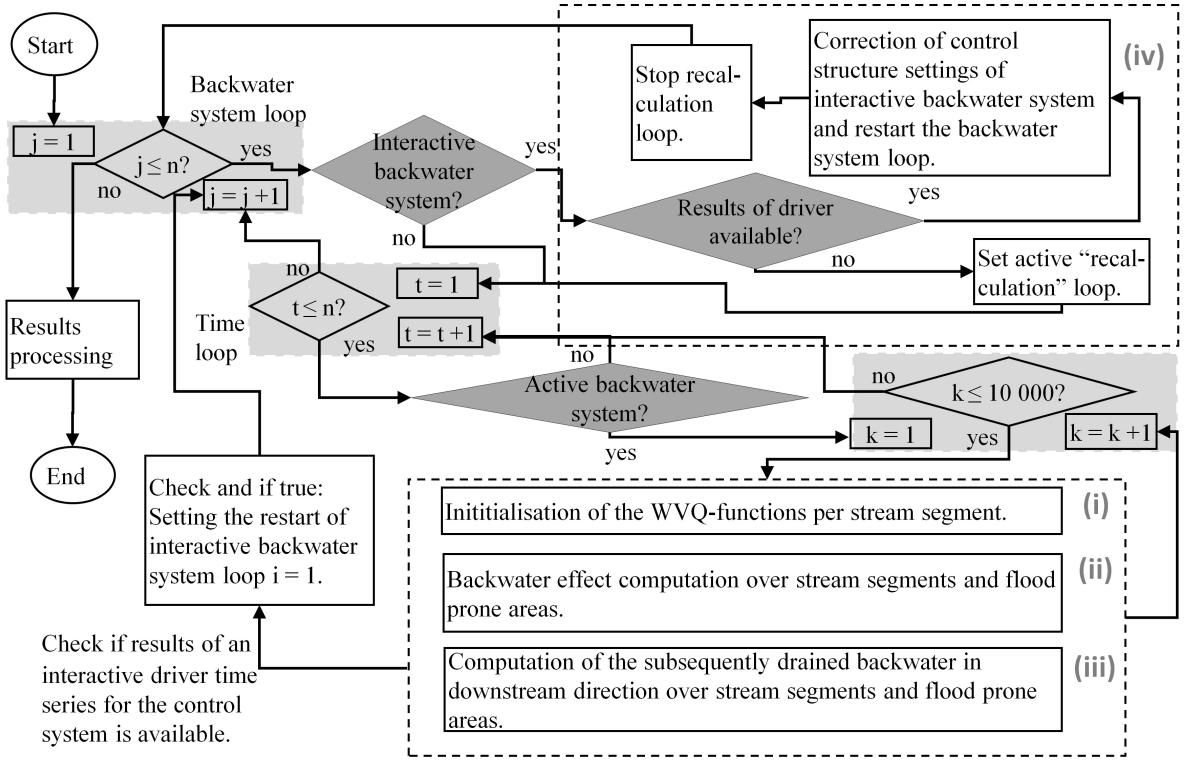

Figure B.7: Flow chart of the algorithm to compute an interactive backwater affected system. This is a reduced version of the flow chart on page 91.

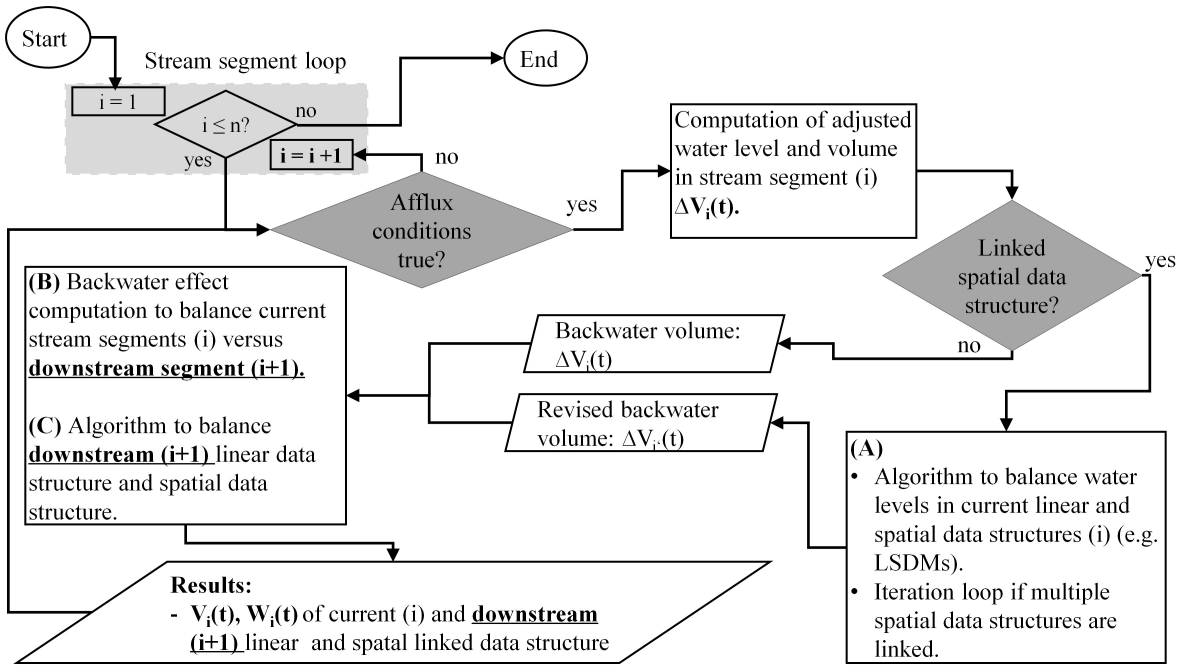

Figure B.8: Algorithm of the method to compute subsequently drained backwater in downstream direction (from stream segment (i) to (i+1)) over streams and areas.

In the algorithm in figure B.8, the water level in the stream segment (i) is reduced by the minimum water level difference ΔW_{min} in the following way: $W_{i'}(t) = W_i(t) - W_{\Delta min}$. The storage volume of the stream segment $V_i(t)$ is defined by the WVQ-relation. The result is the difference in volume $\Delta V_i(t)$ which is routed to a linked structure (i) or directly to the downstream segment (i+1). In case of a linked spatial structure (i) the water level in the linear structure $W_i(t)$ is equalised with the water level in the linked spatial structure $W_{i,area}(t)$ (indicated as process 'A'). The volume in the spatial structure $V_{i,area}(t)$ is reduced respectively. The result is a larger difference in volume $\Delta V_{i'}(t)$ to be routed to the downstream segment. This backwater volume is added to the downstream segment $V_{i+1}(t) = V_{i+1}(t) + \Delta V_{i'}(t)$ and the water level is derived from the WVQ-relation function ($f(W_{i+1}(t); V_{i+1}(t))$). This procedure is indicated with 'B'. If the downstream segment is linked with another spatial structure, the equalisation of water level and volume is done respectively and this is indicated as process 'C'. The processes 'A', 'B' and 'C' are described likewise for the upstream directed backwater computation in section 6.3.2 on page 95.

This calculation routine gives results of the corrected water level $W_i(t)$ and volume $V_i(t)$ for stream segment (i), corrected water level $W_{i,area}(t)$ and volume $V_{i,area}(t)$ for linked spatial structures, corrected water level $W_{i+1}(t)$ and volume $V_{i+1}(t)$ for the downstream segment (i+1) and corrected water level $W_{i+1,area}(t)$ and volume $V_{i+1,area}(t)$ for downstream located linked spatial structures. This algorithm to compute the downstream directed drainage of backwater in figure B.8 is related to the upstream directed backwater computation described in figure 6.10 on page 97, but with a downstream directed computational order.

B.6 Explanation of an interactive backwater affected system

This supplementary material contributes to explain the developed method to model an interactive backwater affected system which is introduced in section 6.3.4 on page 98. Such a system exists when criteria of upstream control structures depend on results of downstream segments, which are at the same time backwater affected and influenced by the inflow from these upstream segments. The criteria defines the activation (opening or closing) of upstream control structures (for instance gates or sluices) to prevent backwater effects further upstream. The algorithm to compute an interactive backwater affected system is illustrated in the flow chart in figure B.7 (iv) to model backwater effects in streams and areas. This flow chart is a reduced form of that one in figure 6.6 (page 91). As long as the driver time series for the criteria of the control structure is not available, a "recalculation" loop is activated. For each additional computation run the index '{k}' is increased '{k+1}'.

An example of an interactive backwater system is presented in figure B.9. In the calculation routine the Water-level-Volume-Discharge (WVQ) relations per stream segment are continuously revised. Three indexes are introduced in figure B.9 to describe the interdependencies between the stream segments ('[x]'), the backwater systems ('(x)') and the computation runs ('{x}'). Each stream segment is labelled with an ordinal from the upstream '[1]' to the downstream segment '[10]'. A stream segment can have only one upstream junction node, but may drain to several downstream junction nodes. That means that a junction node collects the flow of several upstream segments.

Each element belongs to one backwater system. In this example, the first downstream backwater affected system has the ordinal '(1)' and the two tributary systems have the ordinals '(2)' and '(3)'. Each backwater system has a control structure at the downstream segment. The control segments are computed with the "Puls" method described in section 6.2 on page 86. The WVQ-relations, the inflow time series, the storage volume and the outflow distribution to different junction nodes are computed.

In the calculation routines four different processes are computed which are indicated as arrows in figure B.9. The free flood routing computation is indicated in black and is computed in the first computation run '{1}'. In the second computation run '{2}' the backwater effects in upstream or the drainage in downstream direction are computed. These processes are indicated with arrows in grey. Additionally a correction of the flow is computed when the configuration of upstream control structures are changed in a computation run. This is the case for the stream segments upstream and downstream of the control structures in the tributary backwater affected systems (here 'Ctrl 2' and 'Ctrl 3'). The tributary backwater affected systems are indicated in figure B.9 with dashed border lines. The tributary system can be defined on a district scale, representing a subcatchment. Or the tributary system comprises a network of meso scale stream segments. The control structure 'Ctrl 3' (stream segment '[4],(2)') depends on the backwater affected water level of the stream segment [2] (= Ctrl 3 (f[2])) and the control structure 'Ctrl 2' (stream segment '[8],(3)') depends on the backwater affected water level of the stream segment [5] (= Ctrl 2 (f[5]). At the same time,

these control structures drain into those streams which are backwater effected when the downstream control structure 'Ctrl 1' (a tide gate) is closed. The tidal water levels are given at the Node 'Ctrl 1'.

The revisions of control functions (here: 'Ctrl 2' and 'Ctrl 3') lead to changed conditions in outflow ΔQ, storage ΔV and backwater conditions ΔW. The flow regime in the backwater system is influenced by ΔQ in the downstream und upstream segments. For example the computed discharges in the upstream junction nodes of stream segment '[5]' and '[9]' are revised. The changes in the interactive control system settings are indicated in figure B.9 by white arrows in downstream and upstream flow direction together with the index of the control function. After the revision of the interactive control structures and the associated flow conditions, the backwater calculation routines of the tributary system using the methods (i) to (iii) in figure B.7 are continued (see methodology section 6.3 for further details). This is illustrated with another computation run using the index '{k+1}' (here: {3}).

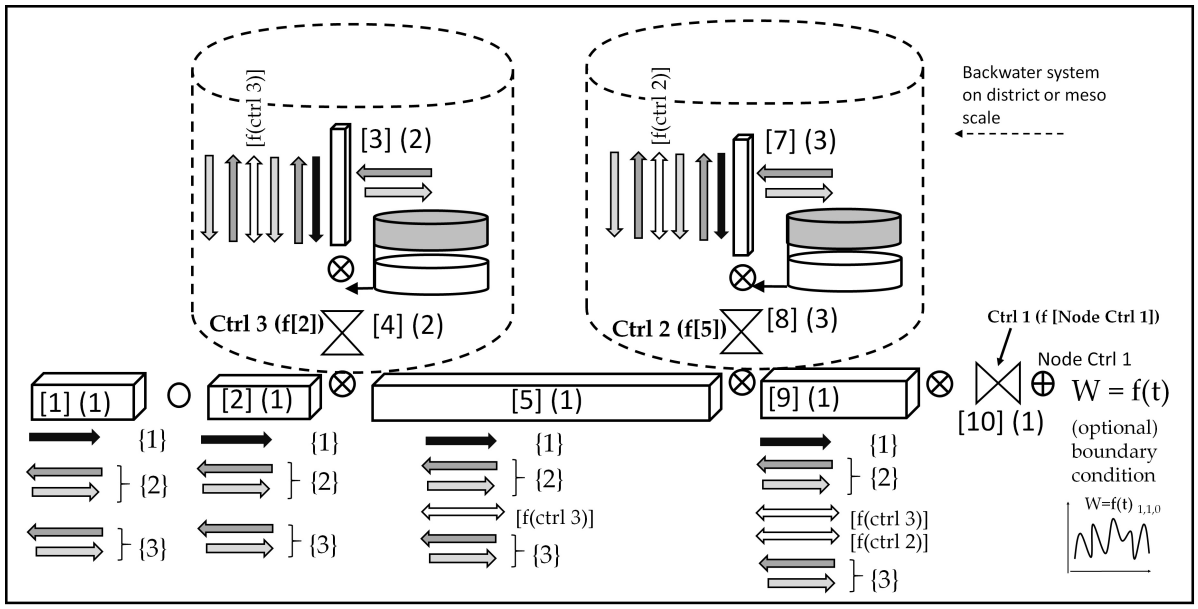

Figure B.9: Scheme of the computation procedure of an interactive backwater affected system. Three indexes are introduced to describe the interdependencies between the stream segments ('[x]'), the backwater systems ('(x)') and the computation runs ('{x}'). (The legend of applied symbols is given in figure B.1.)

C. Supplementary information about the Kalypso simulation platform

The module KalypsoHydrology and the calculation code KalypsoNA are part of the open source project Kalypso which comprises a set of applications and client specific developments. The platform Kalypso is developed according to modern information and communication technologies: WMS-, WFS-Client, WPS-Server, GML-3 Parser, Time Series Service, Report Service[1] (Lippert et al. [2009] and BCE [2018]). It is developed in a cooperation between Björnsen Beratende Ingenieure (BCE) and the Hamburg University of Technology (TUHH). The applied programming language is Java. The model is available on the open source software web-directory "SourceForge.net" (www.sourceforge.net/projects/kalypso/). The Kalypso applications include modelling systems in the areas of rainfall-runoff modelling (namely: KalypsoHydrology), hydrodynamic-numerical modelling (Kalypso1D2D), flood forecasting, flood inundation (KalypsoFlood), flood risk assessment (KalypsoRisk) and the evacuation modelling of flooded areas (KalypsoEvacuation) (see BCE & TUHH [2018]). The modules are provided with a strong functionality on spatial geographical information system (GIS) analysis, time series management and data processing features. These are important functionalities in recent data management practice and software application. The modules of the Kalypso project support the modelling of processes in a computation chain as illustrated in figure C.1.

The implementation of the spatial mapping of georeferenced local data structures in the Kalypso platform has been realised in cooperation with colleagues from BCE. This extension for data exchange between KalypsoNA and KalypsoHydrology for modelling LSDMs was realised in 2013 by the author of this work in cooperation with Gernot Belger (from BCE) and financial support by LSBG (agency for streets, bridges and rivers in Hamburg). Scenario simulations of future urban development projections can be derived from a calibrated basic model using LSDMs which represent adaptation strategies like green roofs, swales or retention areas. The hydrological network is updated on-the-fly (namely during the execution) with the spatial data structures and their interconnections as described in section 4.1 (p. 53).

[1] WMS = Web Map Service, WPS = Web Processing Service, WFS = Web Feature Service, GML = Geography Markup Language

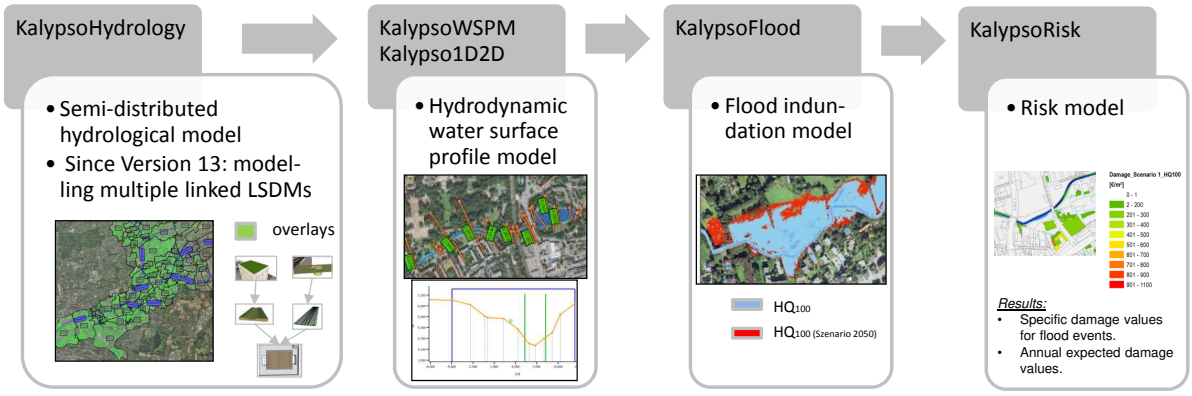

Figure C.1: Overview of the Kalypso project modules (adopted from Hellmers et al. [2015]).

In the process chain of Kalypso, steady state non-uniform rivers hydraulics are computed with a hydrodynamic-numerical model (Kalypso1D2D). In the post-processing phase, the inundated areas and flow depths are computed based on digital terrain data using the module KalypsoFlood. With the module KalypsoRisk the flood risks in the inundation can be determined. Results of model applications are published, for example, in Hellmers et al. [2015] and Hellmers, Manojlović, et al. [2016].

The platform Kalypso supports a GIS-based data management and basic GIS-based functions (such as the intersection of shape files). An example is illustrated in figure C.2. The location and size of an LSDM are defined via shape file import or drawing the LSDM polygons directly with features in the Kalypso platform. Adding a layer of a Web Map Service into the map view supports the definition and visualisation. Different kinds of the same LSDM type are created with tools in KalypsoHydrology or defined in shape files as polygon themes and imported in the model. According to the needs of city planners different designs of the same decentralized measure are to be modelled within one subcatchment. The implemented functions facilitate the import of the geographical location and area of diverse LSDM structures of the same type within the same subcatchment: for example, extensive green roofs, intensive green roofs, cisterns with rainwater harvesting attributes of detached houses and cisterns with rainwater harvesting attributes of administration buildings. The description of the input parameters and the data handling is shown in figure C.3. The "Kalypso Workflow" is shown in figure C.4 on the left side of the window. By activating a view in the list, the data in the model can be edited in the "Feature View". In the example in figure C.4 the input parameters of the LSDMs (which are also known as Sustainable urban Drainage Systems (SUDSs)) are edited per layer. The input parameters using the module KalypsoHydrology and the created extension folder are described in chapter 7.3 (page 104).

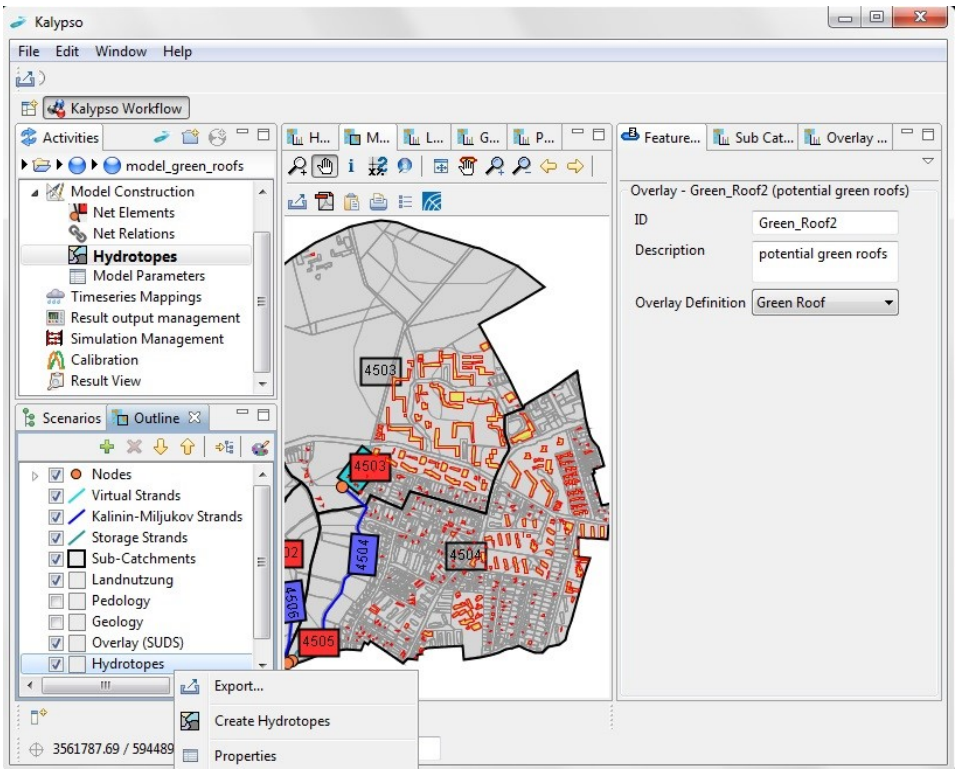

Figure C.2: GIS-based data management and data processing (for example, creation of Hydrological Response Units ("Hydrotopes") via intersection of shape files).

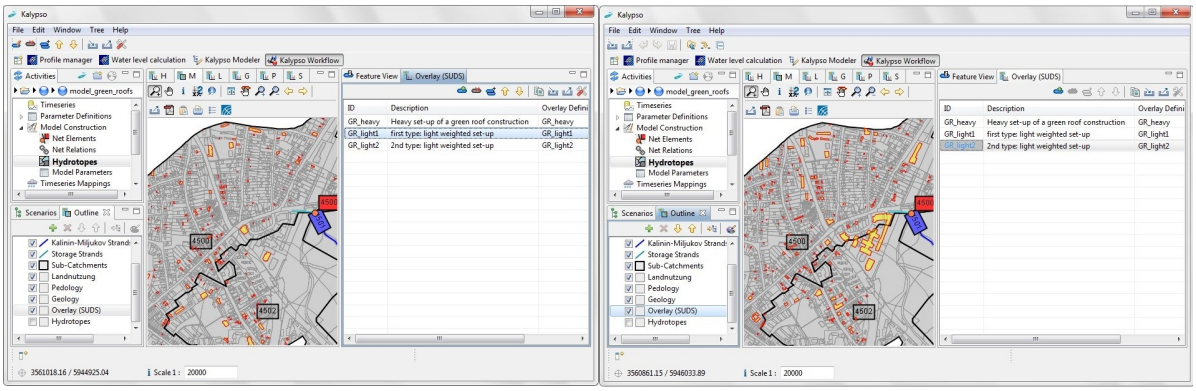

Figure C.3: Exemplified mapping of different LSDM types with specific drainage functionality but different setup can be defined and imported as shape files. In this example, different green roof setups with an intensive green roof design, light green roof design 1 and light green roof design 2 are marked in the map by activating the LSDM type in the list.

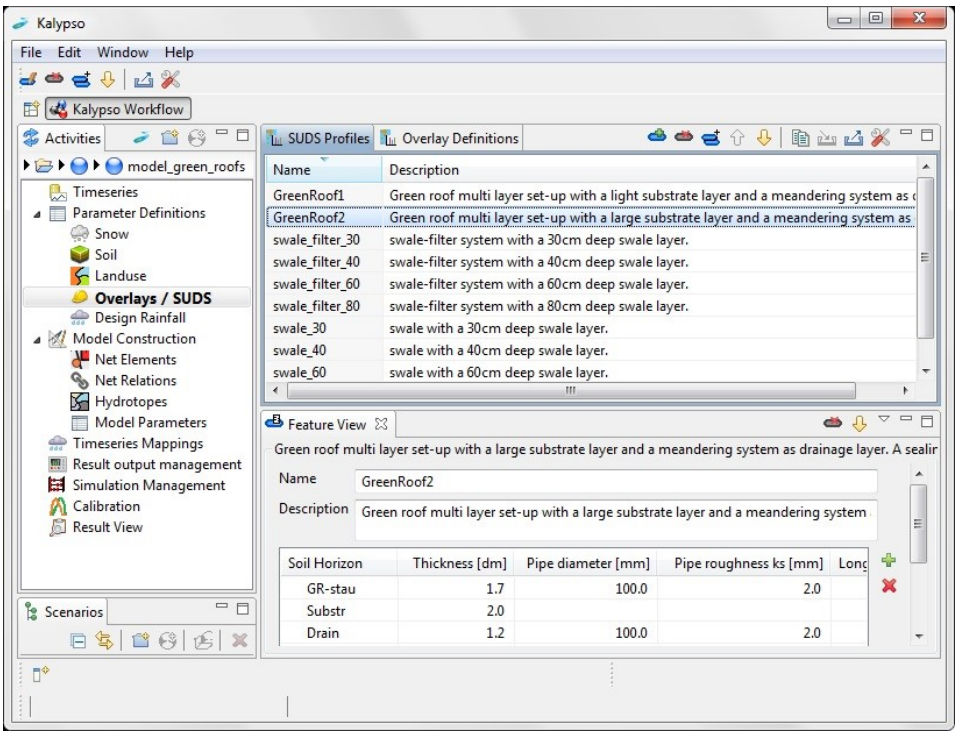

Figure C.4: View of the workflow in the module KalypsoHydrology. In this example, the list of input parameters for multi-layered structures (LSDMs) are shown.

D. Supplementary data and diagrams of the application studies

In this attachment supplementary data and diagrams of the application studies on the local scale of green roof structures (in section D.1) and the numerical model on the regional scale "Dove-Elbe" (in section D.2) are illustrated and explained.

D.1 Calibration and validation results of local scale green roof studies

Local scale studies of different green roof structures are performed and analysed in the laboratory of the TUHH. The observed data is compared with simulated results of the extended numerical model of this work. The procedure and setup of the laboratory studies are reported in recent works which are summarised in the following section D.1.1. Thereafter, the results of the experimental runs for the calibration of the input parameters of the numerical model are presented in section D.1.2. Finally, the results of the experimental runs for the validation of the numerical model output are presented in section D.1.3. The presented calibration and validation results in form of tables, diagrams and scatter plots complement to the findings in section 8.1 (pages 117 ff.)

D.1.1 Particle size distribution curves of the applied substrate materials and reports of related works

Particle size distribution curves of applied substrate materials are determined by laboratory tests (see reports by Fitzner [2015][1] and Rüter [2016][2]). Additionally, the hydrological parameters: wilting point (WP), field capacity (FC) and pore volume (PV) are obtained by these

[1] Fitzner, S. (2015). Ermittlung des Abflussverhaltens vom Optigrün- Dachbegrünungssystem ‚Mäander 30' auf der Grundlage von hydraulischen Modellversuchen: Determination of the discharge behaviour of the Optigrün roof greening system ‚Mäander 30' based on hydraulic model tests (Bachelor Work). Hamburg University of Technology, Hamburg, Germany.

[2] Rüter, R. (2016). Analyse des Regnerückhaltevermögens vom Dachbegrünungssubstrat HansePar AG 4/9-320 auf der Grundlage von hydraulischen Modellversuchen (Projekt Work). Hamburg University of Technology, Hamburg, Germany.

laboratory studies. The tests are performed in the laboratory of the TUHH and described in the following reports which are supervised at the Institute of River and Coastal Engineering of the TUHH: Fitzner [2015][1], Rüter [2016][2] and Hoffmann [2016][3]. The observed raw data of the physical model runs in laboratory are obtained by support of four students and the colleage Justus Patzke (from the Institute of River and Coastal Engineering, TUHH). The layer separation device was invented in 2016 and first experimental output results are reported in Hellmers and Fröhle [2017]; Leber [2017][4]; Schuylenburg [2017][5]; Pasdzior [2017][6] and Patzke et al. [2017]. These works were supervised by Justus Patzke and the author of this work.

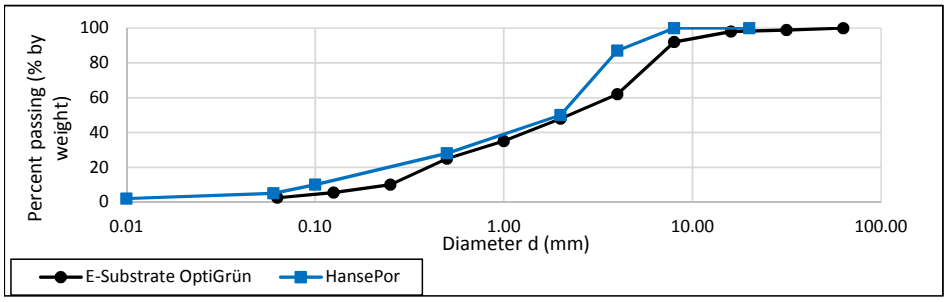

Figure D.1: Particle size distribution curves of the substrate "HansePor" (of the company HanseGrant) and "E-substrate" (of the company OptiGrün), which are tested in the laboratory of the TUHH in 2016 (see reports by Fitzner [2015] and Rüter [2016]).

D.1.2 Results of the calibration runs

A calibration procedure aims to obtain the values of parameters which represent the physical behaviour in a sufficient, but still limited manner. It pursues to transfer calibrated values to model further application studies under changed conditions. The primarily determined values are adjusted by comparing the numerical model results with observed data in laboratory. The output of four different green roof experimental runs of a single layer structure and the output of three different runs of a multi-layered structure are analysed and presented for calibration purpose. The calibration results are obtained by comparing observed with simulated fluxes of the green roof structures. The results are illustrated in diagrams of hydrographs and scatter plots. A legend of the diagrams is given in figure D.2. The different calibration runs are numbered from [1] to [7] with a short label to describe the structure (single layer = SL or multi-layer = ML), substrate layer height H (cm) and gradient I (%). For example run [1] "SL 8H;I6" means a single layered structure with a substrate layer of 8 cm in height and a

[3]Hoffmann, M. (2016). Erstellung und Kalibrierung eines numerischen Modells zur Vorhersage des Abflussvermögens von Dachbegrünung auf der Grundlage von hydraulischen Modellversuchen (Projekt Work). Hamburg University of Technology, Hamburg, Germany.

[4]Leber, P. L. M. (2017). Experimentelle Untersuchung zur Retentionswirkung und zum Abflussverhalten von Dachbegrünungen (Bachelor Thesis). TU Hamburg, Hamburg, Germany.

[5]Schuylenburg, F. D. (2017). Dachbegrünungen als dezentrale Regenwasserbewirtschaftungsmaßnahme: Physikalische Laborversuche zum Abflussverhalten von Retentionsdachaufbauten (Bachelor Thesis). Hamburg University of Technology, Hamburg, Germany.

[6]Pasdzior, P. (2017). Dachbegrünungen als dezentrale Regenwasserbewirtschaftungsmaßnahme: Physikalische Laborversuche am Beispiel von Retentionsdachaufbauten (Bachelor Thesis). Hamburg University of Technology, Hamburg, Germany.

gradient of 6 %. For the calibration and validation procedures, three different types of rainfall events ("P-types") are applied: a rainfall intensity of about 1.9 mm/minute for a duration of 15 minutes (i), a rainfall intensity of about 1.0 mm/minute for a duration of 45 minutes (ii) and a rainfall intensity of about 0.6 mm/minute for a duration of 90 minutes (iii). These rainfall types correspond to statistical rainfall events with a probability of occurrence (T) of once in 100 years (T = 100 a) according to KOSTRA 2010R for the Hamburg inner city region with a tolerance of ± 20 %. According to the three rainfall intensities and durations the time scale of the X-axis and the flux scale of the Y-axis in the diagrams are specified. For the rainfall type (i) the time scale is set to 70 minutes with a maximum of the flux scale of 3.0 mm/minute in the hydrographs and 1.6 mm/minute in the scatter plots. For the rainfall type (ii) the time scale is set to 90 minutes with a maximum of the flux scale of 1.4 mm/minute and a maximum of 1.0 mm/minute on the scatter plot scales. For the third rainfall type (iii) the time scale is set to 140 minutes with a maximum flux scale of 1.2 mm/minute in the hydrograph diagrams and a maximum of 0.8 mm/minute in the scatter plots. The applied scales are visualised in figure D.2. The conclusions of the results are described in section 8.1.3 (see page 123 ff.).

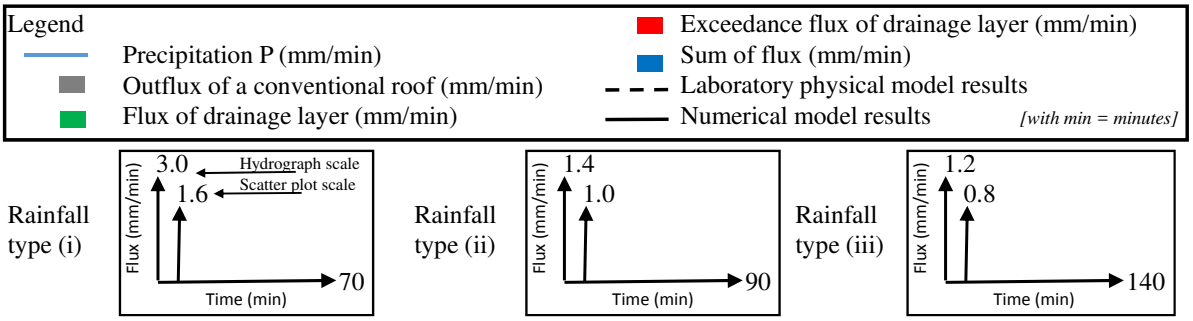

Figure D.2: Applied legend and scales in diagrams as well as scatter plots according to the different rainfall types (i) to (iii).

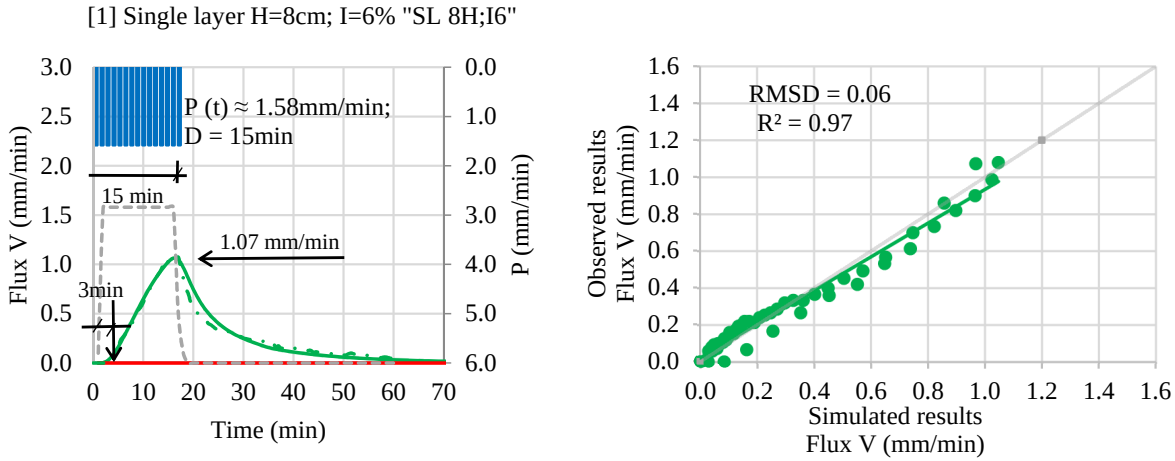

Figure D.3: Run [1] SL H8I6 (P-type i): Single layered structure with 8 cm thickness and 6 % inclination.

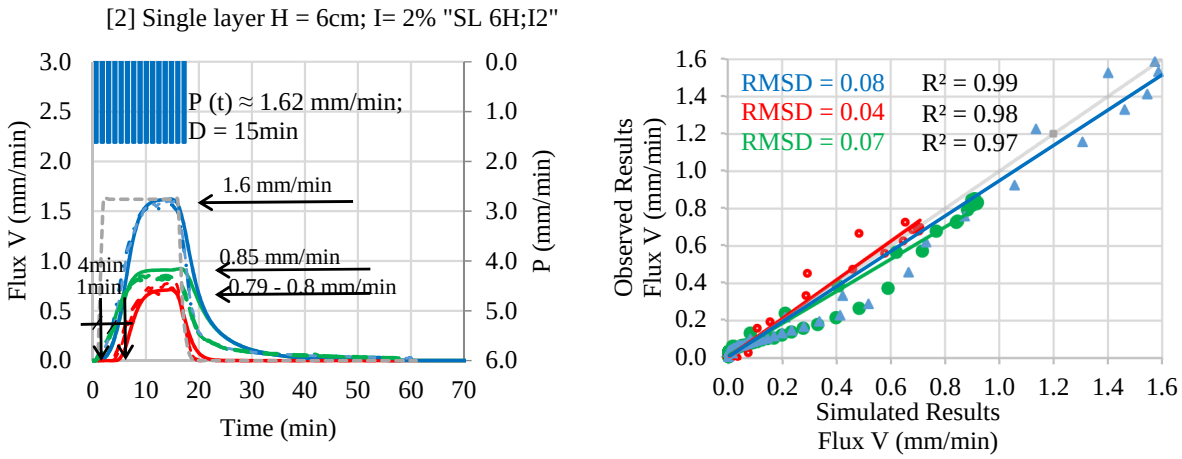

Figure D.4: Run [2] SL H6I2 (P-type i): Single layered structure with 6 cm thickness and 2 % inclination.

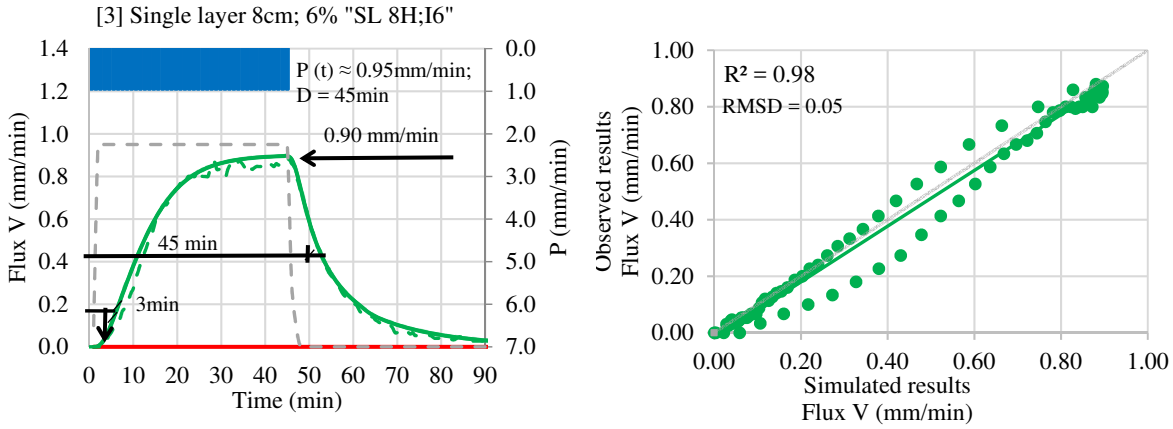

Figure D.5: Run [3] SL H8I6 (P-type ii): Single layered structure with 8 cm thickness and 6 % inclination.

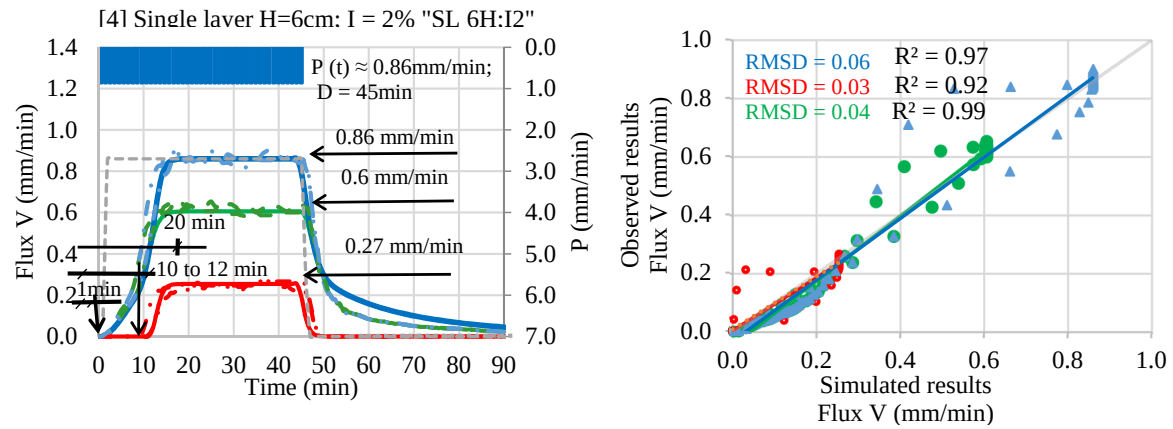

Figure D.6: Run [4] SL H6I2 (P-type ii): Single layered structure with 6 cm thickness and 2 % inclination. A time deviation in the simulated overflow is illustrated. The simulated overflow begins later and ends early as in the observed data.

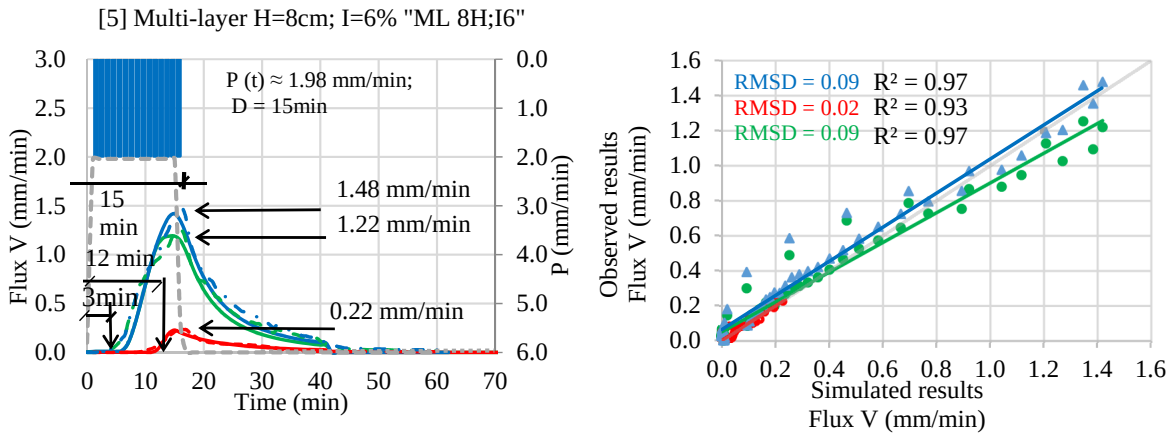

Figure D.7: Run [5] ML H8I6 (P-type i): Multi-layered structure a substrate of 8cm with 6 % inclination.

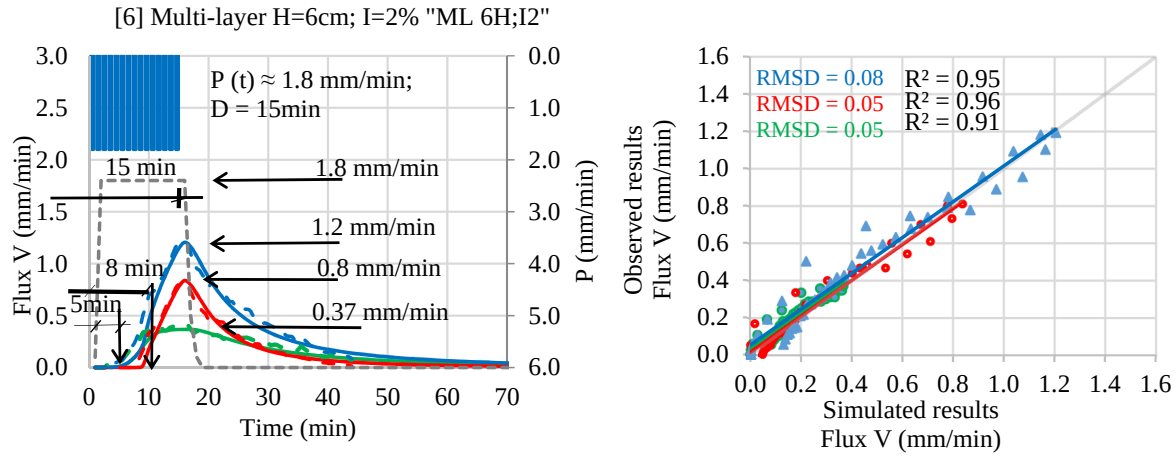

Figure D.8: Run [6] ML D6I2 (P-type i): Multi-layered structure with a substrate of 6 cm and 2 % inclination (adopted from Hellmers and Fröhle [2017]).

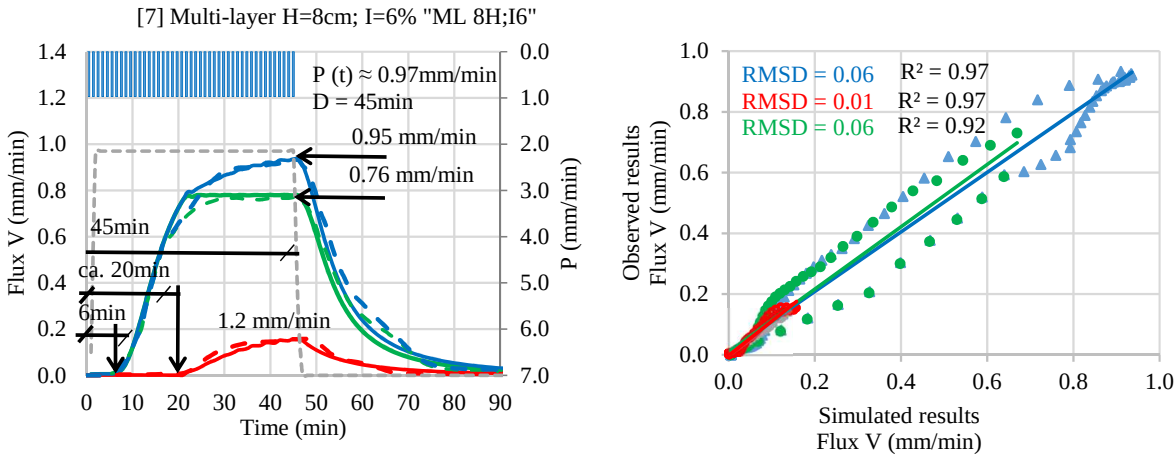

Figure D.9: Run [7] ML H8I6 (P-type ii): Multi-layered structure with a substrate of 8cm thickness and 6 % inclination.

D.1.3 Results of the validation runs

Additionally to the seven experimental runs which are analysed for the calibration of the input parameters, the results of another 15 different experimental runs with the three varying rainfall types are applied in a validation procedure. The obtained input parameter values of the calibration procedure are applied for the model runs in the validation phase. The results of the analysed single layered structures are summarised in table D.1 and table D.2. The results of analysed multi-layered structures are depicted in the tables D.3 and table D.4.

Table D.1: Validation results of the green roof application studies with a single layered structure and rainfall type (i) & (ii).

Rainfall type:		(i)		(ii)	
Structure type:		Single layer (SL) - structure			
Structure details:		[8] SL H=6cm I=6%	[9] SL H=8cm I=2%	[10] SL H=6cm I=6%	[11] SL H=8cm I=2%
Input parameters (of boundary conditions):					
P (t); D*	(mm/ min)	1.6 mm/min; 15min	1.6 mm/min; 15min	0.86 mm/min 45min	0.95 mm/min 45min
V_{ini}	(%)	31.7	36.8	30.6	29.7
Calibration values:					
$f_{H,sat}$	(-)	0.50	0.40	0.50	0.58
$f_{V,sat}$	(-)	-	0.04	-	-
c_0	(-)	0.05	0.16	0.09	0.09
$f_{I,sat}$	(-)	2.00	1.12	1.34	1.34
Results of the evaluation criteria:					
min. lag time / Δ	(min)	1min / < 1min	1min / < 1min	1min / < 1min	1min / < 1min
time to peak / Δ	(min)	15 min / < 1min	15 min / < 1min	44min / <1min	44min / <1min
max. flux peak / Δ	(mm/ min)	1.6 mm/min -0.7%	1.6 mm /min - 5.0%	0.86 mm /min - 0.8%	0.91 mm /min - 0.7%
RMSD	(mm/ min)	0.11 (6.9%)	0.09 (5.6%)	0.06 (7.0%)	0.07 (7.4)
R^2	(-)	>0.95	>0.95	>0.95	>0.95

*P (t) = Rainfall intensity (mm) per minute (min); D = duration in minutes; RMSD = root mean square deviation as total value and (%) deviation of input flux; R^2 = coefficient of determination from the scatter plots; positve delta Δ = overestimation of simulated values; negative delta Δ = understimation of simulated values; "-" means no adjustment of the default value for the model calibration.

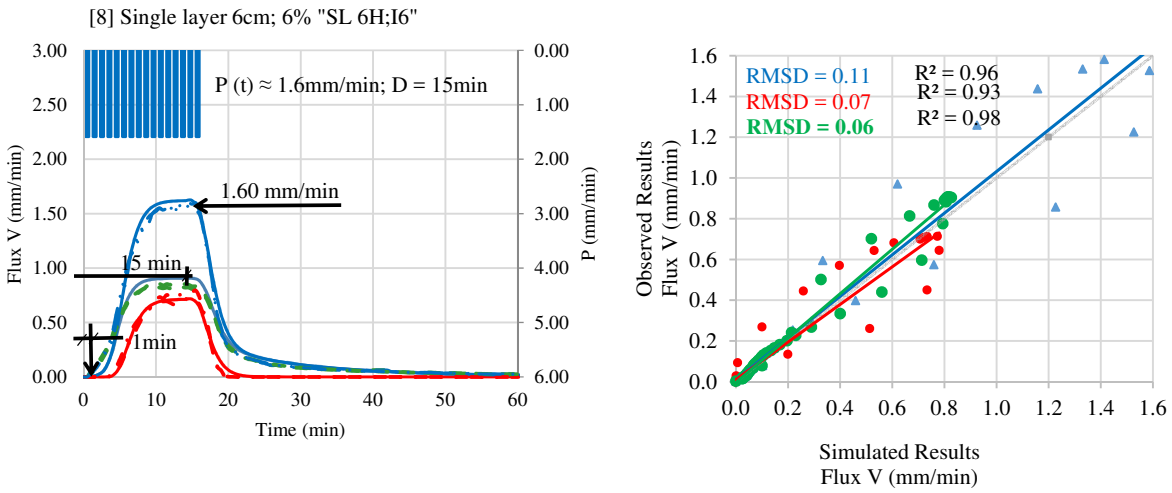

Figure D.10: Run [8] SL H6I6 (P-type i): Single layered structure with substrate of 6 cm thickness and 6 % inclination.

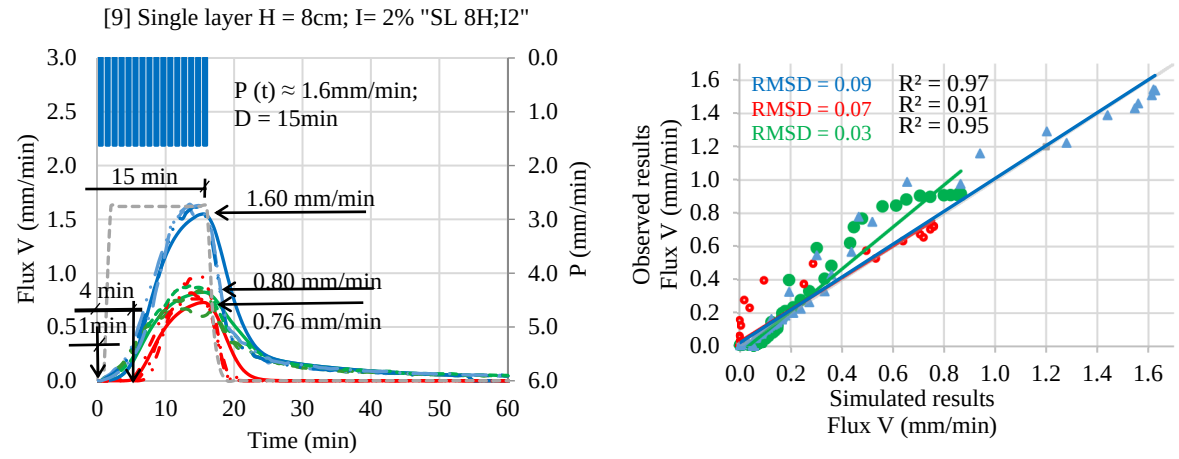

Figure D.11: Run [9] SL H8I2 (P-type i): Single layered structure with substrate of 8 cm thickness and 2 % inclination.

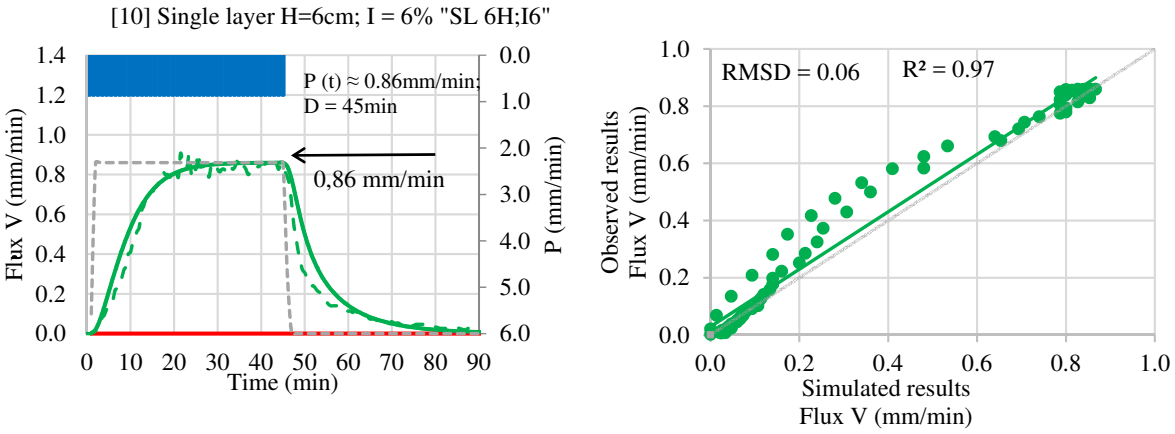

Figure D.12: Run [10] SL H6I6 (P-type ii): Single layered structure with substrate of 6 cm thickness and 6 % inclination.

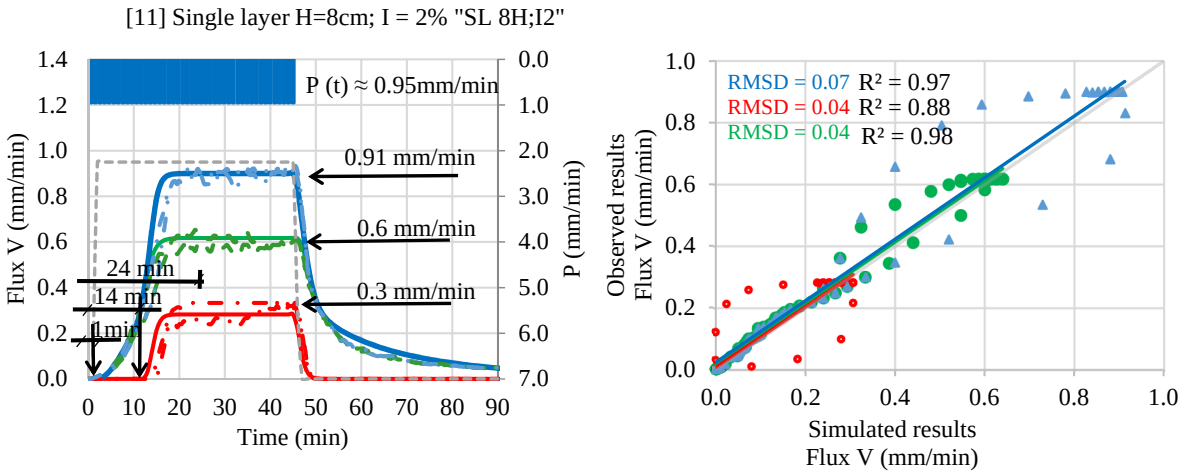

Figure D.13: Run [11] SL H8I2 (P-type ii): Single layered structure with substrate of 8 cm thickness with 2 % inclination.

Table D.2: Validation results of the green roof application studies with a single layered structure for rainfall type (iii).

Rainfall type:		(iii)			
Structure type:		Single layer (SL) - structure			
Structure details:		[12] SL H=6cm I=6%	[13] SL H=8cm I=6%	[14] SL H=6cm I=2%	[15] SL H=8cm I=2%
Input parameters (of boundary conditions):					
P (t); D*	(mm/ min)	0.52 mm/min 90min	0.52 mm/min 90min	0.54 mm/min 90min	0.54 mm/min 90min
V_{ini}	(%)	30.0	34.9	30.0	29.2
Calibration values:					
$f_{H,sat}$	(-)	0.50	0.50	0.50	0.50
$f_{V,sat}$	(-)	-	-	-	0.04
c_0	(-)	0.05	0.05	0.09	0.09
$f_{I,sat}$	(-)	1.34	1.34	1.34	1.34
Results of the evaluation criteria:					
min. lag time / Δ	(min)	2min / < 1min	2min / < 1min	2min / < 1min	2min / < 1min
time to peak / Δ	(min)	40 min / < 1min	40 min / < 1min	20 min / < 1min	30 min / < 1min
max. flux peak / Δ	(mm/ min)	0.52 mm/min /ca. - 0 %	0.52 mm/min /ca. - 0 %	0.53 mm/min /ca. - 0 %	0.53 mm/min /ca. - 0 %
RMSD	(mm/ min)	0.06 (11.5%)	0.04 (7.7%)	0.03 (5.6%)	0.05 (9.3%)
R^2	(-)	>0.95	>0.95	>0.95	>0.95

*P (t) = Rainfall intensity (mm) per minute (min); D = duration in minutes; RMSD = root mean square deviation as total value and (%) deviation of input flux; R^2 = coefficient of determination from the scatter plots; positve delta Δ = overestimation of simulated values; negative delta Δ = understimation of simulated values; "-" means no adjustment of the default value for the model calibration.

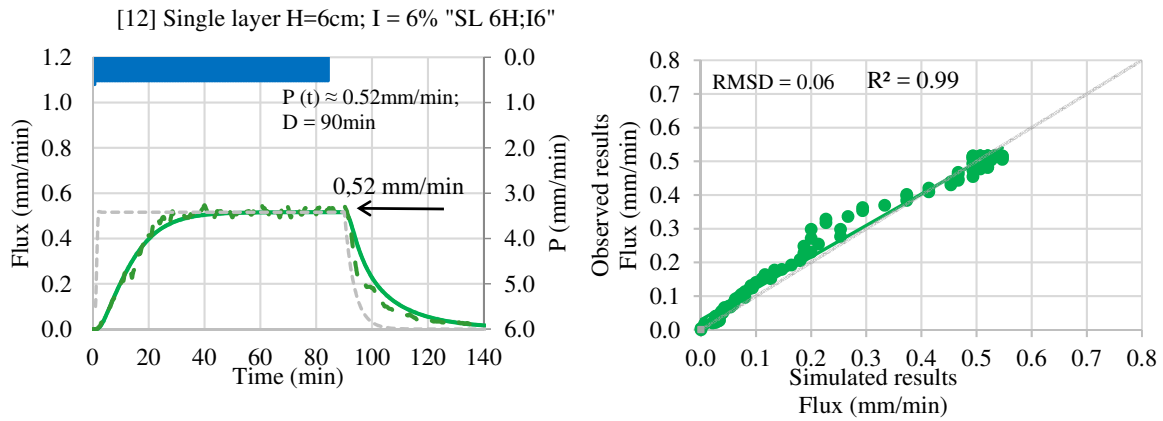

Figure D.14: Run [12] SL H6I6 (P-type iii): Single layered structure with substrate of 6 cm thickness and 6 % inclination.

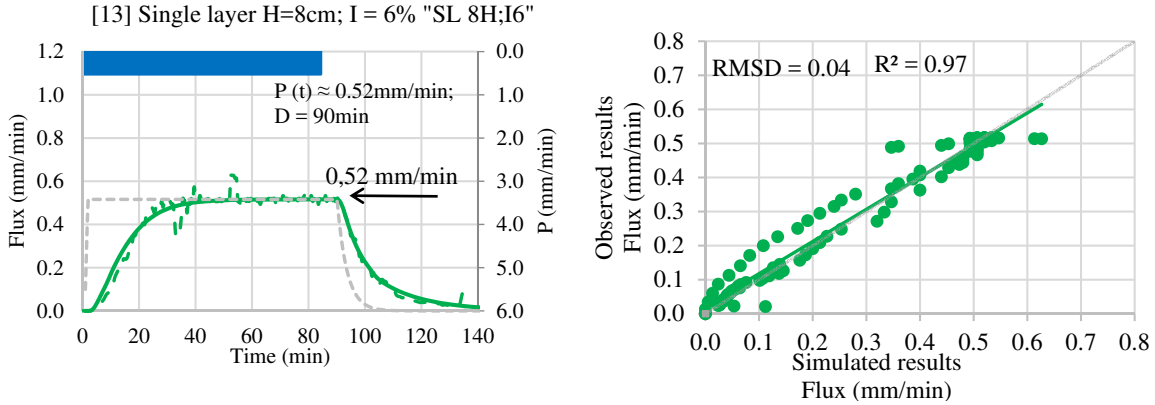

Figure D.15: Run [13] SL H8I6 (P-type iii): Single layered structure with substrate of 8 cm thickness and 6 % inclination.

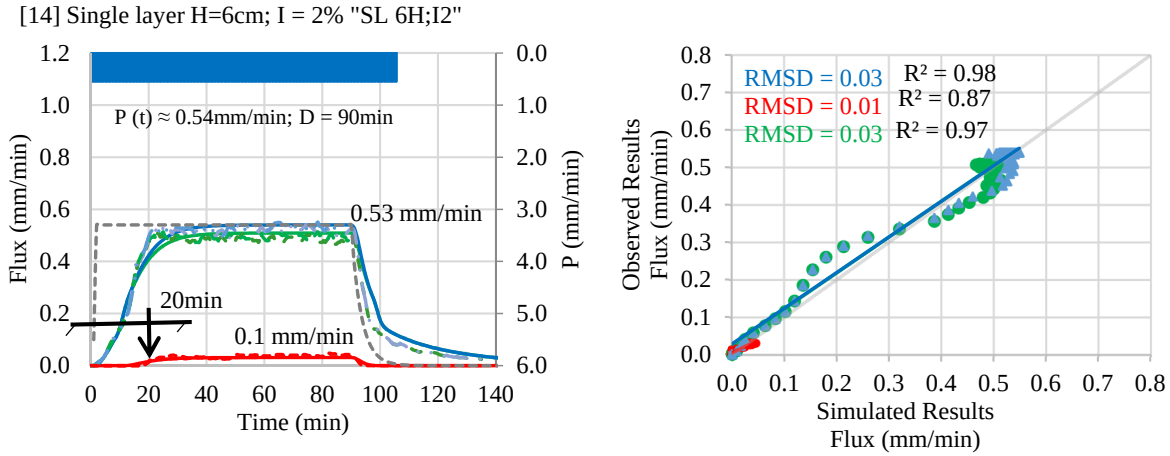

Figure D.16: Run [14] SL H6I2 (P-type iii): Single layered structure with substrate of 6 cm thickness and 2 % inclination.

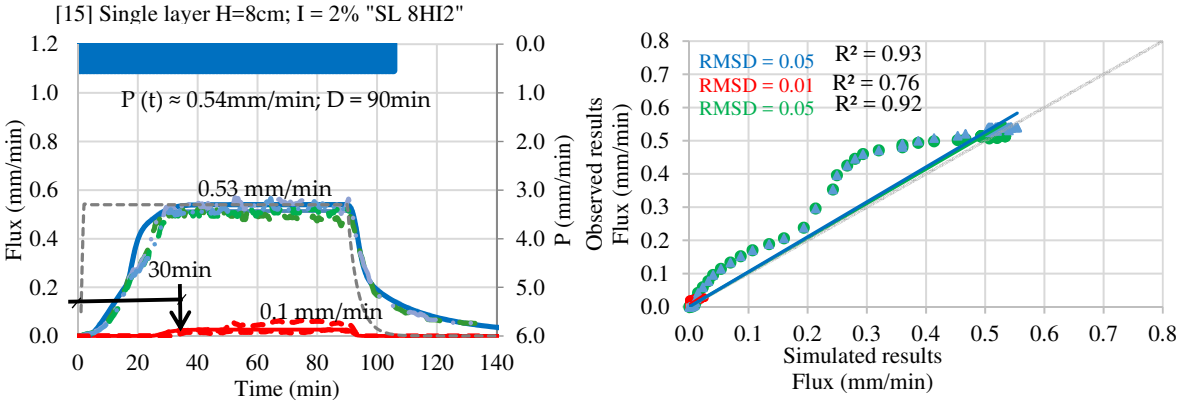

Figure D.17: Run [15] SL H8I2 (P-type iii): Single layered structure with substrate of 8 cm thickness and 2 % inclination.

Table D.3: Validation results of the green roof application studies with a multi-layered structure for rainfall type (i) and (ii).

Rainfall type:		(i)	(ii)		
Structure type:		Multi-layered (ML) - structure			
Structure details:		[16] ML H=6cm I=6%	[17] ML H=6cm I=6%	[18] ML H=6cm I=2%	[19] ML H=8cm I=6%
Input parameters (of boundary conditions):					
P (t); D*	(mm/min)	1.8mm/min; 15min	0.9 mm/min; 15min	1.0 mm/min; 15min	0.88mm/min; 45min
V_{ini}	(%)	22.0	22.2	34.2	25.6
Calibration values:					
$f_{H,sat}$	(-)	-	0.8	-	0.80
$f_{V,sat}$	(-)	-	-	-	-
c_0	(-)	0.08	0.08	0.08	0.08
$f_{I,sat}$	(-)	1.34	1.34	1.34	1.34
Results of the evaluation criteria:					
min. lag time (Δ)	(min)	3min / < 1min	6min / < 1min	8min / < 1min	6min / < 1min
time to peak (Δ)	(min)	15 min / < 1min	45 min / ≈ 1min	45 min / ≈ 1min	45 min / ≈ 1min
max. flux peak (Δ)	(mm/min)	1.3 mm/min - 2.0%	0.9 mm/min -1.0%	1.0 mm/min -0.3%	0.87 mm/min -1.2%
RMSD	(mm/min)	0.05 (2.8%)	0.05 (5.0%)	0.05 (5.0%)	0.03 (3.4%)
R^2	(-)	>0.95	>0.95	>0.95	>0.95

*P (t) = Rainfall intensity (mm) per minute (min); D = duration in minutes; RMSD = root mean square deviation as total value and (%) deviation of input flux; R^2 = coefficient of determination from the scatter plots; positve delta Δ = overestimation of simulated values; negative delta Δ = understimation of simulated values; "-" means no adjustment of the default value for the model calibration.

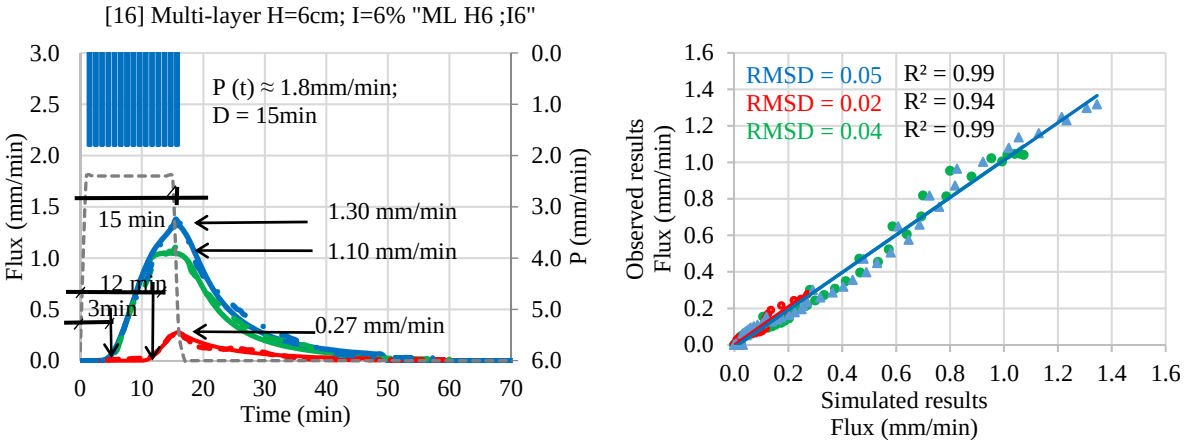

Figure D.18: Run [16] ML H6I6 (P-type i): Multi-layered structure with substrate of 6 cm thickness and 6 % inclination.

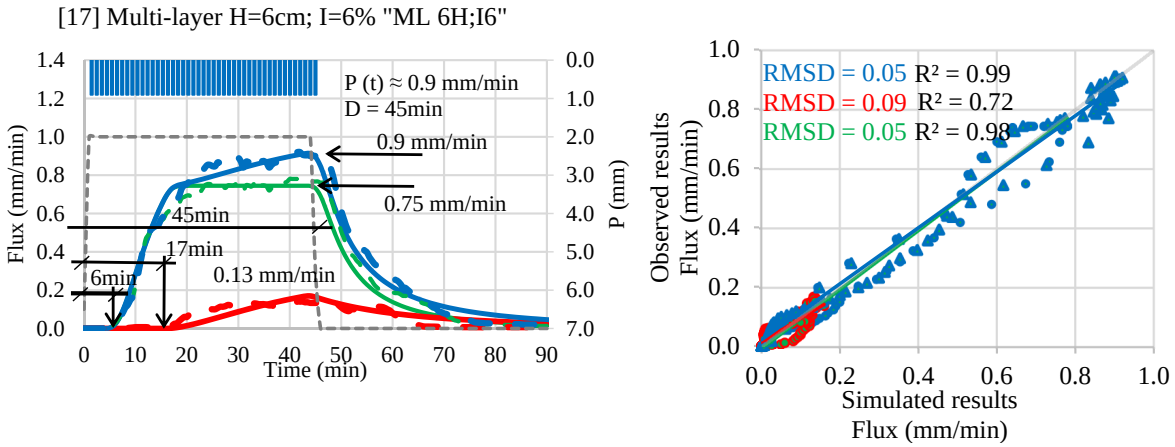

Figure D.19: Run [17] ML H6I6 (P-type ii): Multi-layered structure with a substrate of 6 cm thickness and 6 % inclination.

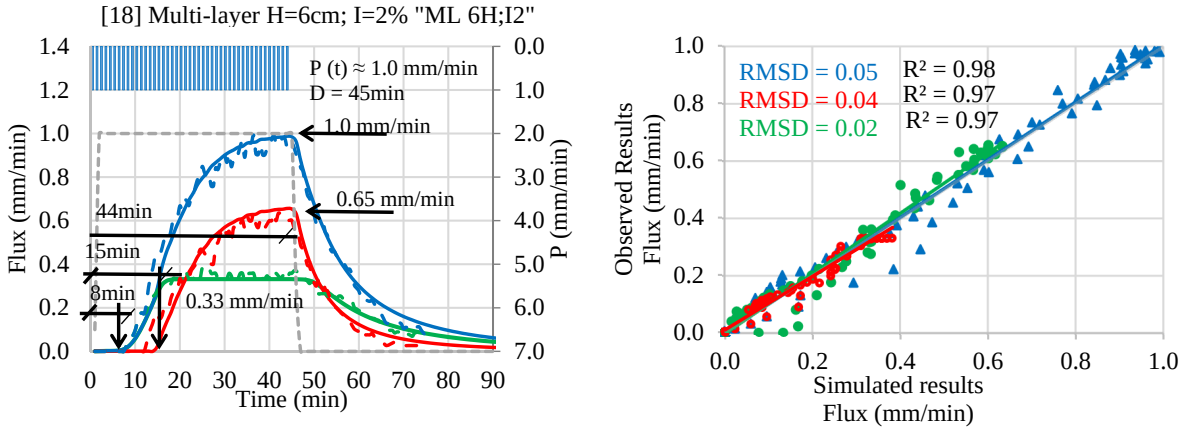

Figure D.20: Run [18] ML H6I2 (P-type ii): Multi-layered structure with a substrate of 6 cm thickness and 2 % inclination. (adopted from Hellmers and Fröhle [2017]).

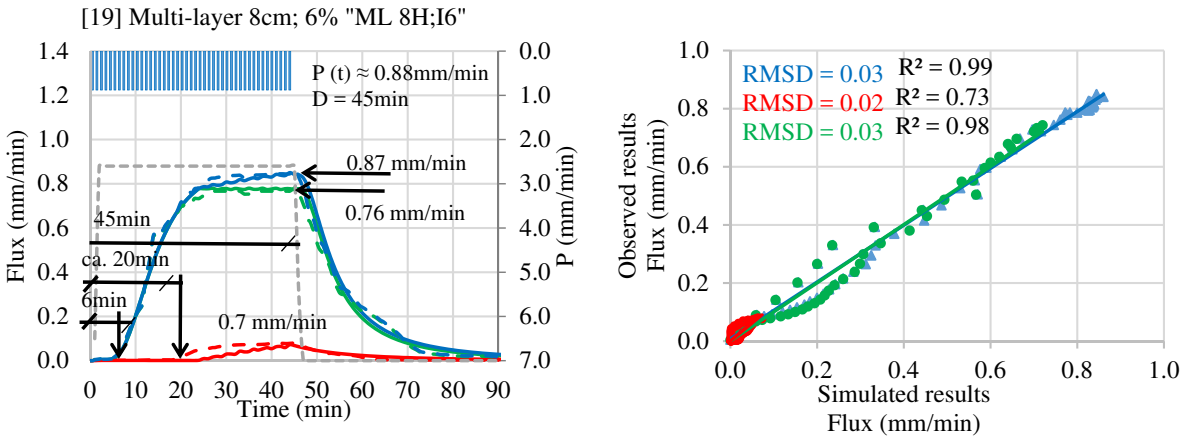

Figure D.21: Run [19] ML H8I6 (P-type ii): Multi-layered structure with a substrate of 8 cm thickness and 6 % inclination.

Table D.4: Validation results of the green roof application studies with a multi-layered structure for rainfall type (iii).

Rainfall type:		(iii)		
Structure type:		Multi-layered (ML) - structure		
Structure details:		[20] ML H=6cm I=6%	[21] ML H=8cm I=6%	[22] ML H=6cm I=2%
Input parameters (of boundary conditions):				
P (t); D*	(mm/min)	0.54 mm/min; 90 min	0.57 mm/min; 90 min	0.6 mm/min; 90 min
V_{ini}	(%)	25.9	25.7	33.5
Calibration values:				
$f_{H,sat}$	(-)	-	-	-
$f_{V,sat}$	(-)	-	-	-
c_0	(-)	0.08	0.08	0.08
$f_{I,sat}$	(-)	1.34	1.34	1.34
Results of the evaluation criteria:				
min. lag time / Δ	(min)	6min / ca. 2min	5min / < 1min	10min / < 1min
time to peak / Δ	(min)	45 min / < 1min	45 min / < 1min	70 min / < 1min
max. flux peak / Δ	(mm/min)	0.54 mm/min - 0.1%	0.57 mm/min - 0.1%	0.6 mm/min - 0.1%
RMSD	(mm/min)	0.03 (5.6%)	0.02 (3.5%)	0.04 (6.7%)
R^2	(-)	>0.95	>0.95	>0.95

*P (t) = Rainfall intensity (mm) per minute (min); D = duration in minutes; RMSD = root mean square deviation as total value and (%) deviation of input flux; R^2 = coefficient of determination from the scatter plots; positve delta Δ = overestimation of simulated values; negative delta Δ = understimation of simulated values; "-" means no adjustment of the default value for the model calibration.

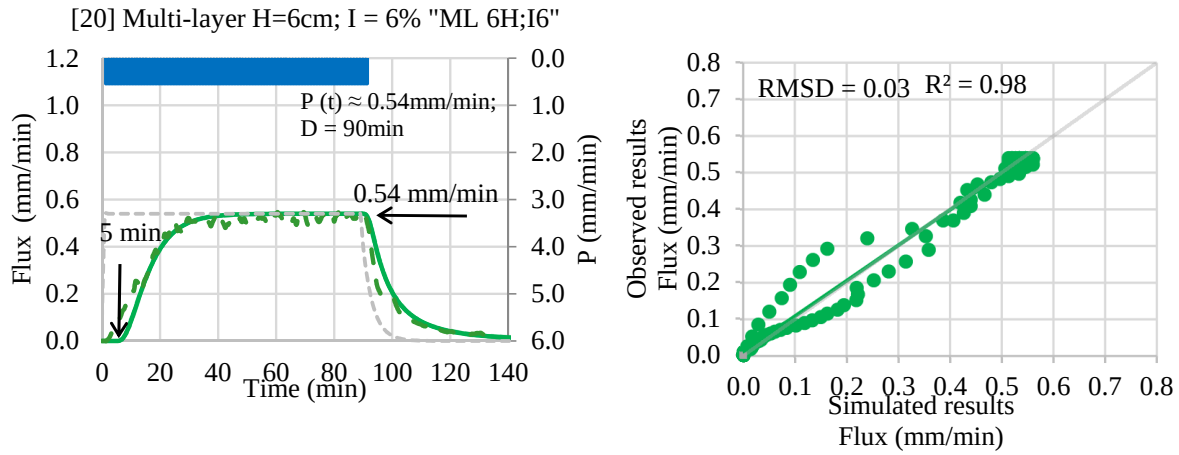

Figure D.22: Run [20] ML H6I6 (P-type iii): Multi-layered structure with a substrate of 6 cm thickness and 6 % inclination.

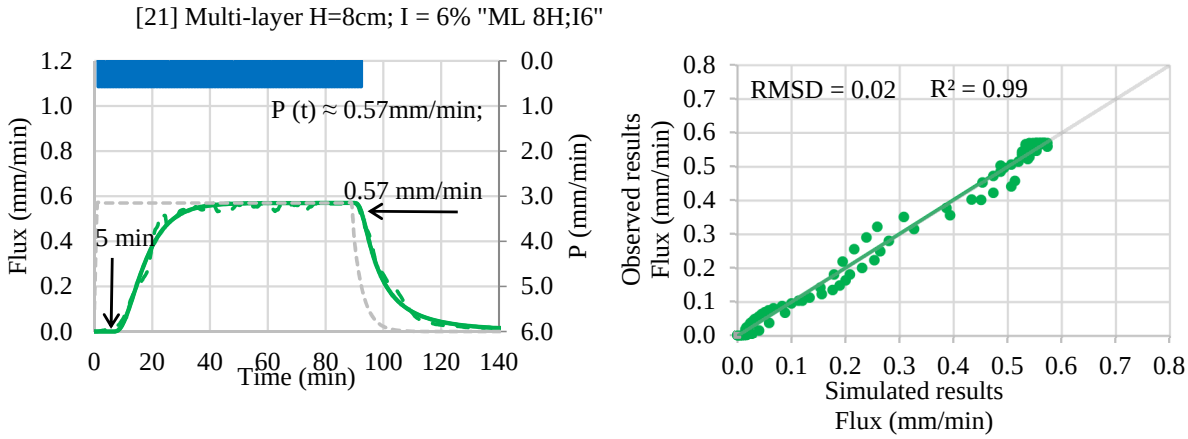

Figure D.23: Run [21] ML H8I6 (P-type iii): Multi-layered structure with a substrate of 8 cm thickness and 6 % inclination.

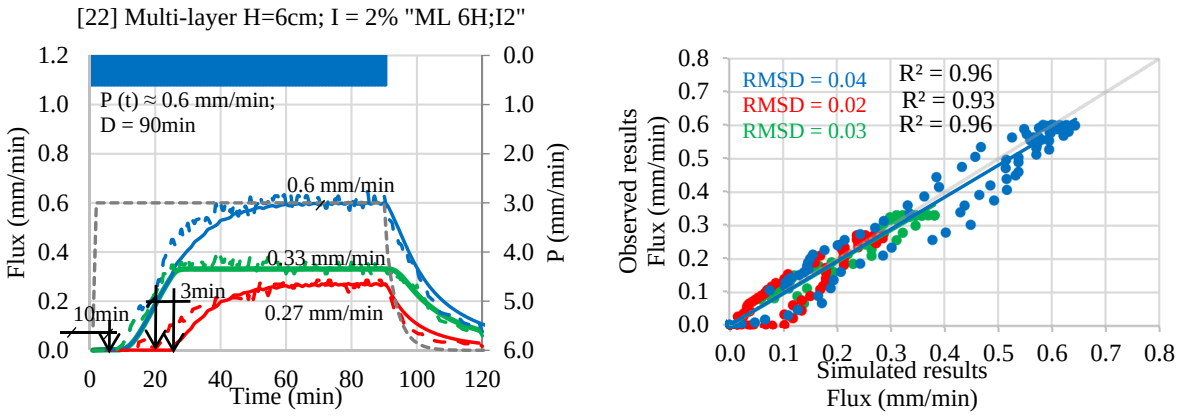

Figure D.24: Run [22] ML H6I2 (P-type iii): Multi-layered structure with a substrate of 6 cm thickness and 2 % inclination.

Soil moisture validation results

For a limited set of four laboratory experiments of the multi-layered structures (namely the runs [16], [17], [20] and [21]) additional soil moisture measurements are analysed. The results of the multi-layered structure with 6 cm thickness of substrate and a gradient of 6 % for the different rainfall types are illustrated. The numerical model results of this work are compared with soil moisture measurements by Giacomelli [2017][7]. He described as well the measuring device and the procedure. The legend is extended with the respective soil moisture data in brown colour (see figure D.25). The different dashed lines point out three runs per experiment. A variation in scales according to the three rainfall types (i) to (iii) is defined.

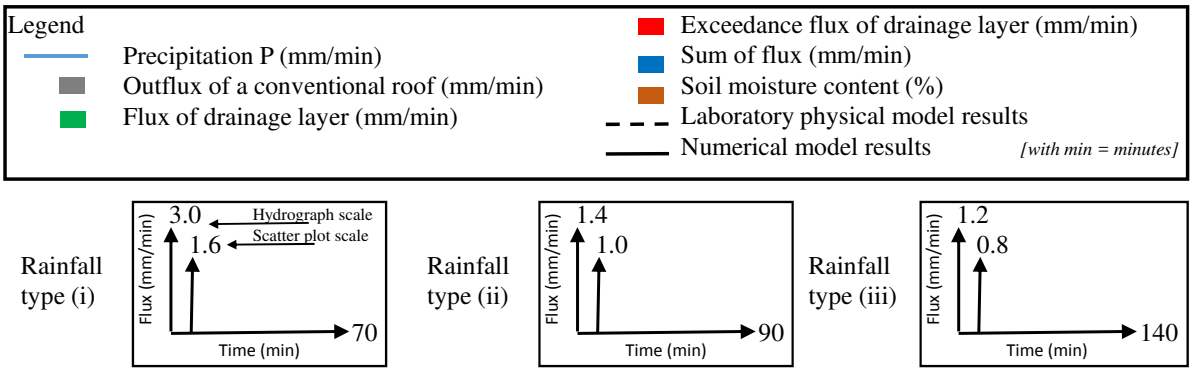

Figure D.25: Legend of the validation results including the numerical and observed output of soil moisture contents.

[7] Giacomelli, M. (2017). Soil moisture content in green roofs: Investigations through laboratory experiments and numerical calculations (Master Thesis). Supervised by Justus Patzke. Examiners: Prof. Dr.-Ing. Peter Fröhle and Dr. Xavier Gabarrell Durany. Hamburg University of Technology, Hamburg, Germany.

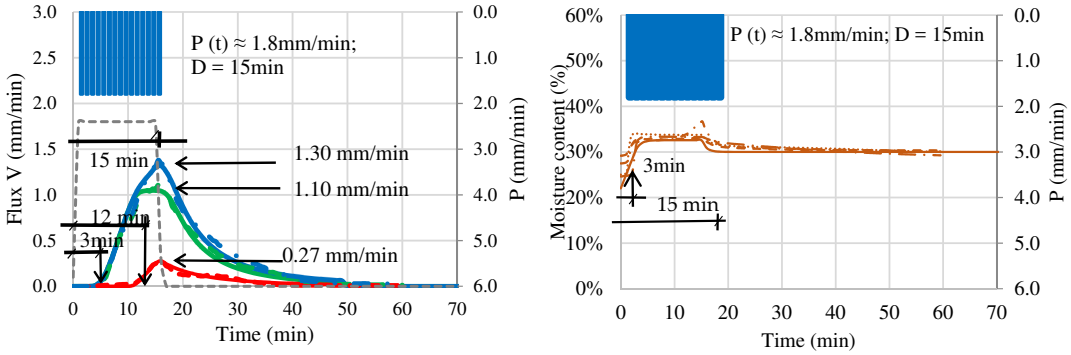

Figure D.26: Flux and soil moisture content results of run [16] ML H6I6 (P-type i): Multi-layered structure with substrate of 6 cm thickness and 6 % inclination.

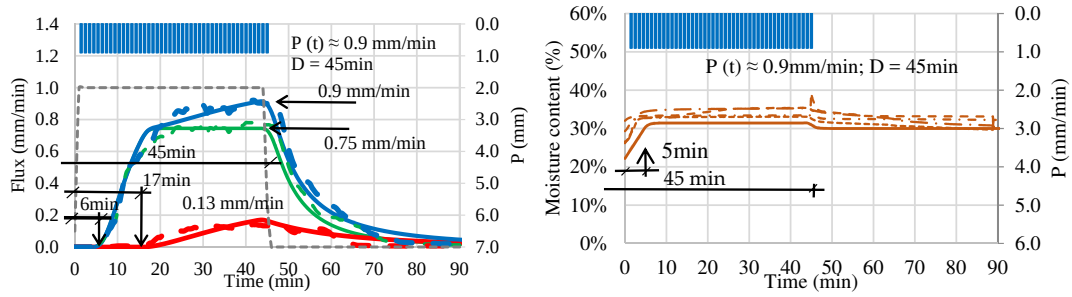

Figure D.27: Flux and soil moisture content results of run [17] ML H6I6 (P-type ii): Multi-layered structure with a substrate of 6 cm thickness and 6 % inclination.

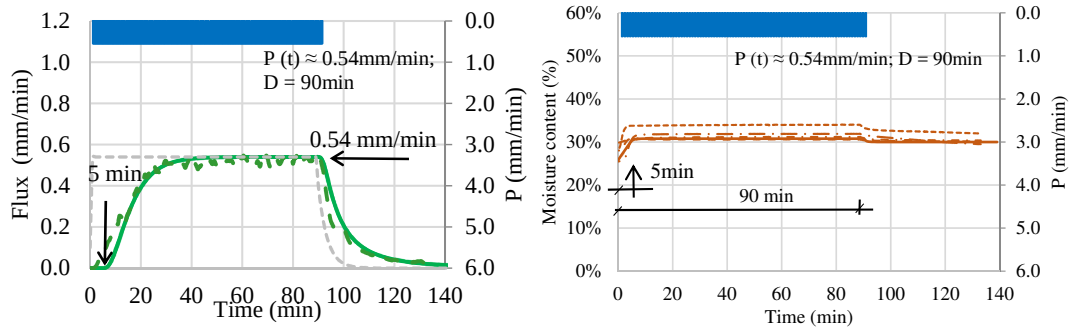

Figure D.28: Flux and soil moisture content results of run [20] ML H6I6 (P-type iii): Multi-layered structure with a substrate of 6 cm thickness and 6 % inclination.

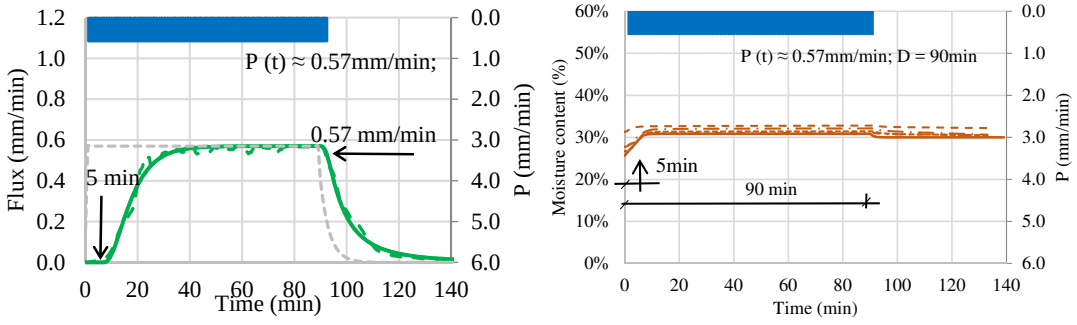

Figure D.29: Flux and soil moisture content results of run [21] ML H8I6 (P-type iii): Multi-layered structure with a substrate of 8 cm thickness and 6 % inclination.

D.2 Supplementary data and diagrams of the meso scale application studies

This attachment D.2 provides supplementary data about the simulated results of the regional scale backwater affected catchment "Dove-Elbe". In the sections D.2.1 to section D.2.4 supplementary maps as well as tables are provided to illustrate the locations and attributes of streams, control structures and LSDMs. In the section D.2.5 and section D.2.6 the results of an evaluation of the generated GIS-based maps and network generation including LSDMs are given. Supplementary information about the evaluation of the developed KM1-method to compute the flood routing and the method to compute backwater effects are provided in section D.2.7 and section D.2.8. The performance of LSDMs to mitigate discharge and water levels in backwater affected streams is analysed for the catchment "Moorfleet". The results are summarised in section D.2.9. The developed and implemented methods to computate the hydrological processes in LSDMs are tested by analysing the output hydrographs in section D.2.10 and with mass-conservation criteria in section D.2.11.

D.2.1 Maps of control structures and profile categories of stream segments

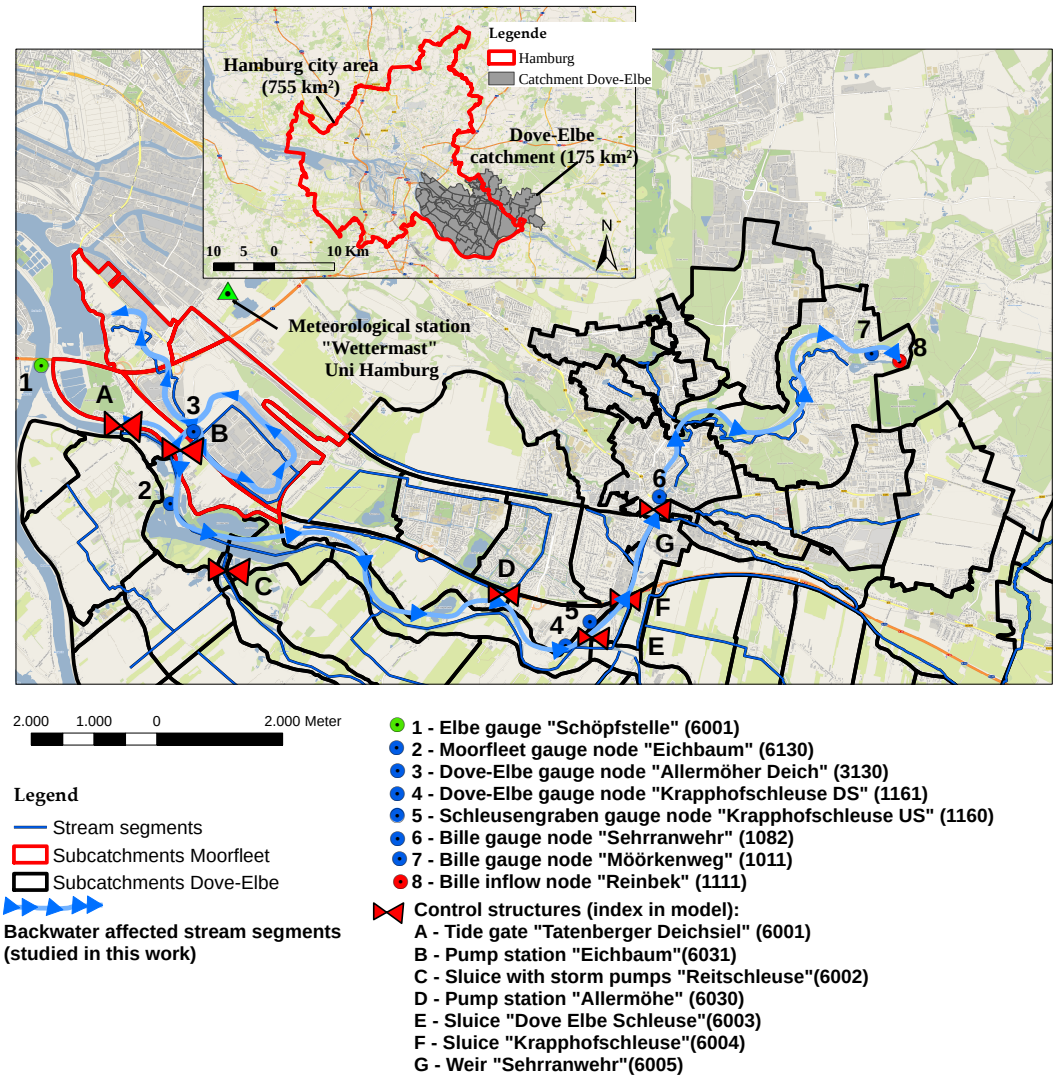

Figure D.30: Map of studied stream segments and control structures. The elements are labelled as follows: gauging station nodes (1 to 8), control structures (A to G), backwater affected stream segments (indicated in light blue) and low lying subcatchments of 'Moorfleet' (indicated in red). The arrows of the backwater affected stream segments (strands) indicate the direction of backwater effects. (background map: www.ows.terrestris.de).

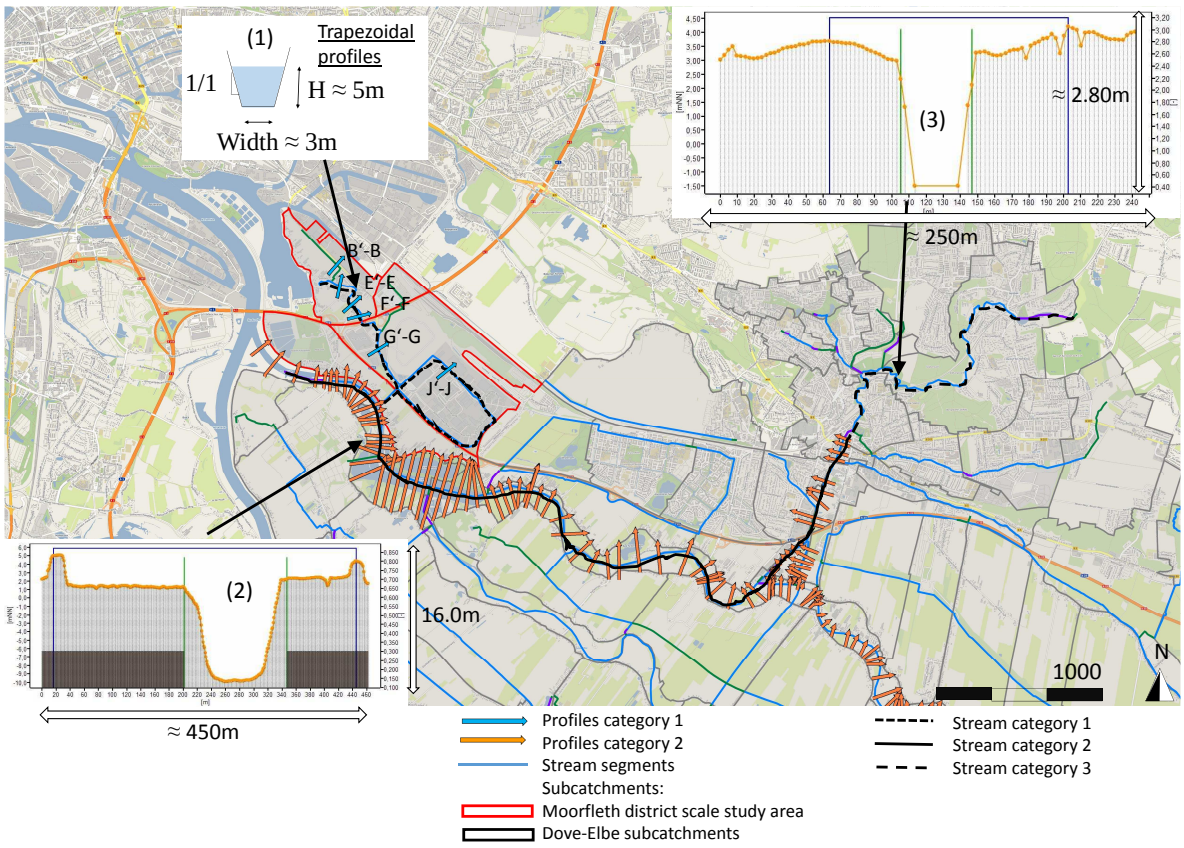

Figure D.31: Map of three categories of stream segment profiles. (1) Stream segments on district scale with trapezoidal profiles, (2) measured profiles with large forelands along the Dove-Elbe stream segments and (3) adopted profiles along the Bille stream segments (background map: www.ows.terrestris.de).

D.2.2 Summary of control structures in the Dove-Elbe catchment

The control structures in the Dove-Elbe study area are listed in table D.5. The structures comprise several control functions which are numbered in the order of activation. The basic control function is given on level (1). When another control function criterion is fulfilled, the control functions are switched. For each time step a different control functions can be activated according to the criteria and the driver time series. These time series can be observed water levels imported into the model or simulated water levels (see "Simulated (W)" in table D.5). The simulated driver time series are computed during the execution of the model. The methodology to activate the control functions is described in section 6.2 (p. 86). The criteria of the control structures in the catchment "Dove-Elbe" are determined on the basis of the report by BWS GmbH [2011].

Table D.5: Summary of control structures and functions of the Dove-Elbe and Moorfleet case study areas. Data is determined on the basis of the report by BWS GmbH [2011].

Control structure name	Index in model	Index in map D.30	Driver type	Driver node index in model	Number of control functions
Tatenberger Deichsiel	6001ctrl	A	Observed (tidal affected) water level stages (W)	6001_ds	2
	(1) Tide gate is opened when the downstream water level in the Elbe river falls below the operational water level in Dove-Elbe over a duration of 30 minutes. (2) Tide gate is closed when downstream water level in the Elbe river exceeds the operational water level (about 0.9 m a.s.l.) in Dove-Elbe over a duration of 30 minutes.				
Eichbaum SW	6031ctrl	B	Simulated (W)	3160	5
	(1) no pumping. (2) minimal intermediate base-level pumping. (3) Starting first pump (1.15 m³/s) when water level reaches -0.85 m a.s.l. (4) Starting second pump (1.15 m³/s) when water level reaches -0.80 m a.s.l. (5) Starting third pump (1.15 m³/s) when water level reaches -0.75 m a.s.l.				
Reitschleuse SP	6002ctrl	C	Simulated (W)	3070	2
	(1) Sluice gate is opened when downstream water level falls below 1.1 m a.s.l. in Dove-Elbe stream segments over a duration of 30 minutes. (2) Sluice gate is closed when downstream water level exceeds a water level of 1.1 m a.s.l. in the Dove-Elbe stream segments over a duration of 30 minutes. Storm pumps are operated with a maximal capacity of 4 x 1.9 m³/s.				
Allermöhe SW	6030ctrl	D	Simulated (W)	3160	4
	(1) no pumping. (2) First full running pump (1.5 m³/s) when water level reaches -0.85 m a.s.l. (3) Second full running pump (1.5 m³/s) when water level reaches -0.80 m a.s.l. (4) Second full running pump (1.5 m³/s) when water level reaches -0.75 m a.s.l.				
Dove-Elbe Sluice	6003ctrl	E	Simulated (W)	1161	2
	(1) Sluice gate is opened when the downstream water level falls below 1.1 m a.s.l. in the Dove-Elbe stream segments over a duration of 30 minutes. (2) Sluice gate is closed when downstream water level exceeds a water level of about 1.1 m a.s.l. in the Dove-Elbe stream segments over a duration of 30 minutes.				
Krapphof Sluice	6004ctrl	F	Simulated (W)	1011	2
	(1) Sluice in operation with an upstream water level of 1.4 m a.sl. (2) Sluice is closed (not in operation) during high water levels and a chute is opened.				
Sehrran Weir	6005ctrl	G	Simulated (W)	1011	1
	(1) Fixed crest weir is closed with an overflow hight on +3.0 m a.s.l. Operational upstream water level is about +3.15 m a.s. l.				

* explanations: SW = Schöpfwerk (pumping station); SP = Sturmpumpen (storm pumps).

D.2.3 Map of surface sealing rates and topographical data (Moorfleet)

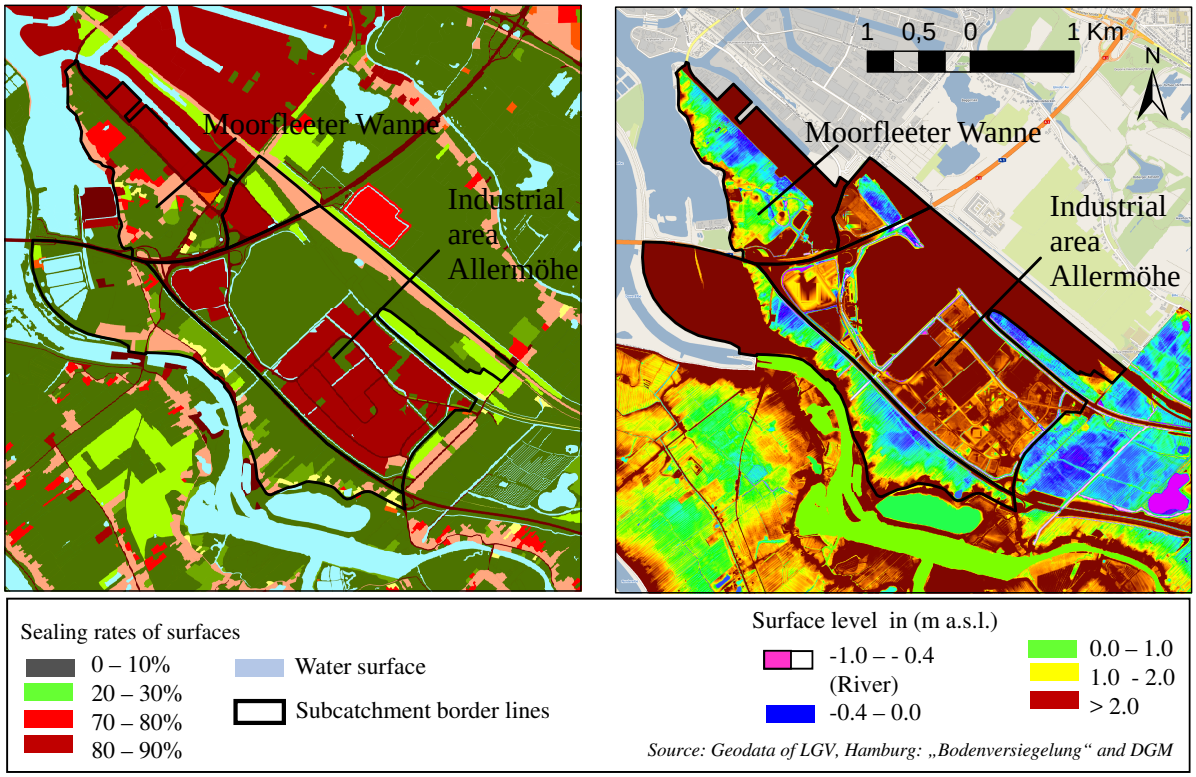

Figure D.32: Map of sealing rates and elevation data of the case study area Moorfleet which is part of the tidal influenced catchment Dove-Elbe (background map: www.ows.terrestris.de).

D.2.4 Map of installed LSDMs in Moorfleet

In the application studies different scenarios are modelled. In scenario 2, LSDMs are installed only in the upstream subcatchment "Moorfleeter Wanne", while in scenario 3 LSDMs are installed in the upstream and downstream subcatchments of Moorfleet. The overall LSDMs comprise 24 green roofs, 23 cistern systems and 7 multifunctional areas. The location of installed LSDMs are illustrated in the map in figure D.33. The area Moorfleet has a size of about 8.42 km^2. The total area of green roofs has a size of about 274 840 m^2 (0.275 km^2) which are coupled to cisterns with a total area of 5376 m^2 (0.005 km^2) and multifunctional areas with a total extent of 47 814 m^2 (0.048 km^2).

Figure D.33: Map of LSDMs installed in the Moorfleet study areas [Scenario 3] (background map: www.ows.terrestris.de).

D.2.5 Evaluation results of the GIS-based mapping of local scale data

To integrate the large number of LSDM data structures per meso scale subcatchment, GIS-based data import and data processing functions are applied. The methodology of the GIS-based mapping is described in section 4.1 (page 53 ff.). Because of the fact, that LSDM data structures are situated within contours of meso scale subcatchments, relevant preset parameters of meso scale attributes are adopted for local scale data structures. These meso scale parameters are defined in shapes to describe the prevailing pedology, geology, landuse and watershed parametrisation. By the intersection of data, Hydrological Response Units (HRUs) are created which are made up of different layers. These HRUs are the smallest spatial units defined in the semi-distributed hydrolological model. The LSDM parameters are lying "over" the HRU parameters and replace them if values are defined. To split the LSDM data structures from the meso scale data structures another spatial intersection is performed.

In this attachment, the results of a model verification concerning the mapping of LSDMs

within the application study Moorfleet is presented. The study area is described in section 8.2 (page 131). The verification procedure of mapping LSDMs is performed in four steps on the basis of different data sources as illustrated in figure D.34 and listed in table D.6.

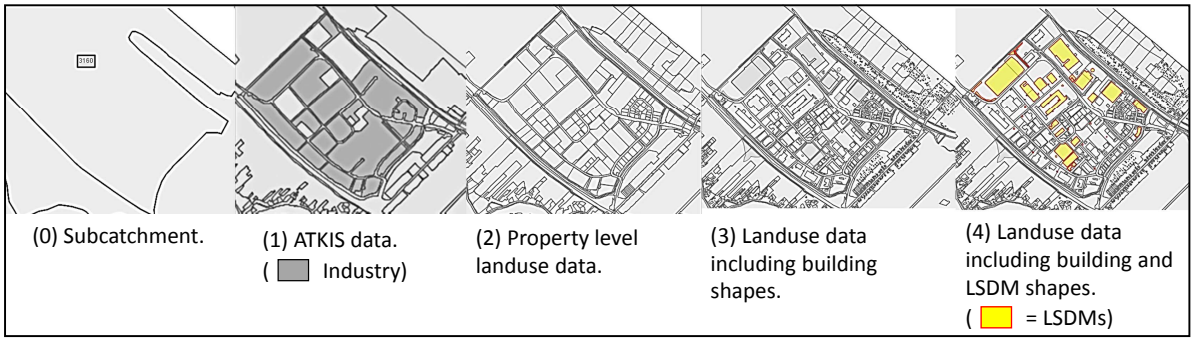

Figure D.34: Illustration of the applied data sources and different steps in the GIS-based data processing.

Table D.6: Verification results of the GIS-based mapping of local scale data using the example of the subcatchment "Moorfleeter Wanne".

Data source	Description	Sealed area (ha)	Permeable area (ha)	Sum of LSDM areas (ha)	Aggregated sum of areas (ha)	Bias	Number of HRUs
0	Spatial size of subcatchment area	--	--	--	159.75	--	--
1	ATKIS data	53.93	105.81	--	159.74	0.01%	105
2	Property level landuse data	44.61	115.02	--	159.62	0.08%	605
3	Landuse data including buildings	44.61	115.02	--	159.62	0.08%	611
4	Creation of landuse data including LSDMs	41.01	113.67	4.94	159.62	0.08%	611

* study of the subcatchment: "Moorflether Wanne" (3150). Areas are given in (ha) = hectare.

In a first step, with data source (1), the object based landuse data of ATKIS[8] is preprocessed and each landuse object is defined with a sealing rate, vegetation type and approximated drained proportion to the stormwater drainage system. In step (2), detailed landuse description data based on drainage information of each property by the Hamburg Water Agency ("Hamburg Wasser") is applied to setup a detailed landuse shape. The data source defines for each property area the spatial proportion which is drained to the stormwater drainage systems. In step (3), the landuse data is updated with the shape file of buildings and in step (4), the final data is intersected with the shape file of LSDMs. After the data processing steps (1) to (4) the proportions of impervious, permeable and LSDM areas are analysed. For the

[8] ATKIS = "Amtliches Topographisch-Kartographisches Informationssystem".

verification test, the aggregated sum of areas after each data processing step is checked to be in congruency with the total area of the subcatchment "Moorfleeter Wanne" (3150). The results are listed in table D.6. This verification procedure checks the "mass-conservation" with regard to computed areas during the GIS-based mapping process. The aggregated sums of areas show a bias of about 0.08 % which meets the evaluation criteria in table 8.10 (see p. 137) to be less than 1 %. The number, kind and size of LSDMs are described in the following section D.2.6.

D.2.6 Evaluation of the hydrological network generation including LSDMs

The model algorithm to create a hydrological network accomplishes a directed order with an explicit start (upstream) and an explicit end (downstream) according to the flow direction. This order defines a directed graph with incoming tributaries. Different types of stream segments allow the distinction between "virtual" (auxiliary connections), "real" (connectors with flood routing features) and reservoir stream segments (including control functions). The method is extended within the scope of this work with additional auxiliary stream segments and junctions nodes on the local scale to create a directed graph, which orders the overlay data structures (namely LSDMs) from the source to the target elements within a hydrological network.

An example of such a net-generation is illustrated in figure D.36 which is created on the basis of the drainage criteria given in table D.7 and the indicated elements in figure D.35. The LSDMs include green roofs (GRs), cistern systems (Cs) and multifunctional areas (MFAs). The developed algorithm prevents the generation of closed loops by circular links among the network elements. The calculation order in figure D.36 shows that the source elements are computed before the target elements. This hydrological network corresponds to scenario 2 where LSDMs are only implemented in the subcatchment "Moorfleeter Wanne" (model index 3150). The scenarios are described in section 8.2.4 (page 134 ff).

Table D.7: Criteria of drainage fractions for the "on-the-fly" network generation including LSDMs (here for the subcatchment "Moorfleeter Wanne", model index 3150).

Source	Drainage fraction (%)	Sink (target)	Source	Drainage fraction (%)	Sink (target)
Subcatchment 3150*	10	MFA1	GR4	100	C2
	8	C2	GR5	100	C2
	2	C3	GR6	100	C3
	1	C1	C1	100	Node 3150
	79	Node 3150	C2	100	Node 3150
GR1	100	C1	C3	100	Node 3150
GR2	100	C1	MFA1	100	Node 3150
GR3	100	C1	MFA2	100	Node 3150

*The surface runoff of sealed areas is drained to LSDMs; Node 3150 is the subcatchment outlet.

Figure D.35: Map of subcatchments and stream segments in the Moorfleet study area, which form the hydrological network in figure D.36.

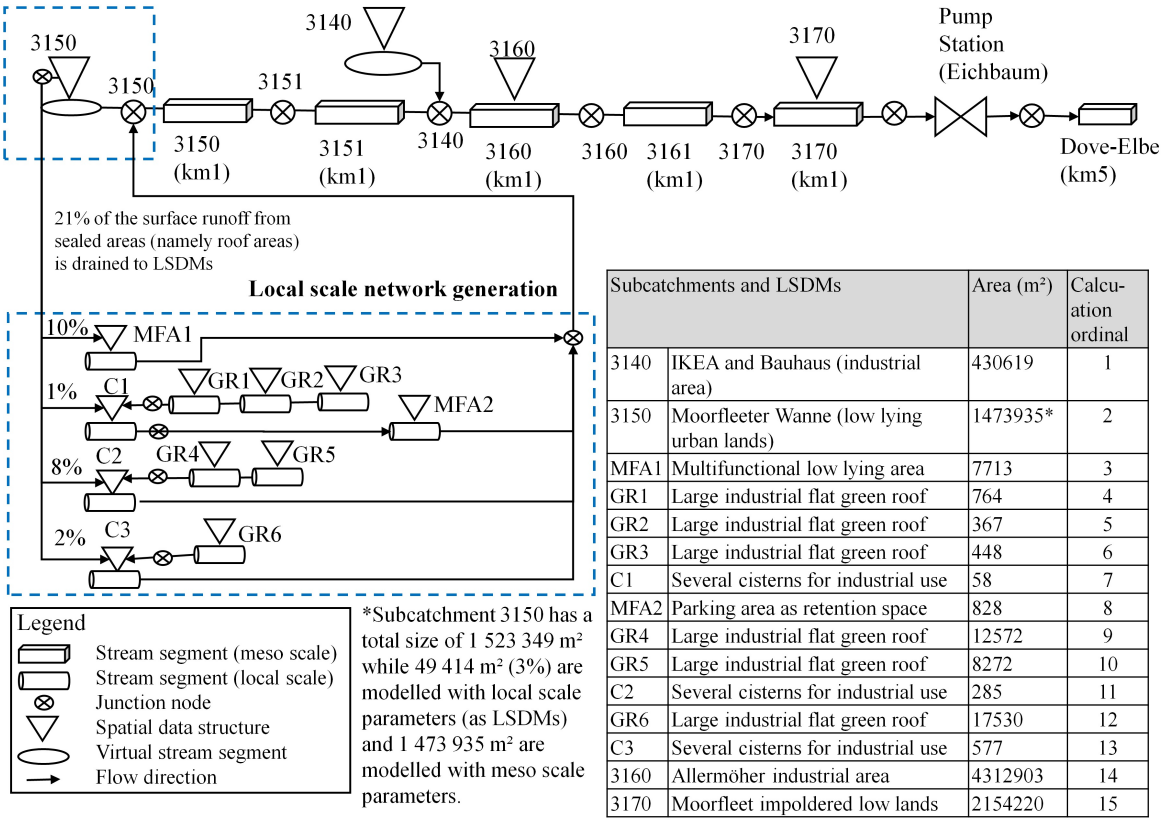

Subcatchments and LSDMs		Area (m²)	Calcu-ation ordinal
3140	IKEA and Bauhaus (industrial area)	430619	1
3150	Moorfleeter Wanne (low lying urban lands)	1473935*	2
MFA1	Multifunctional low lying area	7713	3
GR1	Large industrial flat green roof	764	4
GR2	Large industrial flat green roof	367	5
GR3	Large industrial flat green roof	448	6
C1	Several cisterns for industrial use	58	7
MFA2	Parking area as retention space	828	8
GR4	Large industrial flat green roof	12572	9
GR5	Large industrial flat green roof	8272	10
C2	Several cisterns for industrial use	285	11
GR6	Large industrial flat green roof	17530	12
C3	Several cisterns for industrial use	577	13
3160	Allermöher industrial area	4312903	14
3170	Moorfleet impoldered low lands	2154220	15

Figure D.36: Flow chart of the generated network for the subcatchments in Moorfleet with the drainage criteria of linked LSDMs in table D.7 and calculation ordinals giving an explicit computation sequence.

D.2.7 Evaluation results of the flood routing computation

In this section, the evaluation of the flood routing computation with the developed method "KM1" is explained. The KM1-method is explained in section 6.1 (p. 78 ff). This attachment contributes to the findings in the application study results in Moorfleet (see section 8.3.1, p. 140 ff). First, the flood routing on the local scale is computed and tested with respect to mass-conservation criteria and sensitivity of the input parameters. Secondly, the flood routing computation of stream segments in the subcatchments "Moorfleet" are compared with results of another study. Measurements of gauging stations are not available for this local scale study area Moorfleet, but additional tests of the flood routing and backwater effect computation on the meso scale streams are performed, where measurements are available. That results are explained in the following section D.2.8.

Verification of the "KM1" method to model local scale flood routing: The input parameters for the flood routing method "KM1" are defined per source data structure. An example is given in this section for the LSDM structures shown on the map in figure 8.5 on page 135. The input parameters are summarised in table D.8. The flood routing from green roofs (GRs) to a cistern system (C1) and further on to multifunctional areas (MFAs) is done with circular closed streams using the approach of Darcy Weisbach. The flood routing from MFAs to the receiving streams is done with open water trapezoidal profiles using the approach of Manning-Strickler. The entry "(-)" indicates that the parametrisation is not required for the chosen calculation method "darcy" (Darcy Weisbach) or "manning" (Manning-Strickler).

Table D.8: Input parameters for the computation of the flood routing with the KM1-method. The streams are generated automatically on local scale among LSDMs. The locations of these LSDMs are given in figure 8.5 (page 135).

LSDM name	Width (m)	I_{bank} (-)	K_{st} ($m^{1/3}$ / s)	$H_{bankfull}$ (m)	D_{hydr} (m)	K_s (m)	n = calc_steps	profile form	I_{min} (-)	factor L (-)	calc method
MFA1	0.5	1E-06	30	0.3	-	-	25	angular	0.001	1.5	manning
MFA2	0.5	1E-06	30	0.3	-	-	25	angular	0.001	1.5	manning
GR1	-	-	-	0.1	0.1	0.02	25	circular	0.001	1.5	darcy
GR2	-	-	-	0.1	0.1	0.02	25	circular	0.001	1.5	darcy
GR3	-	-	-	0.1	0.1	0.02	25	circular	0.001	1.5	darcy
C1	-	-	-	0.1	0.1	0.02	25	circular	0.001	1.5	darcy

The results of the flood routing computation are written in output files of the rainfall-runoff model KalypsoNA. For selected elements the results are summarised in table D.9. The difference between inflow and outflow hydrographs is less than 0.01 %. This fulfils the evaluation parameter for the model verification with mass-conservation criteria.

The local scale flood routing computation using the geographical location of the elements is a new algorithm implemented in the rainfall-runoff model KalypsoNA. A different and

Table D.9: Formal parameters of the computed flood routing among LSDMs using the KM1-method. The comparison of inflow volume V_{in} and outflow volume V_{out} is part of the mass-conservation tests.

LSDM (source)	surface level (m a.s.l.)	Target element (sink)	flow path length L (m)	L_c (m)	n (-)	K_c (s)	V_{in} (m³)	V_{out} (m³)	Difference Δ (%)
Input parameters			Formal parameters				Output parameters		
MFA1	-0.8	node 3150*	60.7	110.8	1	3.8	3998.1	3998.1	< 0.01
MFA2	2	node 3150*	37.5	110.8	1	2.4	674.0	674.0	< 0.01
GR1	2	C1	82.0	40.0	2	4.8	42.5	42.5	< 0.01
GR2	2	C1	15.0	40.0	1	4.8	17.1	17.1	< 0.01
GR3	2	C1	30.6	40.0	1	4.8	21.0	21.0	< 0.01
C1	2	MFA2	51.6	40.0	1	4.8	273.4	273.4	< 0.01

* node 3150 is situated on -0.8 m a.s.l

commonly used method in semi-distributed models is the IUH-approach using the retention constants *k* and *n* on the subcatchment scale (see section B.4). It has been one of the objectives of this work to develope a more precise flood routing method without changing the general approach of using a semi-distributed model. Using the IUH method for the flood routing of district scale LSDMs leeds to on overestimation of the retention effects. An example of using the meso scale and the local scale flood routing methods is given in figure D.37. It is concluded that using the IUH method of the meso scale for the local scale flood routing computation and neglecting the geographical location does not give sufficient results. The developed algorithm in this work presents a more precise hydrological method by using the geographical location of structures and the input parameters of stream profiles.

Verification of the "KM1" flood routing method to model the stream segments in "Moorfleet".
The input parameters of the stream segments in the Moorfleet study area are summarised in table D.10. To determine these values, the documented measurements of the profiles in the catchment area "Moorfleet" by Krob et al. [2000] are applied. The analysed storm event in August 2002 took place two years after the measurements. It is assumed that sludge removal changed the roughness as well as bed gradients in comparison to the measurements in 2000.

An adjustment of the input parameters for the flood routing computation has been done on the basis of measured data at the downstream located pumping station for the event in August 2002. The available water level data is limited to this event. A parameter adjustment was required for the cross-sections, the bed level gradient and the Manning-Strickler parameter in the main stream strands. The cross-sections are increased in width with a factor f_{width} ranging between 1.0 to 4.0 to take into account the storage and retention capacity of tributary drainage ditches. The gradient (I_s) measured by Krob et al. [2000] was indicated to be very low (between 0.002 to 0.06 %) by taking into account high sludge levels. The fast reaction of the system is illustrated in figure D.39 with a gradient between 0.1 to 0.5 %

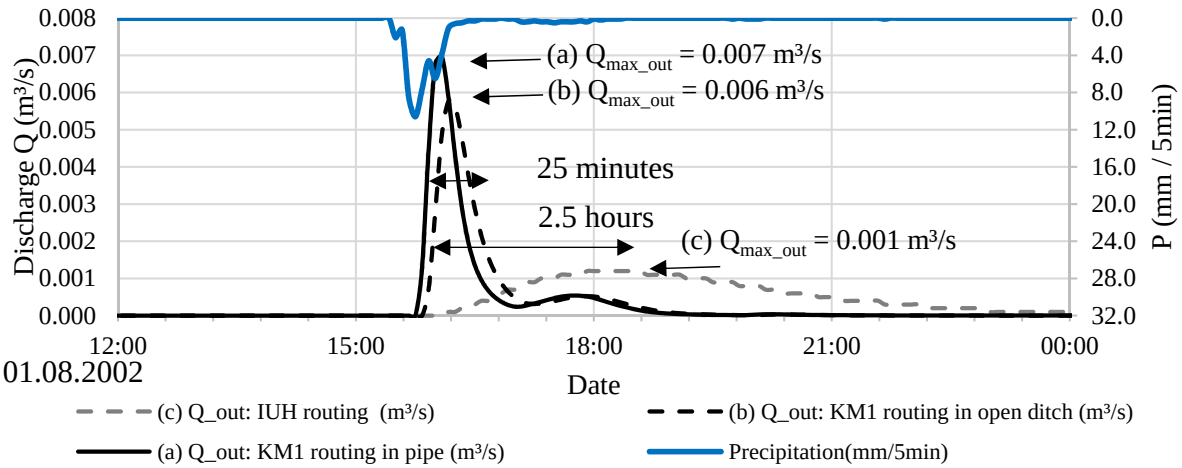

	Method	Description
(a)	KM1-routing	Pipe with a diameter of 30cm over a length of 15m (calculated via geographical location). Time to peak about 20 minutes.
(b)	KM1-routing	Open water swale with 2m width and high roughness over a length of 15m (calculated via geographical location). Time to peak about 25 minutes.
(c)	IUH-method	Using the flood routing approach according to the subcatchment scale parameters. Time to peak about 2.5 hours.

Figure D.37: Results of the sensitivity study using different surface runoff routing methods for the drainage computation from a green roof (GR2) to a cistern (C1). The locations are given in the map in figure 8.5 on page 135.

and a Manning-Strickler roughness (K_{st}) of 30. The adjusted values are summarised in table D.11.

In this work, the discharge Q (m^3/s) is computed on the basis of the wetted cross-section and the velocity calculated with the approach of Manning-Strickler for stationary uniform flow states in the main flow section. The average discharge Q_m is computed among the water level step points and is applied in the KM1-method computation. For each stream segment a result file is written during the execution of the model KalypsoNA.4.0.0 and given in the extension folder. The results of the computed water level (W) and discharge (Q) relations with the KM1-method are compared with the results published in the report by Krob et al. [2000], where a different numerical model was applied. Both W-Q-curves are illustrated in figure D.2.7. These results illustrate the fulfilment of the evaluation criteria in section 8.3.1 (p. 140) with a bias of less than 0.01 %.

The results of the flood routing computation for the event in August 2002 are illustrated in figure D.39 using the unadjusted and adjusted stream segment parameters. The retention effect is illustrated by comparing the inflow and outflow hydrographs. The peak flow is reduced in both cases. The input and output curve data of the stream segments are written in the result files of the extension folder.

Table D.10: Profile data of the stream segments in the Moorfleet study area. The stream segments (indexes 3150 to 3170) are indicated on the map in figure D.35 (page D24). The locations of the profiles (indexes B to J) are given in the map D.31 (page D18).

Stream index	Stream name	Profile index	Stream length L	Bed level height (m a.s.l.) *	Roughness K_{st} ($m^{(1/3)}/s$)	Gradient I_s(m/m) *	Width (m) *	Bankfull height * (m a.s.l.)	I_{bank} (1:m) *	Mean water level (m a.s.l.) *
3150km1	Andreas-Meyer-Graben	B-B'	1216.0	-0.88	25	0.060%	0.9	1.2	0.5	-0.80
3151km1	Moorflether Schlauchgraben (Upstream)	E-E'	1397.0	-1.60	25	0.040%	2.6	1.6	0.8	-0.87
		F-F'	493.0	-1.92	30	0.002%	1.8	1.9	0.8	-0.88
3160km1	Moorflether Schlauchgraben (Downstream)	G-G'	1026.0	-2.30	30	0.002%	3.5	3.3	1.0	-0.89
3161km1	Moorflether Hauptgraben	J-J'	4685.0	-2.35	30	0.004%	3.5	4.3	1.5	-0.91
3170km1	Schöpfwerksgraben	--	247.0	-2.35	30	--	25.0	2.3	0.0	-0.92

* According to measurements given in the report Krob et al. [2000].

Table D.11: Adjusted parameters for the flood routing computation of the Moorfleet study area for the event in August 2002. The basis parameters are reported measurements of the profiles in the year 2000 by Krob et al. [2000]. The index of stream segments is given in figure D.35 (page D24).

	I_s (m/m)	f_{width} (-)	K_{st} ($m^{(1/3)}/s$)
3150km1	0.10%	4.0	30.0
3151km1	0.10%	3.0	30.0
3152km1	0.10%	3.0	30.0
3160km1	0.50%	2.0	30.0
3161km1	0.50%	3.7	30.0
3170km1	0.20%	1.0	30.0

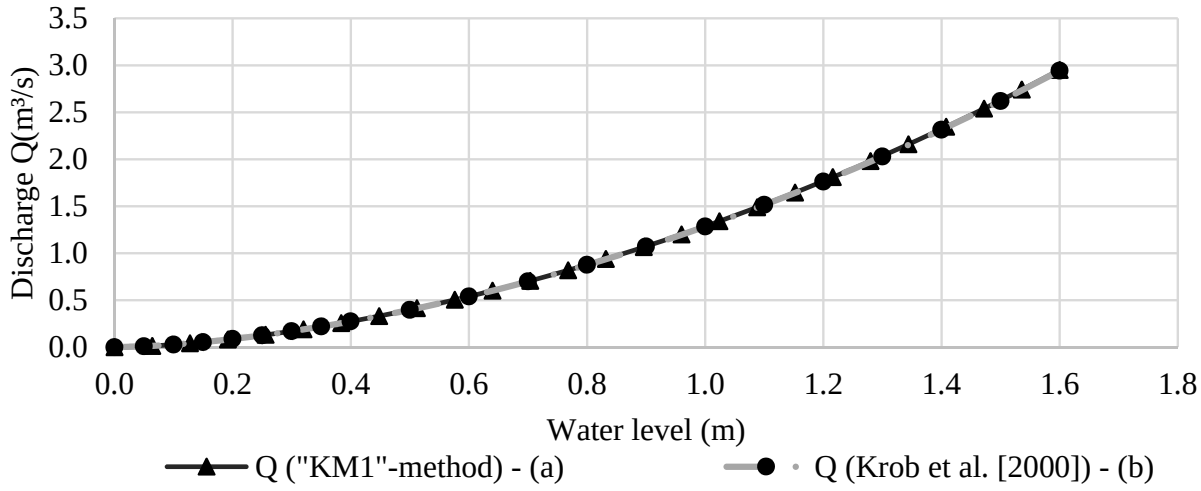

Figure D.38: Simulated relations of discharges and water levels for the profile E-E′ (Moorfleeter Schlauchgraben) using in (a) the developed KM1-method and in (b) results published by Krob et al. [2000] .

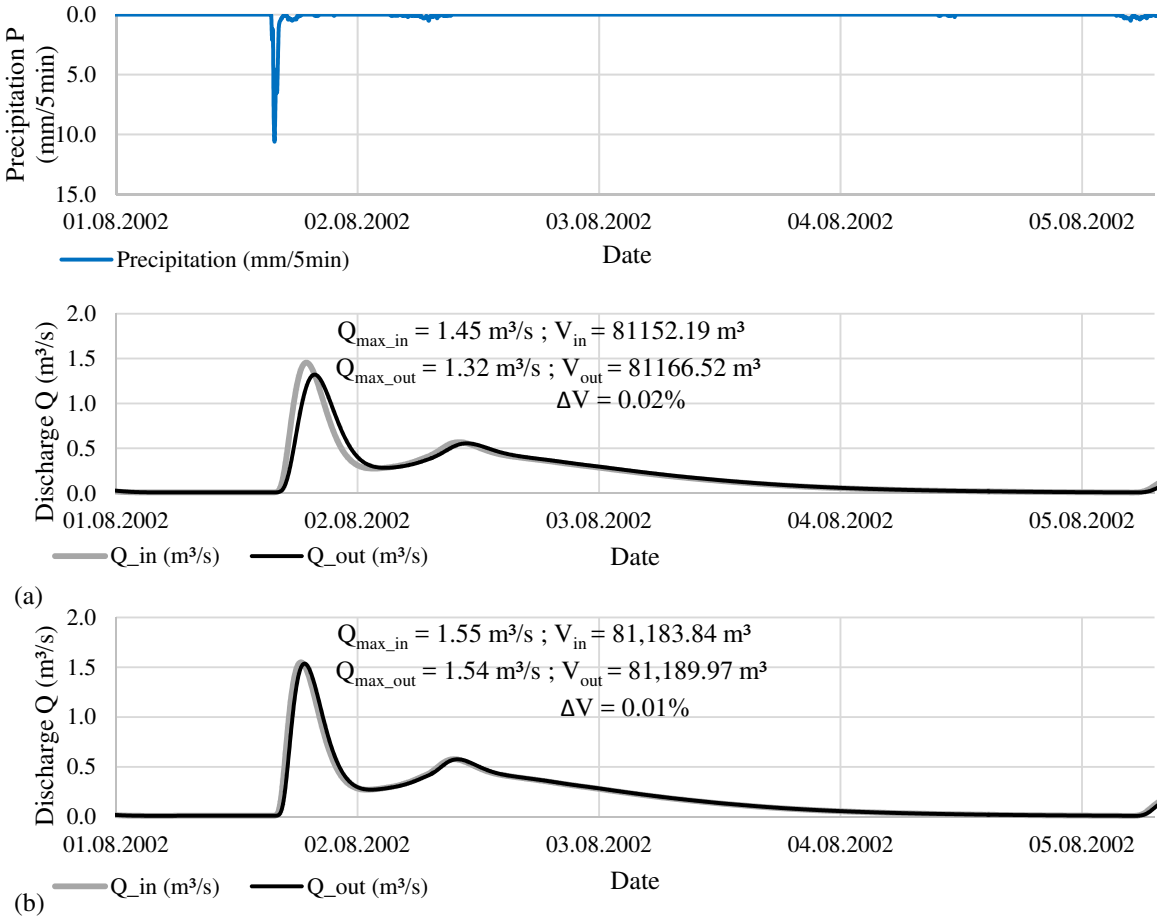

Figure D.39: Results of the stream segment "Moorfleeter Schlauchgraben" (3151km1) using the flood routing method KM1 with the unadjusted parameters in (a) and with the adjusted parameters in (b) for the rainfall event in August 2002.

Table D.12: Computation results of the KM1-method for the stream segment "Moorfleeter Schlauchgraben" (3151km1).

h (m)	lu (m)	A (m²)	R_{hy} (m)	v (m/s)	Q (m³/s)	Q_m (m³/s)	V (m3)	Lc_i (m)
0.00	7.80	0.00	0.00	0.00	0.04	0.00	0.00	64.00
0.06	7.96	0.50	0.06	0.15	0.16	0.08	701.96	84.21
0.13	8.13	1.01	0.12	0.24	0.35	0.24	1413.08	115.20
0.19	8.29	1.53	0.18	0.31	0.61	0.47	2133.35	151.75
0.26	8.46	2.05	0.24	0.37	0.92	0.76	2862.77	189.45
0.32	8.62	2.58	0.30	0.42	1.29	1.09	3601.35	227.60
0.38	8.78	3.11	0.35	0.48	1.69	1.48	4349.09	265.99
0.45	8.95	3.65	0.41	0.52	2.14	1.91	5105.98	304.50
0.51	9.11	4.20	0.46	0.57	2.64	2.38	5872.03	343.06
0.58	9.28	4.76	0.51	0.61	3.17	2.89	6647.23	381.65
0.64	9.44	5.32	0.56	0.65	3.74	3.44	7431.59	420.23
0.70	9.60	5.89	0.61	0.68	4.34	4.03	8225.11	458.78
0.77	9.77	6.46	0.66	0.72	4.98	4.66	9027.78	497.29
0.83	9.93	7.04	0.71	0.75	5.66	5.31	9839.60	535.73
0.90	10.09	7.63	0.76	0.79	6.37	6.01	10660.58	574.11
0.96	10.26	8.23	0.80	0.82	7.11	6.73	11490.72	612.40
1.02	10.42	8.83	0.85	0.85	7.89	7.49	12330.01	650.60
1.09	10.59	9.43	0.89	0.88	8.70	8.29	13178.45	688.71
1.15	10.75	10.05	0.93	0.91	9.54	9.11	14036.05	726.71
1.22	10.91	10.67	0.98	0.93	10.41	9.97	14902.81	764.60
1.28	11.08	11.29	1.02	0.96	11.31	10.85	15778.72	802.38
1.34	11.24	11.93	1.06	0.99	12.25	11.77	16663.79	840.04
1.41	11.41	12.57	1.10	1.01	13.21	12.72	17558.01	877.57
1.47	11.57	13.22	1.14	1.04	14.20	13.70	18461.39	914.98
1.54	11.73	13.87	1.18	1.06	15.23	14.71	19373.93	952.26

Output of the KM1-method:

Characteristical stream length L_c (m)	497.75
Number of linear storages n (-)	3.00
Retention coefficient K_{km} (h)	0.11

D.2.8 Evaluation results of the backwater effect computations

In this attachment the results of computed water levels at gauging stations are presented which are backwater affected. The control structures like tide gates, sluices and pumps are modelled and generate afflux conditions at the downstream segments. The control structures for gates and sluices are indicated in the diagrams with a larger value ("+") for closed and a smaller value ("-") for open status. The control functions are summarised in table D.5 (p. D19). The results are presented in two paragraphs. First the results of the meso scale stream segments "Dove-Elbe" and in the second paragraph the results of the district scale study area "Moorfleet" are illustrated in diagrams. The precipitation is measured at the weather station of the Hamburg University which is located in a distance of 500m north of the study area Moorfleet (see map in figure D.30 on page D17).

Results of backwater effect computations in meso scale stream segments. Stream segments of the Dove-Elbe catchment are described in section 8.3 (p. 139) as part of the application study. During low tide conditions in the Elbe river (water level <0.9 m a.s.l.) the streams drain by free flood routing into the Elbe river. During high tide, the downstream gate is closed and the afflux of water causes backwater effects in upstream direction. Along the backwater affected streams five gauging stations are located. The locations of the gauging stations are indicated in the map in figure D.30 (p. D17). The results for specific events are illustrated in the following diagrams which are ordered from the downstream to the upstream gauging stations. The precipitation events in February 2002 and February 2011 were long lasting over several days with a maximum intensity of 2 mm/5 minutes. The summer event in August 2002 reached an intensity of 10.6 mm/5 minutes. To illustrate the different rainfall intensities in the diagrams the scale of the secondary rainfall axis is varied. Downstream and upstream of the Krapphof sluice, the scale of the water level axis varies in the diagrams, because of a jump in water levels which is operated by that sluice. The backwater effects mostly influence the water levels in downstream segments of the Krapphof sluice. In all diagrams the maximal simulated water level value and the difference between observed to simulated value is given.

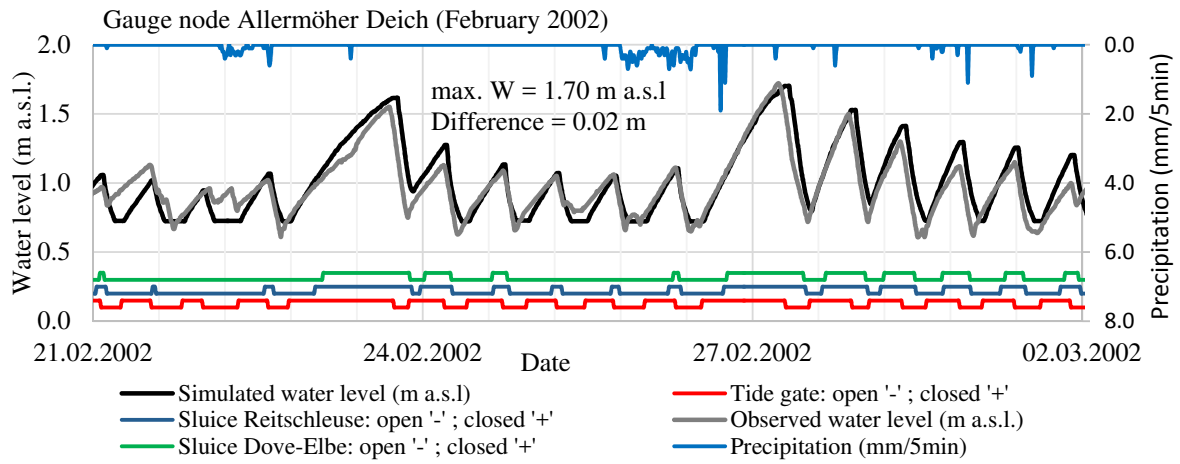

Figure D.40: Simulated and observed water levels at the gauge Allermöher Deich (event February 2002).

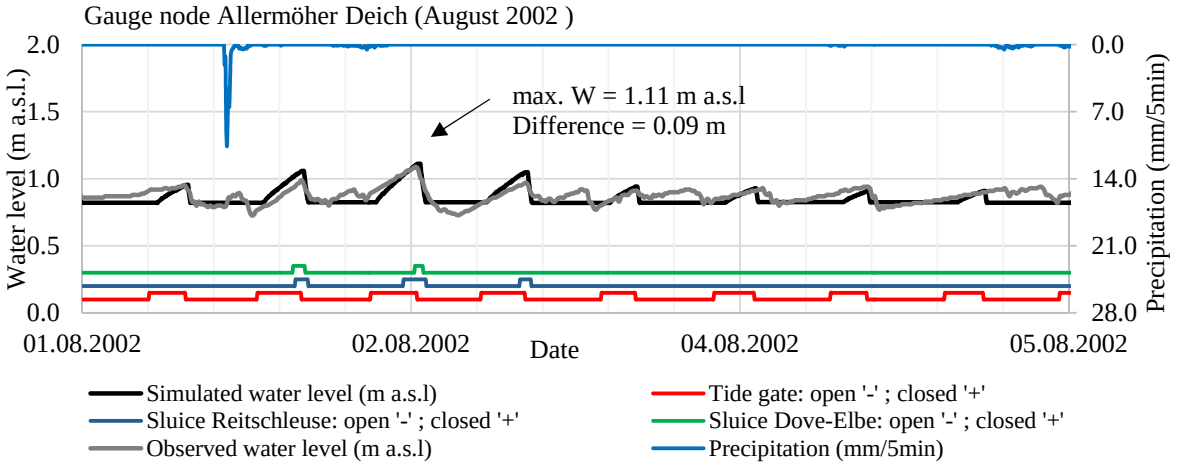

Figure D.41: Simulated and observed water levels at the gauge Allermöher Deich (event August 2002).

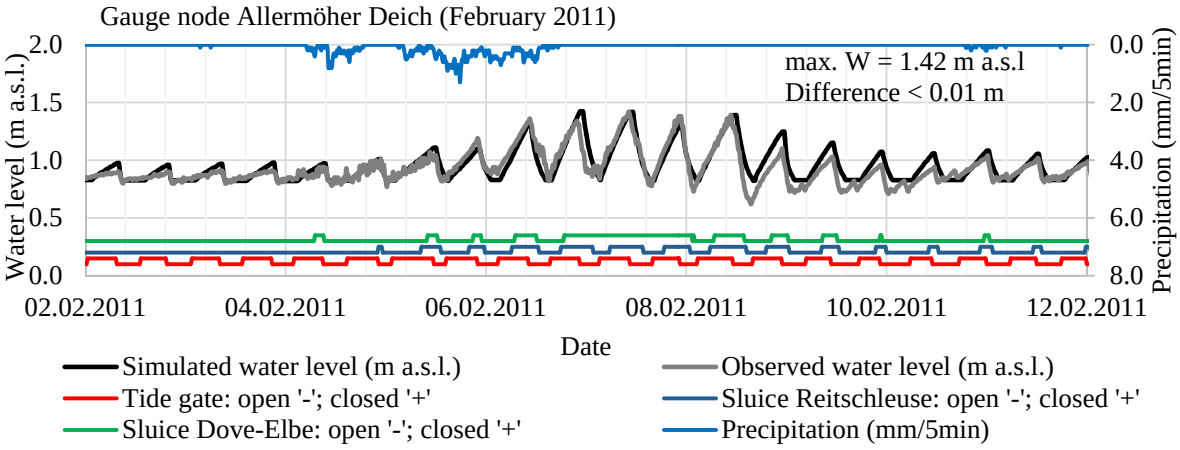

Figure D.42: Simulated and observed water levels at the gauge Allermöher Deich (event February 2011).

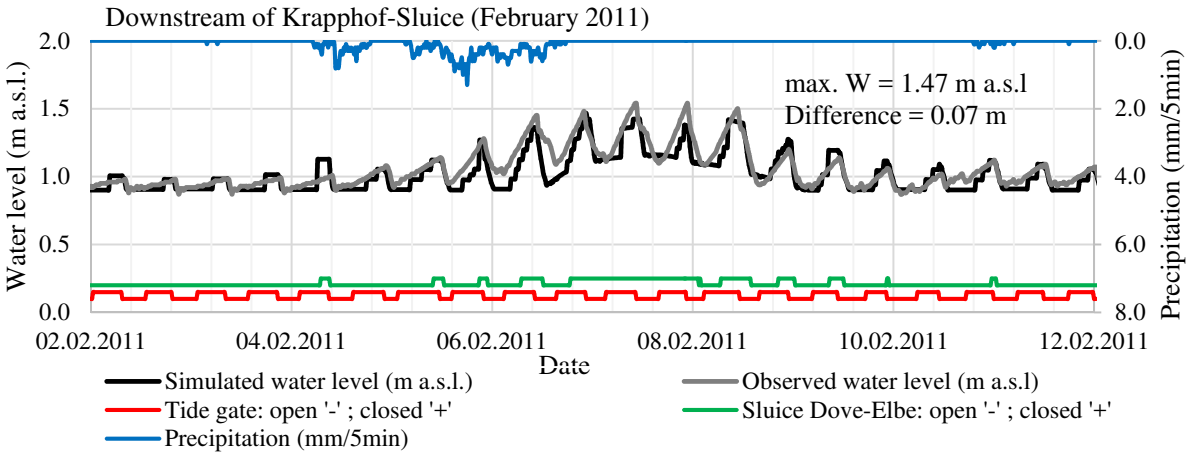

Figure D.43: Simulated and observed water levels at the gauge downstream of the Krapphof sluice (event February 2011).

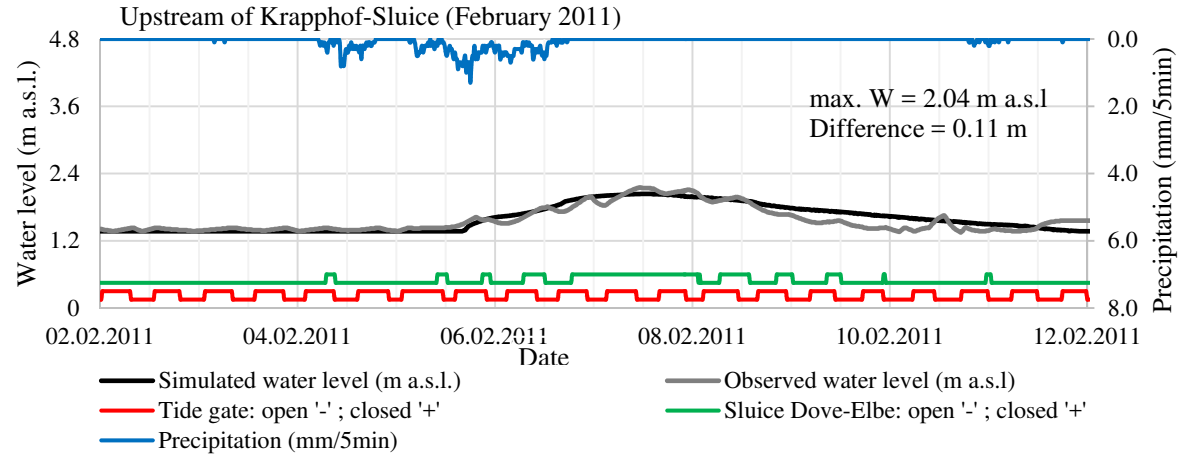

Figure D.44: Simulated and observed water levels at the gauge upstream of the Krapphof sluice (event February 2011).

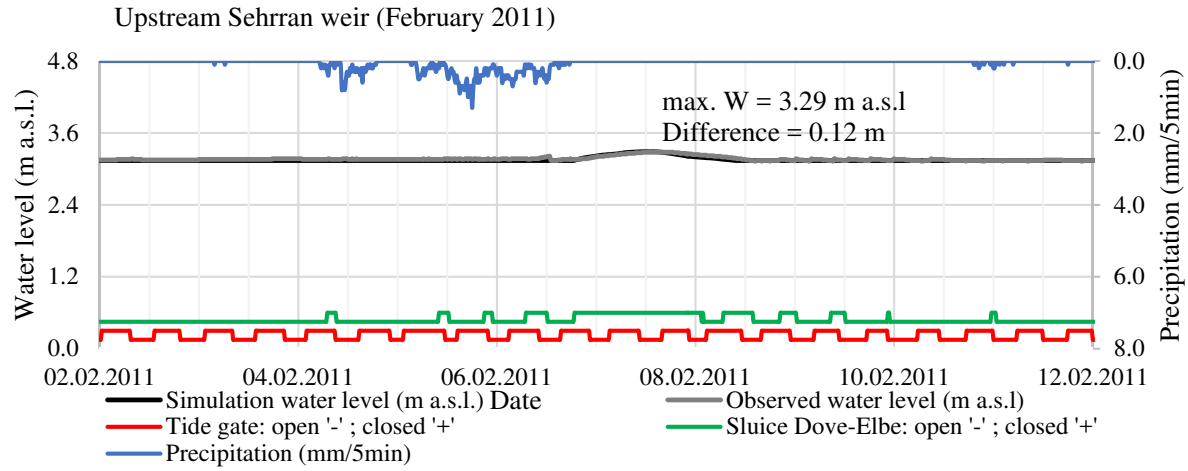

Figure D.45: Simulated and observed water levels at the gauge upstream of the Sehrran weir (event February 2011).

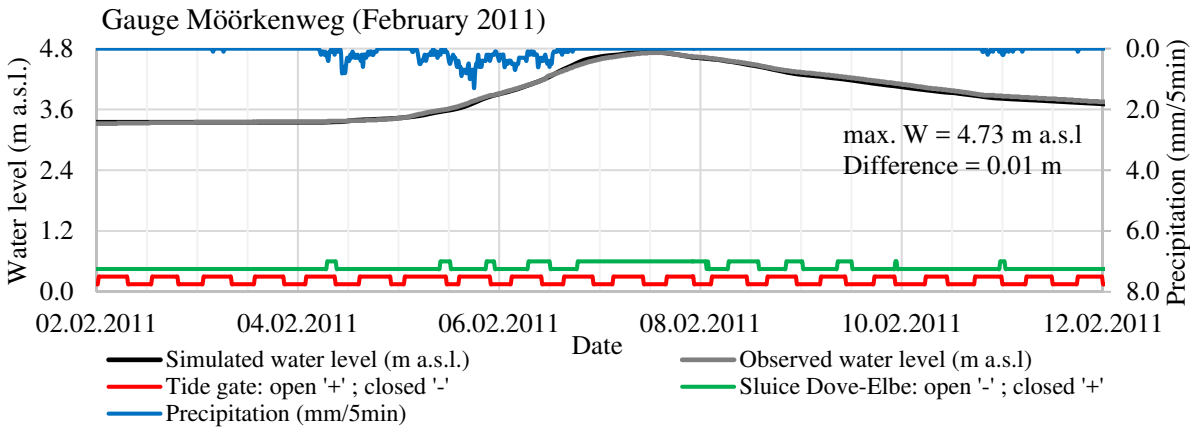

Figure D.46: Simulated and observed water levels at the gauge Möörkenweg (event February 2011).

Results of backwater effect computations in stream segments of "Moorfleet". For the study area Moorfleet rarely observed water level data is available for only one gauge at the downstream located pumping station "Eichbaum". For the rainfall event August 2002 the data is available and applied for a comparison with numerical model results. During that event, the control functions of the pumps are activated according to the upstream water levels at the pumping station. When the water level reached -0.85 m a.s.l the first pump is started. When the water level exceeded -0.80 m a.s.l. another pump started and all three pumps were running when a water level of -0.75 m a.s.l. was exceeded. Each pump has a capacity of 1.15 m^3/s. The results of the computed water levels in comparison to observed water levels are illustrated for the stream segment directly upstream of the pumping station in figure D.47.

The observed and simulated water levels at the pumping station reached a maximum of -0.33 m a.s.l. The rising limb of the simulated water levels agrees with the observed ones, but the simulated water level sinks slower in comparison to the observed water levels. Measurements at the upstream gauging station are not available. Therefore, a comparison of the backwater effects in the upstream segments is not possible. The results in the Moorfleet stream segments are analysed for mass-conservation criteria and sensitivity studies only.

For the event in August 2002, the difference in maximal water level between observed and simulated data is less than 0.01 m. Additionally, the result of the stream segment 3151km1 (Moorfleeter Schlauchgraben) is given in figure D.48 together with the result of the water level on the flood prone area in the subcatchment "Moorfleeter Wanne". A water level of 0.07 m is simulated for the flood prone area over a duration of 3 hours. The results of simulated water levels at the stream segments in Moorfleet are presented in the following section to compare the effect by implementing LSDMs in different scenarios. The objective is a reduction of the water level rise in upstream segments and to mitigate the backwater induced flooding of flood prone areas.

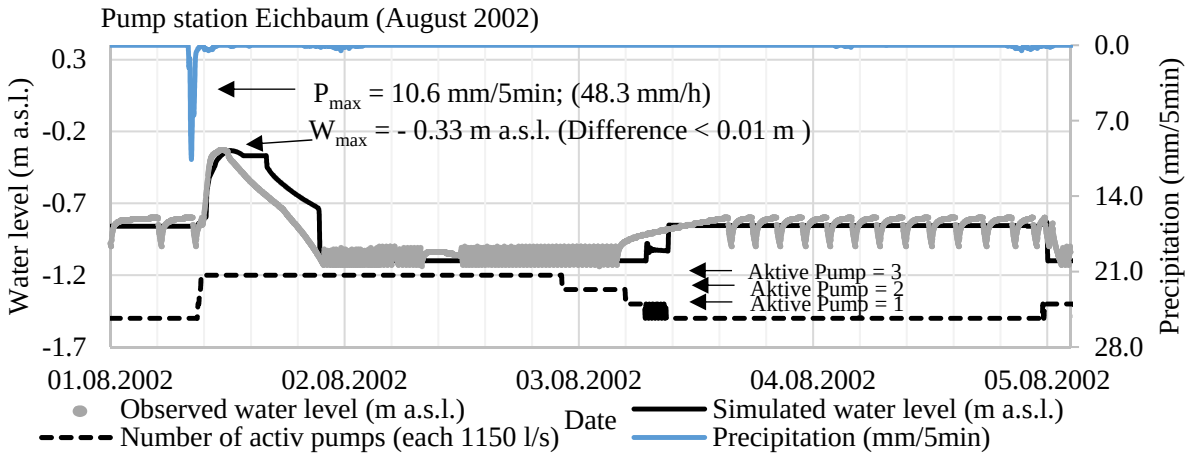

Figure D.47: Results of simulated and observed water levels at the pumping station in Moorfleet (Eichbaum). Additionally, the activation of the three pumps is illustrated.

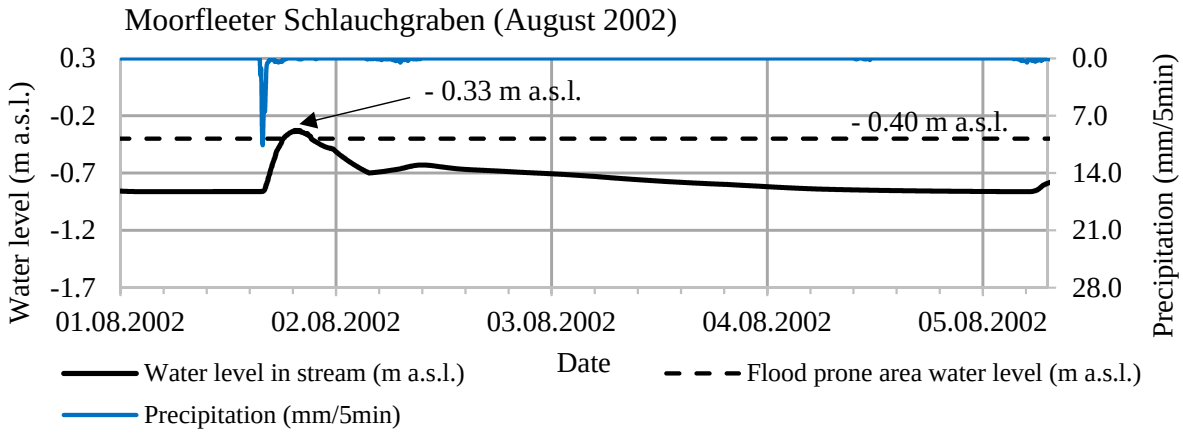

Figure D.48: Results of the simulated water levels at the stream segment Moorfleeter Schlauchgraben (index: 3151km1) and the flood prone area in the subcatchment Moorfleeter Wanne. The flood prone area has a surface level at -0.40 m a.s.l.

D.2.9 Results of application study scenarios to model LSDMs

In this attachment the results of defined scenario studies are presented. The storm event in August 2002 serves as basis to analyse the impacts of three scenarios. First an increase in rainfall intensity (plus 15 %) according to assumed climate change (CC) impacts is defined as "Scenario 1; CC". Secondly, the installation of LSDMs in the upstream low lying lands of Moorfleet are analysed in "Scenario 2". And as "Scenario 3", the installation of LSDMs in all subcatchments of Moorfleet is analysed to mitigate the impacts caused by the increased rainfall intensity. The description of the scenarios is given in section 8.2.4 (page 134). The results are illustrated for the upstream segment of low lying lands (index 3150km1). In the scenarios (2) and (3) the computed water levels in the backwater affected multifunctional area (MFA1) in Moorfleet are depicted with dashed green lines. The scenario results are compared with "status quo" water levels which are explained in the previous paragraphs and depicted in grey colour.

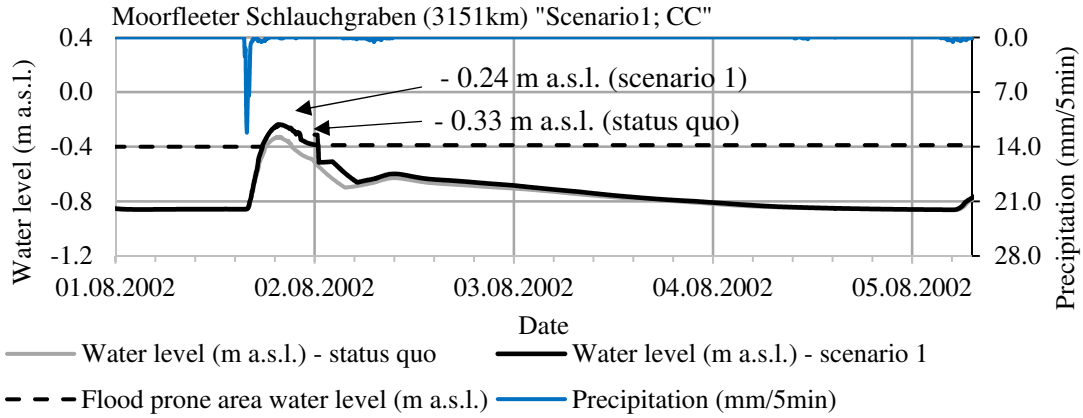

Figure D.49: Computed water levels in scenario 1 (CC) compared to the status quo water levels at the upstream segments in Moorfleet.

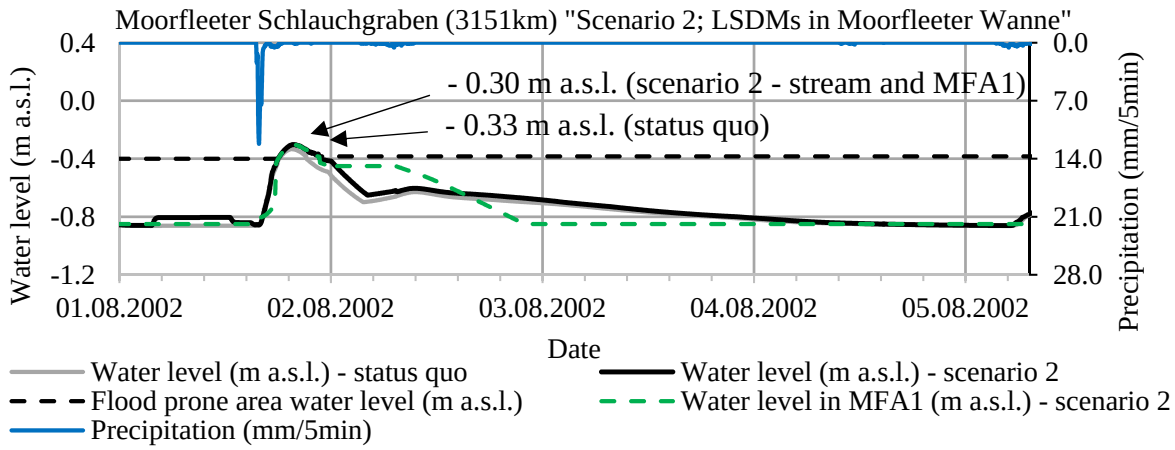

Figure D.50: Computed water levels in scenario 2 (CC & LSDMs) compared to the status quo water levels at the upstream segments in Moorfleet.

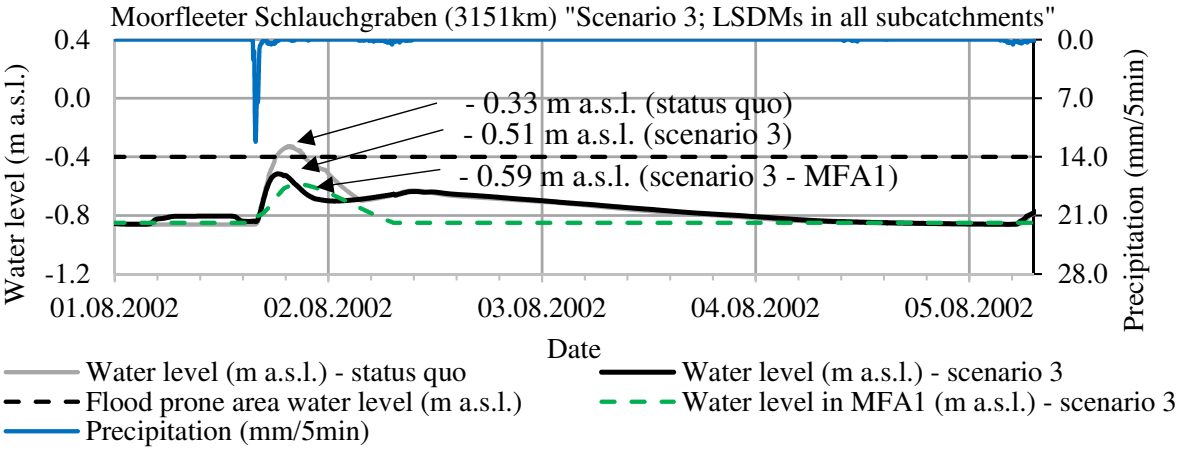

Figure D.51: Computed water levels in scenario 3 (CC & LSDMs) compared to the status quo water levels at the upstream segments in Moorfleet.

The computed discharges at the downstream located pump station (see figure D.52) and at the upstream located node 3151 in the area "Moorfleeter Wanne" (see figure D.53) are depicted to compare the effect of an increased rainfall intensity and the installation of LSDMs on the discharge. The peak discharge is raised by 14 % (from 6.84 to 7.96 m^3/s) by the impacts of an increased rainfall intensity in the climate change scenario. This is mitigated by the installation of LSDMs in the upstream subcatchment to 8 % (7.45 m^3/s). The largest reduction of about 42 % in peak discharge is reached by installing LSDMs in all subcatchments in scenario 3. The presented results in this attachment are explained in section 8.4.1 on page 144 ff.

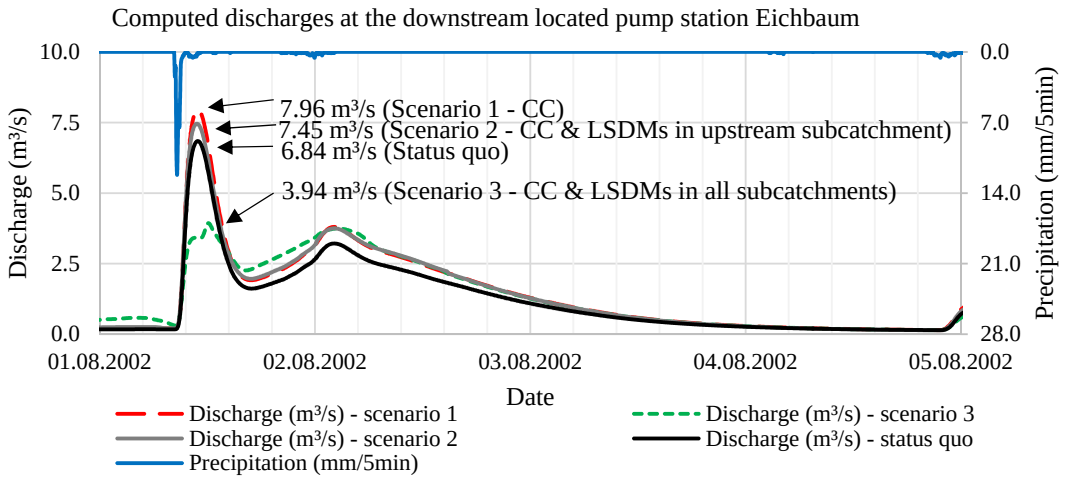

Figure D.52: Computed discharges of the different scenarios in comparison to the status quo at the downstream located pump station Eichbaum.

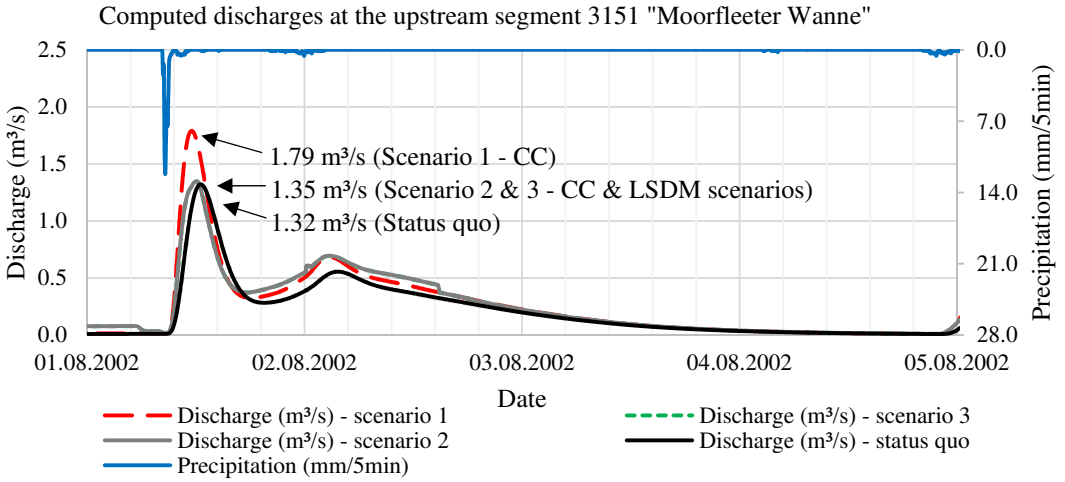

Figure D.53: Computed discharges of the different scenarios in comparison to the status quo at the upstream located node "Moorfleeter Wanne". In scenario 2 the installed LSDMs in the area "Moorfleeter Wanne" are the same as in scenario 3. Therefore, the discharge is equal among these scenarios.

D.2.10 Results of the computed hydrological processes in LSDMs

In this work a methodology is developed and implemented to compute the hydrological processes in LSDMs. The methodology is described in chapter 5 (page 63 ff.). The results of computed processes in two multifunctional areas, three different green roofs and a cistern system are depicted in this attachment. The LSDM scenario studies are described in section 8.2.4 (p. 134). The observed rainfall at the weather station is increased by a climate change impact of plus 15 %. The diagrams comprise two parts. The upper part shows the precipitation and computed evapotranspiration processes. In the lower part, the results of the computed fluxes (in $l/m^2/\Delta t$) and the retained water in form of the water levels within the measures (in mm) are given. Because of the large variations in the dimensions of the measures, the scales of axes are not consistent throughout the diagrams. The maximum values of the simulated processes are labelled in the diagrams.

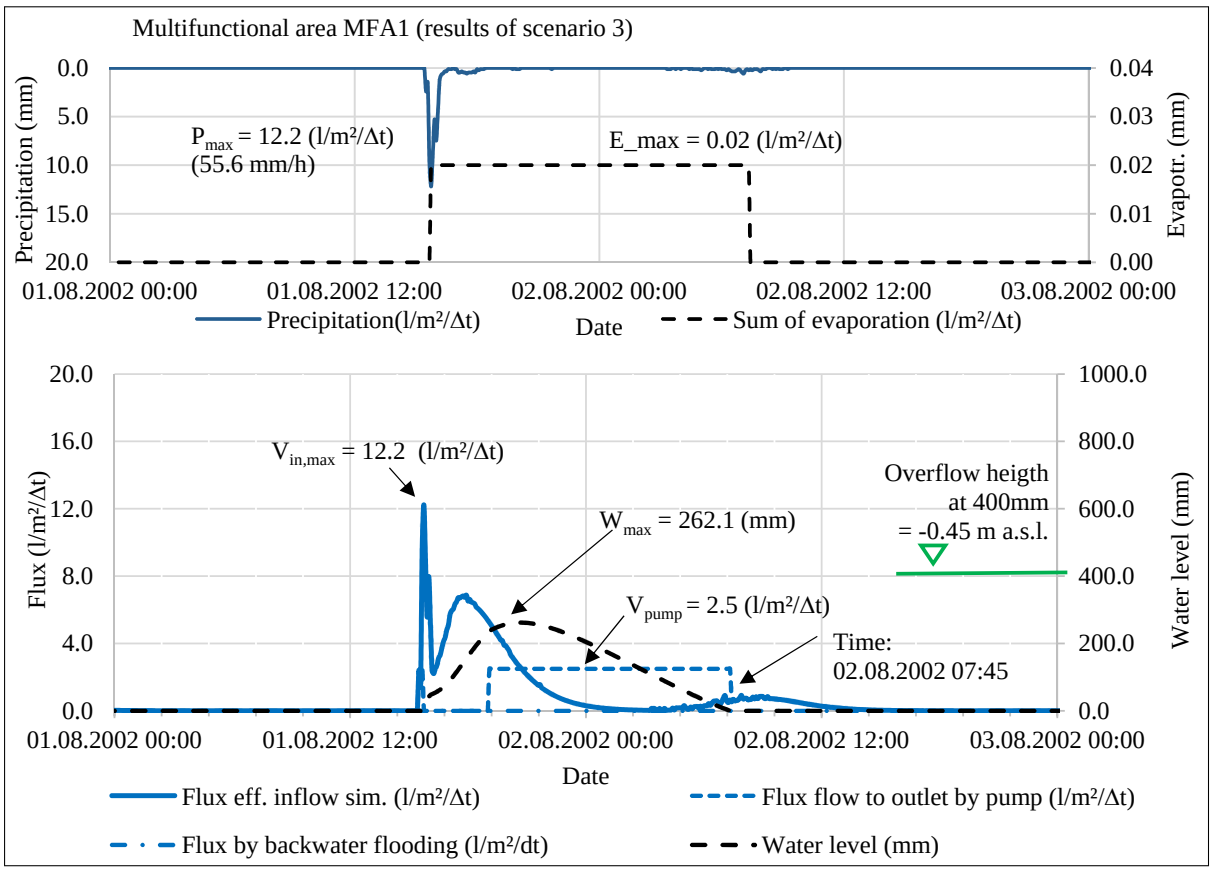

Figure D.54: The multifunctional area (MFA1) is situated on a ground level of -0.85 m a.s.l. with an overflow height of 0.4 m. This area is directly linked to the backwater affected streams in the low lying lands in Moorfleet. In this diagram the result of the MFA1 in scenario 3 is illustrated. The result of scenario 2 with backwater flooding is depicted and explained in figure 8.8 on page 146.

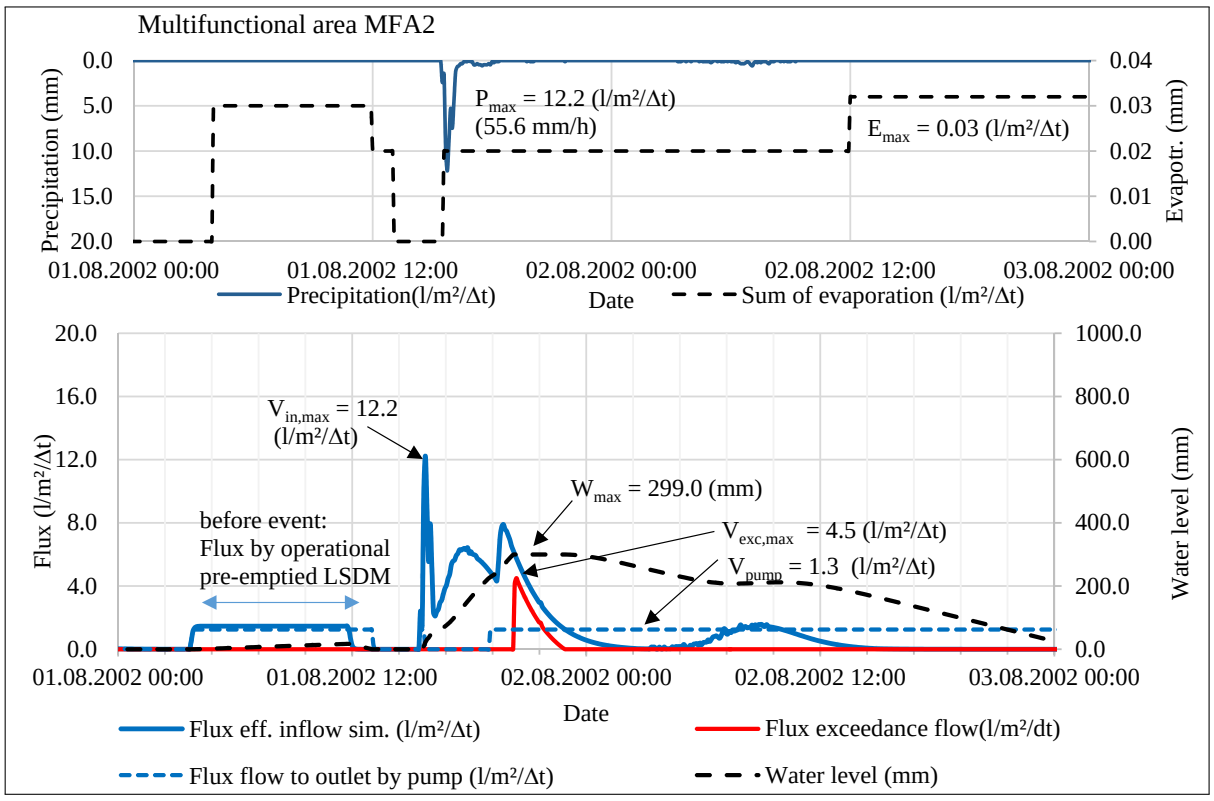

Figure D.55: Results of computed hydrological processes in the multifunctional area MFA2 which is situated on a ground level of +2.0 m a.s.l. (scenario 2 & 3).

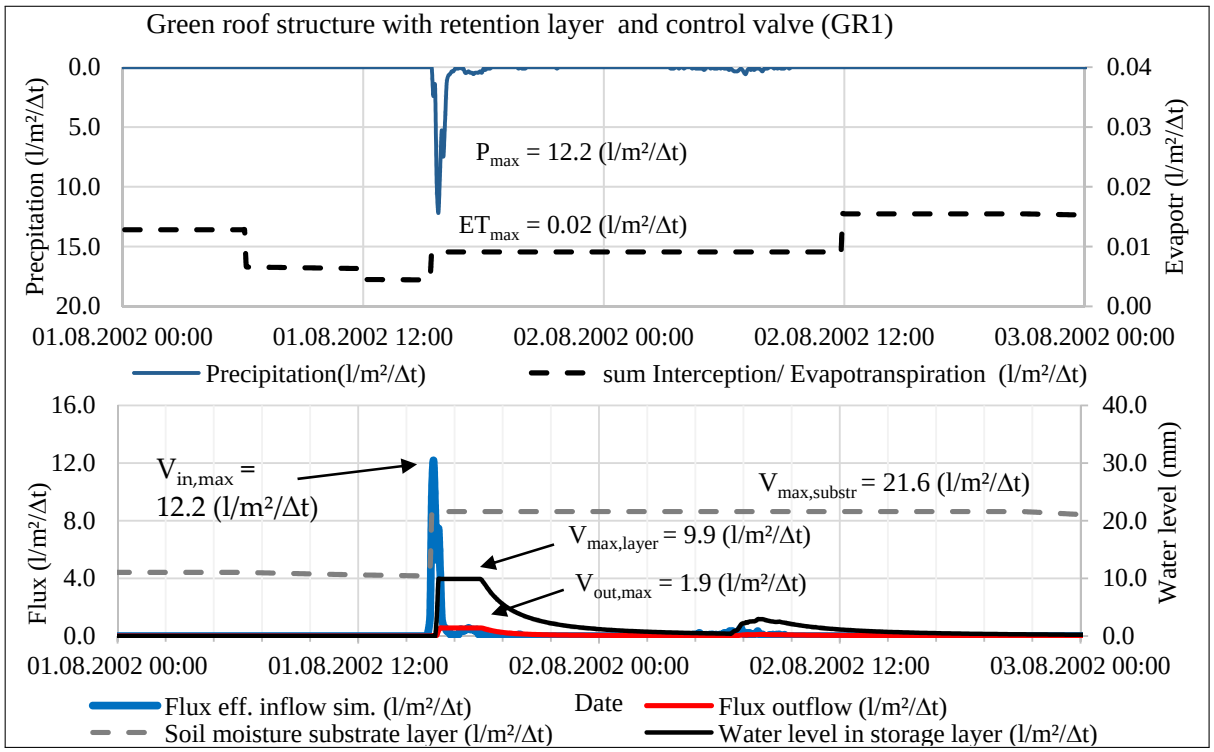

Figure D.56: Results of computed hydrological processes in the green roof GR1 with a retention layer setup and an operational valve with a pre-emptying function (scenario 2 & 3).

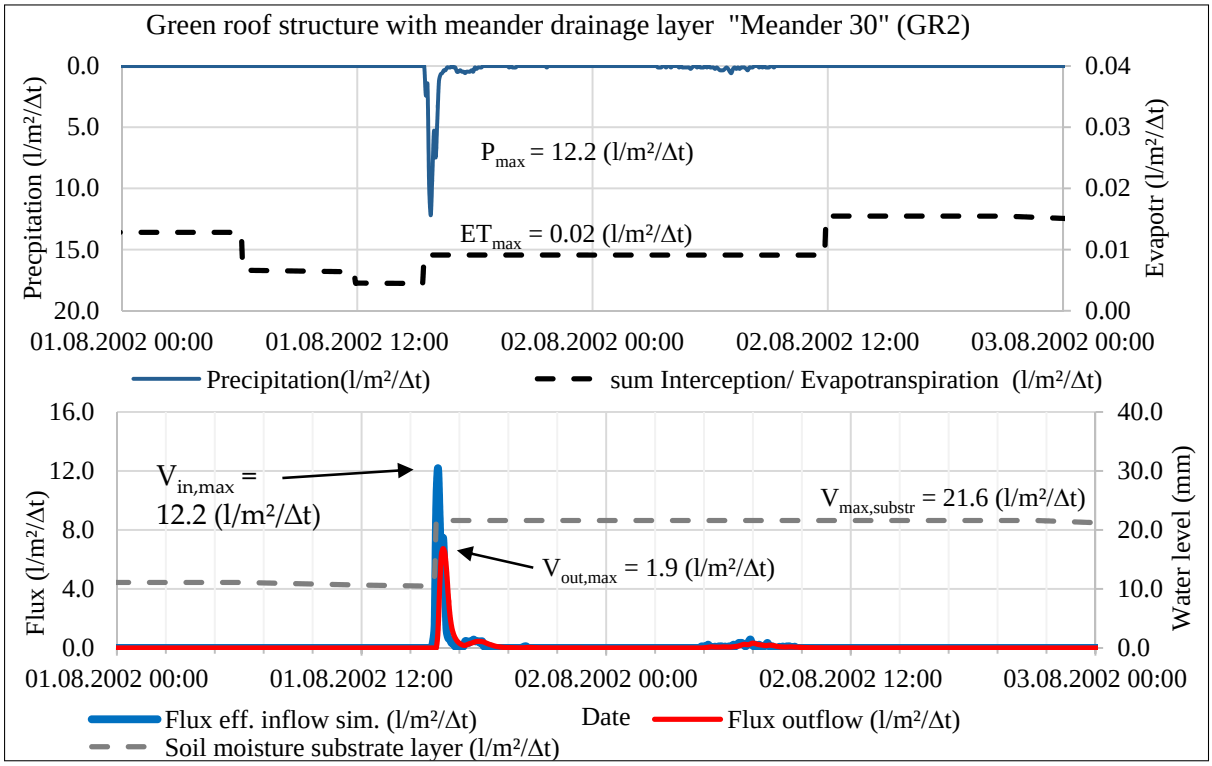

Figure D.57: Results of computed hydrological processes in the green roof GR2 with a drainage layer (scenario 2 & 3).

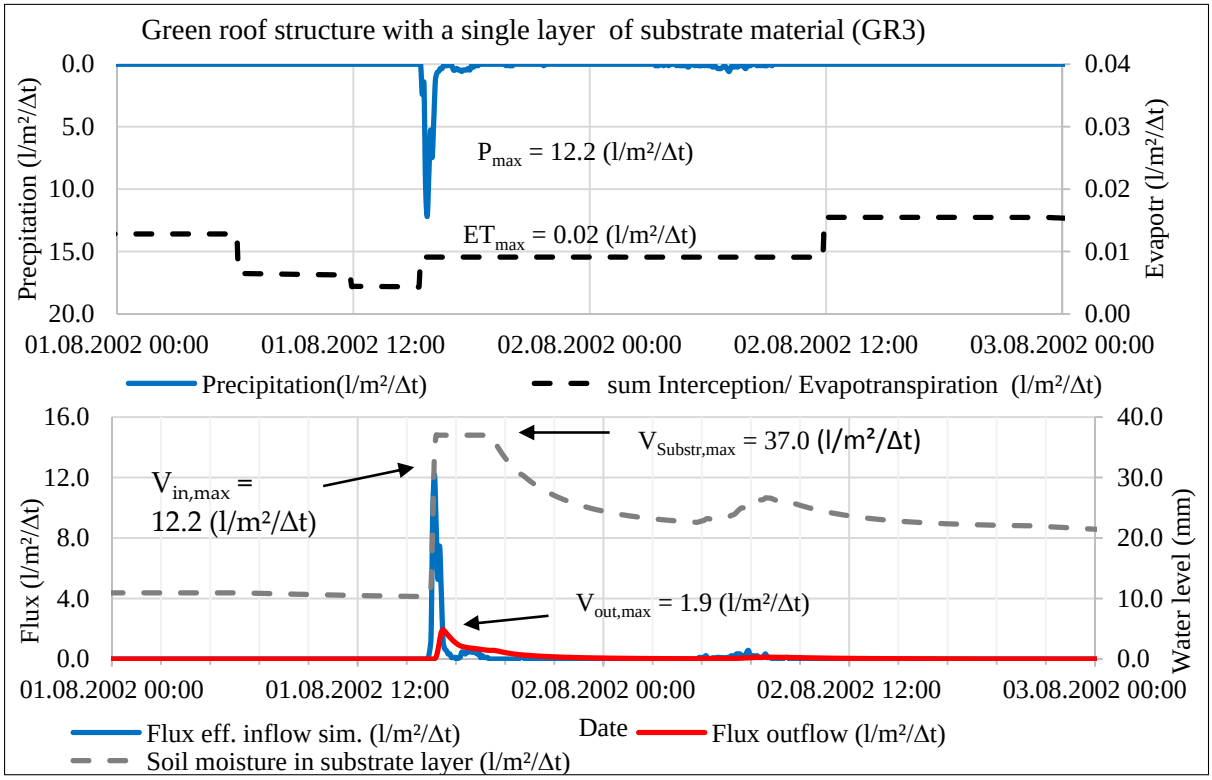

Figure D.58: Results of computed hydrological processes in the green roof GR3 with a single layer structure made up of substrate (scenario 2 & 3).

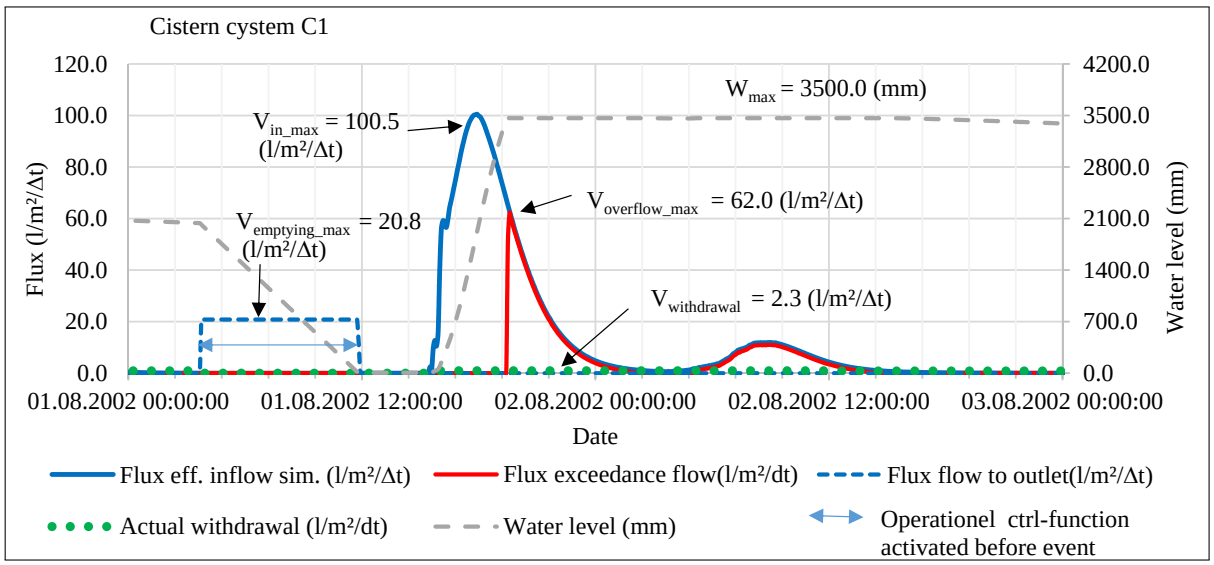

Figure D.59: Results of computed drainage and retention processes in the cistern system C1 with an operational valve for pre-emptying the storage 12 hours before rainfall intensities above 4.5 mm/min are forecasted. The cistern is filled with water from drained roofs. Evaporation processes take not place in the covered system (scenario 2 & 3).

D.2.11 Evaluation results of the mass-conservation in simulated hydrological processes

A verification of the computed hydrological processes in LSDMs is performed by testing the mass-conservation of in- and outfluxes. The computed values are summarised in this attachment. In table D.13 the influxes and in table D.14 the outfluxes are listed. The analysed LSDMs are described in section 8.2.4 (page 134 ff.) and an explanation of the results is given in section 8.4.3 (page 147 ff). The inflow fluxes are computed per unit area of the LSDMs with the equation given in section 8.4.3. The LSDM type (name) is listed in the first row of the tables. The computed effective inflows into these target LSDMs are compared with the computed outflows from the source LSDMs. Further on, losses by interception, evaporation and depression storage are computed. The influx from streams caused by backwater induced flooding occurs only for the multifunctional area (MFA1). A difference between scenario 2 and 3 is only present for MFA1, where backwater flooding occurs in scenario 2 but not in scenario 3.

Table D.13: Results of influxes in l/m^2 and the bias in mass-conservation for the analysed LSDMs.

Description	**Values**							**Unit**
LSDM type	MFA1		MFA2	GR1	GR2	GR3	C1	(-)
Scenario	S2	S3	S2 / S3	S2 / S3	S2 / S3	S2 / S3	S2 / S3	(-)
Area	7713.79		828.18	763.89	367.25	448.23	58.12	(m²)
Run-on fluxes (l/m²):								
Precipitation	97.29		97.29	97.29	97.29	97.29	97.29	(l/m²)
Run-on fluxes from linked areas:								
Influx from impervious areas	442.72		412.35	0.00	0.00	0.00	5876.37	(l/m²)
GR1	0.00		0.00	0.00	0.00	0.00	730.63	(l/m²)
GR2	0.00		0.00	0.00	0.00	0.00	294.03	(l/m²)
GR3	0.00		0.00	0.00	0.00	0.00	361.48	(l/m²)
C1	0.00		330.17	0.00	0.00	0.00	0.00	(l/m²)
Sum of run-on fluxes	540.01		839.82	97.29	97.29	97.29	7359.80	(l/m²)
Interception loss	0.00		0.00	11.24	11.24	11.24	0.00	(l/m²)
Inflow fluxes (l/m²):								
Calculated inflow flux	540.01		839.82	86.05	86.05	86.05	7359.85	(l/m²)
Bias in inflow fluxes from areas	0.00%		0.00%	0.00%	0.00%	0.00%	0.00%	(-)
Inflow by backwater induced flooding:								
Influx from streams	329.98	0.00	0.00	0.00	0.00	0.00	0.00	(l/m²)
Retained exceedance flux	55.37	0.00	0.00	0.00	0.00	0.00	0.00	(l/m²)
Sum of inflow =	925.37	540.01	839.82	86.05	86.05	86.05	7359.85	(l/m²)

Table D.14: Results of outfluxes in l/m² and the bias in mass-conservation for the analysed LSDMs.

Description	**Values**							**Unit**
LSDM type	MFA1		MFA2	GR1	GR2	GR3	C1	(-)
Scenario	S2	S3	S2 / S3	S2 / S3	S2 / S3	S2 / S3	S2 / S3	(-)
Inflow sum (see table D.13) =	925.37	540.01	839.82	86.05	86.05	86.05	7359.85	(l/m²)
Changes in the storage regime (l/m²):								
Initial water content	0.00	0.00	0.00	7.34	7.34	7.19	2277.45	(l/m²)
Difference in water storage over simulation time	0.00	0.00	0.00	8.69	8.70	8.83	556.00	(l/m²)
Outflow fluxes (l/m²):								
Flux to outlet of drainage layers	0.00	0.00	0.00	27.92	64.24	64.58	0.00	(l/m²)
Flux to outlet by control function	937.39	536.20	766.59	36.51	0.00	0.00	2032.41	(l/m²)
Rainwater harvesting	0.00	0.00	0.00	0.00	0.00	0.00	2098.34	
Outflux of excedance flow	0.00	0.00	60.03	0.00	0.00	0.00	2672.82	(l/m²)
Evapo(transpi)-ration	6.30	3.81	13.52	12.85	12.67	12.62	0.00	(l/m²)
Sum of losses and outflow =	943.70	540.01	840.14	85.98	85.61	86.02	7359.57	(l/m²)
Bias in outflow fluxes	1.94%	0.00%	0.04%	-0.08%	-0.52%	-0.03%	0.00%	(-)
Additional losses from fluxes out of the system (l/m²):								
Depression storage	2.42	2.50	1.25	8.85	17.71	17.71	0.00	(l/m²)
Sum of outflow to target =	938.80	537.51	838.89	55.58	46.53	46.87	7359.57	(l/m²)

E. Supplementary comparison of a green roof test result in literature

A supplementary comparison of the results of green roof installations with a slope of 2 % for a rainfall type with an intensity of 0.6 mm/minute is illustrated in this attachment in figure E.1. The results in part (a) are taken from the experimental run [22] which is analysed in this work using a substrate of the company OptiGreen with a thickness of 6 cm. The drainage layer is a patented meander panel with a height of 30 mm of the company OptiGreen and the structure has a gradient of 2 %. In part (b) the result of the study published in Vesuviano et al. [2014] is illustrated. The green roof in (b) is made up of a substrate of the company Zinco (ZinCo, Nürtingen, Germany) with a thickness of 10 cm and a drainage layer of that company. The gradient of the structure is likewise 2 %. Another difference among the tests is the duration of rainfall. In this work a duration of 90 minutes is analysed and in Vesuviano et al. [2014] a duration of only 60 minutes is tested.

The applied numerical method in Vesuviano et al. [2014] is based on a reservoir retention method (first published in Zimmer and Geiger [1997]) using the conceptual parameters "n", "k" and additionally a "delay" factor to fit the numerical model results with the observed green roof test results. In contrast to that conceptual approach, a physical-based method is presented in this work. This method computes the hydraulic conductivity in the substrate based on the Kozeny-Carman approach and computes the attributes of the drainage layer in more detail. For example, the meander 30 panel prolongs the flow path and is modelled with the Darcy-Weisbach approach using the flow path length and the roughness of the material as input parameters. The method to compute the outflow takes into account the size of the outlet by using the approach of Poleni.

Both numerical model results show a good congruency in comparison to the observed data. But the approach presented in this work is physical-based and therefore the parametrisation is transferable to other LSDM structures. This is not possible with the conceptual approach presented in Vesuviano et al. [2014].

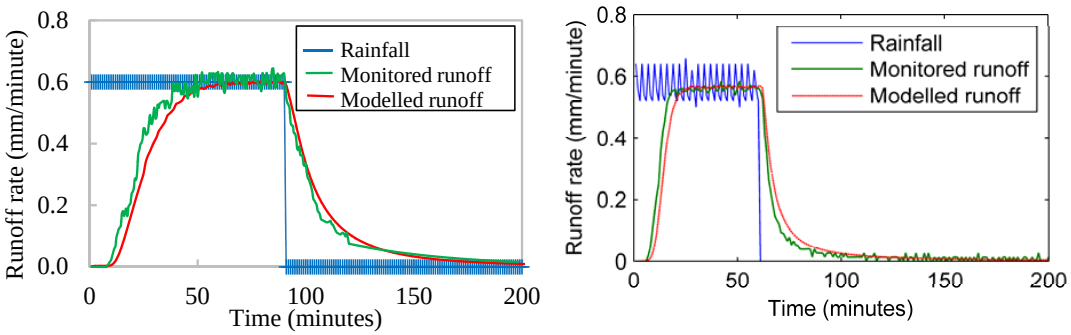

Figure E.1: Comparison between observed and simulated runoff from green roof structures. In (a) an result of this work and in (b) a result from Vesuviano et al. [2014] are depicted. In part (a) the result of run [22] with an OptiGreen structure using a meander 30 panel, a substrate height of 6 cm, a gradient of 2 % and a rainfall intensity of 0.6 mm/minutes over duration of 90 minutes is illustrated. In part (b), the result from Vesuviano et al. [2014] is depicted, where a green roof structure of the company ZinCo is tested. In that structure a ZinCo drainage layer, a substrate height of 10 cm, a gradient of 2 % and a rainfall intensity of 0.6 mm/minutes over a duration of 60 minutes is tested.

22

WASSERBAU
River and Coastal Engineering

DOI: 10.15480/882.2627

TUHH
Technische Universität Hamburg